The copyright of this thesis vests in the author. No quotation from it or information derived from it is to be published without full acknowledgement of the source. The thesis is to be used for private study or non-commercial research purposes only.

Published by the University of Cape Town (UCT) in terms of the non-exclusive license granted to UCT by the author.

University of Cape Town

CONTRIBUTION TO THE UNDERSTANDING OF THE THREE-PRODUCT CYCLONE ON THE CLASSIFICATION OF A DUAL DENSITY PLATINUM ORE

By

Aubrey Njema Mainza

University of Cape Town

Thesis presented for the degree of Doctor of Philosophy in the Department of Mechanical Engineering



UNIVERSITY OF CAPE TOWN

MARCH 2006

ABSTRACT *The detrimental effects exhibited by the conventional hydrocyclone in classifying ores that contain different density components motivated the AMIRA P9 project to look into modifications to the conventional hydrocyclone that can improve separation by component density. In this project a cyclone termed the three-product cyclone has been developed and tested.*

The three-product cyclone is a modification of the conventional hydrocyclone with an additional vortex finder termed the inner vortex finder inserted concentric to the existing one, termed the outer vortex finder, resulting in three products from the same hydrocyclone. The three-product cyclone produces a finer overflow stream, an intermediate overflow stream comprising fine high density particles and medium sized light particles, and a coarse underflow stream.

The work presented in this thesis involved designing an overflow arrangement which allowed interchangeable inner vortex finders to be tested, and a special rig for industrial scale experiments using a 600mm diameter hydrocyclone. A range of experiments were performed to assess the performance of the three-product cyclone and generate the data for model development.

The results indicated that in addition to the design and operational variables that influence classification in the conventional hydrocyclone the length of the inner vortex finder, and the ratio of the area covered by the inner vortex finder orifice to that of the annulus between the inner and outer vortex finder, termed the selection area ratio, had a significant influence on the performance of the three-product cyclone. The selection area ratio had a significant influence in the split between the overflow from the inner vortex finder termed the inner overflow, and that from the annulus - the outer overflow of the three-product cyclone.

Computational Fluid Dynamics (CFD) simulations for the three-product cyclone were performed at JKMRC on behalf of the author. The author interpreted the data and related the flow characteristics from CFD simulations to the trends observed from field trials to enhance the understanding of some underlying principles for the observed trends. From the CFD results it was observed that the inner vortex finder had a significant influence on the both the tangential and axial velocities and that for the fixed spigot the air-core shape is a function of the inner vortex finder diameter and

University of Cape Town

length.

To demonstrate the potential applications of utilising the three-product cyclone in conjunction with the fine screens for the classification of the UG2 platinum ore, comparative pilot plant trials with the conventional hydrocyclone were performed. The results indicated that the combination of the three-product cyclone and fine screens in the processing of the UG2 platinum ore enhances flotation recovery of valuable minerals without diluting the grade.

A model describing separation in the three-product cyclone was developed using experimental data. The description of separation in the model was particle size based and additional relationships for components modelled in terms of the silica and chromite component are included.

University of Cape Town

Contents

1 Introduction **1**

1.1 Background 1

1.2 Motivation 3

1.3 Hypotheses 5

1.4 Objectives 6

1.5 Layout of the thesis 7

2 Literature Review **9**

2.1 Introduction 9

2.2 Reviewed Papers 10

2.2.1 A study of the motion of solid particles in a hydraulic cyclone 10

2.2.2 A further study of the hydraulic cyclone 14

2.2.3 Fundamentals and applications of the liquid cyclone 18

2.2.4 Performance and design of hydrocyclones, parts I - IV. 23

2.2.5 Hydrocyclone fundamentals 31

2.2.6 The selection of cyclone classifiers, pumps, and pump boxes for grinding circuits 35

2.2.7 Modeling and scale up of Hydrocyclone Classifiers. 39

2.2.8 A mathematical model of hydrocyclone classifiers. 43

2.2.9 Hydrocyclone to give a highly concentrated sample of a lighter dispersed phase 48

2.2.10 Water De-Oiling in an Air-Sparged hydrocyclone 53

2.2.11 The effect of two-stage hydrocyclone classification on mineral processing plant performance 57

University of Cape Town

2.2.12 A high performance hydrocyclone design - The Twin Vortex finder 61
2.2.13 The three product hydrocyclone for simultaneous separation of solids, both heavier and lighter than liquid medium. 65
2.2.14 The three-product cyclone - separation performance, potential applications and modelling. 69
2.3 Conclusion 79

3 Types of Cyclones Used for the Classification of the UG2 ore 81
3.1 Introduction 81
3.2 Description of the conventional hydrocyclone 82
3.2.1 Cylindrical section 82
3.2.2 Feed inlet 83
3.2.3 Vortex finder 83
3.2.4 Conical section 83
3.2.5 Spigot and spigot holder 84
3.3 Basic separation principles of the hydrocyclone 84
3.4 Description of the flat bottom cyclone 86
3.5 Comparison of the conventional and flat bottom cyclones 87
3.6 Description of the three-product Cyclone 88

4 Experimental Apparatus 91
4.1 Introduction 91
4.2 The overflow arrangement for the three product cyclone 91
4.2.1 Original overflow arrangement installed on the three-product cyclone 92
4.2.2 Modified JKMRC overflow arrangement 92
4.2.3 The UCT overflow arrangement design 93
4.3 Inner vortex finder mounting techniques 94

University of Cape Town

4.3.1 Collar-reducer system 96
4.3.2 Arrangement of the vortex finders in the three product cyclone 97
4.3.2.1 Outer vortex finders 98
4.3.2.2 Inner vortex finders 98
4.3.3 Changing the inner and outer vortex finders 98
4.4 Description of the industrial scale test rig 99
4.4.1 Location of test rig on the plant 99
4.4.2 The test rig 100
4.4.3 Test rig frame 101
4.4.4 Flow rate measuring tanks 102
4.4.5 Level control switches 103
4.4.6 Sample cutters 104
4.4.7 Pumping and sampling arrangement for the cyclone feed . . . 106
4.5 Pilot plant scale test rig 106
4.5.1 Pilot plant layout 107
4.5.2 Milling rig 107
4.5.3 Cyclone test rig 107
4.5.3.1 Cyclone area 109
4.5.3.2 Sampling area 110
4.5.4 Fine screening rig 111
4.5.5 Flotability characterised test rig 112
4.5.6 Process flowsheet 112

5 Methodology **115**

5.1 Introduction 115
5.2 Exploratory tests for the industrial scale testwork 115
5.2.1 Pre-test planning 116
5.3 Test procedure for the industrial scale testwork 116

University of Cape Town

5.3.1 Experimental apparatus and cyclone dimensions 116
5.3.2 Experimental work 116
5.3.3 Checking solids concentration 118
5.3.4 On site screening using a single screen 119
5.3.5 Measuring stream flow rates 120
5.3.6 Pressure measurements 120
5.3.7 Sampling 121
5.4 Test procedure for the pilot plant scale testwork 122
5.4.1 Start up and operation of the pilot plant 122
5.4.2 Sampling and Flow rate measurements 123
5.4.2.1 Crushed circuit feed 123
5.4.2.2 Mill product stream 124
5.4.2.3 Vibratory screen oversize stream 124
5.4.2.4 Cyclone feed stream 125
5.4.2.5 Cyclone product streams 125
5.4.2.6 Pansep screen oversize and undersize 126
5.4.2.7 Float feed stream 126
5.5 General sample processing procedure 126
5.5.1 Sample preparation 126
5.5.2 Sieve screening 127

6 Industrial Scale Experimental Results and Process Trends 128

6.1 Introduction 128
6.2 Data collection 128
6.2.1 Arrangement of test results 129
6.2.2 Mass balancing 131
6.3 Discussion of experimental results 132
6.3.1 Effect of the inner vortex finder length 132
6.3.2 Effect of the vortex finder diameters 137

University of Cape Town

6.3.3 The selection area ratio 140
6.3.4 The effect of the SAR on overflow streams mass splits 141
6.3.5 Effect of spigot diameter 143
6.3.6 Pressure drop in the three-product cyclone 145
6.4 Efficiency curves 146
6.4.1 Effect of spigot diameter on the cut size 148
6.4.2 Component efficiency curves 148
6.4.3 Effect of the spigot diameter on the component cut size 151
6.5 Reproducibility of experimental data 153
6.6 Summary 154

7 Contribution from the Computational Fluid Dynamics simulations 157
7.1 General hydrocyclone flow modelling 157
7.2 Cyclone modelling using CFD 158
7.3 Three-product cyclone CFD simulations 159
7.3.1 CFD approach 159
7.4 General flow fields 161
7.5 Velocity vectors and profiles 161
7.5.1 Influence of the inner vortex finder length on the velocity profiles and velocity field vectors 162
7.5.2 Velocity field vectors 167
7.6 Influence of the inner vortex finder length on the air-core 168
7.7 Summary 174

8 Pilot Plant Test Results 176
8.1 Introduction 176
8.2 Effect of conical length 176
8.3 Preparation of flotation feed 178
8.4 Flotation results 185

University of Cape Town

8.4.1 Recovery - grade curves 186
8.4.2 Recovery by size curves 187
8.5 Summary 192

9 Model Development and Validation **194**
9.1 Introduction 194
9.2 Three-product cyclone model development 194
9.3 Model equations 195
9.3.1 Pressure drop 196
9.3.2 Flow split 197
9.3.3 Water split 199
9.3.4 Corrected cut size 203
9.3.5 Corrected component cut size 206
9.4 Validation 212
9.5 Model trends and sensitivity analysis 213
9.6 Summary 216

10 Conclusions and Recommendations **227**
10.1 Summary of findings 227
10.1.1 Experimental apparatus and methodology 227
10.1.2 Effect of the operation and design variables 227
10.1.3 Operating pressure 227
10.1.4 Length of the Inner Vortex Finder (LIVF) 228
10.1.5 The Selection Area Ratio (SAR) 228
10.1.6 Cone angle 229
10.1.7 Separation efficiency 229
10.1.8 Computational Fluid Dynamics (CFD) 229
10.1.9 Pilot plant trials 230
10.1.10 Three-product cyclone model 231
10.2 Conclusions 231

University of Cape Town

10.3 Recommendations 233

References 234

Appendix A: Mathematical Definitions.....247

Appendix B: Industrial Scale Three-Product Cyclone Data.....248

Appendix C: Efficiency Curves For The Three-Product cyclone.....276

Appendix D: Pilot Plant Testwork Results..... .315.

Appendix E: Model Development and Validation Summary Data 321

University of Cape Town

List of Figures

2-1 Corrected particle elimination through the overflow, underflow, and annulus products (Figure by Kelsall D. F., 1953). 17

2-2 Schematic representation of paths of particles with a 50 percent chance of reporting either to the overflow or underflow (Figure by E. O. Lilge, 1962). 33

2-3 Coaxial outlet configuration for the hydrocyclone used in the separation of oil from water (figure by Colman, D. A, and Thew, M. T, 1980). 50

2-4 An air-sparged cyclone used for flotation in a centrifugal field (Figure by Jan Miller and Jan Hupka, 1982). 56

2-5 Modified design of the sparger hydrocyclone for the flotation of oil from water. 56

2-6 Two stage hydrocyclone classification configurations. 59

2-7 Schematic of the twin vortex cyclone. 63

2-8 The design and operation of the three-product cyclone (Bednarski 1992) 66

2-9 Effect of the IVF length on size distribution in overflows (Obeng 2003) 71

2-10 Effect of the cross-over and IVF on the size of minerals in the inner and outer overflow streams (Obeng 2003). 72

2-11 Effect of the spigot diameter on size differential between minerals in the overflow at 45% solids (Obeng 2003). 73

2-12 Effect of the spigot diameter on size differential between minerals in the overflow at 30% solids (Obeng 2003). 73

2-13 Conceptual model 1 of the three-product cyclone. 74

2-14 Conceptual model 2 of the three-product cyclone. 75

University of Cape Town

3-1 A schematic illustrating the main components of the conventional hydrocyclone. 82
3-2 A schematic of the two unidirectional spirals in the coventional hydrocyclone. 85
3-3 A schematic of the flat bottom hydrocyclone. 86
3-4 Comparison of the conventional and flat bottom cyclones. 88
3-5 A schematic illustrating the main components of the three-product cyclone. 89

4-1 The UCT overflow arrangement for the industrial scale three product cyclone testwork. 94
4-2 The pilot plant overflow arrangement with the vortex finder mounted to the system. 96
4-3 Photograph illustrating the machining of the collar and reducer . . . 97
4-4 A photograph showing a range of inner vortex finders 99
4-5 Hoisting up the overflow arrangement to change the vortex finders. . 100
4-6 A schematic of the test rig set-up at Eastern Platinum Concentrator. 101
4-7 Testrig frame with tanks for measuring volumetric flow rates prior to installation on the plant. 102
4-8 Illustration of the overflow arrangement on the three-product cyclone. 103

4-9 A photograph of the cyclone overflow sample cutter. 105
4-10 A photograph showing the layout of the pilot plant at Karee concentrator. 108
4-11 The product sump boxes for the three product cyclone. 109
4-12 The compartmentalised sampling system for the pilot plant scale three product cyclone. 110
4-13 Schematic of the pilot plant sampling system for normal operation position. 111
4-14 Schematic of the pilot plant sampling system during sampling position. 112

University of Cape Town

4-15 A photograph of the pilot plant scale Pansep screen 113
4-16 A schematic of the three-product cyclone pilot plant circuit. 114

6-1 Effect of the LIVF on particles reporting to the OFI and OFO streams for the DIVF of 165mm and DOVF of 210mm. 133
6-2 Effect of the LIVF on particles reporting to the OFI and OFO streams for the DIVF of 192mm and DOVF of 230mm. 133
6-3 Particle size distribution for the normal classification configuration of the three-product cyclone. 135
6-4 Particle size distribution for the three-product cyclone with the inner vortex finder terminating in the cross-over region. 136
6-5 Comparison of particle size distributions for the three-product cyclone operated under the reverse classification configuration and those for the conventional hydrocyclone. 136
6-6 Effect of the outer vortex finder diameter on the particles reporting to the overflow streams for the three-product cyclone operated with an LIVF of 775mm. 137
6-7 Effect of the outer vortex finder on particles reporting to the OFI and OFO streams for the three-product cyclone operated with an LIVF of 1025mm. 138
6-8 Effect of the inner vortex finder diameter on particles reporting to the OFI and OFO streams for the three-product cyclone operated with an LIVF of 775mm. 138
6-9 Effect of the inner vortex finder diameter on particles reporting to the OFI and OFO streams for the three-product cyclone operated with an LIVF of 1025mm. 139
6-10 The effect of the selection area ratio on the mass split to the product streams for the three-product cyclone, LIVF = 775 - normal classification configurattion. 142

University of Cape Town

6-11 The effect of the selection area ratio on the mass split to the product streams for the three-product cyclone, LIVF =1025 - reverse classification configurattion. 143

6-12 The Effect of the spigot diameter on particles reporting to the OFI and OFO stream for the three-product cyclone operated with an LIVF of 775mm. 144

6-13 The Effect of the spigot diameter on particles reporting to the OFI and OFO stream for the three-product cyclone operated with an LIVF of 1025mm. 144

6-14 Variation of Pressure with feed volumetric flow rate for short and long vortex finder configurations of the three-product cyclone. 145

6-15 Efficiency curves for the three-product cyclone - run 67. 147

6-16 Effect of the spigot diameter on the d50c for the three-product cyclone operated with an inner vortex finder length of 775mm. 149

6-17 Effect of the spigot diameter on the d50c for the three-product cyclone operated with an inner vortex finder length of 1025mm. 149

6-18 Components efficiency curves for the three-product cyclone. 150

6-19 Components efficiency curves for the three-product cyclone from smoothed assay data. 151

6-20 Effect of the spigot diameter on the component d50c for the three-product cyclone operated with an inner vortex finder length of 775mm. 152

6-21 Effect of the spigot diameter on the component d50c for the three-product cyclone operated with an inner vortex finder length of 1025mm. 152

6-22 Replicate tests for the three-product cyclone with Dovf of 220mm, Divf of 177 mm, LIVF of 775 mm, and Dspig of 95mm. 156

6-23 Replicate tests for the three-product cyclone with Dovf of 220mm, Divf of 198 mm, LIVF of 875 mm, and Dspig of 95mm. 156

University of Cape Town

7-1 Illustration of the computational mesh of the 600mm diameter three-product cyclone 160

7-2 Typical flow fields in the planes (xy) at different Z positions of the interior portion of the conventional and three-product cyclones 162

7-3 Tangential velocity distributions. 165

7-4 Axial velocity distributions. 166

7-5 Velocity field vectors for the conventional hydrocyclone. 168

7-6 Velocity field vectors for the three-product cyclone - inner vortex finder length = 775mm. 169

7-7 Velocity field vectors for the three-product cyclone - inner vortex finder length = 1025mm. 169

7-8 Cross sections of the conventional and three-product cyclones showing the shape of the aircore along the xz – plane. 170

7-9 Comparison of the air-core dimensions in the conventional and three-product cyclone. 172

7-10 Magnified air-core profiles. 173

8-1 The effect of increasing the conical section length of the three-product cyclone on the P80 values. 178

8-2 A schematic of the pilot plant cyclone showing the positions of the vortex finder in relation to the spigot for different conical section lengths. 179

8-3 Comparison of the float feed size fractions from the classification systems ustilising the three-product cyclone with long conical sections and Pansep screens and the conventional hydrocyclone only. 182

8-4 Comparison of the float feed size fractions from the classification systems ustilising the three-product cyclone with a short conical section and Pansep screens and the conventional hydrocyclone only. 183

University of Cape Town

8-5 Distribution of particles in the recycle stream for cyclone configurations with longer conical sections - normal classification configuration. 184
8-6 Distribution of particles in the recycle stream for cyclone configurations with shorter conical sections - reverse classification configuration. 184
8-7 Silica grade - recovery curves for the three-product cyclone circuits and conventional hydrocyclone circuit. 188
8-8 Chromite grade - recovery curves for the three-product cyclone circuits and conventional hydrocyclone circuit. 189
8-9 Valuable sulphide component grade - recovery curves for the three-product cyclone circuits and conventional hydrocyclone circuit. 190
8-10 Recovery - size curves and mass flow rate in the concentrate for the three-product and conventional cyclone circuits. 191

9-1 Correlation observed and predicted pressure drop for the three-product cyclone 197
9-2 Residual plots for the operating pressure. 198
9-3 Comparison between observed and predicted fraction flow split to the OFI of the three-product cyclone 200
9-4 Residual plots for the flow fraction split to the OFI. 200
9-5 Comparison between observed and predicted fraction flow split to the U/F of the three-product cyclone 201
9-6 Residual plots for the flow fraction split to the U/F. 201
9-7 Comparison of observed and predicted fraction of water split to OFI . 203
9-8 Residual plots for the water fraction split to the OFI. 204
9-9 Comparison of observed and predicted fraction of water split to U/F . 205
9-10 Residual plots for the water fraction split to the U/F. 206
9-11 Comparison of the observed and predicted d_{50_cOFI} for the OFI of the three-product cyclone 207
9-12 Residual plots for the d50$_c$$OFI$. 208

University of Cape Town

9-13 Comaparison of the observed and predicted $d_{50_cU/F}$ for the three-product cyclone 209
9-14 Residual plots for the d50$_c U/F$. 209
9-15 Comparison of the observed and predicted $d_{50_cOFI(si)}$ for the three-product cyclone 210
9-16 Residual plots for the d50$_c OFI(si)$. 211
9-17 Comparison of the observed and predicted $d_{50_cOFI(cr)}$ for the three-product cyclone 212
9-18 Residual plots for the d50$_c OFI(cr)$. 213
9-19 Comparison of the predicted and observed $d_{50_cU/F(si)}$ for the three-product cyclone 215
9-20 Residual plots for the d50$_c U/F(si)$. 216
9-21 Comparison of the predicted and observed $d_{50_cU/F(cr)}$ for the three-product cyclone 217
9-22 Residual plots for the d50$_c U/F(cr)$. 218
9-23 Comparison of the observed against predicted operating pressure. . . 218
9-24 Comparison of the observed against predicted fraction flow split to the OFI stream. 219
9-25 Comparison of the observed against predicted fraction flow split to the U/F 220
9-26 Comparison of the observed against predicted fraction water split to the OFI stream. 221
9-27 Comparison of the observed against predicted fraction water split to the U/F stream. 222
9-28 Comparison of the observed against predicted d_{50c} OFI. 222
9-29 Comparison of the observed against predicted d_{50c} U/F. 223
9-30 Comparison of the observed against predicted d_{50c} OFI (cr). 223
9-31 Comparison of the observed against predicted d_{50c} OFI (si). 224
9-32 Comparison of the observed against predicted d_{50c} U/F (cr). 224

University of Cape Town

9-33 Model response to step changes in volumetric feed flow rate. 225
9-34 Model prediction of water fraction to the overflow products. 225
9-35 Model prediction of water fraction to the overflow products. 226
9-36 Model predictions for the variation of the overall and component cut sizes with step changes in LIVF. 226

University of Cape Town

List of Tables

6.1 A summary of the cyclone design variables for the industrial testwork. 129

6.2 Arrangement of experimental results for the three product cyclone test. 130

6.3 Arrangement of results for the conventional and flat bottom cyclones comparative tests. 130

6.4 A summary of the the standard deviation weightings used for mass balancing 132

6.5 Replicate tests for the three-product cyclone with Dovf of 220mm, Divf of 177 mm, LIVF of 775 mm, and Dspig of 95mm 153

6.6 Replicate tests for the three-product cyclone with Dovf of 220mm, Divf of 177 mm, LIVF of 775 mm, and Dspig of 95mm 154

7.1 A summary of the cyclone design variables used in the CFD simulations. 159

8.1 A summary of the cyclone design variables for the cyclone used for the pilot plant trials. 177

8.2 A summary of stream data for the pilot trials tests which included the flotation section. 180

8.3 A summary of stream data for the tests conducted around the comminution and classification sections. 181

8.4 A summary of the flotation test conditions. 186

9.1 A summary of the subsection of data used for model validation. . . . 214

9.2 Details of the data set used as a base case for sensitivity analysis of model trends. 214

University of Cape Town

Dedication

Although the dead can not see their influence and can not hear when spoken to by words of thanks, however, they can be remembered in many ways. To my loving parents Dick and Nsowa Mainza. You will always be in my memory and have a permanent place in my heart.

University of Cape Town

Acknowledgements

Many people have contributed to this work and I say thank you to all. I would like to thank my dear wife Kena for her support during the compilation of this thesis. Special thanks to my supervisor Dr. Malcolm Powell for his patience, encouragement, guidance & support throughout this work; Chisenga Kulya, Andrew McBride, Sonny Mwansa, Jason Waters, and Micheal Bekapi and all the members of the comminution group & MPRU for their assistance with various aspects of this work.

I would like to thank *Dr. Steve Morrell for inventing the three-product cyclone and encouraging the work reported in this thesis to be carried out on this device and for his guidance in setting up the experimental procedure. I would like to thank Dr. Rob Morrison, Prof. Bill Whiten, and Prof. Simukanga for their guidance in the experimental and modelling work; Narasimha for performing the CFD simulations for me; Lonmin for making their industrial & pilot plants available & for assaying the samples generated from this work. Dr. Craig Goodall; Mr. Johan Styen; Mr. Emidio Simbine; & Mr. Aaron Pweto are thanked for the assistance rendered.*

I would like to thank Mr. and Mrs. Knopjes for their parental support, Bertie, Naomi, & Beatrix for lifting my spirits and providing a home that made a big difference in this work; Mr. Mutema Chella, Stella, Precious, and Chalyen Mainza & all my brothers for giving me a reason to smile & carry on after the death of both parents during the period of the thesis; Mrs Frances Powell, Murray and Angus Powell, Mr. Andrew Zulu, Mr. and Mrs. Matambo for their encouragement.

Contributions of my close friend Nelly Moyo, sister Lucy Chella, uncle Stephen Ntswana - who were my pillars of support till their death - are acknowledged.

Lastly but by no means the least, I would like to thank God Almighty Jehovah for giving me life and allowing me to walk this path.

University of Cape Town

University of Cape Town

University of Cape Town

University of Cape Town

Nomenclature and Abbreviations

3-PC	- Three-product cyclone
Conv. cyc.	- Conventional hydrocyclone
Cross-over region	- LIVF where OFI and OFO are identical
Dinlet	- equivalent inlet diameter
$d50_c(cr)$	- chromite cut size
$d50_c(si)$	- silica cut size
d_{50_cOFI}	- cut size to the inner overflow of the three-product cyclone
$d_{50_cU/F}$	- cut size to the underflow of the three-product cyclone
cr, crmt, chrome	- chromite
DIVF	- diameter of the inner vortex finder
DOVF	- diameter of the outer vortex finder
Dspig	- diameter of the spigot
FB cyc.	- Flat Bottom hydrocyclone
IVF	- inner vortex finder
LIVF	- length of the inner vortex finder
LOVF	- length of the outer vortex finder
O/F	- cyclone overflow
Normal classification	Finer overflow from OFI and Intermediate overflow from OFO
OFI	- three-product cyclone inner overflow
OFO	- three-product cyclone outer overflow
OVF	- outer vortex finder
PGEs	- Platinum Group Elements
rem	- remainder
Press	Pressure
Reverse classification	Finer overflow from OFO and intermediate overflow from OFI

University of Cape Town

RoM - Run-of-Mine

SG - Specific Gravity

si, silc - silica

U/F - cyclone underflow

UG2 - Second Upper Ground

University of Cape Town

1

Introduction

1.1 Background

The intention of this thesis is to test a type of hydrocyclone that produces three products instead of the usual two. This required performing modifications to the conventional hydrocyclone to convert it into a hydrocyclone that produces an underflow and two overflow streams, and apply it in the classification of ore that contains mineral components of two different densities.

Comminution is one of the most expensive operations in the mining concentrator departments, and efficient classification is therefore essential to reducing concentrating costs and achieving the correct product size distribution for down stream processes such as flotation. The hydrocyclone is one of the most important classification units in mineral processing and is used in a wide range of circuits for different purposes. A hydrocyclone utilises centrifugal force to classify particles from the feed according to their hydrodynamic properties, namely, density, particle shape, and particle size (Moder and Dahlstrom [1]).

In the mining industry ore is mined from underground or open pit mines and sent to the surface for extraction of valuable minerals which are closely interlocked with non-valuable material, called gangue. In order to extract the metal contained in the run of mine (RoM) ore, heat is used to break down ore minerals in pyrometallurgical processes, while solvents and electricity are used in hydrometallurgical and electrometallurgical processes, respectively. Either one or a combination of the aforementioned recovery processes can be used to extract the valuable material. Smelting, a pyrometallurgical process, is the most commonly used. Vast quantities of energy are consumed in the smelting process and the cost of treating the mined ore directly

University of Cape Town

using this method or indeed any of the other methods mentioned, is much higher than the value of the metal to be recovered. In order to recover the metal profitably, the mined ore is concentrated to produce a small quantity of concentrate rich in the mineral of interest prior to extracting it using any of these recovery techniques. The production of a small quantity of concentrate, rich in the mineral of interest, is achieved through mineral processing (Pyror [2]).

The purpose of mineral processing is to selectively separate a mineral rich concentrate from the barren gangue contained in the bulk RoM ore by using relatively low energy physical methods prior to using the high energy extraction methods such as smelting. Mineral processing starts by freeing the valuable minerals from their associated gangue through a process called comminution. The primary purpose of comminution in mineral processing is to unlock (liberate) the valuables in the ore and reduce the size of the mined ore to meet the particle size requirements for subsequent separation processes.

Comminution involves primarily crushing and grinding operations. Grinding is an energy intensive operation and consumes about 50% of the total concentrator energy. For the concentrator operations to be profitable, grinding must be controlled and optimised so that energy is not wasted in grinding down material to much finer limits which may not bring any further benefits (Wills [3]). The ground pulp is then sent to a classifier device. In these devices the ore particles are separated into coarse and fine fractions, or dense and light fractions relative to the rate of fall through water, or both types of separation depending on the type of classifier used. One such device is a hydrocyclone. The dense, coarse fraction is usually re-circulated to the mill for further grinding and the light, fine fraction from the classifier is sent to the next stage of concentration - usually the flotation process.

The final step in mineral processing involves separating the valuable minerals from the gangue to produce a concentrate. This is usually done by froth flotation which utilises differences in physical-chemical surface properties of particles to effect

University of Cape Town

separation. The process of flotation can only be applied to relatively fine particles. The regulation of the size of particles sent for flotation depends on the type of classifier used and the efficiency at which classification is conducted (Mills [4]).

Classification is one of the most important stages in mineral processing and has been shown to affect both froth flotation and the grinding processes (Colman [5]). If the classification stage is not running effectively numerous problems are encountered in both the flotation and the grinding circuits. Hydrocyclones are among the most common classifiers in the minerals industry today, but are by their nature, imperfect separators. The literature cited in the following chapter shows a number of weaknesses in these classifiers and the amount of research that has been conducted to try and improve them. This thesis gives a description of the work which was conducted using a modified type of hydrocyclone called the three-product cyclone. The motivation for conducting the testwork using this type of cyclone is given in the next section.

University of Cape Town

1.2 Motivation

Conventional hydrocyclones utilise water to classify feed materials into two products termed the cyclone overflow, which comprises the fine, light fraction and the cyclone underflow, which comprises coarse, dense materials. Details of the features and separation principles are discussed in chapters 2 and 3. The major drawback in the classification of the Second Upper Ground (UG2) platinum ore is that it contains a chromite component, whose average density ranges between 4.5 and 4.8, as compared to 2.7 of the bulk silicates (collectively referred to as silica). Silica is the platinum group elements (PGEs) carrying component in the UG2 platinum ore. Chromite grinds down easily to sub 63μm particle size, after which it becomes extremely competent and is problematic to efficiently reduce in size further.

If the conventional hydrocyclone is used as a classification device for the UG2

platinum ore, then due to its high density, the chromite preferentially reports to the cyclone underflow and re-circulates back to the mill even if it is fine enough to escape from the milling circuit. The chromite particles then build up a high circulating load around the mill, only leaving when they are fine enough to be forced out through the cyclone overflow stream. Unlike the high density chromite, the silica component which has a low density reports to the cyclone overflow stream even if it is not fine enough for the contained PGEs to be recovered during the flotation process. This has a number of detrimental effects:

1. The mill loses capacity due to the build up of fine chromite and energy is wasted in grinding down the chromite which is already fine enough.
2. The high proportion of high density, fine chromite particles in the slurry reduces the classification efficiency of the cyclone due to the dense media effect. As a result, the plus 100μm low density silica material reports to the overflow when it is not fine enough for the contained valuable minerals to be recovered during the flotation process.
3. The high proportion of fine chromite particles produced results in high consumption of reagents as well as abstraction of reagent adsorption in the flotation process.
4. The fine chromite particles are entrained in the flotation process and end up reporting to the PGE concentrate due to reduced collector selectivity at such fine sizes.
5. The chromite particles eventually report to the smelter where they have a detrimental effect on the extraction of PGEs as they combine with the magnetite to form a compound that creates a false bottom in the furnace. This results in increased energy requirements at the smelter and a reduction in the furnace capacity as well as considerable losses of the valuable minerals through entrapment.

In order to overcome the classification problems resulting from the presence of chromite in the UG2 platinum ore a new design of the hydrocyclone, namely the

University of Cape Town

three-product cyclone, has been investigated. Although the concept of the three-product cyclone was used in the paper and pulp industry (Bednarski [6]), there is no information outside the AMIRA P9 project on what design is suitable for mineral processing applications. Furthermore, there is no information outside the AMIRA P9 project available in the literature to indicate whether the application of this device could be used to prevent particles from the light silica component from reporting to the overflow when they are not fine enough to be floated and to prevent the over-grinding of the denser chromite component. The three-product cyclone, as it will be shown, has the advantage of producing a middlings product that can be processed separately to maximise the recovery of the PGEs during flotation. Therefore, the purpose of this study is to investigate the performance of the three-product cyclone device at both industrial and pilot plant scale.

In 1963 AMIRA commenced a collaborative research project with the principle aim of optimising mineral processing operations. This applied research project is commonly referred to as "The Mineral Processing Project" or "P9 Project". Over the past 42 years the project has consistently delivered a range of benefits to the sponsors resulting in significant improvements in efficiency at sponsors' operations, including new equipment and new tools to monitor, analyse and model circuits. The project runs in cycles of 3 to 4 years. The research providers for the current extension (fourteenth extension) are the Julius Kruttschnitt Mineral Centre (JKMRC) based at the University of Queensland, the Mineral Processing Research Unit (MPRU) of the University of Cape Town, and McGill University.

University of Cape Town

1.3 Hypotheses

The following are the hypotheses that will be tested in this thesis:

1. Low-density mid-sized particles and high-density fine particles will tend to concentrate into the same region in a hydrocyclone, because of the balance of the different forces acting on the particles to effect separation by size and density.

2. Carefully inserting dual vortex finders in the region where low-density mid-sized and high-density fine particles concentrate can be used to preferentially select a blend of fine high density particles and mid-sized low density particles which can be captured in an extra intermediate stream which is separate from the overflow and underflows streams of the hydrocyclone.

3. Formulating a conceptual model that describes separation within the hydrocyclone will provide a way of assessing hydrocyclones with more than two products because classification is governed by the interaction of forces on the particle and machine design variables and not the discharge orifices.

University of Cape Town

1.4 Objectives

The main goals of this thesis are to establish the critical design and operation parameters of the three-product cyclone and to test the concept of the cyclone that produces a middlings stream in addition to the overflow and underflow in the classification of the dual density UG2 platinum ore. The main aims, which form the work-plan in achieving the goals of this thesis are as follows: -

1. Test the principle of the three-product cyclone using an industrial scale unit for the application of classifying a dual density UG2 platinum ore.

2. Ascertain if the three-product cyclone can produce a middlings product that is useful for overcoming the problem caused by the density differential of the two major components comprising the UG2 platinum ore.

3. Design a method of attaching a range of different diameter inner vortex finders to the same overflow arrangement.

4. Establish critical design parameters for the operation of the three-product cyclone.

5. Evaluate the separation by density in the product streams of the cyclone using silica and chromite assays.

6. Assess the operability, and flotation response of the circuit configuration

involving the three-product cyclone at pilot plant scale.

7. Develop a model describing the effect of the important design and operational parameters on the classification performance of the three-product cyclone.

8. Incorporate mineral components in the three-product cyclone model.

1.5 Layout of the thesis

The above-mentioned objectives and hypotheses are addressed in this thesis which consists of 10 chapters.

Chapter 1 has provided an introduction, motivation, hypotheses, and objectives for this thesis. Chapter 2 provides a literature review that acted as a guide to the design of the cyclone and experimental apparatus, methodology, data analysis and modelling. The relevant literature dealing with design, operation, and modelling studies concerned with the development of hydrocyclones are discussed.

Chapter 3 consists of a discussion of the basic separation principles of the hydrocyclone and detailed descriptions of the types of hydrocyclones used in the classification of the UG2 platinum ore. Chapter 4 discusses the modifications performed to convert the conventional hydrocyclone into the three-product cyclone, design of the 100mm pilot size cyclone, and the design of the experimental apparatus giving descriptions of the critical features of both the industrial and pilot plant test rigs which were specially designed and constructed for this work.

The methodology employed in achieving the objectives of this thesis is given in chapter 5. Included in the methodology are the sampling techniques applied for individual streams, parameters that were varied to achieve the goals of the thesis, and the sample processing techniques employed to obtain stream particle size data.

Experimental results from the industrial scale cyclone and parameters that were found critical in the operation performance of the three-product cyclone are discussed in chapter 6. The results from a computational fluid dynamics study is given

University of Cape Town

in chapter 7, and results from the pilot plant scale experiments are discussed in chapter 8.

Chapter 9 discusses the development and validation of the three-product cyclone model.

The conclusions are presented in Chapter 10 in which significant findings are emphasised. Recommendations for further work that is needed in the classification of particles in the circuit are also presented.

University of Cape Town

2

Literature Review

2.1 Introduction

The objective of this chapter is to provide a literature review related to the development of hydrocyclones in terms of separation mechanisms, design, operation and modelling. Papers dealing with separation principles, effects of various operating and design parameters on cyclone performance, and modelling of hydrocyclones were considered. Papers concerned with the design and development of novel cyclone concepts were reviewed.

A historical review of papers was done in order to highlight the developments in classification using hydrocyclones over the years. In the review, a summary of the important and relevant aspect of each paper is given, then a critical analysis of its usefulness to this work is made. Other aspects of the papers irrelevant to this work may be omitted from the review. The views expressed in the discussion of each paper are those of this author, unless otherwise specified.

The review of the literature acted as a guide in identifying suitable design and operation parameters in hydrocyclones, and in developing the experimental technique for the testwork that was conducted in this study. Papers highlighting relevant experimental techniques and results related to this work were included in the review. Due to the numerous papers dealing with performance, design, and modeling of hydrocyclones only a few which are of particular relevance to this work have been reviewed and many have been omitted. However, the few papers that have been reviewed provide the background of the status of the work in classification using hydrocyclones. The major areas of concern in this study are design, operation, and performance modelling of hydrocyclone units. The review of the papers is arranged

University of Cape Town

in chronological order.

The symbols for various parameters in the papers reviewed have been changed to conform to the standard nomenclature adopted for this thesis.

2.2 Reviewed Papers

2.2.1 A study of the motion of solid particles in a hydraulic cyclone

D. F Kelsall, 1952 [7]

As far back as 1952, Kelsall proposed that to predict the optimum cyclone for any application, the effect of design variables, throughput, feed solids concentration and the type of underflow discharge must be determined. Kelsall's experiments were the first formulated to investigate the motion of particles to determine the mechanism of separation occurring in the hydrocyclone. The aim of his work was to define the practical limits of efficiency and to determine the sources of inefficiencies in the hydrocyclone.

A 75 mm hydrocyclone machined out from perspex was used in the experimental work. The cyclone was constructed in such a way that all the important design parameters could be changed easily.

Kelsall used optical methods to track the trajectories of aluminium particles suspended in water to determine flow patterns in the hydrocyclones. Under suitable ultramicroscope illumination, aluminium particles at selected positions in the cyclone were observed through a microscope with objectives mounted on the disc driven by a small electric motor. The method was based on the principle that any three-dimensional velocity in the cyclone could be resolved into a tangential component (V) in a horizontal plane and at right angles to the radius from the axis of the cyclone, radial component (U) in a horizontal plane along the radius, and a vertical component (W) at right angles to the other two components, that is parallel

University of Cape Town

to the axis of the cyclone. The tangential velocity components were obtained from experimental data while the vertical and radial velocity components for the particle were calculated using equations 2.1 and 2.2, respectively.

$$W = V \tan\theta \tag{2.1}$$

$$U = \frac{V^2}{r} \cdot d_p^2 \frac{(\rho_s - \rho)}{18\mu} \tag{2.2}$$

where: V - measured tangential velocity,

θ - corrected track angle at the same point,

U - radial velocity component,

$\frac{V^2}{r}$ - radial acceleration of the particle at the radius r

d_p - particle diameter in microns,

ρ_s - density of the particle,

ρ - density of water, and

μ - viscosity of the liquid.

Particle tangential velocity components and track angles were measured at selected positions in the hydrocyclone at feed pressures ranging from 70 to 275 kPa. The volumetric flow rates for the underflow and overflow streams were measured for each condition. A series of tests were performed with the products discharging from:

(1) overflow only

(2) underflow only

(3) both the overflow and underflow.

In each series, the diameter of the feed inlet and vortex finder length were kept constant. Although all velocity measurements were carried out with very dilute suspensions of fine aluminium particles there were sufficient particles at all positions within the cyclone for observation. Kelsall related his velocity measurements to cyclone capacity in terms of throughput and a relationship between throughput and

University of Cape Town

the separation efficiency was derived (equation 2.3).

$$d_{50} = \frac{1}{Q_f^{0.56}} \tag{2.3}$$

where: d_{50} - diameter in microns of particle that has a 50% chance of reporting to either the overflow or underflow, and

Q_f - cyclone volumetric throughput.

It was suggested that provided the feed inlet and overflow diameters remained unchanged, an increase in the spigot diameter merely results in an underflow of lower pulp density. This implies that adjusting the spigot alone might not bring about the desired split if other design variables are not manipulated accordingly.

Photographs from his experiments showed a band of particles moving down the outside wall of the vortex finder and turning sharply at the bottom edge of the vortex finder to join the overflow. Other authors referred to the turning band observed by Kelsall as reverse flows (Bradley and Pulling [8], and Hsieh, [9]). Both visual inspection and samples of the band showed more coarser particles than those existing at similar radii at lower levels in the cyclone. Kelsall attributed the short circuit flow to the wall effects at the top of the cyclone and to the existence of the air/water interface and the envelope of zero vertical velocity, which limits the area available for upward flows to the annular area between the air/water interface and the inside wall of the vortex finder. Kelsall concluded that short circuit flow was the major source of inefficiencies in the hydrocylone though no quantitative investigations were conducted. This motivated him to conduct further studies which were reported in the paper entitled "A further study of the hydraulic cyclone."

Discussion

It is generally agreed that Kelsall's study of flow patterns in the hydrocyclone has made a significant contribution in the understanding of the hydrocyclone. However,

University of Cape Town

the relevance of the experiments conducted with either only the overflow or underflow product streams is doubted in the applications of particle classification commonly used in mineral processing and other industries. With regard to the experiments conducted with the material discharging through the cyclone overflow only, it is not clear how that was achieved since there is no mention of any back pressure mechanism on the underflow in the description of the experimental apparatus and methodology.

Exploratory tests where conducted to provide experience with the methodology and these were used to refine the experimental techniques. This is a critical step in setting up a credible experimental methodology for collecting reliable data. The technique was adopted in this work as this is important for tests conducted on industrial plants were measurements of high flow rates are required and representative samples have to be cut from large streams. Exploratory tests are useful in providing information on the design of flow rate measuring vessels and sample cutting equipment. In cases were material from the production plant has to be diverted to the test rig and recirculated back, exploratory tests provide information on a control strategy that enables experiments to be conducted with minimal disruptions to the operation of the production plant.

University of Cape Town

Using the optical method to measure flow patterns in hydrocyclones has an advantage of not disturbing the flow, compared with the Pitot tube methods used by Lilge, [10]. Other workers have conducted flow measurements in hydrocyclones using other techniques such as visual and photographic observation of an injected dye (Bradley and Pulling [8]) and laser doppler anemometry (Dabir and Petty [11], and Hsieh, [9]).

The discussion on the envelope of zero vertical velocity was useful in choosing the positions for the placement of the inner vortex finder in terms of the depth and diameter into the cyclone body. The major setback is that the influence of having dual vortex finders on the velocity profile has not been studied. Due to the absence of

flow information for this system, it can be assumed that the flow patterns are similar to those obtained from conventional hydrocyclones, for the purpose of establishing useful tests on the three product cyclone.

2.2.2 A further study of the hydraulic cyclone

D. F Kelsall, 1953 [12].

Kelsall endeavoured to assess the relative merits of using single point comparison methods (Dahlstrom [13], and Fitch and Johnson [14]) to summarise cyclone efficiencies and to examine the importance of short-circuiting of particles to the overflow.

Kelsall used equation 2.4 to determine the corrected fraction of particles of a given size eliminated through the underflow as a result of cyclone action. It is useful for quantifying the performance of hydrocyclone as it takes into account only the particles that report to the underflow through the action of the centrifugal forces referred to as true classification.

$$\left(\frac{y-x}{100-x}\right) \times 100 \tag{2.4}$$

where: x - percentage of water eliminated through the underflow,

y - experimentally determine fraction eliminated through the underflow.

Tests conducted at different pressures seemed to indicate that the sharpness of separation of the 75 *mm* cyclone improved with increased pressure. A consistent trend was observed for 6 different series of experiments conducted to study the effect of pressure on cyclone performance. A relation between d_{50} and pressure drop suggested that the cut size decreases with increase in pressure drop across the cyclone.

Kelsall's observations appear to imply that for any selected pressure and combination of cyclone dimensions, there was a feed inlet diameter, which resulted in an

University of Cape Town

optimum rate of injection of momentum, and that it bears a simple relationship to the diameter of the overflow orifice. The feed inlet which allow the conditions of maximum rate of momentum injection to prevail resulted in maximum elimination of inefficiencies in the cyclone exits. For the 75 *mm* cyclone the optimum feed inlet diameter was approximated to be between 6.4 and 8 *mm*. The rectangular feed inlet shape appeared to give slightly better efficiencies than the round inlet for all particle sizes and the greatest improvement was obtained with the largest feed openings for the same pressure. However, volume flows were slightly decreased by changing to rectangular feed inlets.

Kelsall's results revealed that decreasing the vortex finder diameter increased the elimination efficiency of the finer sizes, but the coarser sizes increased to a maximum and then decreased with further decrease in the vortex finder diameter. The fall off in the elimination of coarser particles efficiency was attributed to the short circuit flow down the outside walls of the vortex finder.

A decrease in the vortex finder length resulted in an increase in efficiency for finer sizes while a decrease of up to 10% by weight was noted in the coarsest fraction. For short vortex finders the time available for finer particles to leave vertical flows, which eventually reach the vortex finder, is much greater than when a long vortex finder is used. Thus short vortex finders give higher efficiencies for finer fractions and promote short circuit flow for coarse particles. If it is assumed that all coarse particles report to the overflow through short-circuiting, then longer vortex finders would permit such particles a longer time interval to be eliminated from short-circuit flow and eventually discharge in the underflow. This implies that longer vortex finders give increased separation efficiencies for coarser fraction and a decrease in efficiencies for finer particles. A decrease in the elimination efficiency of all sizes was observed with a decrease in the spigot diameter.

The discussion on the effect of both design and operating variables has shown

University of Cape Town

that it is difficult to design and optimise a cyclone to give high separation efficiency. Kelsall [7], in his earlier work identified short circuit flows as the major source of inefficiencies in the performance of the hydrocyclone. To eliminate short circuiting of particles, the conventional cyclone was modified by incorporating an annular take off at the root of the vortex finder in the flat top plate. The annulus provided a way of removing an extra stream through a separate pipe. The pipe was fitted with a valve and a suitable fraction of the total flow was taken off through the annulus by adjusting the valve and the annular discharge flow was limited to 15% by weight.

The actual weight percentages of the three products after incorporating an annular discharge to the cyclone were calculated using equations 2.5 and 2.6, respectively. The overflow was calculated by the difference.

$$\frac{(y-x)}{(100-x-15)} \times 100 \tag{2.5}$$

$$\frac{(z-15)}{(100-x-15)} \times 100 \tag{2.6}$$

where: z - actual percentage by weight of solids discharged through through the annulus.

In the cyclone with the annular discharge, it was shown (figure 2-1) that finer particles have a high probability of discharging through the overflow while coarse particles have a high probability of reporting to the underflow. The intermediate size were shown to have high probability of discharging through the annulus.

Discussion

The unique aspect of his work is that a large number of experiments is required to draw meaningful conclusions from experiments that involve several factors. This appears to be the reason that many workers use his work as a basis for designing cyclones, and for formulating fundamental theories on the operation of the hydro-

University of Cape Town

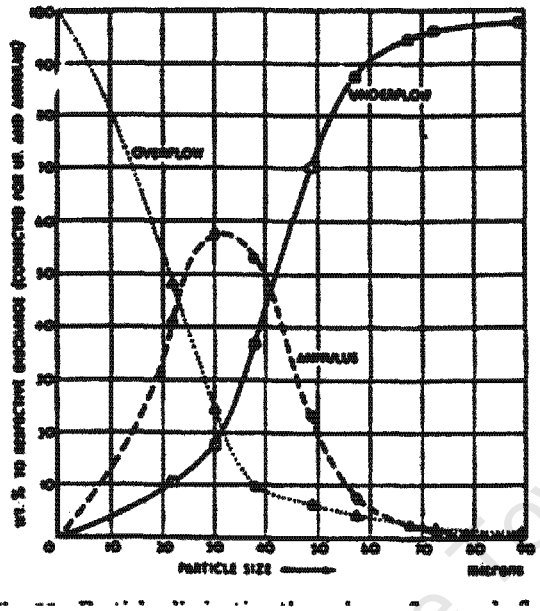


FIGURE 2-1. Corrected particle elimination through the overflow, underflow, and annulus products (Figure by Kelsall D. F., 1953).

cyclone.

The methods of expressing cyclone performance using the cut size (d_{50}) or any other single point methods are insufficient in describing the overall efficiency for the complete size range. These may be useful in situations were a large data base on the ore or type of cyclone is available to provide the missing information. It has been shown by other workers that efficiency curves with different slopes can pass through the same cut size (d_{50}) point (JK monograph, [15]). Kelsall used the percentage of particles eliminated to the underflow due to the cyclone action as an effective way of quantifying the performance of the conventional hydrocyclone. In classification systems involving more than two products using the percentage of particles reporting to one stream as a way of quantifying the performance is inadequate as the presence of two other distinct products makes it impossible to quantify their differences. The method used in quantifying the performance of the cyclone when the annulus was incorporated provided an alternative method for cyclones with three products.

University of Cape Town

Kelsall's work shows that as far back as 1953, the concept of using a cyclone which could provide three products of some sort was viewed as a better way of eliminating inefficiencies which are inherent in conventional cyclones. This provided motivation for refining the design of the cyclone that produces three products in applications treating problematic ores such as the UG2 platinum ore.

The concern that the flow patterns within the cyclone were affected by the portion of the flow that was withdrawn through the annulus are justified considering that the annulus had no protrusion of any form to prevent short circuiting. The situation is assumed to have changed dramatically in the three product cyclone where the annulus is embedded between two vortex finders protruding into the cyclone body. The outer vortex finder in this arrangement is positioned in the same way as that of the conventional cyclone.

The modification of the conventional hydrocyclone to incorporate an annulus has shown that there are a number of modifications that can be done to the cyclone to improve its efficiency. Apart from Kelsall's work, no reference has been found showing a conventional hydrocylone with an annulus modification as a method of improving classification efficiency. The reason for this could be that the annulus modification did not provide any benefits to the industry.

University of Cape Town

2.2.3 Fundamentals and applications of the liquid cyclone

Dahlstrom, D. A. 1954 [16].

Dahlstrom acknowledged that several investigations have been conducted on hydrocyclones which lead to a partial development of the basic fluid dynamics within the hydrocyclone. It was observed that a better knowledge of flow patterns within the hydrocyclone was required to fully understand the operation of the hydrocyclone. A lot of effort has been devoted to examining the flow patterns in the hydrocyclone and a detailed knowledge of flow patterns of spherical or granular particle action is

available in the literature (Kelsall [7], Bradley and Pulling [8], Dabir and Petty [11], and Hsieh [9]).

It was proposed that two spiral flow patterns constitute the major flow patterns within the conventional hydrocyclone. The outer spiral in the hydrocyclone travels towards the spigot of the hydrocyclone while the inner spiral rotates towards the vortex finder. It was suggested that the secondary recirculation pattern is caused by the outer wall of the vortex finder and its accompanying zero velocity, which was in line with Kelsall [7] who concluded that this was the source of inefficiency through the resultant short-circuiting flows. Dahlstrom seemed to agree with the annulus discharge experiments performed by Kelsall as a way of reducing inefficiencies caused by these short circuiting flows in the hydrocyclone.

It was established that the tangential velocity component supplies the centrifugal force factor $V_r^2 r$ for classification and the vertical velocity component influences the magnitude of the flow spirals which determines the volume split. The radial velocity appeared to be the current against which the particles must settle due to the action of the centrifugal force in order to be removed at the underflow.

It was reported that for an increase in the sharpness of classification to be achieved particles must travel through a zone of maximum centrifugal force before reporting to the overflow. It was suggested that 'a plane of no return' exists within the hydrocyclone where a particle can not turn back to be discharged into the overflow stream and that this plane can be calculated from a consideration of pressure distributions within the hydrocyclone. Assuming that there is equal pressure at both discharge points, using the principle of continuity, the plane of no return was found to be a function of the percentage of feed volume reporting to the underflow shown in equation 2.7.

$$x = (L)(V \cdot S) \tag{2.7}$$

University of Cape Town

where: x - vertical distance from the spigot to the plane of no return

L - distance between the vortex finder and the spigot

V·S - feed volume fraction reporting to the underflow

An examination of design and operating conditions was done and empirical relationships were developed. The established energy requirements were given by equation 2.8.

$$\frac{Q_o}{\sqrt{\Delta P}} = K_1(D_o \cdot D_i)^{0.9} \tag{2.8}$$

where: Q_o - overflow volume, gal./min

ΔP - cyclone pressure drop, $ft.$ of fluid

Do - vortex finder diameter, $inch.$

D_i - feed inlet diameter, $inch.$

K_1 - constant

Dahlstrom was the first to suggest a correlation (equation 2.9) for predicting the actual cut size (Dahlstrom [13]). A value of 81 seemed to fit the constant K_2 well for conventional cyclones with a 20° included cone angle.

$$d_{50} = \frac{K_2(D_o \cdot D_i)^{0.68}}{Q^{0.53}}\left(\frac{1.73}{\rho_s - \rho_1}\right)^{0.5} \tag{2.9}$$

where: d_{50} - cut size in μm.

ρ_s - solids specific gravity

ρ_1 - slurry specific gravity

K_2 - constant

The equilibrium radius defined as the radius at which the resultant radial settling velocity of a particle due to centrifugal force equals the inward radial velocity derived from Stokes law (equation 2.2) was in agreement with Kelsall [7]. Values of the equilibrium radii at different levels within the cyclone were calculated for all solids used in the experiments and the 'envelopes of equilibrium' for several particle diameters were obtained. The envelope of zero vertical velocity was obtained and it

University of Cape Town

was found to correspond with the separation cut size from equation 2.9.

Although the cyclone diameter was found to have no direct effect on the cut size and energy requirements, design variables such as the feed inlet, vortex finder, and spigot diameters are sized as ratios of the cyclone diameter (Lynch, et al. [17]). Feed solids concentration, particle shape, and density were shown to have a significant effect on the performance of the cyclone. Although no quantitative expressions were available for the prediction of cut size with hindered settling effects it was indicated that high feed-solids concentration can cause "hindered-settling" effects due to the crowding of the particles, resulting in an increased cut size.

It was observed that the sharpness of classification depends on the solids specific gravity, feed-solids concentration, and 'thickness' of the underflow stream. It was indicated that a thickened underflow gave sharper classification compared to a dilute underflow. Withdrawing underflows at the maximum solids concentration was recommended in operations where sharp classification is required.

The pressure drop across the cyclone is critical in the operation of the device and has a significant influence on the cyclone performance. High pressure drops were found to be undesirable and the law of diminishing returns seemed to apply with respect to lowering of the cut size beyond 140 kPa. Severe wear problems at the spigot are expected at high operating pressures. Due to the severity of wear in some applications, rubber lining is recommended and cyclones should be designed in a way that allows for parts affected by abrasion to be removed (Trawinski [18]).

Since most of the tests conducted on cyclones were done on stand-alone test rigs, Dahlstrom indicated that insufficient studies have been made as to the effects of classification on the rest of the circuit.

Discussion

Flow studies are important in cyclone design and it is perceived that flow studies will be exploited more with the inventions that involve intricate features such as

University of Cape Town

involute feed inlets and vortex finder arrangements for the three product cyclone, coaxial cyclone, and air sparged cyclone. It is expensive to conduct experiments for flow studies but models could be set up in computational fluid dynamics (CFD) that could be used to study flow patterns in these systems without conducting numerous experiments.

Evaluating the velocity components and relating these to the physical classification in the hydrocyclone is an important step in formulating fundamental models for cyclones. In the three product cyclone, aspects of flow which influence flow split to the products will be critical in exploiting the full benefits of this device in many applications.

The derivation of the cut size equation was the most important contribution that Dahlstrom made in the study of hydrocyclones. Due to the importance of this parameter in classification, several varieties of the cut size equations have been published since then: Yoshioka and Hotta [19]; Bradley [20]; Lilge [10]; Rietema [21]; Fahlstrom [22]; Lynch and Rao [23]; Plitt [24]; and Bednarski [25]. Although this is not a complete description of cyclone performance, it provides a reasonable approximation of the size separation in the conventional hydrocyclone. It must be noted that almost all cyclone models developed after Dahlstrom published his cut size derivation, involve the prediction of the cut size. It is useful to have correlations to estimate the cut size, but these do not represent a physical model that can be used to describe separation in the hydrocyclone.

It has been established that feed solids concentration has a profound influence on the design and operation of hydrocyclones [26]. Since the effects of feed solids change with ore density, it is advisable to conduct experiments at different feed solids concentrations and determine the optimum operating concentration for each ore. Though this is known, It was not possible to structure systematic experiments to study the effect of feed-solids concentration in this thesis because of the detrimental effects that changing this parameter could have brought about in the production

University of Cape Town

circuit. However, a consistent way of checking the feed solids concentration was adopted and implemented during the experimental work.

2.2.4 Performance and design of hydrocyclones, parts I - IV.

Rietema, K, 1960 [21].

Rietema was the first to attempt to develop theoretical correlations of hydrocyclone performance based on the Navier-Stokes equations. Rietema discussed the correlations for the pressure drop across a hydrocyclone that he developed, separation power, and some rules for establishing the optimum cyclone design.

Pressure drop across the cyclone has been shown to have a strong dependence on the construction of the cyclone and increases with throughput. In most cases an air core exists and special measures have to be taken to preserve it. It was suggested that the absence of an air core generally results in a decrease in total pressure drop at the same throughput and a reduction in separation efficiency. This contradicts Dahlstrom (1953) who attested that correct application of back pressure to the spigot can be used to eliminate the air core without loss of separation efficiency. If the total pressure drop is insufficient or the solid concentration in the underflow is very high, the underflow discharge changes from a spray-type into a jet-type or drop-type discharge. This condition is undesirable and is termed 'roping'.

Experimental flow patterns seem to indicate that tangential velocities increase as the radius decreases due to the conservation of angular momentum. It was observed that the ideal law of conservation of angular momentum was not strictly obeyed owing to wall friction and internal friction caused by viscosity and turbulence. This suggests that the use of smooth materials in constructing internal surfaces can increase separation efficiency of the hydrocyclone (Trawinski [18]).

The Navier-Stokes equations which describe the hydrodynamic behaviour of fluids in motion were used as a basis for a theoretical derivation of the tangential velocity

University of Cape Town

profile. Due to the complex nature of the problem, special assumptions were made to modify the equations for the solution to be attained. By taking the average time, the turbulent fluctuations were neglected while the quadratic terms were represented in a turbulent kinematic viscosity term ϵ, which was then added to the ordinary kinematic fluid viscosity as shown in equation 2.10.

$$U\frac{\partial V}{\partial r} + W\frac{\partial V}{\partial z} + \frac{UV}{r} = (\nu + \epsilon)\left[\frac{1}{r}\frac{\partial}{\partial r}\left(r\frac{\partial V}{\partial r}\right) + \frac{\partial^2 V}{\partial z^2} - \frac{V}{r^2}\right] \tag{2.10}$$

where: U - radial velocity of the liquid,

V - tangential velocity in the cyclone,

W - axial velocity in the cyclone,

r - radial co-ordinate in the cyclone,

z - axial co-ordinate in the cyclone,

ν - kinematic viscosity, and

ϵ - turbulent kinematic viscosity term.

Applying boundary conditions considering that the cyclone operates with an air core, and that at a free surface no shearing stresses occur and then assuming that V does not depend on z but depends on r only, equation 2.11 was derived. The solution (equation 2.12) was used when considering the influence of turbulence on the separation efficiency.

$$-\frac{U}{r}\frac{dVr}{dr} + (\nu + \epsilon)\left\{\frac{d}{dr}\frac{1}{r}\frac{dVr}{dr}\right\} = 0 \tag{2.11}$$

$$\phi = C_2 - C_1 \exp(-\lambda\sigma)\left(\frac{\sigma}{\lambda} + \frac{1}{\lambda^2}\right) \tag{2.12}$$

where :$C_1 = \frac{\lambda^2}{-\exp(-\lambda) - \lambda\exp(-\lambda) + \left(\frac{\sigma_1^2}{2}\right)\lambda^2\exp(-\lambda\sigma_1) + \sigma_1\lambda\exp(-\lambda\sigma_1) + \exp(-\lambda\sigma_1)}$

$C_2 = 1 + C_1\exp(-\lambda)\left(\frac{1}{\lambda} + \frac{1}{\lambda^2}\right)$

University of Cape Town

$\sigma = \frac{r}{R}$, $\phi = \frac{V_r}{V_o R}$, and $\lambda = \frac{-U_o R}{v+\varepsilon}$

λ - dimensionless parameter describing the tangential velocity profile

σ - ratio of the radius r to the cyclone radius R,

when the cyclone operates with an air core, Retiema equated σ to σ_1.

ϕ - ratio of angular momentum at radius r to inlet angular momentum.

Although Kelsall determined the flow patterns, pressure drop, and separation power he did not derive any correlations for these quantities, [7], [12]. Dahlstrom [13] assumed that the influence of feed inlet and vortex finder diameter were independent and the influence of the Reynolds number was not investigated. These omissions led Rietema to conduct further experiments on cyclone performance because it was felt that reliable pressure drop correlations were essential in solving specific separation problems.

It was observed that pressure drop across the cyclone can not be calculated on the basis of the theoretical tangential velocity profile by integration of the pressure gradient in equation 2.13 as both the dimensionless parameter λ from equation 2.11, and the diameter of the air core vary in an unknown way with the construction of the cyclone and variations in the Reynolds number.

$$\frac{dP}{dr} = \frac{\rho v^2}{r} \tag{2.13}$$

where: $\frac{dP}{dr}$ - pressure gradient over r,

ρ - liquid density,

v - tangential velocity and r is the radius, and

λ - calculated from equation 2.14

$$\lambda = \frac{-U_o R}{v + \varepsilon} \tag{2.14}$$

where: U_o - radial velocity,

University of Cape Town

R - cyclone radius,

ν - ordinary kinematic viscosity, and

ε - turbulent kinematic viscosity, which accounts for the fluctuations in turbulence.

Experiments were carried out using a 75 mm diameter cyclone, with a fixed included cone angle, a variable length and changeable feed inlet, vortex finder, and spigot diameter. Effects of viscosity and the Reynolds number were investigated using water and a mixture of water and glycerol as fluids. In these experiments the overflow and underflow were discharged freely in an open vessel to allow the air core to develop.

In addition to the Reynolds number, solid concentration, and the diameter of the air core, pressure drop was expressed as a function of six geometric parameters as shown in equation 2.15. All the factors from cyclone geometry were represented in the pressure drop correlation.

$$G = \frac{(\Delta P)_t}{\frac{1}{2}\upsilon_i^2} = fxn\left(\frac{D_i}{D_c}, \frac{D_o}{D_c}, \frac{D_u}{D_c}, \frac{L_c}{D_c}, \frac{(L-L_c)}{D_c}, \frac{l}{D_c}, \mathrm{Re}_{inlet}, C, \theta_{ci}, \rho, \frac{gD_c}{\frac{1}{2}\upsilon_i^2}\right) \quad (2.15)$$

where: fxn - abbreviation for function

G - total pressure loss factor,

$(\Delta P)_t$ - total pressure drop

ρ - liquid density

υ_i - inlet velocity,

Re_{inlet} - Reynolds number at the inlet,

D_c, D_i, D_o, D_u - Cyclone, inlet, vortex finder, and spigot diameters,

L, L_c - cyclone length, and cylindrical part length,

l - length of the vortex finder,

C - concentration of solids in suspension,

θ_{ci} - inclination of the cyclone axis to the vertical,

University of Cape Town

g - gravitational acceleration.

After formulating the functional form, Rietema systematically discarded some of the factors such as feed solids concentration and the spigot diameter, whose effects were considered to be negligible. The pressure drop correlation reduced to equation 2.16.

$$E_u = \frac{(\Delta P)_s}{\frac{1}{2}v_i^2} = fxn\left(\mathrm{Re}_{inlet}, \frac{D_i}{D_c}, \frac{D_o}{D_c}, \frac{L}{D_c}, \frac{Q_o}{Q}\right) \tag{2.16}$$

where E_u - cyclone pressure loss factor,

$(\Delta P)_s$ - static pressure loss,

Q_o - overflow flow rate, and

Q - throughput of the cyclone.

It was concluded that the total pressure drop $(\Delta P)_t$ necessary to operate a cyclone consists of three components:

1. the inlet velocity head,
2. friction losses, and
3. the centrifugal head.

The first component is the dynamic pressure produced by the pump to accelerate the feed slurry from rest to the inlet velocity ν_i. The second and third components determine the static pressure loss $(\Delta P)_s$ in the cyclone pressure loss factor represented by $E_u = \frac{(\Delta P)_s}{\frac{1}{2}\rho v_i^2} = G - 1$.

Rietema concluded that the general pressure drop correlation can be split into the Reynolds dependence $f(\mathrm{Re})$, and a function describing the effects of the cyclone geometry.

For particles with higher densities, the radial velocity is directed outwards and when the centrifugal forces are strong enough the particles reach the wall of the

University of Cape Town

cyclone enroute from the cyclone inlet downwards and are separated. Four conditions were identified where a particle was not likely to reach the wall:

1 If the radial velocity of the liquid directed inwards was too large causing the particle to be entrained towards the centre,

2 If the particle enters the cyclone at a great distance from the wall,

3 If the particle's residence time is very short, and

4 On account of turbulence, which causes eddy diffusion to the effect that differences in concentration are evened out.

In deriving the cyclone separation number, Rietema assumed that:

1. the turbulence eddy diffusion had a negligible effect on separation

2. the Reynolds number as related to the particles being separated is sufficiently low for the Stokes law for free fall velocity to apply.

The relation between the static pressure drop and the separation efficiency achieved in terms of the (d_{50}) cut size was given by equation 2.17.

$$\frac{d_{50}^2 \Delta\rho}{\eta} L \frac{(\Delta P)_s}{\rho Q} = \frac{72 C_1}{\pi} \frac{R_1}{D_i^2} \left(\frac{U}{W} L - R_1 \right) \tag{2.17}$$

where: d_{50} - diameter of particle that have a 50% chance of reporting to either the overflow or underflow

$\Delta\rho$ - difference between the density of the solid and that of the liquid

$(\Delta P)_s$ - static pressure drop from inlet to outlet

η - dynamic viscosity

L - total length of the cyclone from the top plate to the apex

C_1 - as defined before

$R_1 = R - \frac{1}{2} D_a - \frac{1}{2} D_i$

R - radius of the cyclone

D_a - diameter of the air core

University of Cape Town

D_i - diameter of the cyclone inlet

U - radial velocity of the liquid

W - axial velocity in the cyclone.

Both the right and left hand sides of equation 2.17 are dimensionless. The right-hand side contains only the cyclone dimensions and velocity ratio, which was found to be constant for a cyclone of a given shape and was equal to the left-hand side. Modifying the above formula resulted in the cyclone correlation number given by equation 2.18.

$$Cy_{50} = \frac{d_{50}^2 \Delta\rho}{\eta} L \frac{(\Delta P)_t}{\rho Q} = CONSTANT \tag{2.18}$$

where: :Cy_{50} - cyclone correlation number based on the d_{50}.

The derivation of a cyclone number which was independent of the pressure drop parameter appears to be a favourable condition for cyclone design.

Discussion

Despite Rietema's attempt to develop a model of cyclone performance based on fundamentals of physics, the complex nature of the system lead him to settle for semi empirical correlations.

Rietema seemed to contradict himself in concluding that within the range of practical applications the tangential velocity profile could be used to calculate the centrifugal head which could in turn be used to determine the static pressure drop. Rietema initially argued that it was impossible to determine the pressure drop from tangential velocity due to the variations of λ and the air core in an unknown manner.

Contrary to the theories based on the assumption that equilibrium conditions prevail in the hydrocyclone (Bradley and Pulling. [8], Tarjan [27]), Rietema suggested

University of Cape Town

that particles with a stability radius smaller than the vortex finder radius were separated towards the wall before reaching their stability radius. However, similar to other authors, the resulting separation efficiency was expressed in terms of the (d_{50}) cut size shown in equation 2.18.

Although pressure drop across the cyclone is undoubtedly an important parameter, Rietema's pressure drop measurements could not be relied upon as they were determined across the cyclone and entire feed line, with the latter showing an appreciable friction. Rietema discussed the effect of several cyclone geometry and operation variables which influence the total pressure drop across a cyclone. However, systematic experiments were not conducted to evaluate the effects of important variables such as feed solids concentration and the ratio of the spigot to cyclone diameter on the total pressure drop across the cyclone. On account of its complexity the influence of feed solids concentration was not examined. The ratio of the spigot diameter to cyclone diameter was not investigated because it is common in practice to obtain the total underflow by adjusting the pressure difference between the overflow and underflow outlets and not by using a certain spigot diameter. The effects of the vortex finder length were discussed but the experimental set up had no provision for its evaluation. The suggested reasons for omitting both the feed solids concentration and the spigot diameter seem inadequate to justify the exclusion of such important variables in the operation of cyclone (Mular *et al.*, [28]). In an attempt to reproduce conditions that are common in mineral processing plants, Rietema allowed the formation of air core in all his experiments.

The concept of representing cyclone performance with a single cyclone number seemed to be attractive, but suffered from several set backs such as not being applicable to the range of types of hydrocyclones that were commonly used in the industry.

University of Cape Town

2.2.5 Hydrocyclone fundamentals

E. O. Lilge, 1962 [10].

Lilge attempted to use fluid flow considerations to analyse the main variables affecting the performance of the hydrocyclone. A total of seventeen variables were investigated and their effect and inter-relationship on mineral beneficiation were evaluated.

Based on fluid flow patterns, fluid velocities, forces acting on individual ore particles, and the paths taken by ore particles, Lilge deduced the basic concepts of hydrocyclone operations. Lilge postulated that the hydrocyclone vessel can be of any shape even cylindrical and not necessarily conical since during operation it forms what was termed the 'theoretical cone'. The effective diameter of the theoretical cone was shown to be related to D_c - the diameter of the cyclone body at the bottom of the vortex finder, and D_u - the spigot diameter at the bottom of the cyclone. The effective height of the theoretical cone was taken as the distance between the bottom of the vortex finder and the spigot.

It was suggested that the radial velocity component is zero for all the points half way between the outside of the air core and the periphery of the theoretical cone at the position level to the bottom of the vortex finder. From the mid point outwards, the radial and vertical fluid velocity downwards increase rapidly, while from the mid points inward the velocity upwards increases slightly. It was stated that the medium and ore particles are forced into the theoretical cone through the annular rig formed by the mid points and the periphery of the cone. Lilge showed that the envelope of zero vertical velocity was defined by the loci joining the mid point at the bottom level of the vortex finder with the point at the circumference of the air core at the level of the spigot. The air core radius was determined using equation 2.19. The radial velocity was shown to increase progressively as the feed descended from the top of the theoretical cone ($h = 0$) down to the spigot ($h = h$).

University of Cape Town

Lilge reasoned that since the envelope of zero vertical velocity was a straight line function its path could be evaluated by considering the radial velocity at the bottom of the vortex finder, then determining one other radial velocity at any elevation on the envelope would provide another point for its loci. It was suggested that this could be done by using the volume of the fluid that reported to the overflow.

$$r_a = 0.083 r_c \tag{2.19}$$

where r_a - radius of the air core from the central axis of the cyclone, and
r_c - radius theoretical cone at the level of the vortex finder opening.

Lilge appears to suggest that the total volume of medium that reported to the overflow was a function of the cone ratio D_u/D_0 and that for a particular cone ratio, the proportion of fluid medium reporting to the overflow is constant for all cone sizes under all operating conditions. As an example, Lilge showed that for the cone ratio of 0.8, 70% of the fluid medium reported to the overflow while 50% reports to the overflow at the cone ratio of 1.0.

The paths followed by particles which according to Lilge had a 50 per cent chance of reporting either to the overflow or underflow are given in figure 2-2. It was reported that the particles which cross the envelope of zero vertical velocity and the envelope of maximum tangential velocity above the intersection point of the two envelopes report to the overflow and below the intersection of the two envelopes, particles may report to the overflow if they can cross the envelope of zero vertical velocity before being ejected into the underflow. The definition of the particles that have a 50 per cent chance of reporting either to the overflow or underflow was given as the particle that starts to cross to the overflow at the intersection of the two envelopes.

The radial velocity at any other point could be calculated using equation 2.20. Since the value $\hat{h}$ at the intersection point of the envelope of zero vertical velocity and the envelope of maximum tangential velocity could be evaluated using equation 2.21,

University of Cape Town

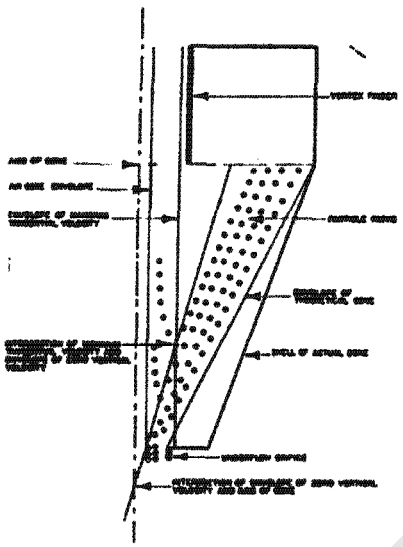


FIGURE 2-2. Schematic representation of paths of particles with a 50 percent chance of reporting either to the overflow or underflow (Figure by E. O. Lilge, 1962).

the radial velocity at this point could be calculated by substituting $\hat{h}$ in equation 2.20.

$$U = \frac{316.6 Q_o}{D_c h} \tag{2.20}$$

$$\hat{h} = \frac{0.337 h}{\cos\theta} \tag{2.21}$$

where: U - radial velocity component

D_c - cyclone diameter

Q_o - volumetric flow rate to the overflow

h - height from the bottom of the vortex finder to the spigot

$\hat{h}$ - height from the bottom of the vortex finder to the intersection of the two envelopes

θ - cone taper angle

Lilge proposed that the percentage weight of other sizes that reported to the

University of Cape Town

underflow had a definite relationship to the size that reports 50 per cent to the underflow. The two expressions termed as the underflow equations for the fine sizes (-106μm) and coarse sizes (+106μm) are given in equations 2.22, and 2.23, respectively.

$$y_2 - y_1 = 2(x_2 - x_1) \tag{2.22}$$

$$x_2 - x_1 = 50 \log \frac{y_2}{y1} \tag{2.23}$$

where: x_1, x_2, y_1, and y_2 are coordinates

Using the two opposing forces that act on the particle in a radial direction to determine whether the particle reports to the overflow or underflow stream and the knowledge of fluid flow in the cyclone, Lilge derived what he termed as the 'cone force equation' (equation 2.24).

$$(\rho_s - \rho_f) d \frac{V_T^2}{r_t} = C_D y_f \frac{U_R^2}{2} \tag{2.24}$$

where: ρ_s - specific gravity of the solid particle,

ρ_f - specific gravity of the fluid,

U_r - radial velocity component,

V_t - tangential velocity component,

r_t - radial co-ordinate at the point where V_t is measured,

r - radial co-ordinate in the cyclone,

C_D - coefficient of resistance of the solid particle.

Discussion

Lilge is the proponent of the cone force equation which is based on the interaction of forces. His proposition that the hydrocyclone vessel can be of any shape since it assumes a conical shape in operation contradicts the mechanisms that have been

University of Cape Town

proposed for types of hydrocyclones that have no conical section such as the flat bottom cyclone in which some strong convective circulating flows in the downward direction have been observed near the wall at the bottom of cyclone (Trawinski [29], Svarovsky [30]). Lilge's proposal ignores the influence of the cone angle on the performance of the hydrocyclone which has since been shown to have a significant effect on the cut size and throughput (Mular and Jull [28], and Schmidt [31]).

Using the envelope of zero vertical velocity and the envelope of maximum tangential velocity to define the particles that have a 50 per cent chance of reporting either to the overflow or to the underflow seemed appealing. The major draw back with Lilge's representation is that the particles that report to the underflow remain undefined. The claim that the particles with a 50 percent chance have been proven mathematically appear to be unsubstantiated considering that the particles can report either to the overflow or underflow starting from the point where the two envelopes intersect down to the point where the envelope of zero vertical velocity intersects the air core while particles that cross above the intersection of the two envelopes have little chance of reporting to the underflow.

Defining the underflow equations on two sizes based on the $106\mu m$ limits the use of the application of the equations to the classification operations that require a cut size close to the $106\mu m$. It is felt that the equation must not be fixed around any size for the classification applications which are known to cover a wide range of cut sizes.

University of Cape Town

2.2.6 The selection of cyclone classifiers, pumps, and pump boxes for grinding circuits

A. L. Mular and N. A. Jull, 1969 [28].

Mular and Jull gave a brief review of cyclone fundamentals, factors considered in the selection of the pumping mechanism including the pump box along with the pip-

ing, and distributors associated with it. The review includes the sizing methodology that may be employed for preliminary design in closed circuits.

It was suggested that larger diameter cyclones tend to give a coarser cut size compared to smaller diameter cyclones. This was attributed to smaller accelerative forces associated with large cyclones. Even though each cyclone size produces a range of accelerative forces, these forces were found to be approximately proportional to the inverse of the cyclone diameter. The vortex finder diameter in cyclones of fixed diameter operating at a constant pressure could be altered to change the cut size. Larger vortex finder diameters were found to produce coarser overflow. Vortex finder diameters in the region of 35 to 40% of the cyclone diameter were recommended. To minimise short-circuiting of coarse particles to the overflow, vortex finders extending below the feed inlet were recommended.

The spigot area is known to be the point of highest wear in the hydrocyclone and a spigot diameter of more than one–fourth that of the vortex finder was recommended, although there was no absolute minimum. Due to the difficulties encountered with optimising the spigot diameter and non existence of models that can accurately determine the optimum size, trial and error with a range of spigots has been recommended (Dahlstrom [32]). Operating the cyclone with an optimum spigot can not be ignored as the spigot is known to determine the critical operating factors such as the solids capacity and the solids content of the underflow. The undesirable condition of roping in the cyclone has been linked to the overload of coarse solids at the spigot or when the underflow is over throttled so that the coarse particles are forced into the overflow stream (Yianatos [33]). For an ore of known density an empirical relation was given for calculating the spigot diameter from the tonnage of material reporting to the underflow and the solids concentration (Equation 2.25).

$$D_u = 4.16 - \left(\frac{16.43}{(2.65 - \rho + \frac{100\rho}{P_u})} \right) + 1.10 \ln(\frac{Q_u}{\rho}) \qquad (2.25)$$

University of Cape Town

where: D_u – recommended spigot diameter in inches

ρ - specific gravity of the ore

P_u – underflow percent solids by weight

Q_u – underflow solids tonnage

The feed inlet area determines the entrance velocity and is one of the factors that govern the tangential velocity at various radii. It was reported that the feed flow rate to the cyclone increases with an increase in the inlet area while decreasing the inlet area results in a slight increase in the pressure drop at similar capacities. In agreement with Dahlstrom's recommendation (1952), Mular and Jull found that a rectangular shaped feed inlet was found to be superior compared with other shapes. These recommendations were made before the development of the involute inlet which is currently believed to be superior.

In conformity with the findings of Lynch and Rao [23], it was observed that the corrected cut size (d_{50c}) is dependent upon particle shape, specific gravity, slurry viscosity, feed size distribution, feed solids concentration, and inlet pressure. The assumption that a certain portion of the feed reports to the underflow by short-circuiting and this amount is directly proportional to the water split to the underflow proposed by Kelsall [12] was adopted in the determination for the corrected cut size (d_{50c}). Mular and Jull seem to suggest that the action of the cone is to squeeze coarse solids toward the centre to obtain a concentrated underflow product. As a result of this small cone angles tend to decrease the separation size and increasing the cone angle tends to increase the separating size.

Mular and Jull admitted that it is difficult to decouple the influence of viscosity and density of the internal slurry medium of the particles being separated within the hydrocyclone. However, it was suggested that the internal slurry viscosity increases with internal slurry density such that at a critical point the viscosity rises sharply for small changes in density. The feed solids concentration is an important

University of Cape Town

operating variable and appears to be an indirect measure of internal slurry viscosity and density.

Equations 2.26, 2.27, and 2.28 are empirical relationships showing the influence the feed solids concentration, pressure drop, and specific gravity of solids, on the corrected cut size, respectively. C1, C2, and C3 are correction factors for the influence of cyclone feed concentration, pressure, and specific gravity respectively ([34]).

$$C_1 = \exp(-0.301 + 0.094v - 0.0356v^2 + 0.0000684v^3) \tag{2.26}$$

$$C_2 = 2.0(\Delta P)^{0.3} \tag{2.27}$$

$$C_3 = \left(\frac{1.65}{(\rho - 1)}\right)^{\frac{1}{2}} \tag{2.28}$$

where : C_1 - relative d_{50c} (relative to the specific gravity of percent solids of 2.65)

exp - means to the base e,

v - volume percent solids

ρ - specific gravity of solids

C_2, C_3 - relative cut size,

ΔP- pressure drop in PSI

In most of the industrial operations the products are discharged at atmospheric pressure. However, if the discharge pressure in the overflow is positive then a greater portion of the feed volume is forced to the underflow, reducing drag toward the overflow and thus making a finer separation.

Centrifugal forces were found to depend on particle mass which is related to particle size and specific gravity. Although particle shape was mentioned among

University of Cape Town

the factors that influence separation in the hydrocyclone, it was not represented in equations 2.26, 2.27, and 2.28. The feed size distribution is known to have a significant influence on separation in the cyclone and it is generally agreed that a coarse feed without fines will coarsen the separation, while a fine feed without coarse particles will give a finer separation. Other than the work of Lynch and Rao [23], and Asomah [35],there has been very little work done to account for the feed size effect on separation.

Discussion

The effects of individual operating parameters on separation in the hydrocyclone and empirical relationships have been discussed. Despite the depth of the findings no attempt was made to integrate these parameters into one relationship that can be used to determine the influence from a combination of these factors on separation. Other authors have attempted to develop relationships involving several operating and design variables: Lynch and Rao [23]; Plitt [24]; Nageswararao [36]; and Svarovsky [37].

Useful recommendations on the pumping arrangement were given in the paper and various design principles for pumps, pump boxes, and hydrocyclones were discussed. Recommendations from their paper were adopted in this thesis when designing the apparatus for the industrial scale experimental work which involved diverting material from the operating plant to the test rig and recirculating it back without causing disruptions to the plant, and pilot plant scale work where the material was pumped from the mill discharge sump to the cyclone located at a height of 12m above the sump.

2.2.7 Modeling and scale up of Hydrocyclone Classifiers.

Lynch A. J. & Rao T. C. 1975, [23].

University of Cape Town

Lynch and Rao suggested that hydrocyclones have a significant influence on the performance of comminution circuits as indicated by the wide variation in the output of the ball mill - hydrocyclone circuit that can be obtained by variations in the classification conditions only. This has major implications on the control of grinding circuits and the efficiency of downstream processes such as flotation.

Tests were conducted on cyclones ranging from 10.2 to 38.1cm diameter, supplied by Krebs Engineers. To ensure geometric similarity no alterations were made to the hydrocyclones and all other fittings were used as received.

The model developed by Lynch and Rao from several experiments was the first widely used empirical model. Unlike the early models, the equations were formulated to show the strong correlation observed between performance criteria such as the cut size and factors such as cyclone geometry, flow rate and feed solids concentration. The general form of the corrected cut size (d_{50c}) correlation is given in equation 2.29. The other performance criteria are given in equations 2.30 and 2.31 representing the feed flow rate and water recovery to the underflow, respectively.

$$\log_{10} d_{50c} = K_1 D_o - K_2 D_u + K_3 D_i + K_4 C_w - K_5 Q_f + K_6 \tag{2.29}$$

where: d_{50c} - corrected cut size,

D_o, D_u, D_i - vortex finder, spigot diameter, and inlet diameters,

C_w - weight percent of solids in feed

Q_f - volumetric feed flow rate

K_1 to K_6 - empirical constants

with d_{50c} in mm, Q_f in l $(\text{min})^{-1}$, and all cyclone dimensions in cm.

$$Q_f = K \times D_o^{0.73} D_i^{0.86} P^{0.42} \tag{2.30}$$

where: $K = 6$ for limestone tests

P - inlet pressure in kPa

University of Cape Town

$$R_f = K_1 \times \frac{D_u}{WF} - \frac{K_2}{WF} + K_3 \tag{2.31}$$

Where: WF - mass flow rate of water in feed (t/h)

K_1 =193, K_2 = 271.6, K_3 = 1.61 for limestone tests

Since the model equations were designed for scale-up determining all the constants (K_1 to K_6) and the efficiency parameter α from tests on a small cyclone using the same feed as that to be treated on the industrial scale was recommended.

For the ores containing a mixture of minerals the reduced efficiency curve had a long tail and did not conform to the regular shapes obtained with other minerals. This feature was unique to ores containing a mixture of minerals with differing specific gravities. However, calculations show that this type of curve for total ore arises directly from summing up the classification results of the individual minerals which behave as predicted by standard reduced efficiency curves. A general form of the required correction for mineral density is presented in equation 2.32 given in the JKMRC monograph [15].

$$\frac{(d_{50c})_a}{(d_{50c})_b} = \left[\frac{(\rho_s)_a - \rho_l}{(\rho_s)_b - \rho_l}\right]^{0.5} \tag{2.32}$$

where ρ_l is the density of the separation medium; a and b denote minerals whose different densities are represented by $(\rho_s)_a$ and $(\rho_s)_b$ respectively. It was concluded from their work that dense minerals have a finer separation size than light ones.

Lynch and Rao gave a simplified approach that can be used to predict the performance of a hydrocyclone operating on a mixture of particles of widely varying specific gravities. Although confirmatory tests on the behaviour of different specific gravity minerals in various hydrocyclone sizes were not carried out, the following conclusions were drawn:

1 The reduced efficiency curve for a mineral is not dependent on hydrocyclone diameter, or outlet dimensions, or operating conditions.

University of Cape Town

2 The reduced efficiency curve determined for a mineral on a small hydrocyclone may be used for scale-up work.

3 The curve is dependent on particle properties such as the specific gravity and shape.

Discussion

Lynch and Rao established their model using both laboratory and industrial conditions. The most important findings in this paper are that for geometrically similar hydrocyclones operating correctly, the reduced efficiency curve is constant for a mineral of fixed feed size distribution irrespective of the hydrocyclone diameter and other operating conditions and that the reduced efficiency curve is dependent on particle properties such as the specific density, size and shape, [38]. If all other variables are kept constant changing the feed size distribution has an effect on both the fraction of water in the feed which enters the coarse product and the d_{50c} value.

The accuracy of the flow meters were checked prior to conducting experiments. It is useful to check all the instrumentation on plants or pilot plants prior to conducting experiments because frequently equipment is either incorrectly calibrated or malfunctioning. Such checks bring to the fore problems that need fixing in terms of instrumentation and ultimately improves the quality and validity of the test data. For the test results to be useful, both design and operating variables must be selected to match those that are used in industrial operations. Although the effects of many parameters were tested, their work was incomplete to the extent that the effect of inlet was not studied and in smaller units the outlet dimensions were not varied.

The major drawback in the Lynch and Rao model is that the effect of the vortex finder on classification efficiency was not considered. Furthermore, most of their data was obtained from tests conducted on limestone and silica and confirmatory tests on

University of Cape Town

the behaviour of different specific gravity minerals in various diameter hydrocyclones were not conducted. Krebs cyclones were used for the experimental work, and the use of the model for significantly different cyclone geometry was not advisable. The requirement to conduct experiments for each ore type to determine the values for the constants in the model limits its application.

The "tail" is due to the fact that the d_{50c} values for the ore is not the weighted average of the d_{50c} values for the components but is biased towards the lower value. The requirement of assuming that the components are fully liberated limits the extend to which the equation can be applied. The draw back is that the shape of the curve was affected by the size distributions of components and their relative proportions. It was concluded that the curves for components remain constant, but they combine to form a composite reduced efficiency curve that is different from the individual components.

Further hydrocyclone research at the JKMRC resulted in a generalised model of hydrocyclones [39], [40], and an alternative model incorporating the angle of inclination [35], [41]. The Nageswararao model is one of the extensively used models and has been incorporated in the JKSimMet simulator for use in design and plant optimisation simulations. A comprehensive review of this model has been performed by Nageswararao et al [42].

University of Cape Town

2.2.8 A mathematical model of hydrocyclone classifiers.

L. R. Plitt, 1976 [24].

Plitt's model appears to be the most widely used model in the study of hydrocyclone performance. After studying and assessing the outcomes from other researchers, Plitt endeavoured to develop a more universally applicable model for hydrocyclones that would give reasonable predictions over a wide range of operating conditions. To obtain greater universality in his model, Plitt decided that the format of the equations in the model should be similar to the theoretical equations and

should include variables that theory predicts to be important. The correlations in his model, were derived from a total of 297 individual experimental data sets. Since most of his experiments did not include data from large diameter hydrocyclones, the results from the work of Lynch and Rao, [23] were added to his 174 tests. These experiments covered a wide range of operating conditions and cyclone geometry. In addition to the five design variables namely; the cyclone diameter, equivalent feed inlet diameter, vortex finder diameter, spigot diameter, and the height between the bottom of the vortex finder and the spigot, the feed pressure and solids content were included. To deal with the seven variables in an organised manner, Plitt organised his tests on a two-level factorial design.

Plitt's model consists of four basic parameters that express: the cut size (d_{50}); volumetric flow split between the overflow and underflow (S); volumetric throughput and pressure drop (Q/P); and sharpness of separation (m) in terms of the operating and design variables given in equations (2.33, 2.34, 2.35, and 2.36).

$$d_{50} = \frac{35 D_c^{0.46} D_i^{0.6} D_o^{1.21} e^{[0.063\phi]}}{D_u^{0.71} h^{0.38} Q^{0.45} (\rho_s - \rho)^{0.5}} \tag{2.33}$$

where: d_{50} - cut size, μm,

D_c, D_i, D_o, D_u - cyclone, feed inlet, vortex finder, spigot diameters in cm,

ϕ- per cent by volume,

h - distance from the bottom of the vortex finder to the spigot, cm,

Q - flow rate of the slurry, m^3/h, and

ρ_s and ρ - are density of solids and density of liquid, respectively, g/cm^3.

$$S = \frac{2.9(D_u/D_o)^{3.31} h^{0.54} (D_u^2 + D_o^2)^{0.36} e^{[0.0054\phi]}}{H^{0.24} D^{1.11}} \tag{2.34}$$

where: S - Volume split,

P - pressure drop, and

ϕ - volume fractions of solids in the feed slurry.

University of Cape Town

$$P = \frac{4.7Q^{1.78}e^{[0.0055\phi]}}{D_c^{0.37}D_i^{0.94}h^{0.28}(D_u^2 + D_o^2)^{0.87}} \tag{2.35}$$

, and

$$m = \exp[0.58 - 1.58R_v]\left(\frac{D_c^2 h}{Q}\right)^{0.15} \tag{2.36}$$

where: m - classification index used a measure of sharpness of classification

R_v - volume recovery in terms of flow split to underflow

Plitt claimed that the ability to calculate the four basic parameters for a given set of conditions would allow the user to determine a complete mass balance which includes size distributions of the product stream. It is doubtful if the four equations alone can give reasonable predictions of the product stream without having to specify at least the feed size distribution since the only parameter related to size in the model is the cut size (d_{50}) which incorporates the F_{50} from the feed size distribution.

It is important to notice that in the cut size equation (2.33), the effects of solid density have been taken into account. Although the term to account for solids effects was incorporated in the model, much work remains to be done in this area to incorporate constraints and abilities to accurately predict multi-phase solid feeds. Plitt assumed that the bypass remains constant and equal to the mass recovery of water in the cyclone feed to the underflow stream, R_f for all specific gravity fractions, shown in earlier work by other authors to be incorrect, (Kelsall, [7], Dahlstrom, [16], Lynch and Rao, [23]). It is necessary to determine the volume split between the overflow and underflow for an accurate determination of the water balance across the classifier using equation 2.37. An iterative solution is required for the above equation since there is dependence between parameters R_f and R_s.

$$R_f = \frac{R_v - \frac{R_s\phi}{100}}{(1 - \frac{\phi}{100})} \tag{2.37}$$

University of Cape Town

where R_v - recovery of fluid to underflow

R_s - recovery of solids to the underflow

ϕ - volume fractions of solids in the feed slurry

Strong correlation was given by the term $\left(\frac{D_c^2 h}{Q}\right)$ in equation 2.36, which is representative of retention time in a cyclone. From that correlation, it was reasoned that with a longer retention time, the particles in the hydrocyclone have a greater chance of being routed to the correct outlet, thus reducing the amount of misplaced material. The classification curve exhibited a relatively large amount of scatter and this was attributed to the large number of reference size intervals (Cilliers and Hinde [43]). Plitt used the scatter in the classification curve to show that the classification index m, which is a calculated parameter, was affected by the scatter resulting from the standardisation procedure which is sensitive to minor errors in size analysis.

Since the size range of interest in Plitt's work was in the sub-sieve, the sizing of the overflow and underflow was carried out using sedimentation hydrometer techniques. Several analyses were repeated using the Andreasen pipet method and no serious differences existed. The sizing data were standardised using an arbitrary fixed $\sqrt[4]{2}$ series of reference sizes and this procedure was carried out by interpolation of the cumulative size curve assuming that the Gaudin-Schumann relationship existed between the measured points. It was claimed that the standardisation technique used introduced an error in the sizing data which affected the determination of the classification index m.

University of Cape Town

Discussion

Plitt used a factorial design to organise his experiments, which is a very useful technique in isolating effects of different parameters compared to the one variable at a time method and reduces the number of experiments required to establish useful relationships from the data. Nageswararao et al. [42] have done a thorough assessment of the Plitt model and compared it to the Nageswararo model and concluded

that both models are useful provided they are fitted with the data obtained under the conditions close to those to be used in future.

Plitt's model is not presented in dimensionless form and apart from being purely empirical, it is dimensionally inconsistent. Like many other workers Plitt used the cut size (d_{50}) as a measure of size classification. Plitt used an exponent m in a Rosin-Rammler type of equations as a measure of sharpness of separation and correlated it to the cyclone diameter D_c, free vortex height h, and the underflow to throughput ratio. However, he admitted poor correlation due to errors particularly in the particle size standardisation procedure.

From Plitt's work the determination of the classification index m was affected by scatter resulting from the standardisation procedure indicating that when converting the sizing data obtained using one sizing technique to another, it is generally incorrect to assume a Gaudin-Schumaan relationship without testing if the relationship holds for the data. The errors introduced through this method are difficult to trace and usually not quantified. Therefore, it wouldn't be prudent to say the error in Plitt's sizing data was very small.

Plitt derived his model using a laboratory set-up and solids density was not specifically investigated in his work. Furthermore, his model assumed a laminar settling relationship, which is not always the case. There is enough evidence at present indicating that hydrocyclones in the mineral industry operate in the turbulent flow regime (Pattersen and Herbst, [44], Neese et all., [45], and Monredon *et al*, [46]). This area deserves further studies, particularly in relation to slurries that contain minerals of differing densities.

The most important conclusion from Plitt's work is that his model equations clearly reveal the independent effects and relative importance of most of the major variables that influence the operations of the hydrocyclone. The feed solids content was found to be the variable that influenced the magnitude of the cut size (d_{50})

University of Cape Town

the most. It was felt that the principle reason was that the effective pulp density increased with increasing solids content. Other factors were hindered settling and underflow crowding (Fahlstrom, [22]). The vortex finder diameter was the second most important variable, which affected the cut size.

2.2.9 Hydrocyclone to give a highly concentrated sample of a lighter dispersed phase

Colman, D. A, and Thew, M. T, 1980 [47].

The Southampton programme on separation using cyclones include the design of units that are used for the separation of lighter dispersed components from liquid. In some cases the primary objective is to maximise the concentration of the dispersed component or to achieve a high yield and quality of a cleaned stream is required (Kimber and Thew, [48]).

If the standard Southampton design was used, indications are that even if all the oil were to be concentrated in a flow 5% of the influent, a low concentration ratio of 20 would be achieved compared with the required ratio of 100. Colman and Thew were requested to develop a hydrocyclone design that would meet the requirement of producing a high concentration of the lighter dispersed component and high quality of the cleaned component. The development of the cyclone with the co-axial overflow for the separation of oil from water is discussed in their paper. Although the discussion is centered on the separation of oil from water, the authors claim that some tests were performed using suspensions of polypropylene.

For their application, a mass balance around the hydrocyclone with steady flow yielded equation 2.38. Rearranging and substituting for the separation efficiency led to equation 2.39.

$$Q_i k_i = F Q_i k_o + (1 - F) Q_i k_c \tag{2.38}$$

University of Cape Town

$$\frac{k_o}{k_i} = \frac{\varepsilon}{F} + (1 - \varepsilon) \tag{2.39}$$

where F - split ratio $=\frac{Q_o}{Q_i}$

F_1 - split ratio $=\frac{Q_{o1}}{Q_i}$

F_2 - split ratio $=\frac{Q_{o2}}{Q_i}$

k - concentration of the dispersed component (by volume)

Q - volumetric flow rate

ε - separation efficiency $= 1 - \frac{k_c}{k_i}$

c - cleaner outlet (depleted dispersed component)

i - inlet

o - overflow (concentrated dispersed component)

o_1 - annular overflow outlet

o_2 - co-axial (central) overflow outlet

The term on the left hand side is the concentration ratio which was required to be higher than 100. Typical results for a 30mm cyclone operating with Kuwait crude oil in fresh water at 15°C (F= 10% and d_i =41μm) gave a separation efficiency of 0.89. After substituting for the concentration ratio and the separation efficiency values into equation 2.39, it was observed that the second term was negligible and the expression could be approximated to equation 2.40.

$$\frac{k_o}{k_i} = \frac{\varepsilon}{F} \tag{2.40}$$

The separation efficiency was found to be a weak function of the inlet flow rate Q_i, raising slowly with flow rate, but at a decreasing rate. To increase the concentration ratio ($\frac{k_o}{k_i}$), F has to be decreased but when F reduces to a few percent it was observed that the value of ε decreased to a very small value. It was concluded that the concentration ratios higher than 100 were not attainable with the standard Southampton cyclone.

University of Cape Town

Modifications to the geometry were considered based on the flow within the hydrocyclone. In the Southampton designs for light dispersion removal, there was no projecting vortex finder and the axially reversed flow was allowed to leave via a port in the overflow end wall. Two reasons were given why this flow had to be removed:

(1) it carried the oil with it in what appeared to be a continuous thin thread, but believed to be discrete droplets

(2) if axially reversed flow was not removed at an adequate rate the vortex core became unstable, broke down and most of the oil was remixed and discharged at the underflow.

Since the oil was concentrated at the centre of the core it was suggested that the overflow outlet be split into two. An annulus that would remove flow necessary for maintaining a stable vortex core, and an inner co-axial outlet that would take out flow carrying the oil. The schematic showing the arrangement of the co-axial outlets is given in figure 2-3.

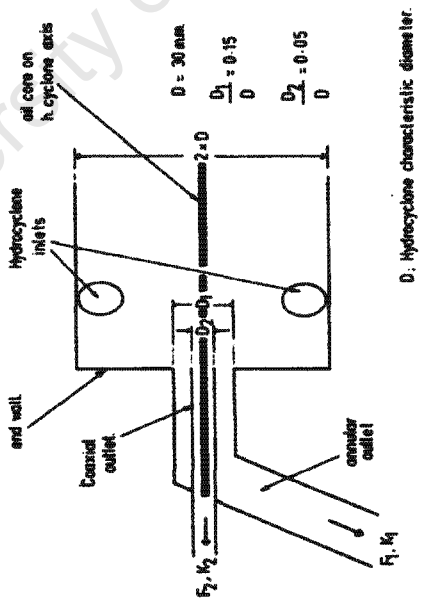


FIGURE 2-3. Coaxial outlet configuration for the hydrocyclone used in the separation of oil from water (figure by Colman, D. A, and Thew, M. T, 1980).

University of Cape Town

It has been found that the annular outlet had a dispersed component concentration k_{o1} which was approximately equal to k_i. The concentration ratio for the co-axial overflow was calculated using equation 2.41. As $F_2 < F$ higher concentration ratios could be obtained using the co-axial arrangement.

$$\frac{k_{o2}}{k_i} = \varepsilon(\frac{1-F}{F_2}) \tag{2.41}$$

The hydrocyclone was constructed using perspex to allow observation of the oil core formed along the axis so that the operations can be controlled to establish the optimum conditions easily. The central outlet in the coaxial arrangement was made from 1.5mm bore hypodermic tubing and the cross section of the annulus was made with the same area as the original outlet.

For the test where F_1 was raised to 10%, it was reported that some of the oil in the core was seen to be diverted into the annulus and this was confirmed with their oil content measurements.

From the comparison of the two cyclone designs it was observed that the separation efficiency of the standard cyclone deteriorated with increase in the flow split while the cyclone with the co-axial overflow was close to the 90% oil removal limiting curve. At split ratios of 2 the concentration ratio for the standard Southampton design was almost zero and increased to a peak value of 30 at a split ratio of 2.5 and then deteriorated with further increase in the split ratio. The trend for the cyclone with the co-axial overflow showed a concentration ratio of 135 at the split ratio of 0.4% and increased to a maximum of 160 at split ratios between 0.5% and 0.6% before dropping down steadily with further increase in the split ratios to a minimum of 80 at the split ratio of 1%. It can be concluded that the cyclone with the co-axial overflow had a substantially superior percentage of oil removal compared to the standard Southampton cyclone.

From the flow patterns shown in the paper, apart from the two distinct regions

University of Cape Town

of the downward and upward flows the upward flow was subdivided into two:

$0.05 < \frac{R}{R_w} < 0.5$ where $\frac{V_z}{V_{\tilde{z}}} \sim$ - 1, in the annulus region, and

$\frac{R}{R_w} < 0.05$ where $\frac{V_z}{V_{\tilde{z}}} \sim$ - 4, in the central core region of the coaxial

The central region was hypothesised to be the region of solid body rotation on the axis of which the lighter dispersed phase was collected and carried rapidly to the overflow outlet.

It appears that Colman and Thew were convinced that the results obtained from their tests could be improved upon by further adjustments to the flow split between the central and annular discharge of the coaxial arrangement. It was pointed out that hydrocyclones incorporating a co-axial outlet were difficult to control due to the extra product stream. Density differential and the size distribution of the dispersed material were seen as major factors influencing the concentration ratios when applying the co-axial cyclone.

Discussion

The study by Colman and Thew showed that the flow split between the two overflow streams was critical in the application of a cyclone which has two overflows in the co-axial arrangement. If the flow split was incorrect the desired results were not attainable. In the experiments conducted by Colman and Thew, the air core was not allowed to develop. It is doubtful if experiments with such a small inner vortex finder would succeed if they were to allow the air core to form. Due to the absence of the air core the dimensions for the two vortex finder orifices are likely to be different to those required for applications where the air core is allowed to form.

The three product cyclone has many similarities with the co-axial cyclone and it appears that although the two cyclones are used for different applications, the separation requirements are influenced by the same factors. Colman and Thew acknowledged the difficulty associated with the control of the cyclone with three products but did not elaborate how they managed to achieve steady operations during the

University of Cape Town

testwork. Control is a major issue for industrial applications and this author would have appreciated more details on the control aspect during the work.

The flow studies conducted do provide some insight on the differences in the velocities between the central core and the annular region, but the information is inadequate in describing the mechanisms that give raise to those differences. Although it is evident that the flow structure for the central core and the annular region are different, it is felt that the flow results presented in their paper can not be used to describe separation in the co-axial outlet cyclone. Although it was mentioned that density differences were critical in the operation of the co-axial cyclone, its influence was omitted in the discussion of the flow structure.

Colman and Thew have shown that a cyclone modified to produce three product streams from the feed streams had superior performance over the standard two product hydrocyclone in the application of separating oil from water. Their paper showed that a cyclone with three outlets was a better option for separating dispersed phases with different density components.

2.2.10 Water De-Oiling in an Air-Sparged hydrocyclone

Jan Miller and Jan Hupka, 1982 [49].

A type of hydrocyclone which was initially developed at the University of Utah for the minerals application but later modified to be applied in the separation of oil from water was reported by Miller and Hupka. This device combines classification characteristics of hydrocyclones and flotation characteristics of columns as a technique for fast flotation of minerals. It has been fittingly referred to as a hydrocyclone (Svarovsky [30]) and a column flotation cell (Goodall [50], and Breed [51]) in classification and flotation studies, respectively. The basic features of an air-sparged hydrocyclone are given in figure 2-4.

University of Cape Town

It consists of a feed inlet, a long cylindrical body, a short vortex finder, and orifices for the discharge of the overflow and underflow products. What makes it unique is that the cylindrical part consists of two concentric cylinders - a non-porous outer cylinder and a porous walled inner cylinder through which air is sparged orthogonally to the tangentially flowing slurry. The non-porous outer cylinder ensures equal distribution of air through the porous walled cylinder. Several designs incorporating the unique features of the air sparged cyclone were tested and the design in figure 2-4 was found suitable for the application in mineral flotation.

In terms of operation, fine particles requiring high force fields to float are fed tangentially through the fed inlet, pass through the separator as a thin layer in swirl flow and travel downward countercurrent to the froth phase which moves upwards in the center of the cyclone. The hydrophilic particles are thrown towards the porous cylinder and are discharged through the underflow while hydrophobic particles attach to the air bubbles sparged radially through the porous wall and travel upwards into the froth phase and are ejected through the vortex finder to the overflow stream. The high shear force at the cyclone wall is believed to generate small air bubbles and provides the high probability of particle/bubble interaction. From the features of the air-sparged cyclone, it can be concluded that the design concept is a mixture of the cyclone and column flotation cell mechanisms in one unit (Breed, [51]).

University of Cape Town

The expression used to calculate the overall separation efficiency E for the oil - water separation with classical hydrocyclone is given in equation 2.42. The same equation was used to evaluate the performance of the air-sparged hydrocyclone

$$E = \frac{Q_o(x_o - x_f)}{Q_f(1 - x_f)} + \frac{Q_u(y_u - y_f)}{Q_f(1 - y_f)} \tag{2.42}$$

Where:

Q_f, Q_o, Q_u - Volumetric flow rate in the feed, overflow, and underflow, respectively

x_f, x_o - Volumetric fraction of oil in the feed and overflow, respectively

y_f, y_o - Volumetric fraction of oil in the feed and underflow, respectively.

The results presented in the paper indicated that the retention time for copper was reduced considerably from the order of ten minutes to under one second and the air-sparged cyclone was superior in terms of capacity.

Discussion

The air-sparged cyclone used in mineral flotation was modified for the application of removing oil from water. Although the application of de-oiling is not of interest to this study, the modification performed to an earlier design is worth consideration. A schematic of the modified design of the air-sparged cyclone for the water de-oiling application is presented in figure 2-5. Other designs of hydrocyclone have been successfully used to separate small amounts of finely dispersed oil in water (Colman et al, [47]).

From the conclusions, it appears that the that the improved air-sparged hydrocyclone was useful for the separation of materials when the density difference between the phases being separated was significant.

The features of interest in this design are the off take pipes for the overflow and underflow product streams. The underflow is discharged through the annulus outside the overflow orifice. This is similar to the overflow arrangement in the three product cyclone where the inner overflow is discharged through the inner vortex finder and the outer overflow is discharged through the annulus between the inner and outer overflow pipe. The differences in the air-sparged cyclone used for minerals flotation and that used for the water de-oiling application highlights the need to change the cyclone design to suit the application. The paper by Miller and Hupka has demonstrated that different designs of the overflow can be achieved to allow for two products to discharge at the roof of the cyclone. Changing aspects of the cyclone design to suit the application assists in developing concepts of hydrocyclones that are more efficient than the conventional hydrocyclones for specific separation requirements.

University of Cape Town

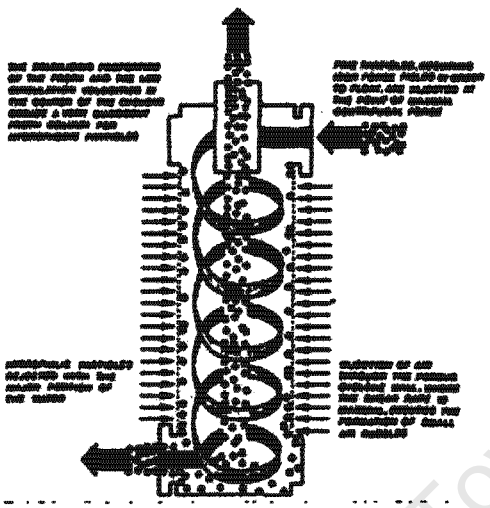


FIGURE 2-4. An air-sparged cyclone used for flotation in a centrifugal field (Figure by Jan Miller and Jan Hupka, 1982).

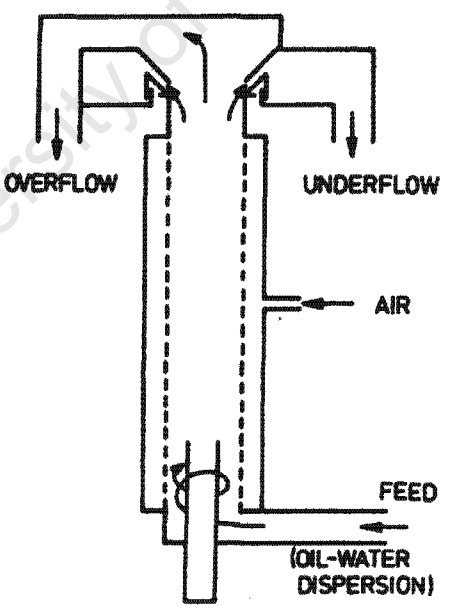


FIGURE 2-5. Modified design of the sparger hydrocyclone for the flotation of oil from water.

University of Cape Town

2.2.11 *The effect of two-stage hydrocyclone classification on mineral processing plant performance*

R. D. Peterson and J. Herbst . 1984 [44].

This paper reported that cyclones are not perfect separators due to turbulence, which causes eddies within the hydrocyclone, and leads to poor separation. In addition, the medium water contributes to imperfect separation in the hydrocyclone. In most cases small particles are carried to the underflow by the water used as the separation media, a situation commonly referred to as short-circuiting through the cyclone. Fine particles returning to the mill through the cyclone underflow result in loss of mill capacity, increased energy consumption by particles being needlessly broken, and poor performance in down stream processes such as flotation where sliming causes loss of recovery.

A number of methods have been proposed to correct the inadequate separation in the conventional hydrocyclone. These methods were classified into two categories. The first category improves separation by changing cyclone components or by water addition at critical points within the hydrocyclone (Kelsall [52]). The second category involves reclassifying a product stream of the hydrocyclone [53].

This paper was concerned with the latter category and it presents the findings from the various aspects of two-stage classification investigated. The experimental results were analysed using a mineral processing plant simulator which was developed at the University of Utah called SIMPLANT . Other important variables that were investigated include mill circulating load, sharpness of classification, water addition, and flotation circuit grade and recovery.

Sampling campaigns were conducted on two stage grinding circuits and a model was developed. Several two-stage classification configurations were evaluated with the aid of the models in the SIMPLANT simulator on the basis of undersize and oversize particles sent to the flotation circuit. Maintaining the mill feed constant,

University of Cape Town

it was found that the proportion of fines returned to the mill decreased and that would consequently result in an increase in mill capacity. It was found that a greater percentage of particles of the desired size range could be sent to the flotation circuit. Since the increase in grinding is one aspect of the process, two stage classification can be considered to be effective if the performance of the entire mineral processing plant is improved.

Four possible configurations for two-stage hydrocyclone classification were identified. In the first case, make-up water was added to the underflow of the first hydrocyclone and fed to the second hydrocyclone and the two overflows were combined to give the final product and the underflow from the second cyclone was returned to the mill (figure 2-6a). In the second case, the overflow stream of the first hydrocyclone plus any additional make-up water became the feed to the second hydrocyclone in the circuit and the two underflows were combined and returned to the mill while the overflow from the second hydrocyclone was sent to the flotation circuit (figure 2-6b). The third case involved feeding the underflow from the first cyclone to the second, but the overflow from the second cyclone was recirculated back to feed the first hydrocyclone in the circuit. The underflow from the second hydrocyclone was sent back to the mill while the overflow from the first hydrocyclone reported to the flotation circuit. The fourth case evaluated was similar to the second case except that the underflow from the second hydrocyclone was recirculated back to the first hydrocyclone.

Paterson and Herbst were of the opinion that the first and third cases would improve separation since fine particles that by-pass the first hydrocyclone pass through a second hydrocyclone hence lowering the overall by-pass of fine particles through the hydrocyclone. The second and fourth cases were thought to give poorer separation since fine particles were given two opportunities to short-circuit into the underflows of the two hydrocyclones.

The basic principles of two-stage cycloning involve either adding water to the un-

University of Cape Town

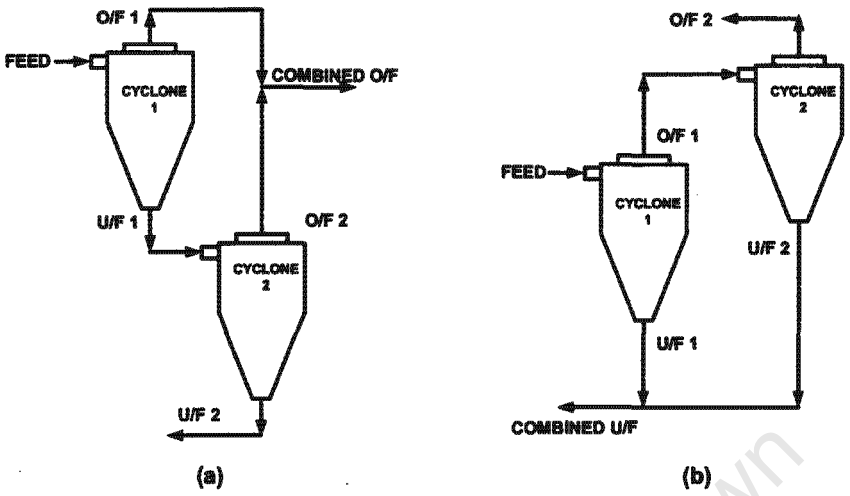


FIGURE 2-6. Two stage hydrocyclone classification configurations.

derflow stream of the first stage and feeding it to the next cyclone and combining the overflow streams from both the first and second cyclones to form the final overflow stream, or adding make up water to the overflow stream from the first cyclone and feeding it to the second cyclone, while the two underflow streams are combined and returned to the mill. It was noted that many configurations of multi-stage cycloning can be obtained, but they are all based on the principles in the two cases mentioned above (Dahlstrom and Kam [54], Kelsall et al. [55]).

It was pointed out that to accurately evaluate one-stage versus two-stage classification, it is important to test the configuration in conjunction with a closed grinding circuit followed by a flotation circuit. This is difficult to achieve on an industrial plant as well as at a pilot plant due to the cost involved as well and extended down time required to change the circuit configuration. The difficulty associated with running the industrial plants at steady-state which may sometimes require a sophisticated control system was also noted as one of the obstacles in conducting such testwork (Rogers et al. [56], Stratton [57]). To overcome these problems, they chose to use a mineral processing simulator. The computer program used consists a combination of several unit operation models which were available. Among the unit operation

University of Cape Town

models included in the simulator were a cyclone model, a grinding liberation model, and a flotation model.

The results from the testwork showed that the percentage liberation of chalcopyrite in the combined overflow of the two stage was essentially the same with that of the single stage and so were the flotation circuit's grade and recovery. However, some important changes were noted such as the reduction in the circulating load from 195 to 100%, and the percent solids in the underflow from 78 to 63%. It was concluded that the changes were an indication of a cleaner separation obtained with the configuration where make-up water was added to the underflow of the first cyclone and fed to the second cyclone and the two overflows combined to give the final product whereas the underflow from the second cyclone was recirculated to the mill.

Discussion

Although Paterson and Herbst claimed that a well tested mineral processing simulator (SIMPLANT) was used, the models for liberation and flotation are still in their infancy at this stage. It is therefore doubted if the liberation results from those models were adequate for evaluating the performance of the circuit. However, empirical and semi mechanistic models for most of the unit operations have proved to be useful in predicting the performance of many circuits (Dahlstrom [13], Bradley [58], Lynch and Rao [23], Plitt [24], Mishrai [59]).

It would be justified if they used the models just to evaluate certain aspects of liberation and flotation. The use of a simulator can help to cut the cost of having to do more than necessary tests provided the models in the simulator are reliable and well tested. It is important to understand the limitations of the models so that the pitfalls of using them outside the range of application is avoided. Simulators can be helpful in evaluating the performance of mineral processing circuits and unit operations, however, it must be noted that simulators are only as good as the models behind them. The integrity of the data used in the simulators must be checked if

University of Cape Town

reliable results are to be obtained. Care must be exercised when collecting data for use in simulators and the validity of the simulator tested against the response of the circuits to changes in operating conditions. Simulators with tested models can be useful in comparing performances of different circuit configurations (Lynch [60]).

In order to evaluate the effects of a two-stage classification, a single-stage case was used as a basis for comparison. When evaluating the performance of one configuration versus another a true reflection of the performance can be achieved only if the operating conditions, such as the feed to the configuration being tested and to the base case, are kept the same. In the case of the multi-stage cyclone tests it would be useful to use a single-stage conventional hydrocylone as a basis for comparison.

The disadvantage of using a two-stage or multi-stage cycloning, is the addition of water to the underflow which might not be good for applications were the control of solids concentration is critical. However, if it is not desirable to have large particles in the overflow, configurations where the overflow is fed to the second cyclone might be useful. The two or multi-stage cycloning also suffers from the difficulty of having many units to control rather than just one.

The two stage configurations cycloning systems presented in the paper were used to either reduce the by-pass of fine material into the underflow or reduce the by-pass of coarse material into the overflow and none had a capability of simultaneously reducing the by-pass of fines into the underflow and coarse particles into the overflow. While for most ores it is helpful to implement either of the two options, the UG2 platinum ore requires a classification system which would achieve both simultaneously.

2.2.12 A high performance hydrocyclone design - The Twin Vortex finder

K. Heiskanen, A. Vesanto, and H. Eronen, 1987 [53].

The Twin Vortex cyclone from hereafter referred to as the TC cyclone is a com-

University of Cape Town

bination of two different cyclones. The main idea behind this type of cyclone is to reduce the high by-pass fraction, which is usually in the order of 10 - 30% in conventional cyclones and hence reduce the amount of fines that report to the underflow.

Heiskanen et al designed the TC cyclone based on the idea of water replacement first proposed by Kelsall, [52]. The first part of the TC cyclone is a conventional cyclone with the conical section replaced with a cylindrical part that has a larger diameter than the main body. This cylindrical part, which is the washing section has an adjustable central cone and water addition holes in it as shown in Figure 2-7 (the two illustrations in paper are put into one diagram by the author of this thesis).

The second part of the TC cyclone is an ordinary hydrocyclone whose function is to do solid-liquid separation to yield a cleaner underflow and a dilute fine overflow which can be recirculated to dilute the fresh feed to the cyclone resulting in an improved classification (figure 2-7).

. During separation in the first part of the TC cyclone, the coarse product enters the

washing section from the gap between the cone and the cyclone body. Water is added to the expanded body in such a way that a zone is created where the pulp density is lowered just at the gap. As the centrifugal velocity prevails, particles will circle into this zone and through it. Due to the difference in pulp density and depending on the volume balance in the washing unit, water will move upwards. This creates a balance between the forces resulting from the downward vertical velocity and upward water velocity. As a result, the small and light particles in the downward stream are swept back upward into the main body volume. Heavy and large particles move down the zone. They are then removed to the second part of the TC cyclone that separates material into the final coarse product and water that may contain some fines.

The aim of their study was to compare the performance of the TC cyclone with a conventional cyclone on both industrial and pilot plant scale. In their experiments

University of Cape Town

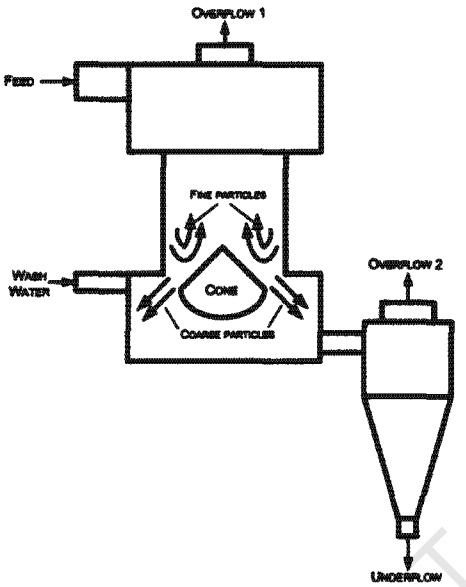


FIGURE 2-7. Schematic of the twin vortex cyclone.

the slurry from the TC cyclone could not be recirculated because the water in the products decreased the slurry densities and this could have adversely affected the feed densities. The parameters measured in the pilot and industrial plant tests were: densities of all pulp streams, feed pressure, amount and pressure of water added, and particle size distribution of all pulp streams. The separation efficiency curve was determined as the probability of coarse particles that report to the final underflow combining both overflows in the calculation. The reduced efficiency curves were calculated but did not differ significantly from the non-reduced curves for the TC cyclone. This was due to the relatively low amounts of by-pass fines.

Since the TC cyclone has three different products, the grade efficiency curve was not the best way to describe efficiency. As the TC cyclone is a low by-pass piece of equipment, mass recoveries were calculated but the fraction of by-pass was impossible to estimate from the water balance.

From the tests it was seen that the TC cyclone had certain benefits when compared to the conventional cyclone. The grade efficiency of the TC cyclone was found to

University of Cape Town

be better with all the test materials. In the TC cyclone, the by-pass of fines to the underflow decreased and the coarse product contained less fine particles compared to the conventional underflow. Unlike in conventional hydrocyclones, in the TC cyclone the separation limit can be adjusted while the unit is in operation by changing the amount of wash water. The pressure drop of the TC cyclone was found to be smaller than the pressure drop of the conventional cyclone.

Discussion

The TC cyclone technology produces three different products and although Heiskanen *et al* used the grade efficiency curve to evaluate its performance, they admitted that it was not the best way of describing its performance.

In their experimental work, it was not possible to re-circulate the underflow because the pulp densities were decreased due to the large amounts of water added in achieving the objectives of the work. In most milling circuits it is inescapable to re-circulate the coarse product to the mill to further liberate the valuable minerals. In the case of the TC cyclone, re-circulating the highly dilute underflow would lead to a drop off in milling capacity a condition that must be avoided. Since water affects the mass recovery of feed solids to various products, it is expected that the overflow in the TC cyclone will contain more fines compared to the conventional cyclone, but may be highly diluted and ending up being unsuitable for flotation which requires 30 - 40% solids by volume.

It was indicated the cut size for the TC cyclone increased with increased wash water. This shows that although an underflow stream devoid of fines could be obtained by increasing the amount of wash water to the cyclone, the overflow coarsened limiting the extend to which this could be of benefit.

The most outstanding improvement in the use of the TC cyclone is the decrease of the by-pass of fines to the underflow. Despite this improvement the two overflows and

University of Cape Town

the underflow may be too dilute for subsequent processes, rendering it impractical in industrial applications. Strictly speaking, the TC cyclone is a modified two stage cycloning system which fulfils the objective of obtaining an underflow devoid of by pass fines but might still suffer from coarse material in the overflow stream.

Despite the setbacks mentioned in the discussion, this paper has shown that there are a number of improvements needed in the cycloning technology to improve operating efficiencies.

2.2.13 The three product hydrocyclone for simultaneous separation of solids, both heavier and lighter than liquid medium.

Bednarski S. 1992 [6].

Bednarski was the first to report the concept of a cyclone that produces three distinct products from one feed stream termed 'the three product cyclone'. His paper presents the design and some basic operating principles for the three product cyclone (figure 2-8)which was used in the separation application in industrial processes treating petroleum, food, pulp, and paper. A few applications of that relatively new type of hydrocyclone for the separation of solids both heavier and lighter than water as well as other suspension systems were discussed and recommendations with regard to its operation were given.

Most of the operations involve separation of two-phase suspensions, whereas in some cases, suspension systems consisting of two or more solids with different densities need to be separated. Devices based on the action of various forces are applied for separation of systems in this category and sometimes different physical properties of solids and suspensions are improved in order to achieve effective separation. Due to many problems associated with separation, solutions were being sought to find other devices that can provide efficient and economical methods of achieving separation. From Bednarski's work, the three product hydrocyclones appeared to

University of Cape Town

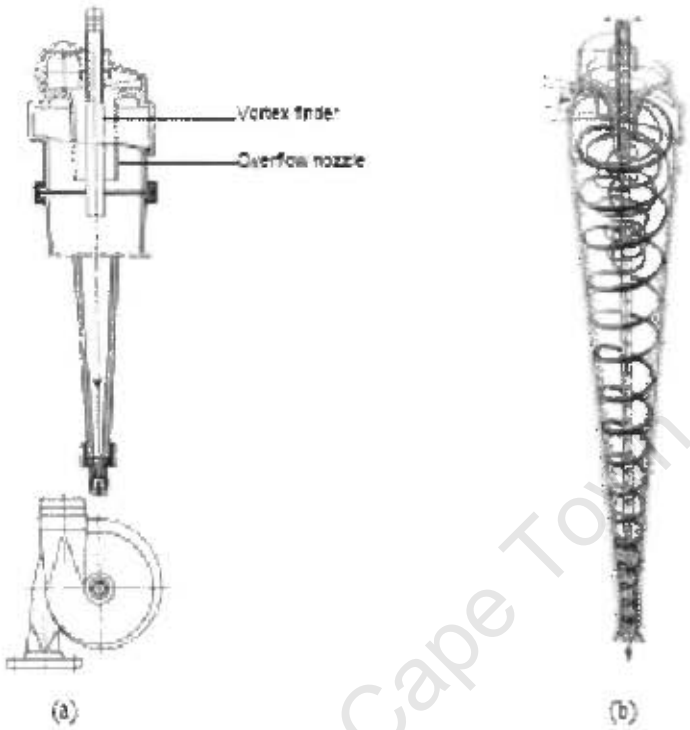


FIGURE 2-8. The design and operation of the three-product cyclone (Bednarski 1992)

be the kind of devices which distinguished themselves by high effectiveness, process intensity, low cost and simplicity in their construction.

The construction and operation principle of the three product cyclone does not differ considerably from that of the conventional hydrocyclone. After the removal of the inner vortex finder, it works like the conventional hydrocyclone which produces two products. Due to the circulating movement of the suspensions in the device, displacement of solid particles of different density takes place. The three product hydrocyclone can work within a wide range of pressures and from Bednarski's experience with the three product cyclone unit, it was mentioned that throttling the inner and outer overflows gave the advantage of not having to overcome the hydrostatic pressure of a column of 0.5 - 1.5 m, which to a high degree prevents plugging of the underflow hole and eliminates the air core in the hydrocyclone axis.

University of Cape Town

Selection of the diameter and other constructional parameters of the three product hydrocyclone depend on its application. For the three product cyclone to separate effectively, it was recommended that the feed inlet diameter should be in the range $D_i = (\frac{1}{6}$ to $\frac{1}{4})\ D_c$. Similarly the outer vortex finder and spigot diameters should be in the ranges; $D_{ovf} = (\frac{1}{4}$ to $\frac{1}{3})\ D_c$, and $D_u = (\frac{1}{15}$ to $\frac{1}{8})\ D_c$, respectively. Depending on the suspension properties, the inner vortex finder diameters should be in the range $D_{ivf} = (\frac{1}{20}$ to $\frac{1}{10})\ D_c$.where D_i, D_{ovf}, D_u, D_{ivf} and D_c are the feed inlet diameter, outer vortex finder diameter, spigot diameter, inner vortex finder diameter, and the cyclone diameter, respectively.

In the same paper, Bednarski came up with the following empirical equation for calculating the capacity for the three product cyclone, which was based on the measured flow rates:

$$V_n = K_B D_i D_{ovf} \left[\left(1 - \frac{D_i}{D_c}\right)\left(1 - \frac{D_{ovf}}{D_c}\right)\right]^{0.5} \times \Delta P^n \tag{2.43}$$

Where:

$$K_B = \left[0.21 + \frac{0.018}{\left(\frac{0.04t\varphi}{2}\right)}\right] \frac{D_c + 20}{D_c + 10} \left[1 - \frac{S}{D_c}\right]^{0.5} \left[\frac{D_c + L}{D_c + L_o}\right]^{\frac{1}{6}} \tag{2.44}$$

$\Delta P = P_o - P_p$, which is Pressure drop between the pressure before the feed P_o and the pressure in the overflow connector P_p of the hydrocyclone.

S - width of the feed inlet

L_{ovf} - immersion depth of the outer vortex finder

L - length of the cylindrical part of the cyclone

t - acceleration due to gravity

φ - cone angle

$n = B\xi \left(\frac{D_c}{d_o}\right)^m$

$B = 0.467$ – constant,

ξ - shape factor of the hydrocyclone head which for the discussed construction is

University of Cape Town

$\xi = 1$ and for all the others ξ is less than 1,

m is a coefficient depending on the roughness of the internal parts of a hydrocyclone, for smooth surfaces m = 0.12, for rough surfaces m is greater than 0.12.

It was concluded that the three - product cyclone is an off shoot of a conventional cyclone and that it can be applied in the separation of two, and three phase suspension systems. Despite the fact that the separation of three phase systems is complicated and usually requires devices that occupy a large space, the three product cyclone was viewed as a device that can be used to separate two, and three phase suspension systems with an advantage of occupying very little floor space and have a low capital cost and can be reasonably cheap on maintenance.

Discussion

Bednarski's paper is the only published work outside the AMIRA P9 project discussing the existence and application of the three product cyclone. Bednarski's work was based on the application of the three-product cyclone in the petroleum, food, pulp and paper industries. Most of his experiments were involved with separation of oil-water emulsions polluted with grease and solid particles like metallic fillings and non-metallic elements from the rubber abrasive disks.

The general ideas like the operation of the unit and design parameters are still applicable in the separation of minerals of different densities as mentioned in his conclusion. Bednarski did not permit the formation of an air core in the vortex finder, a situation that is almost inescapable in cyclones used in mineral processing operations (Rietema, [21]). He was of the view that large diameter three product cyclones were more efficient in the simultaneous separation of solid particles to give fines, middlings and coarse fractions as products, an application that has been investigated in this thesis.

Bednarski pointed out that flow rate measurements were important in the study of the performance of the three product cyclone as well as in the development of a

University of Cape Town

model to predict the volumetric capacity of the unit. In the design of the test rig for this thesis, the importance of obtaining reliable flow rate measurements in the operation of the hydrocyclone was realised and a provision for obtaining flow rate measurements from three of the four streams around the cyclone was incorporated in the design and building of the test rig for the testwork in this thesis. Furthermore, recommendations that were given regarding the inner, and outer vortex finder diameters provided a starting point for the experimental work.

The most important conclusion from his paper was the recognition that the three product hydrocyclone is just an offshoot of the conventional hydrocyclone which can be applied in the separation of two-phase and three-phase systems. This was an important conclusion in that most of the basic calculations for the three product cyclone can be done in the same way as a conventional hydrocyclone. It was stated in the paper that among the numerous units involved in simultaneous separation of three-phase mixtures, the three product hydrocyclone has the same advantages as the conventional cyclone of being the simplest, cheapest, most effective, lightest and occupying little floor space. This paper has shown that there is still a lot of scope in the area of classification using hydrocyclones and that certain modifications can be done on the conventional hydrocyclone so that separations involving multi-phase systems can be achieved using hydrocyclones.

University of Cape Town

2.2.14 The three-product cyclone - separation performance, potential applications and modelling.

Obeng D. P. 2003 [61].

In his work Obeng performed tests using three-product cyclones of 150 and 254mm diameters and supplemented his test data with 48 tests performed by the author of this thesis using a 600mm hydrocyclone in a parallel project, as acknowledged on pages 59 and 72 of his thesis, to assess and model the device. The first three-product cyclone in mineral processing tests for industrial application was invented

by Morrell [62] and Obeng's work was aimed at assessing if this device could be used to generate a more suitable feed for flash flotation, for use in fine separation application, in conjunction with micro screens to provide feed for flotation; desliming applications, and to achieve improvement of overall classification with respect to the denser mineral fractions in feed materials that have mineral mixtures. As part of the AMIRA P9 project his work also sought to provide a database that can help in the understanding of the likely mechanisms of separation in the three-product cyclone.

To assess the performance of the three-product cyclone on ore containing different densities, magnetite and silica mixtures which have densities of 4.7 and 2.7 respectively, were used. These minerals were chosen because they are of high purity and could be separated easily using a Davis tube without having to use assay methods. In addition to the tests performed at the JK Centre, Obeng conducted some tests at WMC's nickel operations to demonstrate potential applications of the three-product cyclone in providing feed for the flash flotation.

Obeng mass balanced his data using JKMBal incorporated in JKSimMet software by treating the three-product cyclone as two cyclones in series. However, an equation was given in his thesis that can be used to mass balance the three-product cyclone data as a single unit. This method using JKSimMet was utilised by the author of this thesis to mass balance the experimental data.

From the analysis of the data it was concluded that the three-product cyclone produces three distinct products depending on the length of the inner vortex finder Obeng showed that a number of variables have an influence on the separation performance of the three-product cyclone. The inner vortex finder length and the spigot diameter were found to be the critical ones. It was shown that increasing the inner vortex finder length resulted in the coarsening of the inner overflow product and a cross-over length was observed after which the inner overflow became the intermediately sized overflow and the outer overflow the finer product (figure 2-9). Obeng observed that the length of the inner vortex finder had a substantial influence on the

University of Cape Town

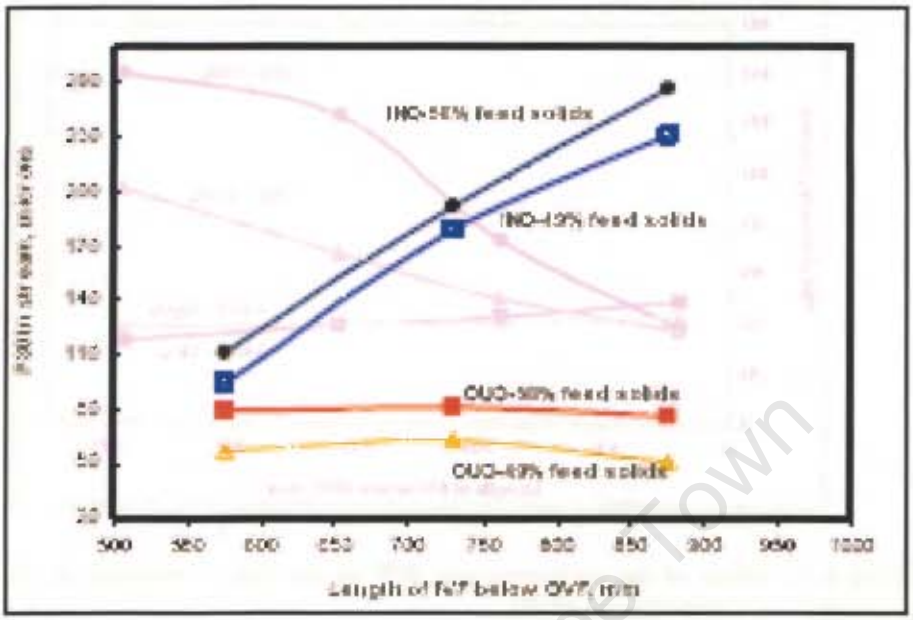


FIGURE 2-9. Effect of the IVF length on size distribution in overflows (Obeng 2003)

minerals in the inner overflow streams while the minerals in the outer overflow appeared to be unaffected (figure 2-10). It must be noted that Obeng performed most of the tests using long inner vortex finders extending below the cross-over length. The effect of the spigot diameter on minerals at different particle sizes is illustrated in figure 2-11 and figure 2-12. Obeng showed that at 45% solids there was a substantial difference between magnetite and silica in the inner overflow (figure 2-11. At 30 % solids the differences in the magnetite and silica were not as substantial as those observed at 45% feed solids (figure 2-12).

In assessing the potential applications, it was shown that the three-product cyclone could be used to provide feed that has a suitable size distribution for flash flotation. Using the three-product cyclone with an inner vortex finder length extended deep down into the conical section below the cross-over region, Obeng found that the percent solids and size distribution of the nickel and magnetite in the outer overflow stream (fines stream) were similar to those for a conventional overflow, and

University of Cape Town

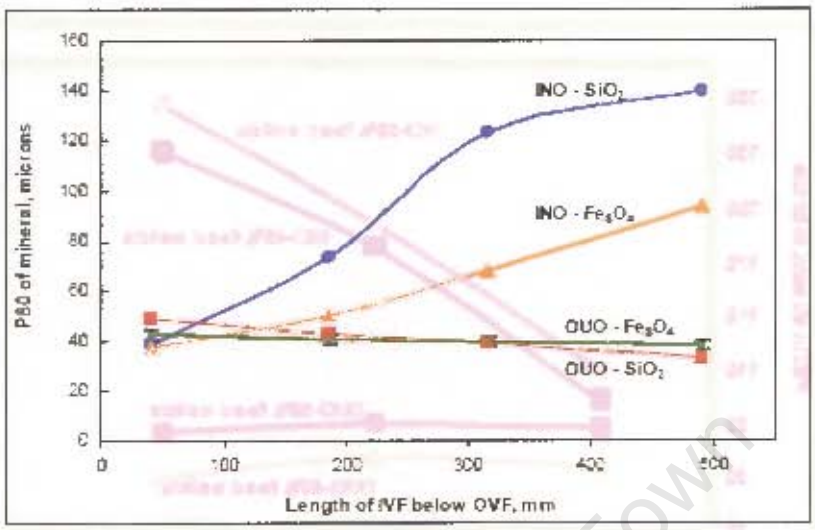


FIGURE 2-10. Effect of the cross-over and IVF on the size of minerals in the inner and outer overflow streams (Obeng 2003).

percent solids and size distribution of the nickel and magnetite in the inner overflow stream (intermediately sized stream) were substantially lower than those for the conventional hydrocyclone underflow, and were in the required range for a flash flotation feed.

The application of a micro screen to screen out the oversize material prior to flotation was assessed using results from simulations performed for the magnetite-silica slurry. From the simulation results Obeng indicated that the nickel and magnetite with the size distribution in the suitable range for the subsequent processing stage would increase by 13.5 % and 14 %, respectively, if the three-product cyclone was used and the undersize from the micro screen was combined with the finer overflow. It was concluded that the three-product cyclone was suitable for this application.

Using the experimental data, a model treating the three-product cyclone as two conventional cyclones in series was developed. Two methods of arranging the conventional cyclones in series were tested. In the first method the feed to the three-product cyclone was feed to the first cyclone to produce an overflow and underflow which

University of Cape Town

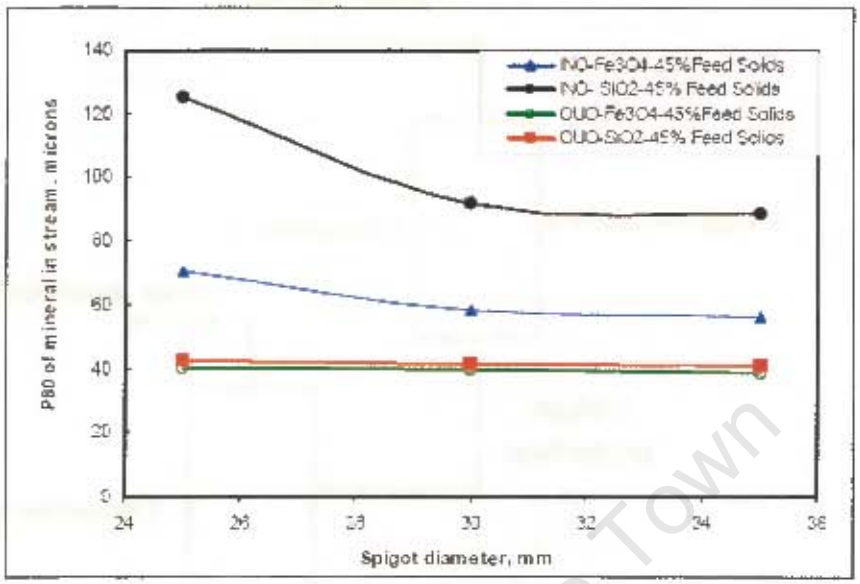


FIGURE 2-11. Effect of the spigot diameter on size differential between minerals in the overflow at 45% solids (Obeng 2003).

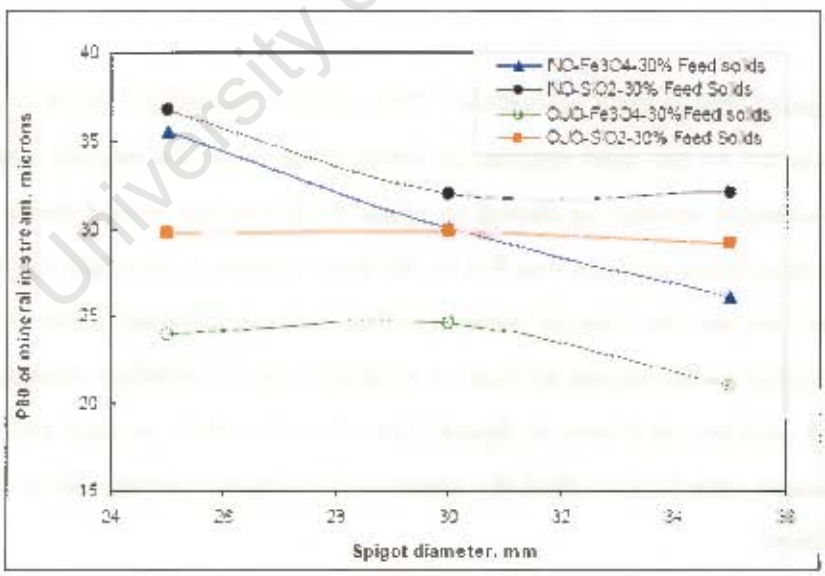


FIGURE 2-12. Effect of the spigot diameter on size differential between minerals in the overflow at 30% solids (Obeng 2003).

University of Cape Town

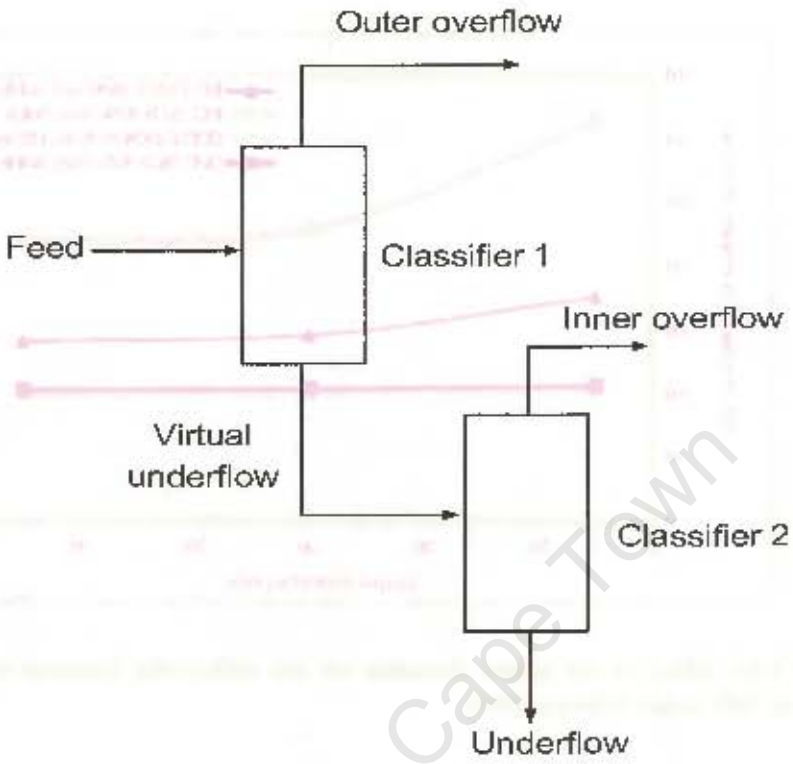


FIGURE 2-13. Conceptual model 1 of the three-product cyclone.

University of Cape Town

was termed 'the virtual underflow'. The 'virtual underflow' from the first cyclone was then fed to the next cyclone in series to produce the second overflow and the final underflow stream, as shown in figure 2-13. For the second method the feed to the three-product cyclone was fed to the first cyclone to produce the underflow and overflow termed the 'virtual overflow'. The 'virtual overflow' from the first cyclone was then fed to the second cyclone to produce the two overflow streams of the three-product cyclone, as shown in figure 2-14. This was done so that each classification stage can in turn be modelled like a conventional hydrocyclone using efficiency curve parameters.

After obtaining efficiency curve parameters, Obeng then modified the Nageswararao model [40] for the feed flow, d50c, water split and volumetric recovery, and Xiao's model [63] for the sharpness of separation, by incorporating the influence of the

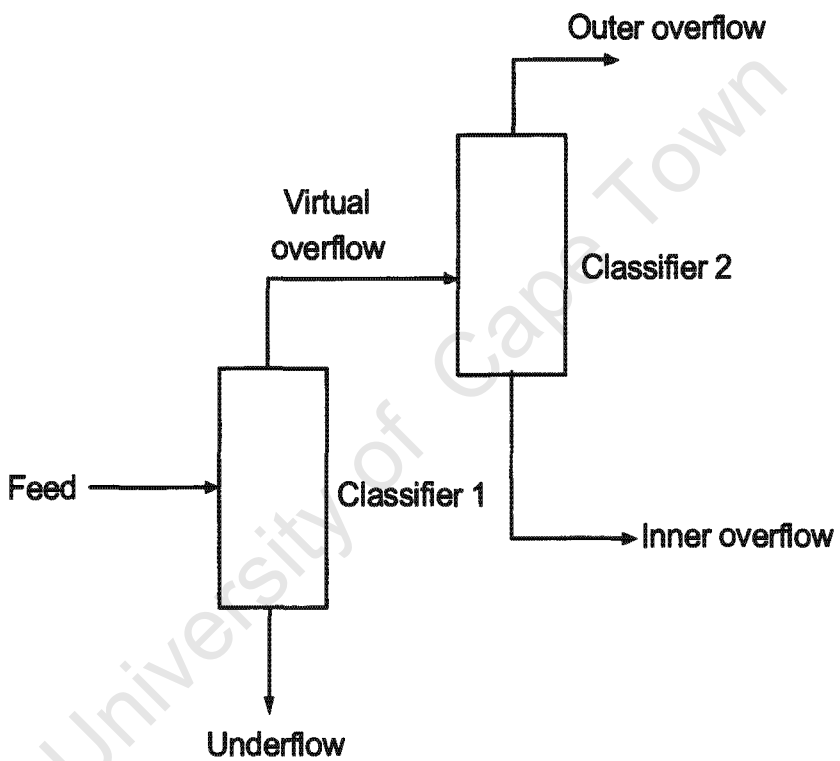


FIGURE 2-14. Conceptual model 2 of the three-product cyclone.

University of Cape Town

additional vortex finder. After testing the two methods of arranging the cyclones in series against the modified equations from Nageswararao and Xiao, it was found that the method of reclassifying the 'virtual underflow' fitted the data better. This method was then selected and used to develop the final model in his work.

The final model developed in Obeng's work comprise seven equations (equation 2.45 to equation 2.51) describing the:

- Q_f – volumetric feed flowrate (m3/h)
- $d_{50c}C1$ – first stage cyclone cut size (mm)
- $d_{50c}C2$ – second stage cyclone cut size (mm)
- R_fC1 – first stage cyclone water recovery to the underflow (%)
- R_fC2 – second stage cyclone water recovery to the underflow (%)
- $\alpha C1$ – first stage cyclone sharpness of separation parameter
- $\alpha C2$ – second stage cyclone sharpness of separation parameter

$$Q_f = \frac{72.65P^{0.59}{D_c}^{1.82}(D_i)^{0.01}\left(D_u^2 - D_o^2\right)^{0.08}\exp(-0.5076C_v)\left(\frac{LIVF}{H}\right)^{0.06}}{h^{0.36}\left(\frac{DIVF}{D_c}\right)^{0.08}} \tag{2.45}$$

$$d_{50c}C1 = \frac{13.66D_c^{1.52}\left(\frac{D_o}{D_c}\right)^{0.76}\left(\frac{D_u}{D_c}\right)^{0.10}\lambda^{0.85}\left(\frac{L_c}{D_c}\right)^{2.16}}{\gamma^{0.08}\left(\frac{D_i}{D_c}\right)^{0.22}\theta^{1.13}\left(\frac{LIVF}{H}\right)^{0.40}\left(\frac{DIVF}{D_c}\right)^{0.14}} \tag{2.46}$$

$$d_{50c}C2 = \frac{0.46D_c^{0.37}\left(\frac{D_o}{D_c}\right)^{2.28}\left(\frac{D_i}{D_c}\right)^{1.38}\gamma^{0.13}\lambda^{0.71}\theta^{0.17}\left(\frac{L_c}{D_x}\right)^{1.57}\left(\frac{LIVF}{H}\right)^{1.12}}{\left(\frac{D_u}{D_c}\right)^{0.90}\left(\frac{DIVF}{D_c}\right)^{0.28}} \tag{2.47}$$

$$R_fC1 = \frac{2.92\lambda^{0.16}\gamma^{0.09}\theta^{0.72}\left(\frac{DIVF}{D_c}\right)^{1.01}}{\left(\frac{D_o}{D_c}\right)^{0.82}\left(\frac{Du}{D_c}\right)^{0.35}\left(\frac{D_i}{D_c}\right)^{0.19}\left(\frac{L_c}{D_c}\right)^{0.57}\left(\frac{LIVF}{H}\right)^{0.42}} \tag{2.48}$$

University of Cape Town

$$R_fC2 = \frac{14.57D_c^{0.66}\left(\frac{D_o}{D_u}\right)\left(\frac{F_{40}}{D_o}\right)^{0.01}\theta^{0.20}\left(\frac{h}{D_c}\right)^{0.51}\left(\frac{LIVF}{H}\right)^{0.10}}{\mathrm{Re}^{0.19}\left(1-C_v\right)^{1.21}\left(\frac{DIVF}{D_c}\right)^{1.12}} \tag{2.49}$$

$$\alpha C1 = \frac{1.86\left(\frac{D_i}{D_c}\right)^{0.27}\mathrm{Re}^{0.11}\left(\frac{LIVF}{H}\right)^{0.22}\left(\frac{DIVF}{D_c}\right)^{0.24}}{\left(\frac{D_u}{D_c}\right)^{0.33}\left(\frac{h}{D_c}\right)^{0.27}} \tag{2.50}$$

$$\alpha C2 = \frac{0.46\left(\frac{D_u}{D_c}\right)^{0.14}\left(\frac{D_i}{D_c}\right)^{0.13}\mathrm{Re}^{0.20}}{\left(\frac{h}{D_c}\right)^{0.60}\left(\frac{LIVF}{H}\right)^{0.04}\left(\frac{DIVF}{D_c}\right)^{0.62}} \tag{2.51}$$

where:

D_c – cyclone diameter (m)

D_i – cyclone equivalent inlet diameter (m)

D_o – outer vortex finder diameter (m)

D_u – spigot diameter (m)

DIVF – diameter of the inner vortex finder (m)

LIVF – length of the inner vortex finder (m)

L_c – cyclone cylindrical length

θ - cyclone cone angle (degree), but in radians for the alpha equations

h – cyclone free vortex height (m)

H – cyclone total height (m)

C_v – volumetric fraction of solids in the feed slurry

Re – Reynolds number

F_{40} – feed 40 % passing size (mm)

F_{80} – feed 80 % passing size (mm)

λ - hindered settling correction term

$$y = \left(\frac{P}{\rho_p g D_c}\right)$$

P – cyclone inlet pressure (kPa)

University of Cape Town

ρ_p – cyclone feed slurry/pulp density $\left(\frac{t}{m^3}\right)$

Discussion

Obeng highlighted the presence of the cross-over length but did not discuss its importance in the choice of the inner vortex finder length for the three-product cyclone. His work focused more on the long inner vortex finders extended below the cross-over length and the recommendations presented were therefore biased towards that area.

Due to the non-availability of a pilot facility for the three-product cyclone to be operated in conjunction with the micro screens, Obeng recommended further work in this area. This is addressed in the present thesis.

Obeng modelled the three-product cyclone by using two cyclones in series to provide two overflow streams, so that the efficiency curve parameters for the conventional hydrocyclone can be used in describing the model for the three-product cyclone. It appears that the method may be suitable for the three-product cyclone where only two cyclones in series are required. If cyclones producing more products are developed it may be complicated to model such systems using conventional hydrocyclones in series. It is also a concern of this author that the best way of constructing the cyclone in series model would depend on the length of the inner vortex finder. Obeng's work was dominated by a long inner vortex finder, so naturally used a conceptual model that splits the underflow of the first cyclone. Additionally, the component data indicates that the three-product cyclone does not perform in the same way as cyclones in series, so in this thesis an alternative modelling approach is taken.

Obeng did not include an equation for predicting the flow split to the products of the three-product cyclone. Due to the presence of the additional vortex finder which results in three products, flow split is critical in the prediction of the performance of the three-product cyclone. This is an area to be tackled in this thesis.

University of Cape Town

Obeng performed work with mixtures of minerals and used the data in the discussion but the model does not include equations for predicting the cut size for the different minerals in the feed. In addition his model does not take into account the mineral components which were analysed in his work. In the application involving minerals of different densities [64], the prediction of mineral components which behave differently as shown in his analysis would consolidate the model capabilities. The aspect of modelling the flow splits to the overflows and the classification of different density mineral components is considered a critical area in extending the three-product cyclone modelling work, and will be tackled in this thesis.

2.3 Conclusion

The review of literature has shown that a lot of work has been done in terms of quantifying the performance of the hydrocyclone classifiers. It has shown that considerable effort has been devoted to improving the separation efficiency of hydrocyclone classifiers due to their ability to handle high throughputs while they occupy a small floor space. Although experimental work has been done on both small test cyclones and large industrial units, a large number of these experiments were conducted on small test units and scaled up to industrial plant units.

It was shown that despite its apparent simplicity in operation, the flow regimes in the cyclone are complex. This makes the task of developing a series of equations defining operating characteristics of cyclones or a mathematical model of cyclones based on hydrodynamic or theoretical considerations almost impossible. The difficulty associated with modelling hydrocyclones have been evident in the models reviewed and almost all the models endeavour to describe the cut-size rather than the overall performance or separation of the hydrocyclone. From the large number of experiments conducted, models have been developed where mathematical descriptions of separation and efficiencies within the hydrocyclone classifiers are given. These models are very useful for design purposes as well as in the prediction of a

University of Cape Town

range of operation conditions that are important in cycloning techniques. Although most of the models developed to date are empirical or semi-empirical, that suffer from a restriction in the range were they can be applied, the literature has shown that the development of these models has shed more light in the study of hydrocyclones and there is no doubt that numerous benefits can be derived by using these models.

The literature has highlighted some areas that need attention in improving the operation of the hydrocyclone unit and has shown that different modifications can be made to the hydrocyclone for use in a range of applications. Work has been done to try and improve cyclone performance by reducing the by-pass material to the products by injecting water in a section of the cyclone, using multi-stage cycloning, and in some cases types of hydrocyclones that produce three products have been used. Apart from being helpful in designing the test rig for use in the experiments and highlighting areas that could be modified on the cyclone, the literature was also useful in developing the experimental procedures for this test work.

The next chapter discusses the hydrocyclones used in the UG2 platinum ore classification circuits and the cyclone termed the three-product cyclone which has shown potential in addressing the classification challenges in this dual density ore.

University of Cape Town

3

Types of Cyclones Used for the Classification of the UG2 ore

3.1 Introduction

Hydrocyclones have been used for decades and the review of literature has shown that the unit was being investigated from as far back as 1949 [13]. According to Svarovsky [30], the first patent on conventional hydrocyclones used for the removal of gritty solids from water was obtained by Breteny in 1891 in the United States of America. However, hydrocyclones didn't receive much attention until Driessen started conducting work in the coal washing applications with these devices (Driessen [65]). It is now common practice in various industries to use hydrocyclones for different separation applications which include: liquid clarification, slurry thickening, solids classification, or sorting according to density or particle shape.

University of Cape Town

Due to the broad range of applications, it is expected that different cyclone designs and operation criteria are employed to achieve the objectives in various applications. The review of literature in chapter 2 has shown that several changes have been effected to the hydrocyclone over the years with a view to improving performance and to suit the needs of the different separation applications. In this chapter, the basic separation principles of the hydrocyclone are discussed and descriptions of the types of hydrocyclones used for the classification application on the UG2 platinum ore experimented with in this thesis are given.

3.2 Description of the conventional hydrocyclone

A conventional hydrocyclone classifies particles from the feed material into two products, namely, the cyclone overflow and underflow streams through the action of the centrifugal, drag and gravity forces on the particles. A schematic showing the main components of a conventional hydrocyclone is given in figure 3-1. These are discussed in detail in sections 3.2.1 to 3.2.5.

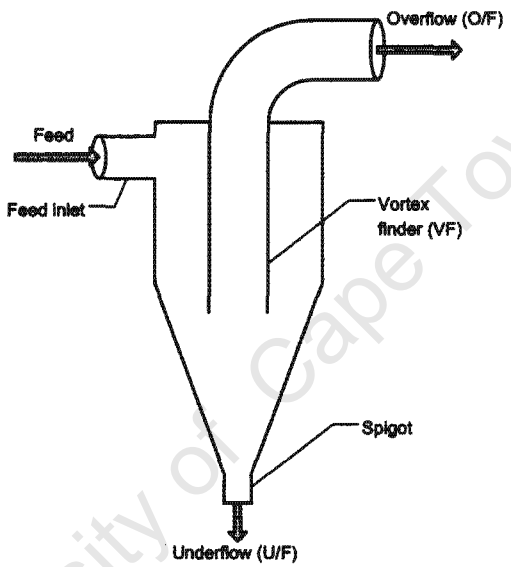


FIGURE 3-1. A schematic illustrating the main components of the conventional hydrocyclone.

University of Cape Town

3.2.1 Cylindrical section

The conventional cyclone is basically a cylindrical tube covered with a flat plate on top which has provision for inserting a vortex finder and mounting the overflow pipe. The cylindrical part is the upper section of the cyclone in which the inlet discharges the material and the vortex finder extend concentrically into this chamber. In conventional cyclones, it has been observed that a longer cylindrical section results in a finer separation with a decrease in the sharpness of classification. It is believed that hydrocyclones with longer cylindrical sections can handle higher throughputs at

the same pump speed. The size of the cyclone is quoted using the internal diameter of the cylindrical part.

3.2.2 Feed inlet

The inlet is the part through which feed slurries are introduced into the cyclone. The feed inlet pipe joins the cylindrical tube tangentially near the top of the cylindrical tube. The inlet area determines the entrance velocity of the particles. The pressure is measured at the point just before the feed enters the feed chamber of the cyclone, so a pressure gauge is usually situated at the feed inlet pipe to measure the operating pressure. Most cyclone inlets are rectangular in shape, and the entry can be effected in either tangential or involute forms. It has been shown in the literature that those with an involute type have a larger entry radius, which reduces turbulence and results in improved classification and a considerable reduction in wear (Trawinski [18]).

3.2.3 Vortex finder

The removable section called the vortex finder is inserted through the top plate covering the cylindrical tube and extends below the feed inlet. Apart from preventing short-circuiting of feed materials directly into the overflow stream, the vortex finder carries the cyclone overflow material out of the cyclone through the top where an overflow pipe is fitted. In most hydrocyclones, the vortex finder terminates well above the junction of the cylindrical section and conical section. For the hydrocyclones used in the UG2 ore longer vortex finders are preferred to minimise the excessive by-pass of coarse silica into the overflow caused by the density differences of the two main mineral components in this ore (Mainza et al. [66]).

3.2.4 Conical section

At the bottom of the cylindrical tube, a conical section is usually fitted for most of the hydrocyclones used in mineral processing. The function of the cone is to squeeze

University of Cape Town

the centrifuged solids towards the centre of the device to obtain a concentration of solids that are ejected through the spigot. Mular and Jull [28] observed that small cone angles give finer separation but at a decreased sharpness of classification . Large included cone angles ensure a coarse separation and low recirculating load. The conical part of the cyclone is usually made up of several removable parts bolted together to make a cone. This allows for replacement of worn out parts at a low cost. The conical part of the hydrocyclone has an included angle and for the conventional hydrocyclone this angle is normally less than 25°. The conical part of the industrial scale test hydrocyclone used in this work had an included angle of 20°. At the end of the conical section there is a removable outlet nozzle called the spigot or apex from which the material from the cyclone underflow stream is ejected.

3.2.5 Spigot and spigot holder

The spigot is mounted to the spigot holder located at the lower end of the conical section of the cyclone body. The spigot holder is usually designed to allow rapid replacement of the spigot. This could be done by loosening the clamp and twisting the spigot for clamp mounted spigots or undoing the screws and twisting the spigot for screw mounted spigots. Inspecting the lower end of the conical part of the cyclone for wear is easily done by removing the spigot. The spigot is made in such way that continuity is maintained between the spigot and the rest of the cyclone. Spigots used in the testwork were made from a highly abrasive resistant rubber material produced by Metquip.

University of Cape Town

3.3 Basic separation principles of the hydrocyclone

A typical hydrocyclone as discussed in section 3.2 contains no moving parts and separation in the vessel is achieved by pumping the slurry tangentially into the stationary cylindrical-conical body. The tangential pumping of the slurry into the hydrocyclone causes swirling and this generates centrifugal force within the device.

3. Types of Cyclones Used for the Classification of the UG2 ore

It has been shown that the separation action in the hydrocyclones is based on the centrifugal forces created within the body of the vessel (Arterburn, [34], Monredon et al. [46]).

The flow pattern in the hydrocyclone has two distinct helical flows with one moving downwards and the other upwards, both spinning in the same direction. A schematic illustrating the two helical flows in the hydrocyclone is shown in figure 3-2. The incoming fluid has been shown to flow downwards in a circular path in the outer region of the cylindrical part and then follows a helical path in the conical section of the hydrocyclone vessel. A portion of the fluid from the downward outer helical path discharges through the spigot while a portion of the flow reverses its vertical direction and joins the inner upward helical path and leaves through the vortex finder into the overflow at the top.

University of Cape Town

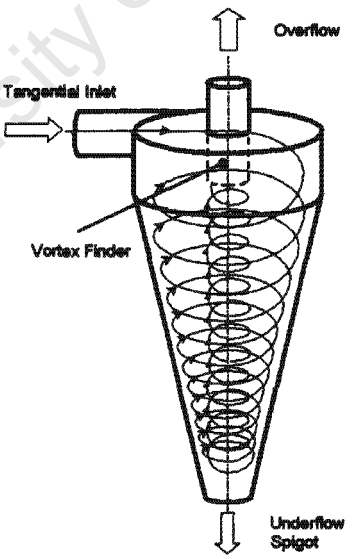


FIGURE 3-2. A schematic of the two unidirectional spirals in the coventional hydrocyclone.

3.4 Description of the flat bottom cyclone

The flat bottom cyclone is basically a conventional hydrocyclone with a long cylindrical section and an almost flat bowl shaped bottom as shown in figure 3-3 (Schmidt, [31]). The flat bottom cyclone has all the features of the conventional hydrocyclone except the conical section is either absent or has a large included angle rendering its influence on classification negligible. In the most common flat bottom designs, the conical section is absent and has a central discharge for the cyclone underflow stream as shown in figure 3-3. In some cases the cone angle in flat bottom cyclones can be 120° - 160° for structural strength reasons (Trawinski [29], [67]).

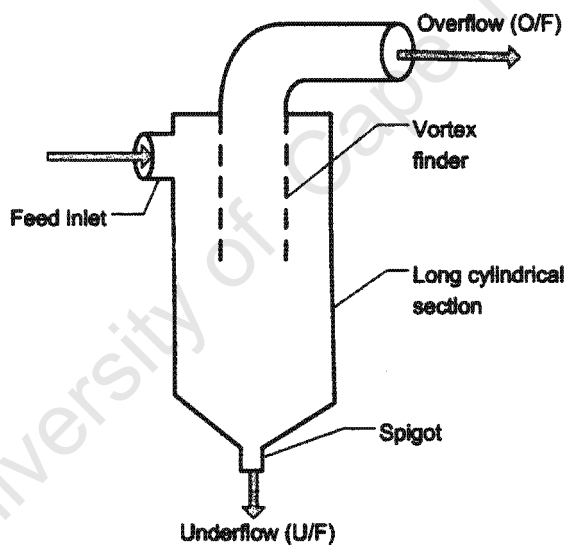


FIGURE 3-3. A schematic of the flat bottom hydrocyclone.

Hydrocyclones with large angles were shown to be widely applicable for purposes of sorting according to particle size and density (Rietema, [21], Svarovsky, [30]). Due to the classification problems caused by the big differences in densities between the chromite and silica components in the UG2 ore, flat bottom cyclones were adopted in some operations to promote classification by density and size (Mainza [66]). Results from the tests conducted in this thesis, which are discussed in chapter 6, have

University of Cape Town

shown that classification problems have not been resolved by the use of this type of cyclone. Trawinski [67], observed some convective circulating flow near the bottom of the cyclone which was attributed to the vortex being slowed down by wall friction (Svarovsky, [30]).

3.5 Comparison of the conventional and flat bottom cyclones

The efficiency curves from the stream size and assay data for the conventional and flat bottom cyclone are presented in figure 3-4. It appears that the flat bottom gives a coarser cut and the overall efficiency curve is flatter than that of the conventional cyclone of the same size. The corrected cut size for the flat bottom cyclone was 185μm while that for the conventional cyclone was 80μm. This agrees with the observations made by Schmidt and Turner [31].

It can be seen that both cyclones have a significantly high fraction of silica in the plus 100μm reporting to the overflow stream. The conventional cyclone had a corrected $d50_c(si)$ of 114μm while that for the flat bottom cyclone was 195μm. For the UG2 platinum ore which requires sub100μm particles for the flotation process, the coarse cut sizes given by the two types of cyclones would lead to a loss of recovery.

The corrected chromite cut sizes ($d50_c(cr)$) for the conventional and flat bottom cyclones were 78μm and 145μm, respectively. The flat bottom cyclone appear to be cutting coarser in general compared to the conventional cyclone. Having a coarser $d50_c(cr)$ for the UG2 ore has the advantage of entraining less chromite in the concentrate. The overall efficiency curve for the conventional cyclone tends to follow the chromite component in the sub 100μm size range and deviates towards the low density silica component at coarser sizes. For the flat bottom cyclone the silica, chromite and overall curve were similar in the fractions above 200μm and deviated with decrease in size.

University of Cape Town

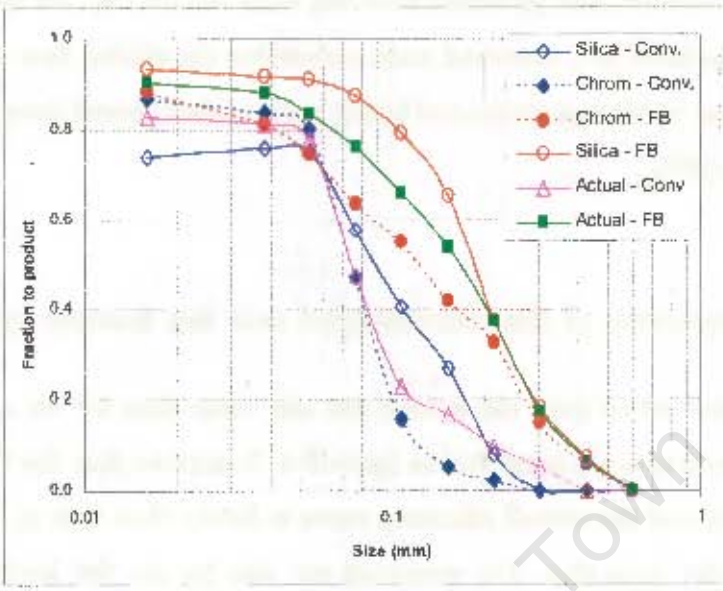


FIGURE 3-4. Comparison of the conventional and flat bottom cyclones.

3.6 Description of the three-product Cyclone

In addition to the attempts to improve the classification efficiencies in the UG2 platinum ore circuits using the flat bottom cyclones, different combinations of design variables have also been tested. In some cases, longer vortex finders - terminating deep in the cylindrical section of the hydrocyclones - have been installed, as opposed to common practice in the base metal industry - of using vortex finders that terminate well above the junction between the conical and cylindrical sections. Some plants operate with two stages of hydrocyclones.

Despite making all these changes in the design parameters of the hydrocyclone, the problems caused by the differences in the component densities of the UG2 platinum ore have not been resolved. The detrimental effects of classification by density in the conventional hydrocyclones motivated the AMIRA P9 project to look into alternative classifier designs or modifications to the conventional hydrocyclone that can provide improved separation by component density. One tool that could potentially be used to minimise or eliminate the dense media effect is the three-product

University of Cape Town

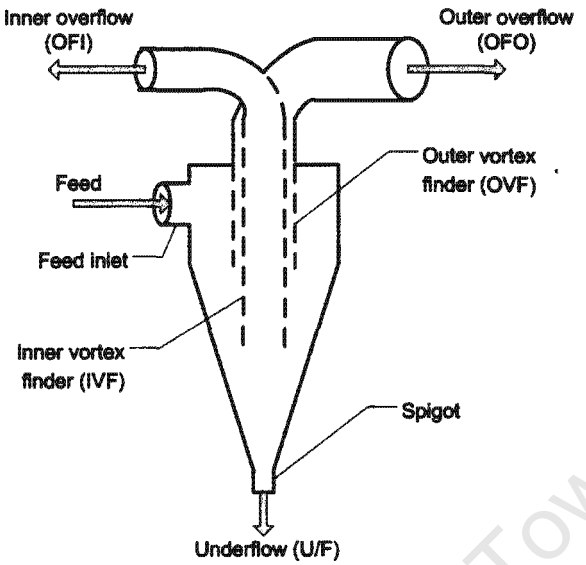


FIGURE 3-5. A schematic illustrating the main components of the three-product cyclone.

cyclone, Morrell [62].

This section gives a detailed description of a cyclone whose design has been altered to give three products instead of two, as with the conventional hydrocyclone. As mentioned in the first and second chapters, the three-product cyclone is just a modification of the conventional hydrocyclone with an additional vortex finder inserted concentric to the existing vortex finder in the conventional hydrocyclone [6]. A schematic of the three- product cyclone is given in figure 3-5.The existing vortex finder is termed the outer vortex finder (OVF) and the additional one which has a smaller diameter the inner vortex finder (IVF). The three-product cyclone contains all the parts described under the conventional cyclone.

The concept of the three-product cyclone developed from the need to produce three unique products from a single feed stream by using one unit. This type of cyclone produces fines from one of the overflow streams, middlings from the other overflow stream, and a coarse underflow stream from the spigot. The product from the inner vortex finder is termed the inner overflow (OFI) and the product from the annulus - the gap between the inner and outer vortex finder, is called the outer

University of Cape Town

overflow (OFO). To retain the conventional abbreviation of O/F for Overflow, the description of inner or outer is added after OF.

The major difference between the three-product cyclone and the conventional hydrocyclone is the insertion of an additional vortex finder concentric to the existing one which gives a third product stream. Due to the additional overflow product stream, the design of the overflow arrangement was modified to accommodate the additional vortex finder, and the outlet overflow pipe for this third product stream (Mainza et al. [68]). In terms of the operation, the three-product cyclone uses a smaller spigot and operates at a much higher pressure than a conventional cyclone of the same size (Obeng [61]).

Due to an increase in the number of product streams in the three-product cyclone, more measurements than those required from the conventional hydrocyclone test-work were required to obtain useful and quality data. However, taking representative samples and reliable flow rate measurements from large a diameter hydrocyclone is a difficult task and requires using carefully designed experimental apparatus. The next chapter discusses the design of new features which makes the three-product cyclone unique to that of the conventional, and flat bottom hydrocyclones, and the specially designed pieces of experimental apparatus which were used in the experimental work to evaluate the performance of the three product cyclone on both industrial and pilot plant scales.

University of Cape Town

4

Experimental Apparatus

4.1 Introduction

The previous chapter discussed the types of hydrocylones used in the UG2 platinum ore classification and a description of the three-product cyclone was given. The purpose of this chapter is to highlight the new features which makes the three-product cyclone design unique to that of the conventional and flat bottom hydrocyclones, and to describe the experimental apparatus used in both the industrial and pilot plant scale experimental work. Due to the differences between the commonly used hydrocyclone and the three-product cyclone, two separate test rigs for the industrial and pilot plant scale were specially designed and built to test the concept of the three-product cyclone in the classification of the UG2 ore.

The cyclone dimensions and the ranges of the design variables for the testwork performed using a 600mm cyclone are listed in Table 6.1.

4.2 The overflow arrangement for the three product cyclone

The major difference between the three-product cyclone and the conventional hydrocyclone is the presence of the extra vortex finder inserted concentric to the existing one to provide the third product stream. As a result of this a different overflow arrangement had to be designed to accommodate different diameter inner vortex finders. In this section, special attention is given to describing the changes made to the overflow arrangement to allow for two distinct overflow streams to be discharged simultaneously from the same hydrocyclone.

At the time this work commenced, three-product cyclones were installed at a num-

University of Cape Town

ber of concentrators in South Africa but none of those the author investigated were operational. These devices did not produce three distinct products in accordance with the concept of the three-product cyclone. An assessment was carried out by the author and it was realised that the major problem was the design of the overflow arrangement installed on these hydrocyclones.

4.2.1 Original overflow arrangement installed on the three-product cyclone

The original overflow arrangements installed on two of the three product cyclones were unsuccessful in producing the two distinct overflow streams required in the three product cyclone set-up. This was mainly due to the poor design of the original overflow arrangements used on both cyclones and two major problems were identified: firstly, the inner and outer overflow pipes diverged at different heights above the roof of the hydrocyclone resulting in a pressure difference between the two overflow outlet pipes. This resulted in little or no flow in the inner overflow stream whose overflow discharge pipe was much higher above the roof of the cyclone than that of the outer overflow. Secondly, the construction of the overflow pipes had sharp bends which caused turbulence that resulted in poor slurry flow and subsequently poor separation in the hydrocyclone.

University of Cape Town

4.2.2 Modified JKMRC overflow arrangement

To overcome the problems in the original overflow arrangement, an overflow arrangement design for the three product cyclone produced at the Julius Kruttschnitt Mineral Research Centre (JKMRC) was adapted and modified for use in large diameter cyclones treating material with a high chromite content. Plants treating high chromite content ores suffer from wear problems in slurry transport pipes, pumps and equipment like hydrocyclones and sumps. Therefore, provision for high wear rates had to be taken into account when making the overflow arrangement for the dual overflow cyclone.

Two major design considerations were followed in making the overflow arrangement. The first was that the inner and outer overflow pipes curved out at the same pipe-centre height from the roof of the cyclone to avoid differences in the pressure head between the inner and outer overflow discharge pipes ([69]). The overflow pipes were kept as close to the cyclone roof as possible to minimise siphoning problems that are associated with such overflow arrangements. The second was that no sharp bends were allowed in the overflow pipes, so as to minimise turbulence. The overflow pipes were designed to discharge freely into the flow rate measuring tanks at atmospheric pressure and were not allowed to extend below the roof of the hydrocyclone, so as to prevent siphoning problems.

4.2.3 The UCT overflow arrangement design

The UCT overflow arrangement design used in the testwork for this thesis incorporated all the design aspects discussed in section 4.2.2 and had additional features to allow for the installation and use of a wide range of inner vortex finder diameters with the same overflow arrangement. The critical features of this overflow arrangement are discussed in this section.

The overflow arrangement has two discharge pipes for carrying the inner and outer overflow separately. The outer overflow discharge pipe was made up of a 250mm-90° standard bend welded to a standard 250-200mm standard reducer pipe. A 200mm-90° standard bend was welded at the smaller end of the reducer to direct the flow into the flow rate measuring tank. The inner overflow discharge pipe was inserted into the 250mm standard bend with a collar attached at the end for mounting the inner vortex finder using the collar reducer system which is discussed in section 4.3.1. This was done to allow for a range of inner vortex finders to be mounted concentric with the outer vortex finder. A short 200mm pipe was welded on the other side of the bend before joining a 200mm standard bend for directing the flow into the volumetric flow rate measuring tank. Both the inner and outer overflow pipes curved

University of Cape Town

out at the same pipe-centre height from the roof of the cyclone and the products were discharged freely into the flow rate measuring tanks, which were open on top. A picture of the overflow arrangement (upside-down) used in the work is given in figure 4-1 and a photograph of the overflow arrangement being installed is presented in figure 4-5.



FIGURE 4-1. The UCT overflow arrangement for the industrial scale three product cyclone testwork.

The layout of the pipes in the UCT overflow arrangement design made it possible for any leaks in the pipes to be noticed immediately. There was enough clearance between the inner and outer overflow pipes to avert the danger of blockages in instances when there is tramp oversize in the overflow streams.

University of Cape Town

4.3 Inner vortex finder mounting techniques

The mounting mechanism of the vortex finders is critical in testing the large diameter three product cyclone in a production setup. Due to the importance of testing different vortex finder diameters and lengths, various designs incorporating interchangeable inner vortex finders without changing the entire overflow arrangement were investigated.

Welding the inner vortex finder to the overflow arrangement was one of the options that was considered and it was implemented when mounting the inner vortex finder to the overflow arrangement for exploratory tests to trial the concept of the modified overflow arrangement. However, using a welded joint to mount the inner vortex finder to the overflow arrangement would have made it very difficult to test a range of diameters and lengths for the inner vortex finder during the experimental work. It would have required cutting the tested vortex finder pipe and grinding the whole area prior to welding another pipe on to the overflow arrangement. It could have been difficult to maintain a smooth surface on the pipe if welding was going to be used for mounting the inner vortex finders. This could lead to turbulence at the joint, and wear rates could have been unduly high due to weakness at the joint resulting from the uneven surface created by the weld. Reduction in the inner vortex finder diameter without proper reducer mechanisms would be a problem with the welding option.

Grooves/slots were considered and rejected on the basis of the high wear rates that were expected in the region around the joint. Apart from allowing the material from one stream to flow into the other, grooves/slots could have provided a point of weakness in the vortex finder structure which could have lead to a reduction in its operational life span.

Threading the whole pipe with square threads was considered and it seemed to be a good option, but could not be implemented due to the large diameter pipes that were being used as inner vortex finders. Apart from the constraint of dealing with large diameter pipes, the test ore had a high chromite content and it was feared that if the chromite particles entered the thread, replacing the vortex finders at those large diameter pipes after each experiment could have been difficult. For the pilot plant cyclone, two collar-reducer system mounting methods were adopted. Two separate overflow arrangements were manufactured (figure 4-2) one set had a collar-reducer system whose collar was threaded with square internal threads and

University of Cape Town

the reducer had square external threads and the other set had grub screws with square threads.



FIGURE 4-2. The pilot plant overflow arrangement with the vortex finder mounted to the system.

University of Cape Town

After considering all the possible options, the collar and reducer system with grub screws was selected as the method for mounting the inner vortex finder for the industrial plant scale experimental work.

4.3.1 Collar-reducer system

The collar-reducer method with grub screws was the preferred method for mounting the inner vortex finder to the overflow arrangement for the industrial scale testwork and one of the two overflow arrangement sets for the pilot plant scale testwork. The collar and reducers for mounting the inner vortex finders were made at the central workshop at Eastern Platinum Limited. Two identical collars and eight reducers with different outlet diameters were made to accommodate a range of different diameter pipes used as inner vortex finders during the testwork. The reducers were made by machining out solid round bars of mild steel. The reducer fitted tightly to the collar to avoid flow of slurry from one overflow stream to the other during operation.

On each collar, eight equi-spaced M10 threads were tapped around it. The reducers



FIGURE 4-3. Photograph illustrating the machining of the collar and reducer

were made to fit the collar and on each reducer eight-M10 threads were tapped in positions corresponding to the threads on the collar. To make sure that the threaded holes in all the reducers matched those of the collar, the collar and reducers were placed in the work piece holder and the positions were carefully marked out using a dial gauge as shown in figure 4-3. Grub screws were used to hold the inner vortex finder to the overflow arrangement using the collar-reducer technique shown in figure 4-3. Grub screws had the advantage of fitting flush with the reducer after being screwed in position.

University of Cape Town

4.3.2 Arrangement of the vortex finders in the three product cyclone

The main functions of the dual vortex finders in the three product cyclone are to prevent the short-circuiting of coarse material into the overflows and to promote differential separation of the overflow streams by both size and component density. As discussed in section 3.4, the unique feature of the three product cyclone is the existence of two concentric vortex finders.

4.3.2.1 Outer vortex finders

The outer vortex finder was mounted in the same way as vortex finders in the conventional hydrocyclone. It was inserted into the cyclone from the roof and held in place by the bolts and nuts on the flange at the roof of the cyclone and the flange below the overflow arrangement, as in a conventional hydrocyclone. Standard vortex finders for a 600mm diameter cyclone, manufactured from highly abrasive-resistant rubber material produced by Metquip were used in the experimental work.

4.3.2.2 Inner vortex finders

For test purposes, inner vortex finders were made by welding different diameter non-standard thin section pipes to the corresponding reducers. The inner vortex finder was attached to the overflow arrangement using the collar and reducer system discussed in section 3.6. Eight grub screws were used to ensure that the inner vortex finder was held firmly to the overflow arrangement and was able to withstand high slurry flows associated with cyclones. The inner vortex finder descended into the cyclone body concentric to the outer vortex finder to maintain uniform flow of the slurry within the periphery of both vortex finders. Six pipes of different diameters were welded to the reducers to serve as inner vortex finders in this test work. A photograph depicting non-standard pipes welded to reducers to form inner vortex finders (before grinding the bottom edges smooth) is shown in figure 4-4.

4.3.3 Changing the inner and outer vortex finders

To change the inner and outer vortex finders, the overflow arrangement was hoisted up using chain-blocks as shown in the picture in figure 4-5. The outer vortex finder was removed by lifting it up and out of the cyclone while the inner vortex finder was removed by undoing the grub screws holding the reducer part of the vortex finder to the collar of the overflow arrangement.

University of Cape Town



FIGURE 4-4. A photograph showing a range of inner vortex finders

4.4 Description of the industrial scale test rig

The industrial scale experiments were conducted at Eastern Platinum Concentrator, a Lonmin concentrator which treats UG2 ore mined from three different underground shafts. The concentrator has two treatment plants termed A and B section. Each section has primary and secondary processing stages in a mill-float and then mill-float configuration. The testwork was conducted on the material from the secondary mill of B section. The set-up of the test rig is discussed in sections 4.2.1 to 4.2.7.

4.4.1 Location of test rig on the plant

The test rig was located three levels above the secondary mill discharge sump. This was at the same level as the conventional cyclone of the same dimensions which was in the plant's production circuit, and this was done to ensure an adequate pressure head for the material from the three product cyclone test rig to flow back to the mill discharge sump without having to pump it back. All the material that was pumped



FIGURE 4-5. Hoisting up the overflow arrangement to change the vortex finders.

to the test rig returned to the plant's production circuit via the mill discharge sump, with the exception of the samples obtained for analysis, as shown in the schematic in figure 4-6.

An agitator was not necessary in the mill discharge sump because there was no accumulation of solids in the sump since all the material that reported to the three product cyclone test rig was sent back into the production circuit. Apart from that, the mixing from the mill discharge and the returning flows was intense enough to keep the solids in suspension.

4.4.2 The test rig

The closed circuit test rig set-up for the industrial scale study is shown in 4-6. The test rig is comprised of a specially adapted 600mm diameter Multotec cyclone that was placed on a custom-built frame. The feed to the three product cyclone was pumped from the 3.2 m^3 secondary mill discharge sump using a 110 KW-4 bar Weg variable speed pump. The cyclone feed pressure during the test work was controlled by varying the pump speed at the mill discharge sump. Two pumps were operated from the mill discharge sump to pump the feed material to the secondary flotation production circuit and to the test rig simultaneously (figure 4-6). This arrangement

University of Cape Town

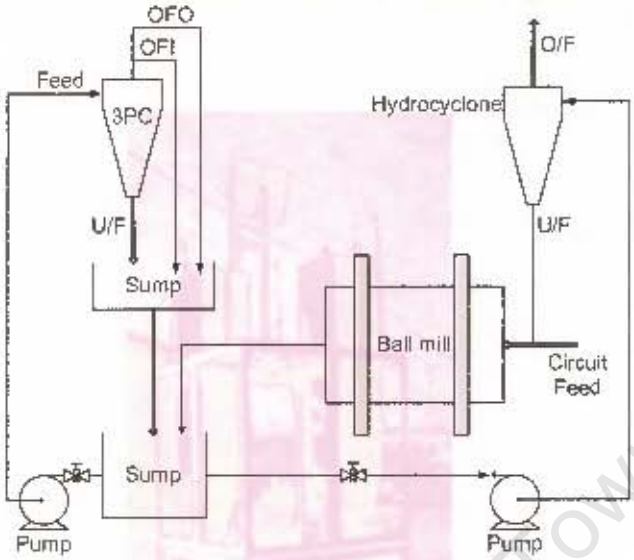


FIGURE 4-6. A schematic of the test rig set-up at Eastern Platinum Concentrator.

required careful control and details of the control strategy used during the testwork are discussed in Chapter 5.

4.4.3 Test rig frame

Figure 4-7 shows part of the framework for the three product cyclone test rig. The rig had three rectangular frames constructed from angle iron and they were bolted together. The top frame held two identical tanks for measuring the inner, and outer overflow flow rates. The three product cyclone was mounted next to the two flow rate measuring tanks on the top. This was done to allow the inner, and outer overflow to be freely discharged into two separate flow rate measuring tanks at atmospheric pressure. The space surrounding the tanks and the cyclone was closed with mentis grating and was used as a platform for changing the vortex finders as well as for process observations. The picture in figure 4-8 shows the arrangement of the cyclone, the inner and outer overflow pipe, the top half of the two flow rate measuring tanks, and the process observation platform. The frame located at the bottom held the combined products sump where all the product streams from the cyclone were

University of Cape Town

collected prior to being returned to the production circuit via the secondary mill discharge sump.



FIGURE 4-7. Testrig frame with tanks for measuring volumetric flow rates prior to installation on the plant.

University of Cape Town

4.4.4 Flow rate measuring tanks

The two identical tanks at the top were used for taking flow rate measurements from the inner, and outer overflow streams. Each tank had a volumetric capacity of 0.52 m^3. The combined products sump at the bottom was designed to hold slurry up to a volume of 2.10 $m^3$and this tank was used for measuring the feed flow rate. The flow rate measuring tanks were fitted with ATS actuators at the discharge end, which were designed to open and close automatically. The actuators comprised a butterfly valve each, which was opened and closed by a 4 bar, 80 × 250mm stroke piston operated by a 240 volts solenoid. Butterfly discharge valves with a diameter of 150mm were mounted at the bottom of each overflow flow rate measuring tank and a 250mm diameter discharge valve was mounted on the combined products



FIGURE 4-8. Illustration of the overflow arrangement on the three-product cyclone.

sump. This was done in order to allow the full flow of the streams to pass through without building up a head in the tank. This was essential for taking reliable flow rate measurements and in preventing segregation that might have taken place when taking flow rate measurements.

The tanks for measuring flow rates were big enough to give reliable measurements and the mechanism allowed a quick drain to prevent disturbances in the production circuit. A simple calculation based on timing accuracy over time to fill was conducted to test this. The timer accuracy of the level sensors is better than 0.1s. As identical sensors were used for the start and finish levels there should be no discrepancy in the trigger point relative to slurry level adjacent to the sensor. The filling time was of the order of 10s, so the accuracy is better than (2x0.1s)/10s, which is 2%. Rubber lined rectangular converters were fitted at the discharge end of each overflow flow rate measuring tank to minimise spraying of the discharge, and allow a proper sample to be cut for analysis.

4.4.5 Level control switches

Initially infrared level switches were installed on the rig for measuring flow rates. The infrared optical level sensors rely upon light transmitting properties of the process

University of Cape Town

material when measuring the level. Two non-contacting infrared level switches were mounted near the bottom and top of each flow rate measuring tanks. The level sensors were mounted on transparent fibre glass panels designed to allow for smooth operation of these sensors. During the commissioning phase of the test rig it was realised that splashing slurry activated the sensors which caused erroneous readings. When they failed to operate they were removed and replaced with Ajax level switches

.

Two Ajax float level switches were fitted at different depth levels in each tank for measuring the slurry levels in the tank. The Ajax level switches use mercury to complete the circuit. The level switches were fitted in such a way that the float was allowed to bend downwards perpendicular to the horizontal so that as the slurry filled the tanks, the level switch moved upwards and tilted to the horizontal. When the level switch comes into the horizontal position, the mercury completes the circuit and the timer on the control panel starts up. The second switch for detecting the slurry when it reached the upper level operated in a similar way except that when the slurry moved the level switch to its horizontal position, the counter on the timer at the control panel stopped counting and the opening mechanism for the discharge valve was activated. In each of the two overflow flow rate measuring tanks, the lower level switch was mounted 0.150 m from the bottom of the sump and the upper level switch was mounted 1.300 m above the lower one. In the combined products sump the lower level switch was positioned 0.200m from the bottom of the sump and the upper level switch was located 1.200 m above the lower one.

4.4.6 Sample cutters

Three custom-made identical sample cutters were designed and manufactured for the test work. The sample cutters for the overflow streams were designed to hold 2.5 litres of sample. The sample cutter mouths were $300mm$ long and $20mm$ wide. The sample cutter for the cyclone underflow stream had a cutting mouth of $400mm$ long

University of Cape Town

and $40mm$ wide and was designed to hold 5.0 litres of sample. The sample cutters were designed with a steep fall angle of 60° to allow high density materials to exit from the bottom without settling inside the sample cutter (figure 4-9).



FIGURE 4-9. A photograph of the cyclone overflow sample cutter.

Rubber hose pipes with $25.4mm$ diameters were used to carry the samples from the overflow sample cutters to the discharge spouts located on the combined products sump. Similarly a discharge $50.8mm$ diameter rubber hose pipe was used to carry the cyclone underflow sample from the sample cutter to the discharge spout on the rig. The hose pipes were allowed to move with a fall angle ranging from 45° to 60°. This was done to avoid choking the pipes. Three outlets for the sample discharge pipes were made in the wall of the combined products sump. These were designed to give the correct fall angle to the pipe and to allow proper operation of the sample cutter. They were properly sealed to avoid slurry leaks.

Samples from the inner overflow, outer overflow, and underflow were taken using automatic sample cutters driven by separate 24V 8 bar-80×250mm stroke pistons fitted on the rig. Each sample cutter was controlled independently by a switch from

University of Cape Town

the control panel. The switches controlled the flow of both electric current and air pressure that activated the automation.

To ensure adequate air supply to all the actuators and sample cutters a six-way splitter air manifold was designed and installed on the rig. Preliminary work showed that this was essential to achieving reliable and consistent activation of the sample cutters and actuator valves simultaneously.

4.4.7 Pumping and sampling arrangement for the cyclone feed

The pipe for supplying the feed slurry to the test rig consists of two steel reinforced elephant rubber hose pipes and rubber lined mild steel pipes. One rubber hose was connected to a T-piece pipe that carried the slurry feed from the pump delivery pipe and this was joined to a metal pipe on the other end. Rubber lined mild steel pipes were used in the middle section of the feed pipe to supply the required height, due to their relatively low cost compared to the cost of steel reinforced elephant rubber hose pipes. One end of the second steel reinforced elephant rubber hose pipe was connected to the mild steel pipe and the other to the cyclone feed inlet.

The pressure pipe sampler was positioned in the centre of the pipe connected to one end of the T-piece on the cyclone feed pipe. The pressure pipe sampler was used for taking the feed sample by diverting part of the stream and collecting it in a bucket. The pressure pipe sampler was correctly baffled to promote mixing of the feed slurry before the split. To avoid causing fluctuations in the operating pressure of the cyclone, samples were cut at the start and end of the test.

4.5 Pilot plant scale test rig

The promising results from the industrial scale tests conducted at Eastern Platinum concentrator motivated further testwork at pilot plant scale. The aim of the pilot plant tests was to evaluate the applicability of the classification system involving

University of Cape Town

the three product cyclone and fine screens in the circuit. It was critical to conduct testwork on the circuit that involved grinding and flotation in order to assess the recirculating loads in the grinding circuit and the recovery of values in the flotation circuit. The pilot plant circuit tests provided an opportunity to assess the operability of the proposed classification circuit configuration for the UG2 ore application. A brief description of the pilot plant facility at Karee concentrator is given in sections 4.5.1 to 4.5.6. Only the sections of the pilot plant facility which were used for this thesis are discussed.

4.5.1 Pilot plant layout

To test the concept of the three product cyclone at pilot plant scale, the classification rig which included the cyclone and fine screen rig were designed and installed in the existing pilot plant facility which had the milling and flotation rigs. The layout of the section of the pilot plant used in this study is shown in figure 4-10.

4.5.2 Milling rig

Ore pre-crushed to 100% minus 6mm was stored in a feed hopper equipped with load cells for weighing the feed. The feed hopper was designed to hold approximately 3 tons of ore. Grinding was done using a 0.93m diameter $\times$ 1.5m long roller driven ball mill. The mill was equipped with a variable speed drive. A seasoned ball charge with a size range from 12mm to 50mm balls was used as grinding media. The mill was fitted with a discharge grate with 10mm diameters discharge holes at an open area of 20%. The mill product was discharged on to a vibratory screen fitted with a 600μm aperture wire-mesh.

4.5.3 Cyclone test rig

The cyclone test rig was specially designed for a small diameter three product cyclone that can be operated in a single or multi-stage classification circuit with fine screens. The cyclone rig was located 12m above the mill discharge sump to allow

University of Cape Town



FIGURE 4-10. A photograph showing the layout of the pilot plant at Karee concentrator.

the slurry from the products to report to subsequent process stages in the circuit without having to pump it. The cyclone rig occupied two levels termed the cyclone area, located at the topmost level of the pilot plant, and the cyclone sampling area which was a level below the cyclone area (figure 4-10). Apart from the feed sample which was obtained from the vibratory screen undersize at the mill discharge sump, sampling of the cyclone products was conducted using the sampling system installed at the sampling area.

4.5.3.1 Cyclone area

Figure 4-11 shows the arrangement of the cyclone and sump boxes at the cyclone area and figure 4-12 presents the layout of the sampling system at the cyclone sampling area. In this area, the cyclone is mounted on a specially designed frame which allows the two cyclone overflows and underflow streams to discharge freely into separate 50l sump boxes as shown in figure 4-11. The sump box for the cyclone underflow had an additional launder installed to allow the cyclone to be operated at various angles of inclination. Flexible blue tube hose pipes were connected at the discharge end of each sump box to transport the products to the sampling area. A pressure gauge was installed at the cyclone feed inlet.



FIGURE 4-11. The product sump boxes for the three product cyclone.

University of Cape Town

4.5.3.2 Sampling area

The sampling area located one level below the cyclone area was equipped with the sampling system for taking samples from the cyclone products. A sump box partitioned into three separate compartments corresponding to the three products was installed. Each compartment was further subdivided into two separate sections. The partition between the sections obtained after subdividing the compartments did not reach the top of the sump box so that the pipes carrying the material could be positioned in the sump box to avoid any splashing as shown in figure 4-12. Each of the two sections in the compartment had a discharge pipe at the bottom. On each of the compartments one of the discharge pipes was for transferring slurry from the cyclone rig to the subsequent unit in the circuit and the other was for sampling purposes.

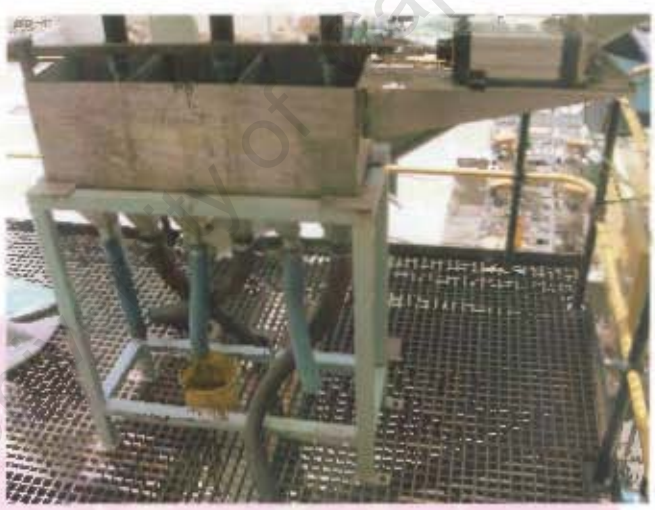


FIGURE 4-12. The compartmentalised sampling system for the pilot plant scale three product cyclone.

The flexible blue tubes from the sump boxes at the cyclone area were then connected to a light channel bar which was mounted on top of the sump box shown in figure 4-15. The channel bar was connected to a pneumatically driven ATS piston. Rectangular metal caps were fitted to the discharge end of each flexible blue

tube hose pipe. The channel bar was positioned directly above the sump to allow each flexible blue tube to discharge the slurry in the corresponding section without splashing.

The installation allowed slurry from the three-product cyclone to report to the subsequent process units in the circuit continually, and when the piston is activated the slurry from the streams is discharged into the respective sampling buckets for a set time interval as illustrated in the schematics in figure 4-13 and 4-14. This allowed for all the products to be sampled for the same duration under the same piston stroke. The positions marked P represent the streams reporting to the subsequent process units in the circuit and S is the sampling bucket.

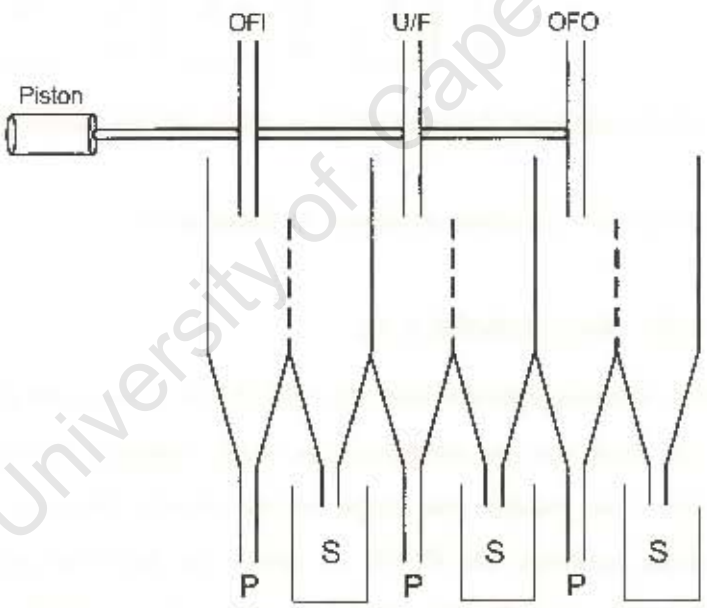


FIGURE 4-13. Schematic of the pilot plant sampling system for normal operation position.

4.5.4 Fine screening rig

A fine screen technology termed Pansep screens was used for screening the middlings product. Screen panels with 100mm apertures were installed on the screening rig.

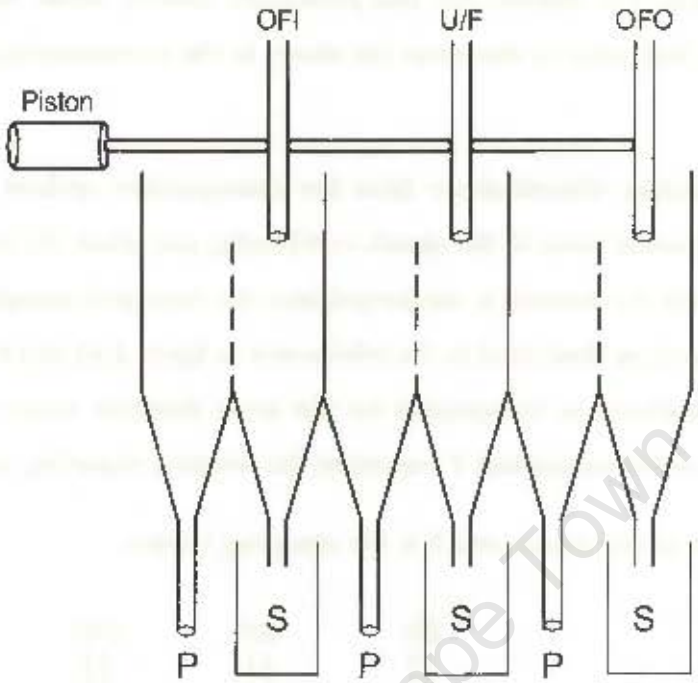


FIGURE 4-14. Schematic of the pilot plant sampling system during sampling position.

Water spray bars were installed as shown in figure 4-15.

4.5.5 Flotability characterised test rig

The Flotability characterisation test rig (FCTR) is a flotation pilot plant with a number of cells that can be configured to study different circuit configurations. Flotation studies are outside the scope of this thesis. However, some tests were conducted which included the FCTR to assess the flotation performance of the circuit configuration involving the three product cyclone. Details of its design and operation were reported by Coleman et al. [70].

4.5.6 Process flowsheet

A schematic of the grinding and classification sections of the pilot plant is presented in figure 4-16. Pre-crushed ore was transferred in the feed hopper using a pneumatic

University of Cape Town



FIGURE 4-15. A photograph of the pilot plant scale Pansep screen

hoist. The ore was then feed to the mill using a variable speed conveyor belt which discharged the material directly in the ball mill feed chute. Water was added to the ore in the feed chute to maintain a mill discharge slurry of 78% solids by mass.

The ground material was then discharged on to a vibratory screen with screen apertures of $600\mu m$. The screen oversize was recirculated to the mill for further grinding while the screen undersize was discharged into the sump and then pumped to the cyclone rig located 12m above the sump using a 15kW environtech centrifugal pump. The cyclone was located at this level to allow slurry from the cyclone to flow to the subsequent process units in the circuit without having to pump it. The centrifugal pump at the mill discharge sump was equipped with a variable speed drive to allow for flexibility in the cyclone feedrate control.

The cyclone underflow was recirculated to the mill for further grinding while the finer overflow from the three product cyclone was sent to the FCTR for flotation. The middlings overflow stream was sent to the Pansep screens for reclassification to remove all the plus $100\mu m$. The screen oversize which is predominantly plus $100\mu m$ was preferentially recirculated to the mill to be reground. The Pansep screen undersize was combined with finer overflow and fed to the flotation circuit.

University of Cape Town

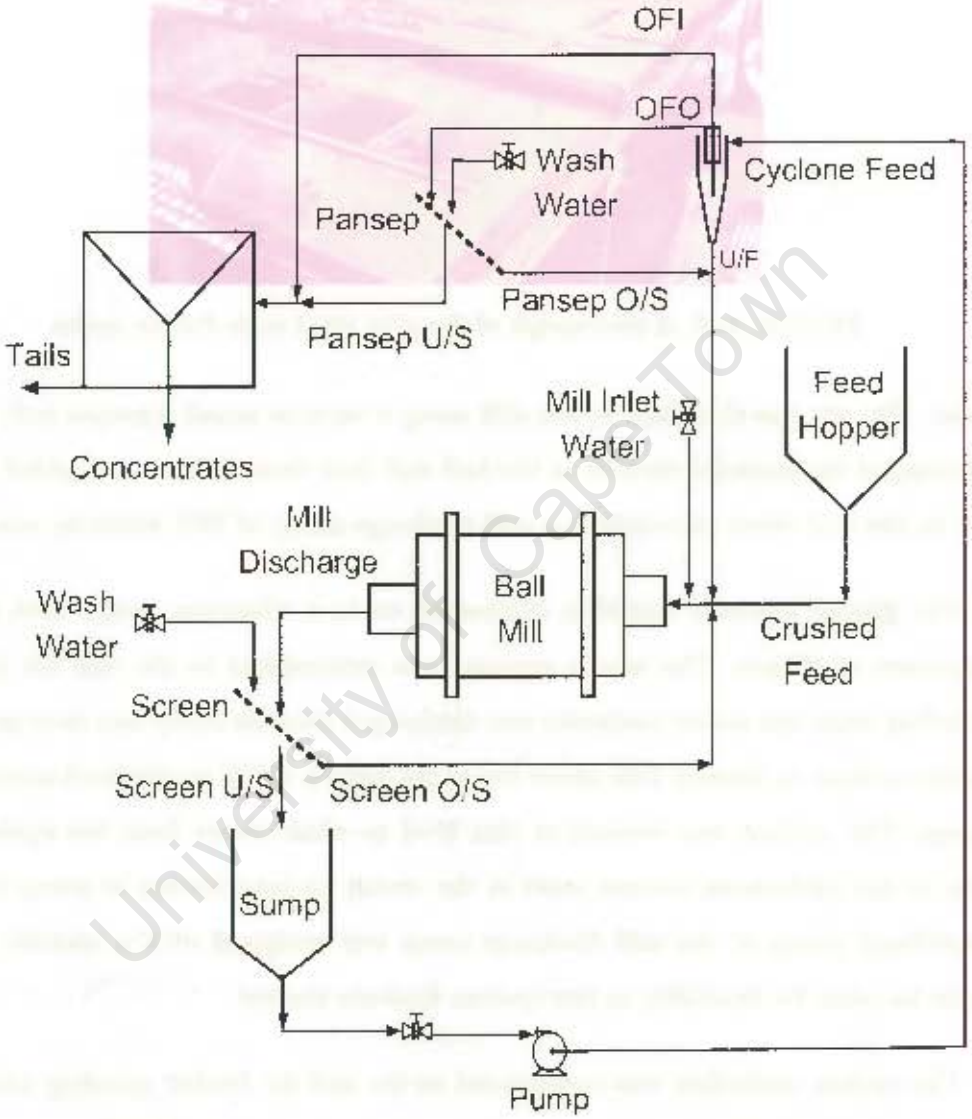


FIGURE 4-16. A schematic of the three-product cyclone pilot plant circuit.

University of Cape Town

5

Methodology

5.1 Introduction

This chapter is devoted to giving a description of the experimental methodology employed in obtaining the results used in testing the concept of the three product cyclone in the UG2 platinum ore classification application. The industrial scale experimental work was conducted at Eastern Platinum concentrator which treats UG2 platinum ore. Pilot plant tests were performed using the Lonmin pilot plant facility located at Karee concentrator and the UG2 ore from Eastern Platinum concentrator was used.

University of Cape Town

5.2 Exploratory tests for the industrial scale testwork

A series of exploratory tests were conducted prior to embarking on the principal testwork. These provided experience in the methods which were used in the work and resulted in several useful refinements in the development of the test rig and the technique for performing the experiments. Exploratory tests were used to assess the design of the overflow arrangement and the ease of changing the vortex finders which was critical to the experimental work. The data from these experiments were not used as part of the findings for the experimental work. However, the exploratory tests were used to investigate the sizes of tanks needed for volumetric measurements, the appropriate sample cutter dimensions as well as the effectiveness of sample cutter designs with regard to cutting representative samples. These tests also provided ball-park dimensions for the vortex finders and spigots for the experimental work.

5.2.1 Pre-test planning

A number of measurements and mini-tests were conducted prior to embarking on the principal test work. These provided information required for circuit control with a dual pump arrangement on the same sump, and a check on the effectiveness of the chosen equipment and methodology. They also awarded an opportunity to practice the chosen data collection techniques, and the experimental technique to ensure that the data collected during the tests was useful and valid.

5.3 Test procedure for the industrial scale testwork

After refining the methodology using exploratory tests, a major test program was drawn up, and testwork carried out using the procedures discussed in sections 5.3.1 to 5.3.6.

University of Cape Town

5.3.1 Experimental apparatus and cyclone dimensions

Prior to embarking on the testwork, the cyclone diameter, length of the cylindrical part, feed inlet equivalent diameter, cone angle, and the length of the conical section were measured and recorded. The dimensions of the tanks used for volumetric flow rate measurements were taken and recorded.

Prior to installation at the beginning of each test, the actual dimensions of the outer vortex finder diameter, inner vortex finder diameter and length, and the spigot diameter were taken and recorded in the test note book. This was done to allow for wear, and to ensure that the parts had not been incorrectly changed. Both the inner and outer vortex finders were inspected for possible wear and observations were recorded for each test.

5.3.2 Experimental work

The pump at the mill discharge sump was activated and the valve feeding the three product cyclone was fully opened. The section of the plant containing the test rig

was switched from automatic control, where the plant usually operates, to manual control. The pump speed for the conventional cyclone feeding the flotation circuit for the production plant was set at maximum speed and the pump feeding the three product cyclone was slowly adjusted until the required cyclone feed flow rate was reached. The solids concentration for the feed and overflow products were checked using the methods discussed in section 5.3.3. If they turned out to be less than the plant requirement, adjustments were made to try and achieve the required percent solids. Prior to cutting test samples on-site size analysis was conducted using a $75\mu m$ sieve screen to ensure that the cyclone was giving a consistent product. This method was used to determine the stability of the cyclone operation. During this time, the speed of the pump at the mill discharge sump was adjusted to obtain the required pressure drop across the cyclone. The test rig was allowed to run for 2 - 3 hours time to attain steady state.

University of Cape Town

There was little control on the feed solids concentration during the test work. The experiments were conducted with material that was used in the production circuit where the flotation response is very sensitive to the changes in feed solids concentration. The feed solids concentration did fluctuate in the production circuit, and the author of this thesis was not allowed to vary it much for test purposes. However, the tests were conducted only when the plant was running at the optimum feed solids concentration and the test was abandoned if changes outside the acceptable operational range were noticed. This is one of the fundamental difficulties of conducting on-site experimental work in a production environment. Patience, being prepared to wait for many hours or even for another day if necessary to obtain the desired test conditions, was essential. It is often necessary to set up a good working relationship with the plant operators so as to obtain their cooperation in stabilising the circuit performance. Plant operating conditions are varied with changes in the ore and it was difficult to duplicate conditions from one test to another.

5.3.3 Checking solids concentration

The solids concentration by mass of the two overflow product streams and the feed were checked on site during the stabilisation period and while conducting the tests. Two methods were employed in checking the solids concentration of the products. The first involved using a Marcy scale. The Marcy scale was calibrated using plant water by filling the empty Marcy cup with plant water and re-setting the scale to a plant water reading. The same Marcy cup used in the calibration was used to check the solids concentration of the two overflow product streams and the feed during the test. The other method involved filling up a tared 20 litres bucket with slurry up to the $20l$ mark and weighing it on a scale. The solids concentration of the sample was calculated using equation 5.1. Equation 5.1 was used to obtained an on-site approximation of the solids concentration.

$$\%Solids = \frac{\rho_s\left(\left(\frac{M_p}{V}\right) - 1\right)}{\left(\frac{M_p}{V}\right)(\rho_s - 1)} \times 100 \tag{5.1}$$

Where: ρ_s - specific gravity of the ore,

M_p - weight of the sample, and

V - volume of the bucket.

A comparison between the reading from the Marcy scale and the solids concentration obtained by weighing a known volume of sample was made on the spot. Although the measurements from the two methods did not give the same result the difference was small enough for the methods to be relied upon. The Marcy scale does not give an accurate reading in high density ores and this could have been the reason for the small deviations in the solids concentration measurements from the two methods. The on-site solids concentration measurements were not used in the analysis of results. The solids concentration measurements obtained from the wet and dry masses from the samples were used in the data analysis. However,

University of Cape Town

these methods were found reliable for checking the solids concentration from the two overflow streams, and the feed, and the rapid application was ideal for on-site testing.

5.3.4 On site screening using a single screen

The on site screening using a 75μm screen was done to assess if the operating conditions were stable (Kojovic [71]). For on-site screening a sample is carefully cut and poured into a measuring cylinder. The sample is then weighed and the volume measured and recorded. The sample is then wet screened using a 75μm screen. After ensuring that all the sub 75μm particles have been screened, the oversize is placed back into the measuring cylinder. Extra water is then introduced so that the volume of the plus 75μm particles and additional water is equal to the volume occupied by the sample prior to screening out the sub 75μm particles. The plus 75μm particles and additional water are then weighed and the mass recorded. The percentage passing 75μm is calculated using equations 5.2 to 5.5:

$$\mathrm{a} = \text{original sample mass} \times \frac{\%\ \text{solids of the sample}}{100} \tag{5.2}$$

$$\mathrm{b} = \text{mass of (plus 75}\mu\text{m + extra water)} \times \frac{\%\ \text{solids of (75}\mu\text{m + water)}}{100} \tag{5.3}$$

$$\%\ \text{plus 75}\mu\text{m} = \left(\frac{\mathrm{b}}{\mathrm{a}}\right)\times 100 \tag{5.4}$$

$$\%\ \text{sub 75}\mu\text{m} = \left(1\text{-}\ \frac{\mathrm{b}}{\mathrm{a}}\right)\times 100 \tag{5.5}$$

University of Cape Town

5.3.5 Measuring stream flow rates

For each test, flow rates of the cyclone feed and the two overflow streams were measured. Three independent measurements were taken; at the beginning, in the middle and at the end of each test. The feed stream flow rate was measured from the combined products sump where the two overflow streams and the cyclone underflow combine before being returned to the mill discharge sump.

Flow rate measurements were obtained by closing the butterfly valve at the bottom of the flow rate measuring tank and allowing the slurry to accumulate in the tank. When the slurry reached the first level switch, the timer located on the control panel was activated to start counting and stopped counting immediately the slurry reached the second level switch and the valve underneath the tank opened to discharge the slurry.

To obtain the flow rate measurements, the one stream at a time approach was taken to avoid disturbances in the production circuit which was in closed circuit with the test rig. Flow rate measurements from the overflow streams were obtained first and then the feed stream. The readings were obtained from the timer and recorded. The automation of the flow rate measuring technique allowed for reliable measurements to be obtained with minimal disruptions to the production circuit and there was no danger of spillage of material due to overfilling of the flow rate measuring tanks.

5.3.6 Pressure measurements

Throughout the duration of the test, pressure readings were taken from the industrial pressure gauge situated at the feed stream a few centimetres before the cyclone inlet. Pressure readings were taken at five minute intervals for the duration of the test and the readings were recorded in a test note book.

University of Cape Town

5.3.7 Sampling

Samples were cut at five-minute intervals for the test period of 40 minutes using the automatic sample cutters fitted to the test rig. Samples from the three product streams were taken simultaneously by pressing all three automatic sample cutter switches. For each stream a dummy sample was cut first, followed by the primary sample for analysis - called the 'A sample', and then a backup sample for storage - called the 'B sample'. The dummy sample was cut to make the inside of the sample cutter 'dirty' and consistent throughout the sampling process. The backup samples taken during the test were stored and were only discarded after the final project report was completed. These dried samples were given a safe storage area, for safekeeping over a period of five years. They were used only if a mistake was noticed or there was some doubt in the results obtained from the primary sample.

For the first few tests a sample of the feed slurry was taken using the pressure pipe sampler at the beginning and end of each test. This was done to avoid variations in the feed pressure during the test period. However, it was noticed after processing the samples from the first set of tests that the pressure pipe sampler gave a poor feed sample. Pressure pipe samplers with incorrectly designed baffles usually give poor samples. The application of pressure pipe sampler in ores containing high density minerals should be limited to very fine streams (Morrison [72]). In the subsequent tests, the feed sample was cut manually using a pelican sample cutter from the pipe returning material from the test rig to the mill discharge sump. The sampling point was located at point where the returning flow from the combined product streams discharged into the mill discharge sump.

All 9 samples from a sampling point were poured into the same sample bucket. The primary and backup samples had separate buckets. The advantage of this method was that there were $\frac{1}{9}$ the number of samples than if individual samples were processed and analysed. Samples were then filtered, dried, and packed in well-

University of Cape Town

labelled plastic bags. These were then stored according to the test numbers to avoid sample swaps during processing. The sample processing procedure is laid down in section 5.5.

A total of eighty two industrial scale tests including 18 repeat tests were conducted to evaluate the performance of the three-product cyclone in the UG2 classification application. The test methodology for the pilot plant testwork conducted at Lonmin pilot plant is discussed in section 5.4.

5.4 Test procedure for the pilot plant scale testwork

After gaining experience with the operations of the pilot plant through the exploratory tests which were conducted prior to the principal work, the actual experiments were performed using the apparatus described in section 4.3.

The cyclone parts selected for the testwork were measured and installed before the test and measurements were recorded in the test note book. Prior to starting up the pilot plant, a sufficient quantity of bags containing pre-crushed ore were transferred into the hopper using the pneumatic hoist in readiness for the test.

5.4.1 Start up and operation of the pilot plant

The pilot plant was started up using the sequence described in this section. The mill inlet water, vibratory screen water and Pansep wash water were all opened to pre-determined flow rates to maintain a mill discharge of 78% solids and the cyclone feed of 50% solids by mass, respectively. The Pansep screen was started up first followed by the cyclone feed pump. After ensuring that the Pansep screen and the cyclone feed pump were operational, the vibratory screen and the mill were started up. After inspecting all the units to ensure that they were running well, the crushed feed was then started up and the mill speed was adjusted to the maximum speed which corresponded to 65% of critical speed.

University of Cape Town

The plant was allowed to run for a few minutes and then the feedrate was adjusted by changing the conveyor belt speed until the required feedrate was reached. The pump speed for the cyclone feed was adjusted until a balance between the sump level and the required cyclone feed pressure was attained. The sump level was then allowed to fluctuate to maintain a consistent feed pressure at the cyclone inlet.

To determine the stability of the plant, the solids concentration of the cyclone feed, overflows, underflow, and Pansep undersize streams were measured using the techniques discussed in section 5.3.3. Minimal fluctuations in the plant feed and other flows in the circuit as well as the pulp densities was considered to be an indication of stability. Due to the small amounts of flow encountered at pilot plant scale the volume of the vessel was reduced from $20l$ to $5l$ for the technique of determining the solids concentration from the mass of the slurry using equation 5.1. On-site screening was implemented using a 75μm aperture screen for the cyclone overflows. To speed up the screening process a 300mm diameter screen was used. The full procedure is discussed in section 5.3.4.

University of Cape Town

5.4.2 Sampling and Flow rate measurements

In addition to taking samples for size and component analysis by size for all the streams in the circuit, flow rate measurements from selected streams were obtained. Flow rate measurements are critical in performing the mass balance to assess the integrity of the data. Mass splits around the classifiers in the circuit were important in evaluating performances of individual process units as well as the overall pilot plant circuit performances. A description of the techniques used for obtaining samples and flow rate data for various streams in the circuit is discussed in this section.

5.4.2.1 Crushed circuit feed

The sampling point for this stream was located at the point where the feed conveyor belt discharged the crushed feed into the mill feed chute. The sample was obtained by placing a $200mm \times 150mm$ tray below the lip of the conveyor belt to allow

the whole stream to discharge on the tray. Each cut was taken over a period of 10 seconds at sampling intervals of 5 minutes. The sample from each cut was weighed and both the mass and actual time of sampling were recorded in the test note book. The mass taken out of the circuit was approximately $1\frac{1}{2}$ - 2% of the total feedrate which is small to have any significant influence on the stability of the circuit.

5.4.2.2 Mill product stream

The sample from the mill product stream was taken at the point where the launder from the mill discharge trunnion discharged the material on the vibratory screen. A custom made tray was used to obtain the sample from this stream. The whole stream was allowed to discharge on the tray for a pre-determined time for each cut. A composite sample was obtained by cutting samples at 5 minute intervals for the duration of the test.

5.4.2.3 Vibratory screen oversize stream

The vibratory screen had no provision for discharging the oversize automatically. Due to the absence of an automatic screen oversize discharge mechanism, the screen oversize was continuously scraped off the screen manually and placed in tarred buckets during the test. The time taken for each load to accumulate on the screen was recorded. The buckets were then weighed and recirculated back to the mill for further grinding. The recirculated screen oversize was fed back into the mill at intervals close to the rate at which it was scraped off the screen. This was done to mimic the operations in typical plants where the screen oversize is recirculated back to the mill at the rate of its production. Every ten minutes one bucket containing the scraped screen oversize material was retained as a sample for further analysis. The masses and time for each bucket were taken, recorded and used to determine the mass flow rate.

University of Cape Town

5.4.2.4 Cyclone feed stream

The sample from the screen undersize which was pumped to the cyclone as feed was obtained at the vibratory screen undersize discharge spout located at the mill discharge sump. A $5l$ bucket was placed at the discharge spout and a sample of the whole stream was taken and the sampling person ensured that the duration for the cuts was consistent.

To obtain flow rate measurements, three timed samples were taken using $20l$ buckets at the beginning, in the middle and at the end of each test. For each of these samples the vibratory screened undersize was collected over a period of 5 to 6 seconds. The flow rate measurements were obtained at those three intervals to avoid upsetting the flows around the circuit. The samples were weighed wet, filtered, dried and then weighed again to obtain dry masses.

5.4.2.5 Cyclone product streams

The samples for analysis and flow rate measurements were obtained using the automatic sampling provision installed on the pilot plant test rig. To obtain the samples from all the product streams simultaneously the sample cutter was manually activated to move into the sampling position and the sample was collected over a pre-determined period.

Like the cyclone feed, flow rate measurements were obtained at the beginning, in the middle and at the end of each test to avoid causing disturbances to other parts of the circuit. These were obtained by allowing the material to discharge in the designated buckets for a period of 5 to 6 seconds. Since all the product samples were obtained by activating the same piston, the mass split among the products were obtained directly from flow rate samples and checked using data from analysis samples.

University of Cape Town

5.4.2.6 Pansep screen oversize and undersize

The Pansep oversize and undersize samples were obtained by placing the respective pipes in labelled buckets. The time taken to collect the material for each cut was noted and recorded. The A samples for analysis and B samples for back up were also used for determining the mass flow rates of these streams.

5.4.2.7 Float feed stream

The sample from the float feed was obtained by collecting the whole stream in a bucket. Samples from this stream were obtained in 5 minute intervals for the duration of the test. Only the A sample for analysis was obtained from the float feed.

The flow rate for the float feed was obtained at the beginning and end of the test by collecting the material into a labelled bucket for a period of 5 to 6 seconds.

A samples for analysis and B samples for back up were cut at each sampling point with the exception of the screen oversize, Pansep products, and float feed. The samples from all the streams were weighed wet, filtered, dried, and then weighed to obtain dry masses. The dried samples were kept in labelled plastic bags for further processing. The procedure for sample processing is laid out in section 5.5.

University of Cape Town

5.5 General sample processing procedure

5.5.1 Sample preparation

For each sample, the total sample was weighed wet, while still in the collection bucket, which had been previously tared. After pressure filtering it using a tared filter paper, the sample was then placed in a tray and oven dried at about 80°C. The dried sample was weighed and the percent solids by weight calculated from the wet and dry masses.

5.5.2 Sieve screening

The sample was split on a rotary splitter to produce a sub-sample of at least 300g. The sub-sample was weighed and then wet screened at a 32 μm sieve screen. The vibratory sieve frame was used to hold and vibrate a 32 μm laboratory sieve screen while the material and water were being introduced onto the sieve. The sieving process continued until only clear water was discharging from the undersize. The undersize from the 32 μm was collected in a clean bucket. The oversize was wet screened on the 125 μm screen. The the oversize was placed on a tray and dried while the undersize was further wet screened at 90 μm.The procedure was repeated for the undersize from the 90 μm to obtain fraction for 63 μm, 45 μm, and 32 μm.The undersize from the 32 μm was collected in a clean bucket and combined with the sub 32 μm from the first pass and then filtered, and oven dried at 80°C. The dried material was then weighed and stored for further analysis.

The dried oversize from the 125 μm screen was sized on a stack of standard sieve screens from a 710 μm sieve screen down to 125 μm. A sieving time of 20 minutes was maintained for each stack of screens for every sample. The Roland vibratory sieve shaker was used to hold and vibrate the stack of laboratory sieve screens. Each size fraction was weighed and stored separately for assays by size analysis.

University of Cape Town

University of Cape Town

6

Industrial Scale Experimental Results and Process Trends

6.1 Introduction

The apparatus and methodology used to generate the experimental results for this thesis are described in chapters 3, 4, and 5. These chapters have shown that a lot of effort was put into designing and constructing the experimental apparatus, and into developing the procedures applied for the testwork in an attempt to obtain good quality data. A total of 82 tests including repeats were conducted using a 600mm three-product cyclone mounted on a custom built test rig described in chapter 4. The purpose of this chapter is to present results from the industrial scale field trials and process trends for the critical design and operational variables from the experimental data. A method of assessing the performance of the three-product cyclone is proposed. To show the influence of density of different mineral components found in the UG2 platinum ore, component assays for chromite and silica were analysed.

University of Cape Town

6.2 Data collection

The cyclone dimensions and the ranges of the design variables for the testwork performed using a 600mm cyclone are listed in Table 6.1. The cyclone diameter, inlet diameter, cylindrical length, and cone angle were kept constant. For the three-product cyclone tests the outer vortex finder length was kept constant at 675mm which is a typical vortex finder length for the standard 600mm diameter conventional, and flat bottom cyclones applied for classification of the UG2 platinum ore.

TABLE 6.1. A summary of the cyclone design variables for the industrial testwork.

Variable	**Dimension**
Cyclone diameter, mm	600
Equivalent inlet diameter, mm	160
Length of cylindrical part, mm	655
Slanting length of conical part, mm	770
Cone angle	20°
Outer vortex finder internal diameter, mm	210 - 230
Inner vortex finder internal diameter, mm	150 - 209
Inner vortex finder length, mm	0 - 1025
Outer vortex finder length, mm	675
Spigot diameter, mm	70 - 105

6.2.1 Arrangement of test results

The data obtained from each test was arranged in tables containing all the critical data as illustrated in Table 6.5. Similarly data for the conventional and flat bottom cyclones was arranged as illustrated in Table 6.6. A range of variables was covered in the testwork some of which were highlighted by the literature to affect the performance of cyclones in general. Since no data was available on the performance of the three-product cyclone in mineral processing applications when this testwork commenced, in addition to the variables that influence conventional hydrocyclones in general, the tests were performed to study the influence of variables unique to this type of cyclone. The cyclone was positioned in a vertical orientation for all the tests performed.

The data collected for each test included: stream flow rates, percentage of solids, and particle size distributions. Assays by size were performed for 40 tests analysing for chromite and silica. The top portion of the table presents the stream solids flow rate (tph), stream water flow rate (tph), chromite head assay (%), silica head assay (%), and solids S.G. A complete data set for the industrial scale three-product cyclone testwork is given in Appendix B.

University of Cape Town

TABLE 6.2. Arrangement of experimental results for the three product cyclone test.

Run67 Dcyc 600 DOVF 220 DIVF 192 LOVF 675 LIVF 775 Dspig 95 Press 88												
	Solids	Water	Chromite	Silica	SG							
Feed	322.2	335.1	18.3	24.2	3.8							
Ofi	99.1	208.5	16.1	29.9	3.8							
Ofo	46.2	75.7	21.6	25.1	3.8							
Uf	177.0	50.9	34.4	12.4	3.8							
Size	Feed	Crmt	Silc	Ofi	Crmt	Silc	Ofo	Crmt	Silc	Uf	Crmt	Silc
0.710	0.2	0.0	0.0	0.0	0.0	0.0	0.0	0.0	0.0	0.3	0.0	0.0
0.500	0.1	0.0	0.0	0.0	0.0	0.0	0.0	0.0	0.0	0.1	0.0	0.0
0.355	0.3	1.3	14.0	0.0	0.0	0.0	0.0	0.0	0.0	0.6	4.3	45.4
0.250	1.9	5.3	9.5	0.0	0.0	0.0	0.2	0.0	0.0	3.4	17.1	30.8
0.180	5.3	8.7	12.7	0.3	0.0	0.0	0.9	5.6	46.3	9.3	25.5	19.8
0.125	10.9	10.3	11.3	1.7	0.0	0.0	3.6	4.1	47.1	18.0	31.5	14.6
0.090	21.7	17.2	29.7	6.4	8.0	39.2	10.8	11.6	39.7	33.1	36.2	8.2
0.063	15.6	20.6	30.5	9.2	6.6	44.0	15.6	19.4	26.0	19.1	46.1	8.4
0.045	10.8	18.0	30.7	14.1	7.8	44.8	18.5	22.2	19.4	6.9	34.2	10.7
0.032	5.6	20.2	26.2	9.6	11.6	34.7	10.0	28.5	19.6	2.2	31.7	14.2
0.000	27.8	23.5	21.8	58.7	21.8	23.2	40.4	25.1	22.5	7.1	25.9	18.8

TABLE 6.3. Arrangement of results for the conventional and flat bottom cyclones comparative tests.

Run 36 Dcyc 600		DVF 220		LVF 675 Dspig 95			Press 57	
	Solids	Water	Chromite	Silica	SG			
Feed	333.0	347.9	25.3	19.9	3.8			
O/F	164.0	296.1	23.9	22.0	3.8			
U/F	169.0	51.8	34.9	9.7	3.8			
Size	Feed	Crmt	Silc	Conv. O/F	Crmt	Silc	Conv. U/F	Crmt	Silc
0.710	0.0	0.0	0.0	0.0	0.0	0.0	0.1	0.0	0.0
0.500	0.1	2.5	7.9	0.0	0.0	0.0	0.4	16.9	27.0
0.355	0.2	3.5	6.9	0.0	0.0	0.0	1.0	23.1	21.0
0.250	0.6	3.8	6.6	0.1	0.0	0.0	2.1	22.6	21.8
0.180	2.2	8.5	25.2	0.7	4.8	38.7	6.2	25.4	19.4
0.125	7.8	13.5	30.9	3.6	6.6	37.0	18.2	34.2	10.4
0.090	22.8	20.8	23.6	10.1	15.6	28.0	34.3	37.1	6.5
0.063	18.5	26.3	18.0	19.9	25.6	18.2	22.6	38.5	5.9
0.045	10.7	29.2	15.1	14.7	26.9	17.0	4.3	34.0	10.3
0.032	2.7	27.0	17.6	3.7	26.1	18.2	0.9	31.2	13.0
0.000	34.4	27.4	19.4	47.3	25.9	18.4	10.1	27.8	16.4

University of Cape Town

6.2.2 Mass balancing

Data collected from plant surveys is always subject to error from sampling and assay. Additional uncertainties are introduced from unavoidable variations in operating conditions. The usefulness of the data from the testwork for quantifying the performance of the process unit for modelling purposes is highly dependant on the quality and consistency of the data collected. Therefore, prior to performing any further analysis the experimental data was mass balanced using Excel spreadsheet and JKMbal - a mass balancing program in the JKSimMet software - to assess the self consistency and integrity of the data.

Since there is no three product cyclone unit in the JKSimMet simulator, two cyclones arranged in series were used to represent the three product cyclone in the mass balance. In this arrangement, the two overflow streams were combined to reconstitute the feed to the second cyclone in series. To run the JKMbal program, experimental data was entered in the experimental columns. For each stream the data entered included: solids flow rates; percentage of solids calculated from the wet and dry sample masses; the specific gravity of the ore; size distributions; and the standard deviations (Morrison [73]). The weightings suggested by Whiten (JKSimMet Manual [74]), were used in all tests. A summary of the guidelines to the weightings used is given in Table 6.4. The same procedure used for mass balancing particle size data was used for component assay data. Details of the mass balance formulation for the three-product cyclone were reported by Obeng [61], and Wiegel [75].

From the experimental data, it was noticed that the feed sample for the first 15 tests was not representative despite all the improvements made to the pressure pipe sampler. It was observed that the pressure pipe sampler was classifying and the problem was not minimised by installing a different design of baffles. The feed stream data for these tests was reconstituted using experimental flow rate and size distribution measurements from the products stream. Both Excel and JKSimMet

University of Cape Town

TABLE 6.4. A summary of the the standard deviation weightings used for mass balancing

Tag	Weighting
Morrison solution	20
Consistent assays	10
Feed, TPH	1
Measured flow rate	2% of actual value
Calculated flow rate	5% of calculated value
Measured size distributions	Standard Whiten SD values
Reconstituted size distribution	Greater than Unit

were used in reconstituting the feed stream data. For subsequent tests the feed sample was obtained from the combined streams return pipe as discussed in section 5.3.7. After assessing the data quality, trends were generated to isolate variables that had a significant influence on the performance of the three-product product.

6.3 Discussion of experimental results

Trends from the experimental data revealed that a number of design and operational variables have a significant influence on the performance of the three-product cyclone. These include the: length of the inner vortex finder; ratio of the area for the annulus between the inner and outer vortex finder to the inner vortex finder orifice; spigot diameter; and the operating pressure. The following discussion presents a qualitative assessment of the data and trends. Simple trend lines are used only to highlight trends in the data, fitting of the data occurs in the modelling chapter, and detailed discussion of the significance of the fitted trends is presented after that.

6.3.1 Effect of the inner vortex finder length

To establish the effect of the inner vortex finder length (LIVF) on the performance of the three-product cyclone, a range of tests involving different inner and outer vortex finder diameter combinations were performed. For each set of these tests all the other design variables were kept constant and the LIVF was varied between 775mm and 1025mm.

University of Cape Town

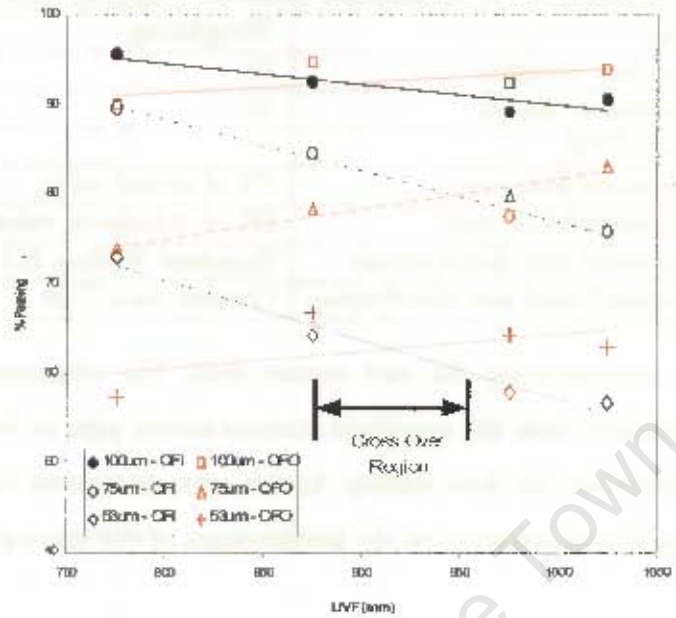


FIGURE 6-1. Effect of the LIVF on particles reporting to the OFI and OFO streams for the DIVF of 165mm and DOVF of 210mm.

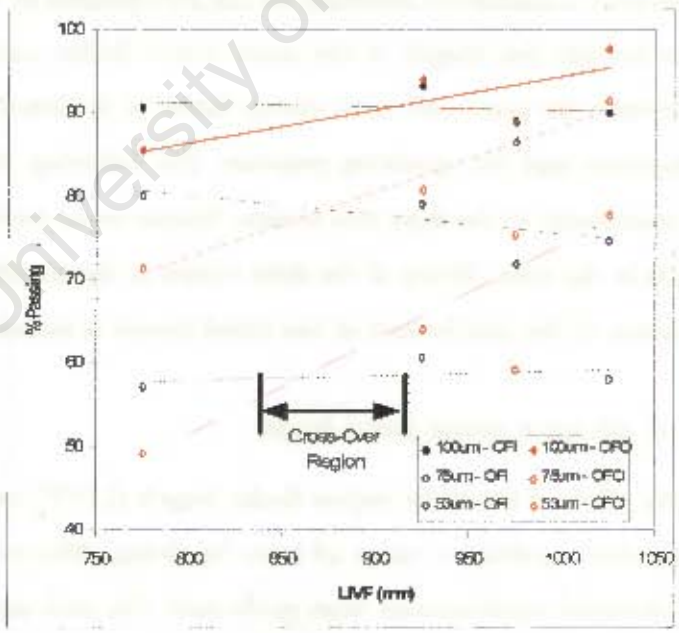


FIGURE 6-2. Effect of the LIVF on particles reporting to the OFI and OFO streams for the DIVF of 192mm and DOVF of 230mm.

University of Cape Town

Figures 6-1 and 6-2 show the effect of the LIVF on the percentage by weight of particles passing 100, 75, and 53μm of the OFI and OFO streams for the inner and outer vortex finder diameter combinations of 165mm and 210mm, and of 192mm and 230mm, respectively. This is similar to what Milin et al [76] observed when they inserted a secondary vortex finder in the hydrocyclone in an attempt to eliminate short-circuit flow. It was observed that the percentage by weight of particles passing 100, 75, and 53μm for the OFI stream was higher than that for the OFO stream at the LIVF of 775mm. At this LIVF the finer overflow product was discharged through the OFI stream and the intermediate sized overflow product through the OFO stream. This is termed the normal classification configuration. It was observed that the percentage by weight of the particles passing 100, 75, and 53μm for the OFI stream decreased as the LIVF increased while the percentage in the corresponding fractions for the OFO stream increased. When the LIVF is positioned in the transition zone called the "cross-over region", the product size distributions for the OFI and OFO streams are similar. When the inner vortex finder length is extended below the cross-over region, reverse classification is exhibited. In this case, a finer overflow product is discharged through the OFO stream and an intermediate sized overflow through the OFI stream.

Typical stream size distributions for a vortex finder combination of 165mm inner and 210mm outer at the LIVFs of 775mm, 875mm, and 1025mm are given in Figures 6-3, 6-4, and 6-5, respectively. The size distribution for the conventional overflow appear to lie between the OFI and OFO streams of the 3-product cyclone while the underflow for the three-product cyclone seem to be similar to that for the conventional cyclone at the coarse end, but deviates at sub-100 μm (Figure 6-5).

A shift in the position of the cross-over region from the LIVF range of 875 - 975mm to the LIVF range of 850 - 925mm was observed when the inner, and outer vortex finder diameters combination was changed from 165mm and 210mm to 192mm and 230mm, respectively (Figures 6-1 and 6-2). From this it can be concluded that the

University of Cape Town

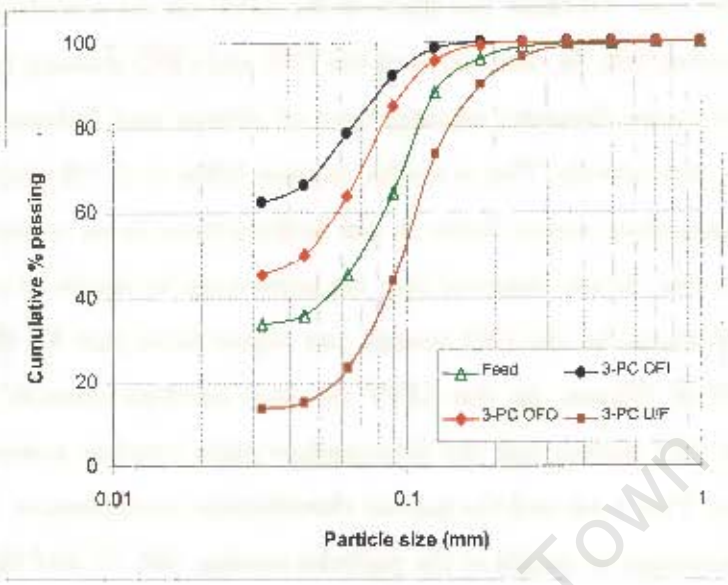


FIGURE 6-3. Particle size distribution for the normal classification configuration of the three-product cyclone.

position of the 'cross-over region' is influenced by both the LIVF and the combination of vortex finder diameters used. Knowledge of the 'cross-over region' is critical in utilising the three-product cyclone as it indicates the regions where the LIVF can be positioned to provide three-distinct products. For the three-product cyclone to be beneficial, the LIVF must be positioned either above or below the 'cross-over region' to obtain normal or reverse classification, respectively. Positioning the LIVF in the 'cross-over region' result in two identical overflow streams which may not differ significantly to the conventional cyclone overflow. However, significant differences in the size distributions between the inner and outer overflow streams have been shown when the inner vortex finder was positioned further away from the 'cross-over region'.

The inner vortex finder length was found to have a significant effect on the classification of the three-product cyclone and influences whether the cyclone is operated in the normal, 'cross-over region', or reverse classification configurations. It can be concluded that the three-product cyclone produces three distinct products provided it is not operated with the LIVF positioned in the cross-over region. Both the normal

University of Cape Town

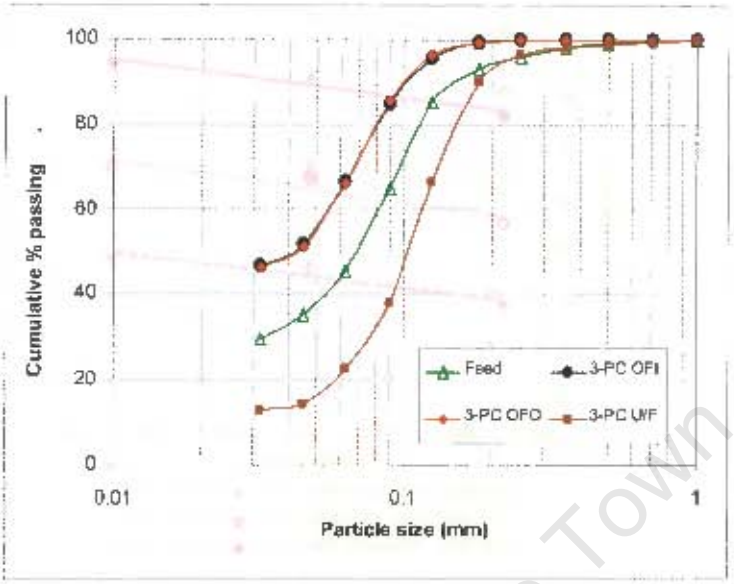


FIGURE 6-4. Particle size distribution for the three-product cyclone with the inner vortex finder terminating in the cross-over region.

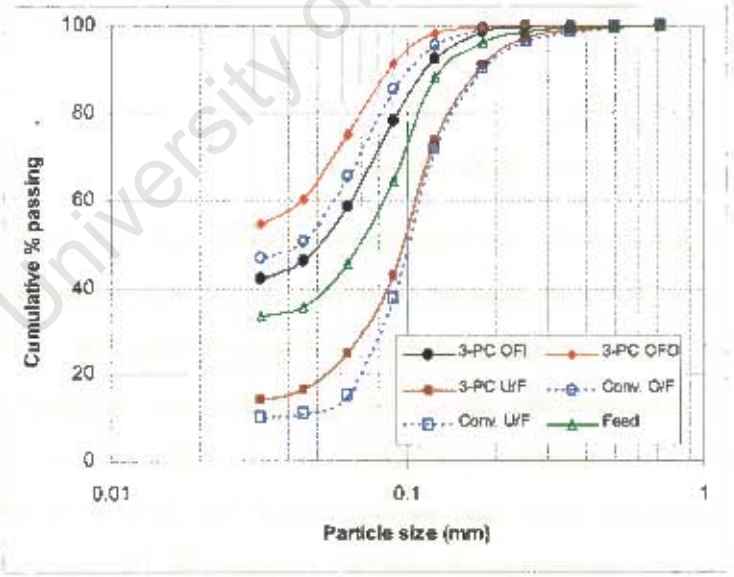


FIGURE 6-5. Comparison of particle size distributions for the three-product cyclone operated under the reverse classification configuration and those for the conventional hydrocyclone.

University of Cape Town

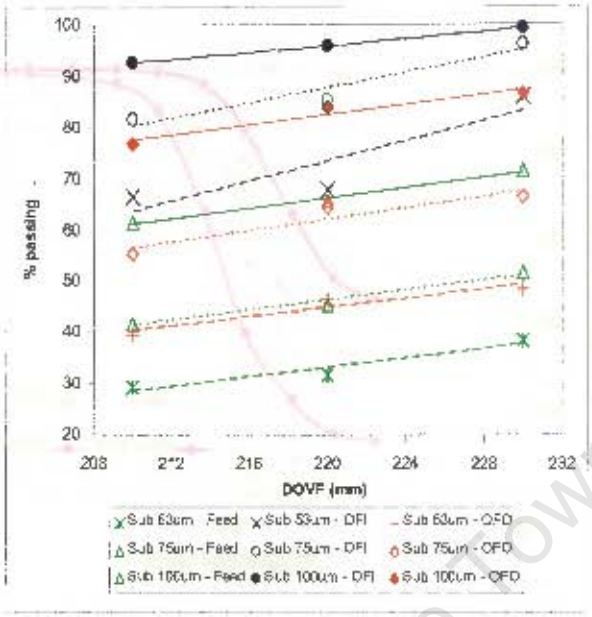


FIGURE 6-6. Effect of the outer vortex finder diameter on the particles reporting to the overflow streams for the three-product cyclone operated with an LIVF of 775mm.

and reverse classification modes produce a middlings product suitable for screening, but operating the 3PC in the cross-over region doesn't produce a useful middling product.

6.3.2 Effect of the vortex finder diameters

The vortex finder diameter has been shown to affect flow split, water recovery to the underflow, and other performance characteristics of the conventional hydrocyclone, making it one of the important design variables affecting the cyclone performance (Bradley, [77] and Svarovsky, [30]). This section discusses the effect of the two vortex finder diameters on separation performance of the three-product cyclone.

Figure 6-6 and 6-7 show that varying DOVF has little or no effect of practical significance on the percentage of particles passing 100, 75, and 53 μm for the OFI and OFO streams for the normal, and reverse classification configurations of the three-product cyclone, respectively. The differences observed can be attributed to the variations in the feed size distributions, as they follow the slight changes (arising

University of Cape Town

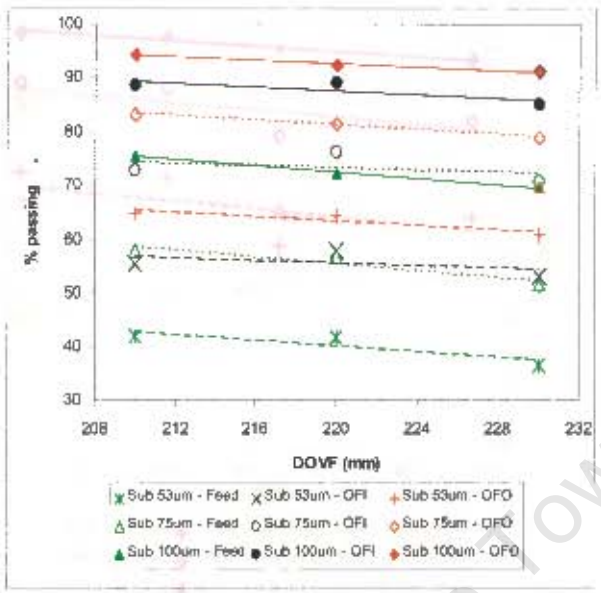


FIGURE 6-7. Effect of the outer vortex finder on particles reporting to the OFI and OFO streams for the three-product cyclone operated with an LIVF of 1025mm.

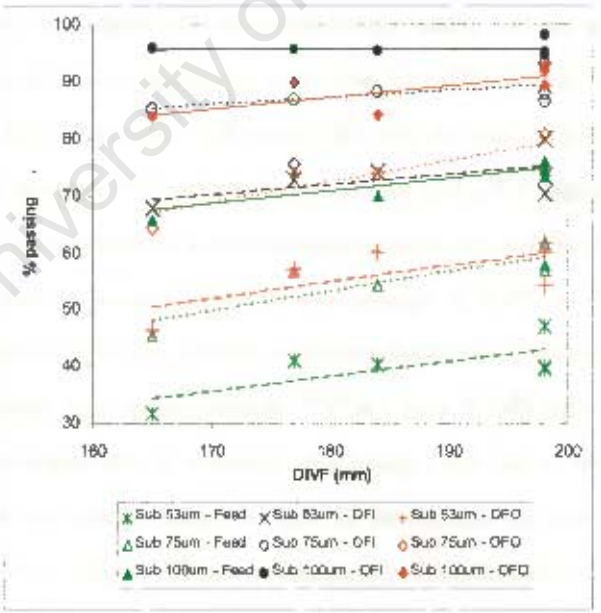


FIGURE 6-8. Effect of the inner vortex finder diameter on particles reporting to the OFI and OFO streams for the three-product cyclone operated with an LIVF of 775mm.

University of Cape Town

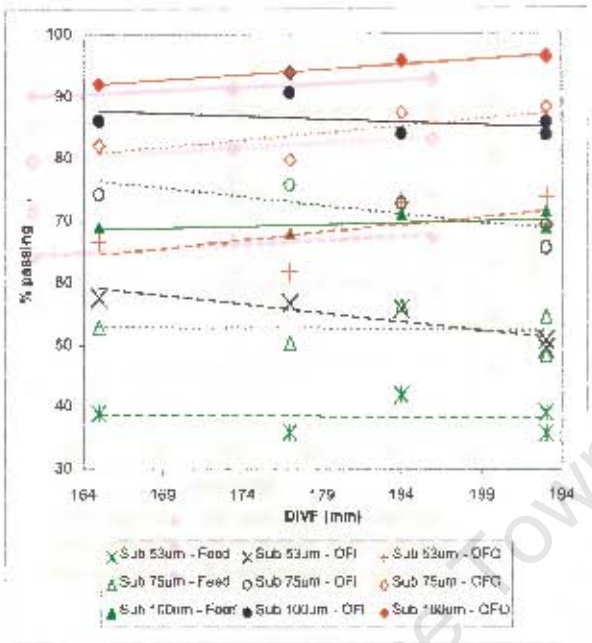


FIGURE 6-9. Effect of the inner vortex finder diameter on particles reporting to the OFI and OFO streams for the three-product cyclone operated with an LIVF of 1025mm.

from fluctuations in the plant operation) of the feed size distribution. Similarly, varying the DIVF has no effect of practical significance on the percentage of particles passing 100, 75, and 53 μm for the OFI and OFO stream for the normal classification configuration (Figure 6-8), but the fractions in the OFI appear to be coarsening with increase in the DIVF for the reverse classification configuration (Figure 6-9). Varying either the DIVF or DOVF appear to to give similar trends with the exception of the reverse classification configuration where the OFI coarsens with increase in the DIVF. Since the DIVF and DOVF variations do not change the percentage of particles reporting to the OFI and OFO streams in the respective fractions, the two design variables can be combined in one variable which can be used to assess the effect of the dual vortex finder arrangement on flow split to the product streams.

For the normal, and reverse classification configurations considered, the percentage of particles passing 100, 75, and 53 μm for the OFI were significantly different from

the percentage of particles passing the respective fractions in the OFO streams, which can render the three-product cyclone attractive for flowsheets that can treat the two overflows using different process routes to maximise recovery of the valuable mineral.

6.3.3 The selection area ratio

The presence of two vortex finders in the three-product cyclone required a new design parameter for evaluating the effect of the dual vortex finders on the cyclone performance. It will be shown in the next section that the area available for flow to the annulus between the inner and outer vortex finders can be altered by either keeping the inner vortex finder (IVF) constant and changing the outer vortex finder (OVF) or keeping the OVF constant and changing the IVF. The ratio of the area of the annular orifice between the inner and outer vortex finders to the inner vortex finder orifice termed: the Selection Area Ratio (SAR), is the design variable used in the three-product cyclone to evaluate the effect of the dual vortex finders on cyclone performance. The SAR is defined as:

$$SAR \quad \frac{OVF\ cross\ sectional\ area - IVF\ cross\ sectional\ area}{IVF\ cross\ sectional\ area} \tag{6.1}$$

Where: SAR – Selection Area Ratio
OVF – outer vortex finder
IVF – inner vortex finder

The thicknesses of the inner vortex finder (pipe thicknesses ranged from 1.5 to 3 mm) were excluded in working out the SAR. The SAR given in equation 6.1 does not take into account the influence of the air-core on the flow split. This is due to the difficulty associated with getting meaningful measurements of the air-core in operational cyclones. The shape and dimensions of the air-core for the three-product cyclone set-up were obtained from computational fluid dynamics simulations as discussed in Chapter 7 of this thesis.

University of Cape Town

6.3.4 *The effect of the SAR on overflow streams mass splits*

The effect of the SAR on the fraction of solids in the feed reporting to the OFI, OFO, and U/F streams for the normal and reverse classification configurations of the three-product cyclone are shown in Figures 6-10, and 6-11, respectively. It can be seen that at small SARs a higher fraction of the feed reports to the OFI product stream, while a relatively low fraction reports to the OFO product stream. It was observed that increasing the SAR resulted in a decrease in the mass fraction reporting to the OFI product stream while the mass fraction reporting to the OFO product stream increased. At higher SARs the fraction reporting to the OFO product stream is significantly higher than that being discharged through the OFI product stream. In essence the curves for the OFO and OFI mirror each other, as would be theoretically expected. Similar trends for the split to the overflow streams were observed for both the normal and reverse classifications configurations. The fraction of solids reporting to the U/F of the three-product cyclone appeared to decrease slightly with increase in the SAR. The scatter observed in the data can be attributed to different operating conditions such as variations in the feed solids concentration. It can therefore be concluded that the SAR has a significant influence on the mass split to the product streams of the three-product cyclone.

This section has shown that the suitability of the three-product cyclone in the potential applications depends on the capability of producing two distinct overflows at mass splits that satisfy the requirements for the subsequent processes. In the plants treating the UG2 platinum ore, it has been found that when the conventional cyclones are used, coarse silica particles report to the overflow even if they are not fine enough to be floated while the chromite particles re-circulate to the grinding mill even if they are fine enough to escape from the grinding circuit. In the UG2 platinum ore application the three-product cyclone can be utilised to capture a middlings product containing the silica and chromite particles that are misplaced in the conventional cyclone. This stream can then be screened using fine screens with

University of Cape Town

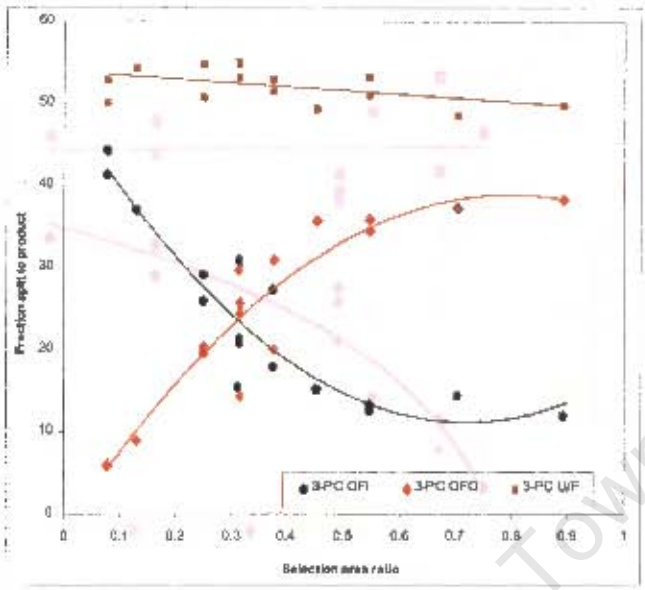


FIGURE 6-10. The effect of the selection area ratio on the mass split to the product streams for the three-product cyclone, LIVF = 775 - normal classification configurattion.

100μm apertures to prevent oversize silica particles from reporting to the flotation process and fine chromite from building up a huge re-circulating load. The screen undersize can be sent to the subsequent process while the oversize can be sent to the mill for further grinding. For the fine screen to operate efficiently the feed rate must be controlled and for the Lonmin UG2 ore application the desired mass split to the intermediate stream was between 15 and 20 % of the total feed.

To obtain the overflow containing the intermediate sized particles at the desired mass splits suitable to the application the inner and outer vortex finder combination has to be chosen carefully to attain the SAR that can achieve this. For the 600mm diameter three-product cyclone, Figure 6-10 and 6-11 indicates that a split of 15 - 20% in the middlings product can be obtained by using SARs of 0.28 - 0.35 for the normal classification configuration, and of 0.65 to 0.75 for the reverse classification configuration. The presence of two additional design variables; the LIVF and SAR which can be used for controlling separation in terms of particle size classification and solids split to the products makes the three-product cyclone attractive for most

University of Cape Town

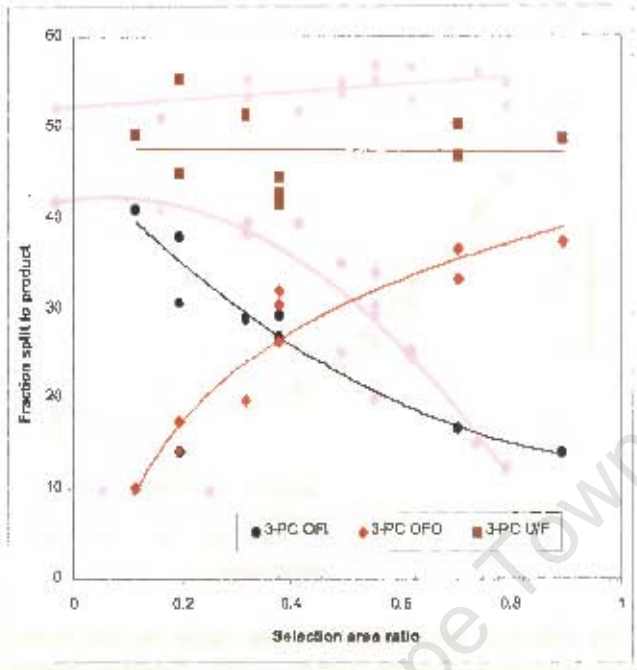


FIGURE 6-11. The effect of the selection area ratio on the mass split to the product streams for the three-product cyclone. LIVF =1025 - reverse classification configurattion.

flowsheet applications. In line with Bradley's [58] suggestion that throttling the annulus in the cyclone with an annular discharge could be used for control purposes, the test cyclone for this thesis had a collar and reducer system described in section 4.3 specially designed to allow different diameter inner vortex finders to be used.

6.3.5 Effect of spigot diameter

The effect of varying the spigot on the percentage of particles passing 100, 75, and 53μm for the OFI and OFO streams for the normal, and reverse classification configurations of the three-product cyclone are given in figures 6-12 and 6-13, respectively.

For the normal classification configuration it was observed that the percentage of particles passing 100, 75, and 53 μm for the OFI and OFO streams increased slightly with increase in the spigot diameter. No significant differences were observed when the spigot diameter was increased from 70 to 95 for the reverse classification configuration for DIVF of 165mm and DOVF of 220mm (Figure 6-13). However,

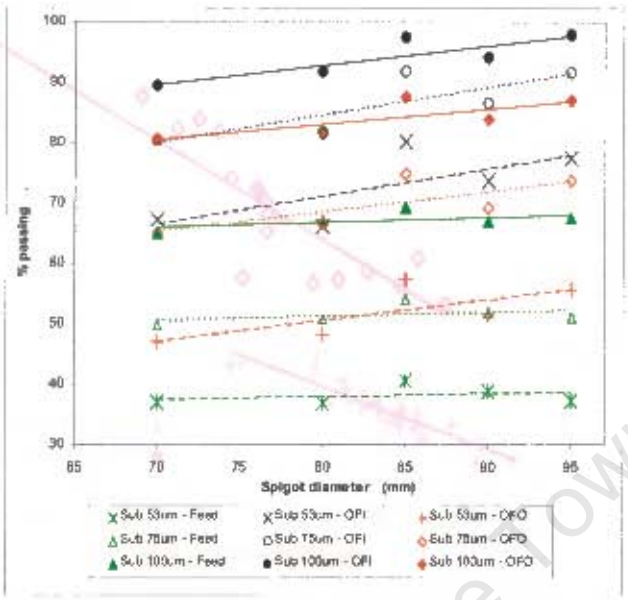


FIGURE 6-12. The Effect of the spigot diameter on particles reporting to the OFI and OFO stream for the three-product cyclone operated with an LIVF of 775mm.

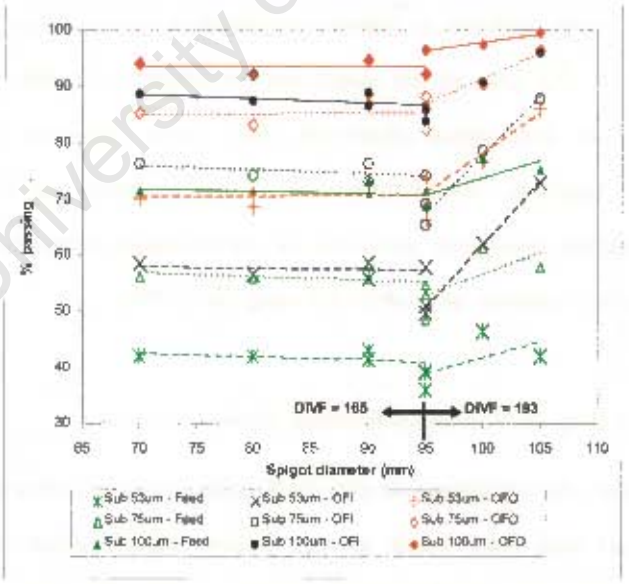


FIGURE 6-13. The Effect of the spigot diameter on particles reporting to the OFI and OFO stream for the three-product cyclone operated with an LIVF of 1025mm.

University of Cape Town

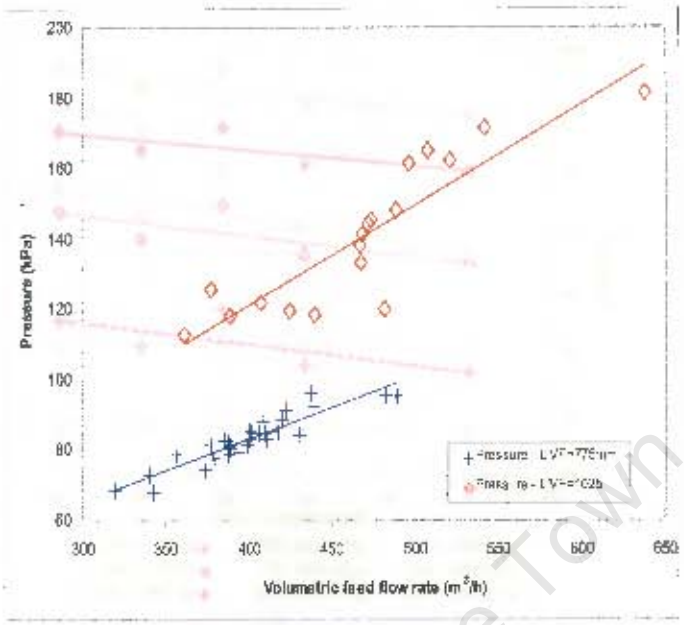


FIGURE 6-14. Variation of Pressure with feed volumetric flow rate for short and long vortex finder configurations of the three-product cyclone.

for the DOVF of 220mm and DIVF of 193mm it was observed that reducing the spigot diameter from 105mm to 95mm resulted in the coarsening of both the OFI and OFO streams. For this larger inner vortex finder extending deep down into the conical section, the differences observed could have been due to the proximity of the inner vortex finder to the cyclone wall leaving a small gap for slurry to flow and promoting migration of coarser particles to the overflow streams due to the crowding effect when smaller spigots are used (Obeng, [61], [69]).

6.3.6 Pressure drop in the three-product cyclone

Figure 6-14 shows the variation in the feed inlet pressure with volumetric feed flow rate for the short and long inner vortex finder configuration of the three-product cyclone. It was observed that generally pressure increased with increase in the volumetric feed flow rate.

The results indicate that operating the three-product cyclone with longer in-

ner vortex finders require a significantly higher pressure than that operated with a shorter inner vortex finder. It appears that for the same volumetric feed flow rate the configuration with the long inner vortex finder required a higher pressure than that with the short inner vortex finder. Scatter was observed in the data especially for the long vortex finder configuration which was attributed to the variations in operating conditions such as the feed solids concentration. It can be concluded that the feed volumetric flow rate and the inner vortex finder length have a significant influence on the operating pressure of the three-product cyclone.

6.4 Efficiency curves

Traditionally, the separation performance of hydrocyclones is measured and modelled using efficiency curves. Efficiency curves have the advantage of describing the particle separation across the whole size distribution and incorporating mass flow rates in the assessment. The formulation of efficiency curves and the parameters that can be derived from these were discussed by other workers:Tromp [78]; De Kok [79]; Kutepov [80]; Svarovsky [30]; and Wills [3] . An efficiency curve can be described by three properties: height; width; and shape of the curve. The height usually corresponds to the water split for wet classifiers denoted 'C', then the width at 0.5 is the corrected cut size ($d50_c$) (Whiten [81]). For conventional cyclones the curve maybe normalised by plotting $\frac{efficiency}{c}$ vs $\frac{size}{d50_c}$ to obtain the reduced efficiency curve (Kojovic, [82], Nageswararao, [36]).

The same formulation used to generate efficiency curves for the conventional hydrocyclones was applied to the three-product cyclone, but with additional curves to represent the inner and outer overflow streams. The traditional efficiency curve parameters have been redefined to accommodate multiple products. The underflow curve is represented by its inverse to make comparisons with the OFI and OFO curves easy. The efficiency curves are taken as fractions recovered to the separate products from the same feed. Therefore, for each size fraction the sum of the recoveries from the

University of Cape Town

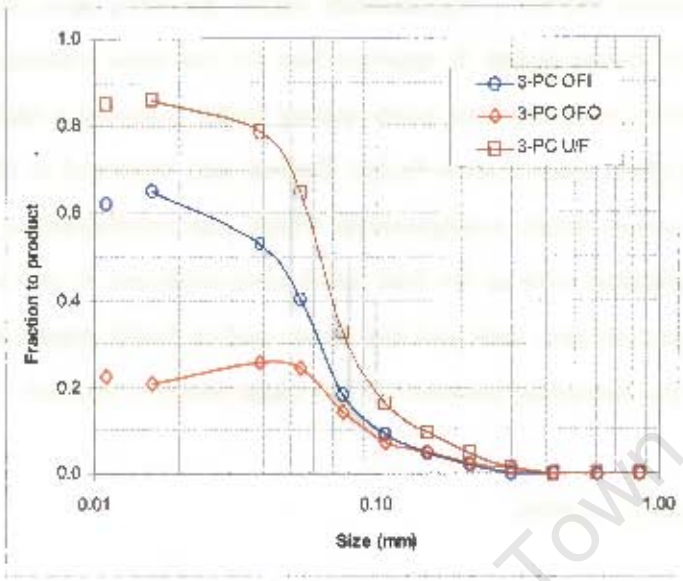


FIGURE 6-15. Efficiency curves for the three-product cyclone - run 67.

products is unity. The experimental data was fitted to the Whiten alpha curve expression (equation 6.2) to obtain efficiency curve parameters for model development [81]. The overall size, chromite, and silica d50c values for the inner overflow and underflow were obtained using the Whiten alpha curve expression. Alpha values for the inner overflow and the underflow curves were also obtained. These were not used in the model due to the large scatter Obtained [81]. The efficiency curve parameters used for model development are given in Appendix E.

$$Eo\left(\frac{d}{d_{50c}}\right) = C\left(\frac{\exp(\alpha)-1}{\exp\left(\alpha\frac{d}{d_{50c}}\right)-\exp(\alpha)-2}\right) \tag{6.2}$$

where: α - reduced efficiency curve sharpness parameter

d - mean particle size, mm,

d_{50c} - corrected cut size, mm,

C - percentage recovery of water to overflow.

Eo(d) - percentage of feed material of size d reporting to overflow.

Figure 6-15 shows typical actual efficiency curves for the three-product cyclone

University of Cape Town

generated using particle size information and stream mass flows. Each stream is represented by an efficiency curve describing the fraction of the feed reporting to that product. The curve for the cyclone underflow is represented by the combined overflow so that it can be easily compared to the curves for the OFI, and OFO streams. The water split fractions are shown as points at the finest size of each curve. It can be seen that for all the curves the fractions increase with decrease in particle size to a value approximately equal to the water split to that product. The efficiency curve to the underflow is the sum of the respective fractions in the OFI and OFO. Therefore, efficiency curves to any two products can be used to describe separation in the three-product cyclone. The corrected cut size $d50_c$ is more appropriate in the three-product cyclone than just the d50 value because one or both of the overflow curves may not reach the 0.5 fraction as demonstrated in Figure 6-15 where the curve to the annulus terminates at the fraction just above 0.2. The $d50_c$ for the three-product cyclone is the size corresponding to the mid-point fraction between zero to the fraction equal to the water split.

6.4.1 Effect of spigot diameter on the cut size

Figure 6-16 shows that the $d50_c$ for all the product streams increases with decrease in the spigot diameter for the normal classification configuration. For the reverse classification configuration the $d50_c$ for the overflow products increases while that of the underflow decreases with increase in spigot diameter (Figure 6-17). The overflow streams coarsen with decrease in the spigot diameter due to the particles being pushed into the upward flow as a result of the constriction in the spigot orifice.

6.4.2 Component efficiency curves

Using the assay data and component densities the contribution of each component was calculated and component efficiency curves plotted. Assays by size were obtained for silica (si) representing the low density component and chromite (cr) representing the high density component. The remainder of the components were not assayed

University of Cape Town

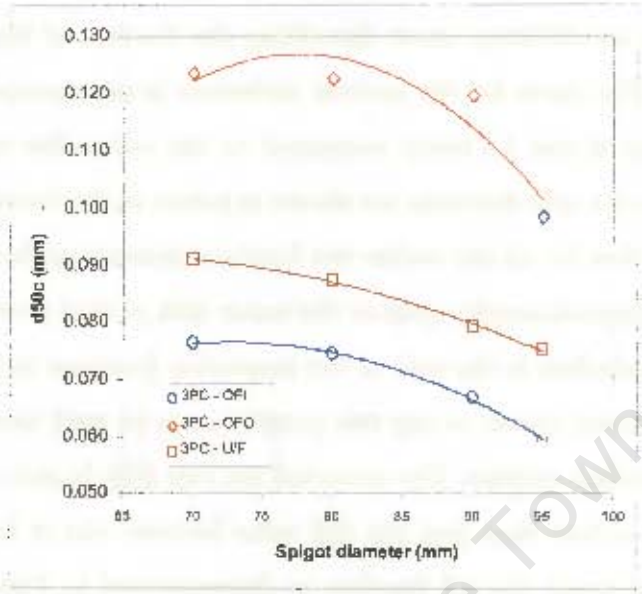


FIGURE 6-16. Effect of the spigot diameter on the d50c for the three-product cyclone operated with an inner vortex finder length of 775mm.

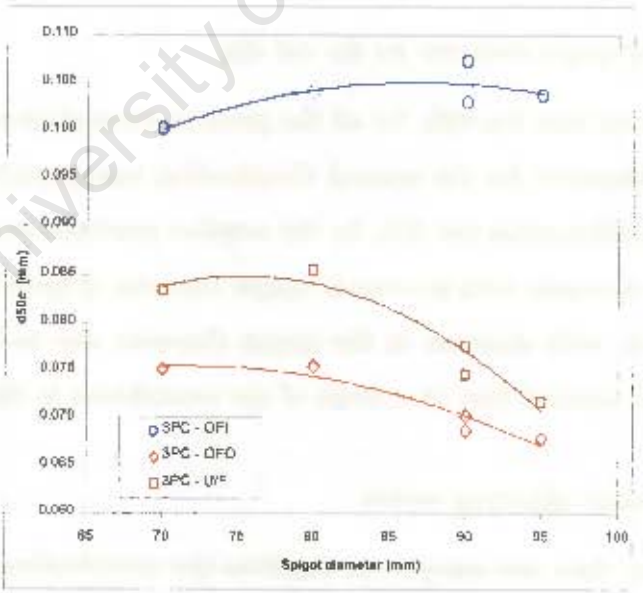


FIGURE 6-17. Effect of the spigot diameter on the d50c for the three-product cyclone operated with an inner vortex finder length of 1025mm.

University of Cape Town

for and are collectively represented by the remainder (rem) in the analysis. The efficiency curves for the chromite, silica, and remainder components for the three-product cyclone are presented in figure 6-18. From the component efficiency curves representing the product streams it can be seen that for each product the efficiency curve for silica - the lighter component - is classified at a coarser size, and chromite - the heavier component - at a finer size. This is similar to the observations made by Laplante and Finch when they were analysing the origin of unusual efficiency curves [83]. The remainder appear to be close to the overall size curve. Efficiency curves for all the 41 tests where assays by size data was obtained are presented in Appendix C.

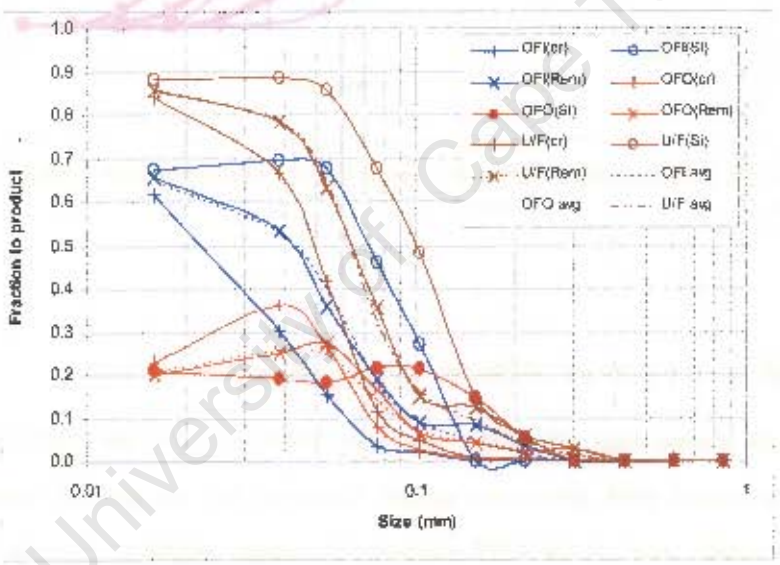


FIGURE 6-18. Components efficiency curves for the three-product cyclone.

The component efficiency curves figure 6-18 were smoothed to obtain the curves shown in figure 6-19. The efficiency curves were smoothed to remove the inconsistencies that are generally associated with assay data, [84]. During the smoothing process the uppermost point, the component $d50_c$, and the lowest point were preserved. This enabled consistent efficiency curve parameters to be obtained from assay data. However, due to the difference between the experimental efficiency curves

and the smoothed curves, the efficiency curve parameters used in the analysis and modelling were from the unsmoothed curves.

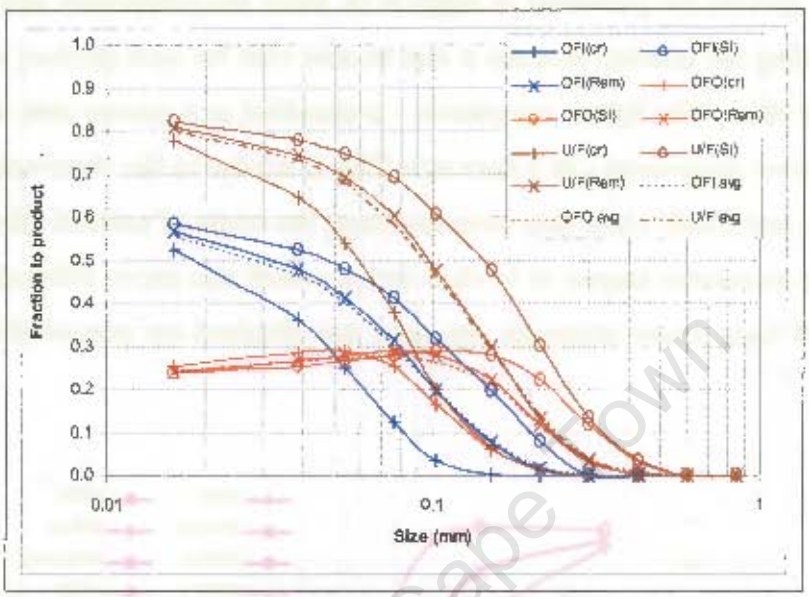


FIGURE 6-19. Components efficiency curves for the three-product cyclone from smoothed assay data.

6.4.3 Effect of the spigot diameter on the component cut size

Figure 6-20 shows that the silica cut size ($d50_c(si)$) for the OFO and underflow streams increased with decreased spigot diameter for the normal classification configuration while that of the OFI streams decreased slightly. For the reverse classification configuration, 6-21, the $d50_c(si)$ for the overflow products increased when the spigot was reduced from 95 to 80mm. The $d50_c(si)$ decreased with further reduction of the spigot diameter from 80mm to 70mm. For the reverse classification configuration the $d50_c(si)$ underflow appeared to increase slightly when the spigot diameter was reduced from 95 to 80mm and no changes where observed when the spigot diameter was reduced from 80 to 70mm.

The chromite cut size ($d50_c(cr)$) for the OFO and underflow streams appear to increase with decreased spigot diameter for normal classification configuration while

University of Cape Town

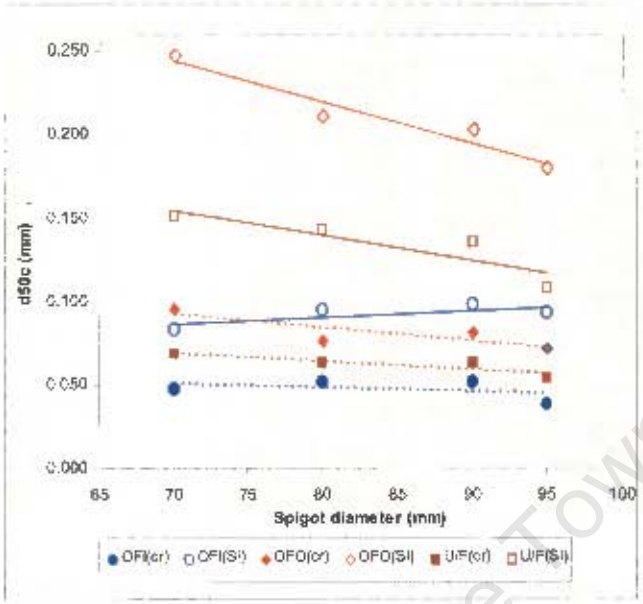


FIGURE 6-20. Effect of the spigot diameter on the component d50c for the three-product cyclone operated with an inner vortex finder length of 775mm.

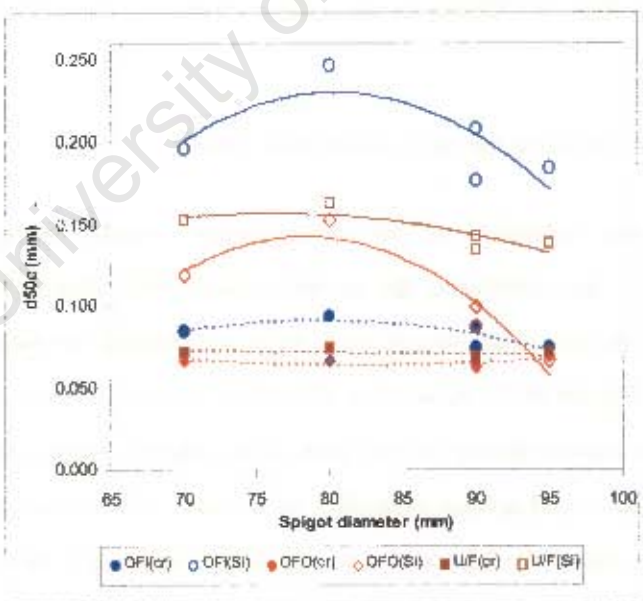


FIGURE 6-21. Effect of the spigot diameter on the component d50c for the three-product cyclone operated with an inner vortex finder length of 1025mm.

University of Cape Town

TABLE 6.5. Replicate tests for the three-product cyclone with Dovf of 220mm, Divf of 177 mm, LIVF of 775 mm, and Dspig of 95mm .

Run No.	46	47	Coefficient of variance, %
Feed TPH solids	327.4	310.6	3.8
Feed % solids	48.3	47.7	0.9
Mass split to OFI, %	36.8	36.2	1.2
Mass split to OFO, %	9.0	8.2	6.6
Mass split to U/F, %	54.2	55.6	1.8
d50c OFI, mm	66.1	66.4	0.3
d50c OFO, mm	86.4	84.3	1.7
d50c U/F, mm	65.4	67.7	2.4
% passing 75 μm OFI	88.0	86.6	1.1
% passing 75 μm U/F	31.2	33.2	8.5
P80 OFI, μm	0.062	0.064	2.2
P80 U/F, μm	0.141	0.134	3.6

no changes were observed for the OFI stream. For the reverse classification configuration no changes were observed in the $d50_c(cr)$ for the OFO and U/F with decrease in spigot diameter while those for the OFI stream appear to increase with a reduction in the spigot diameter from 95 to 80mm. The $d50_c(cr)$ exhibited a slight decrease with further reduction in the spigot diameter from 80mm to 70mm.

6.5 Reproducibility of experimental data

To determine the reliability of the measurements taken during the experimental work and to test the validity of the model, repeat tests were performed for some of the conditions. In this work repeat tests were performed on different days from the primary tests. Figure 6-22 shows the efficiency curves for two test runs performed using the outer vortex finder of 220 mm, inner vortex finder diameter of 198 mm, length of 775 mm, and spigot diameter of 95 mm. The corresponding mass splits to the products and d50c values are presented in Table 6.5. It can be seen that the result are reproducible.

Figure 6-23 shows the efficiency curves for test runs performed using the outer vortex finder of 220 mm, inner vortex finder diameter of 177 mm, length of 875

TABLE 6.6. Replicate tests for the three-product cyclone with Dovf of 220mm, Divf of 177 mm, LIVF of 775 mm, and Dspig of 95mm .

Run No.	38	79	Coefficient of variance, %
Feed TPH solids	299.0	302.7	0.9
Feed % solids	43.3	46.0	4.3
Mass split to OFI, %	11.40	12.04	5.5
Mass split to OFO, %	28.6	30.58	4.7
Mass split to U/F, %	60.2	57.38	3.4
d50c OFI, mm	72.87	73.54	0.65
d50c OFO, mm	75.87	78.70	2.8
d50c U/F, mm	70.64	68.77	1.9
% passing 75 μm OFI	81.2	81.1	0.2
% passing 75 μm U/F	31.5	28.9	6.1
P80 OFI, μm	0.074	0.075	0.9
P80 OFO, μm	0.135	0.139	2.1

mm, and spigot diameter of 95 mm, and the and corresponding mass split and d50c values are given in Table 6.6. It can be seen that tests performed under these cyclone variables were reproducible with small variations that are expected on an industrial plant. It was observed that in both sets of tests analysed the feed % solids is different between tests, which is a consequence of plant variation. The coefficients of variation in table 6.6 and ?? show that the results are reproducible. It can therefore be concluded that the observed trends are reproducible and that the difference between the low and high variable is significant.

6.6 Summary

The three-product cyclone produces three distinct products when operated in normal and reverse classification configurations while no significant differences in the OFI and OFO size distribution are observed if operated in the 'cross - over region'. The LIVF can be used to control the particle size classification in the three-product cyclone by either positioning the inner vortex finder above or below the 'cross-over region'.

The SAR influences the flow split between the OFI and OFO product streams.

University of Cape Town

The SAR can be used to control the flow split to the OFI and OFO streams if the cyclone design has provision which allows interchangeable inner and outer vortex finder diameters such as a reducer -collar system for the inner vortex finder.

To describe separation in the three-product cyclone using efficiency curves, curves to at least two products are required. If two curves are specified the third one can be calculated from the two. The same formulation used for the overall efficiency curves is applicable for component efficiency curves. Component efficiency curves have shown that the light component classifies at a coarser cut size while the heavy component classifies at a finer cut size for all the product curves.

For the normal classification configuration, the underflow, and the intermediate sized stream coarsened with decrease in spigot diameter for both the overall size curves, and the silica, and chromite component curves. For the reverse classification configuration, the underflow, and the OFO stream coarsened with decrease in spigot diameters for the overall size curves, while the OFI cut size decreased slightly.

University of Cape Town

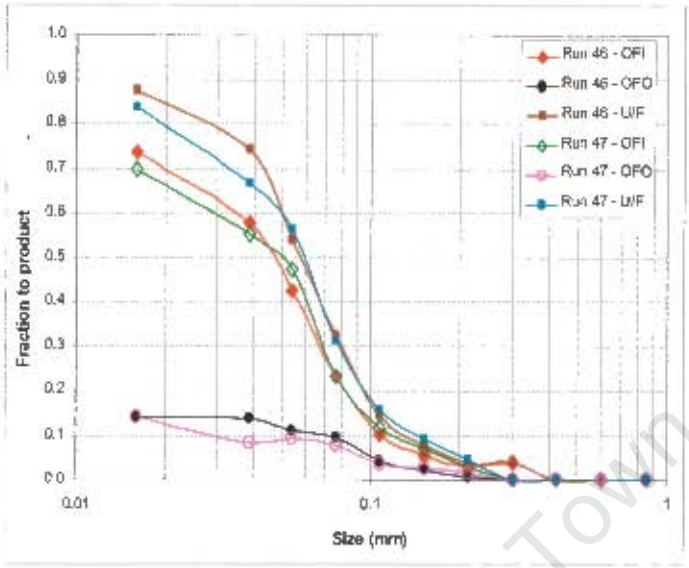


FIGURE 6-22. Replicate tests for the three-product cyclone with Dovf of 220mm, Divf of 177 mm, LIVF of 775 mm, and Dspig of 95mm.

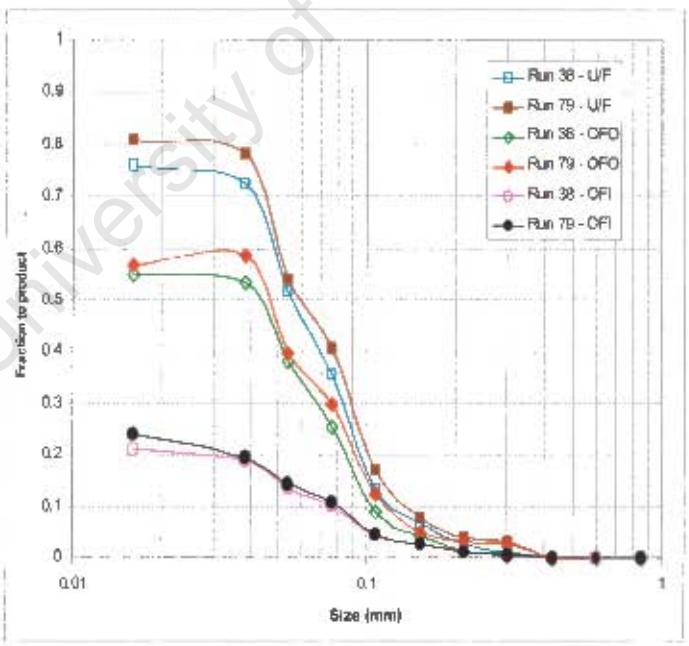


FIGURE 6-23. Replicate tests for the three-product cyclone with Dovf of 220mm, Divf of 198 mm, LIVF of 875 mm, and Dspig of 95mm.

University of Cape Town

7

Contribution from the Computational Fluid Dynamics simulations

Computational Fluid Dynamics (CFD) simulations were performed by Mr. Narasimha Mangadody of the JKMRC, based at the University of Queensland in Australia, on behalf of the author and the results were analysed and interpreted by the author. Simulations were performed for the conventional and three-product cyclone on a two phase system containing only water and air. Although no solids were present in these simulations, valuable flow information was obtained. It was useful to conduct simulations with water and air only to study the flow behaviour of the medium which has a significant influence on solids separation within the hydrocyclone and to obtain information on aspects of flow that can not be measured from plant trials, such as the air-core dimensions. For the two types of hydrocyclones studied, the liquid velocity profiles, the air-core, and other flow characteristics were analysed.

University of Cape Town

7.1 General hydrocyclone flow modelling

As far back as 1952, Kelsall [7], indicated that knowledge of flow within the hydrocyclone was an important aspect of design and modelling of these units. Due to the complexity of the physics and flow behaviour in the hydrocyclone, empirical models have been developed for design and optimisation. However, it is still acknowledged that a good understanding of the flow behaviour in the hydrocyclone is required for any significant improvements to be made in the design and operation of these units (Statie et al. [85], Monrendon [46]). Many studies have been done focusing on theoretical studies using the Navier Stokes equations. These, in the CFD framework, along with experimental work such as that performed by Hsieh - where Laser Doppler

Anemometry (LDA) was used to study flow in the hydrocyclone. Flow studies using LDA and applied numerical methods used to model the observed flow behaviour, have no doubt contributed to the understanding of fluid flow and separation in the hydrocyclone (Rietema [21], Hsieh and Rajamani [86], Bloor and Ingham [87]). In all these studies it was found that although the construction of the hydrocyclone is relatively simple, flow behaviour is complex, making prediction difficult. Despite the challenges associated with this task, most of the previous studies have shown the significance of studying the flow in any type of hydrocyclone (Kelsall [7], Bradley [20] [8], Monrendon [46], Narasimha et al. [88], Chakraborti [89]).

7.2 Cyclone modelling using CFD

Advances in computational technology in recent years have led to models based on fundamental fluid flow taking central stage as tools that will enhance the understanding of flow fields within the hydrocyclone and bring about improvements in the design of these process units. The commercially available CFD package Fluent is one of the efficient means to study the fluid dynamics of many physical systems and it has been used widely in engineering applications, including modelling flow in hydrocyclones. The use of CFD will go some way to alleviate the problems of using empirical engineering models based on correlation formulae established for a limited range of parameters dictated by the experimental data. Statie et al [85], indicated that CFD and other numerical tools can give high quality information on separation performance and shed more light on the influence of different geometric and flow parameters. Therefore, uncertainties raised by these effects can be significantly lessened by modelling the devices and simulating the behaviour.

Since the three-product cyclone is an off-shoot of the conventional hydrocyclone, tools used for modelling flow in the conventional hydrocyclone can be applied to the three-product cyclone as the two types of cyclones exhibit similar general flow characteristics, (Bednarski [6]). Although the general flow characteristics in the three-

University of Cape Town

TABLE 7.1. A summary of the cyclone design variables used in the CFD simulations.

Variable	Dimension
Cyclone diameter, mm	600
Equivalent inlet diameter, mm	160
Length of cylindrical part, mm	655
Slanting length of conical part, mm	770
Cone angle	20°
Outer vortex finder internal diameter, mm	220
Inner vortex finder internal diameter, mm	165
Inner vortex finder length, mm	0, 775, 925, 1025
Outer vortex finder length, mm	675
Spigot diameter, mm	95

product cyclone are similar to that of the conventional cyclone, the presence of an extra vortex finder in the three-product cyclone changes the local flow behaviour in the vortex finder region and variations in the length of the extra vortex finder lead to significant changes in the magnitudes of some flow parameters.

CFD simulations were performed to study the flow fields in the three-product cyclone and comparative studies were performed on the conventional hydrocyclone of the same size. The aims of the study were: to compare the flow fields between the three-product cyclone and conventional hydrocyclone; and to study the effect of the inner vortex finder length on flow within the hydrocyclone.

7.3 Three-product cyclone CFD simulations

A summary of the cyclone dimensions and design variables used in the experimental work are given in table 7.1. The geometry of the cyclones is given in figure 3-1 and 3-5.

7.3.1 CFD approach

Fluent version 6 was used to perform simulations [90]. The computational mesh (185,000 grid nodes) used in the simulation illustrated in figure 7-1 was constructed. A mesh with a similar number of nodes was used for the conventional hydrocyclone

University of Cape Town

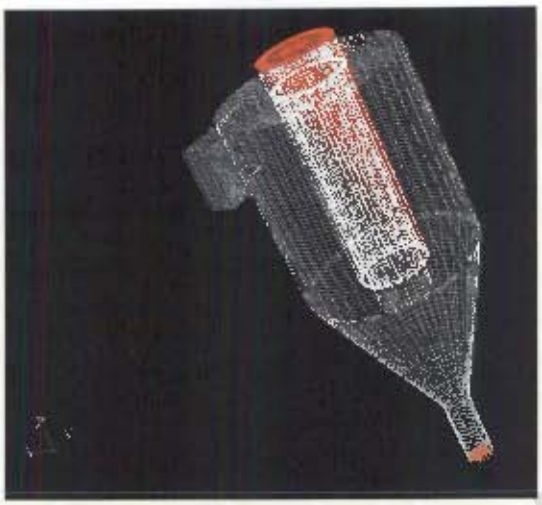


FIGURE 7-1. Illustration of the computational mesh of the 600mm diameter three-product cyclone

velocity simulations. Detailed theoretical and practical considerations for hydrocyclone modelling using CFD have been discussed by many authors and only a brief description is given in this thesis (Hsieh and Rajamani [86], Narasimha et al. [88], Brennan [91], Slack et al. [92], Pericleous eat al. [93], Cullivan et al. [94], [95], [96]).

The CFD simulations were conducted using Fluent with 3d body fitted grids for both the three-product cyclone and the conventional hydrocyclone. Simulations have been conducted using Large Eddy Simulation (LES) turbulence model. The LES model was chosen because it has been shown to predict the velocity profiles at different locations of flow correctly, and to provide a realistic parabolic shape for the air-core (Delgadillo and Rajamani [97]). The air-core has been resolved using the Volume of Fluid model (VOF). The simulations were performed using water and air only. A grid independence test was performed and the results didn't deviate from those provided in this thesis. The convergence criterion used showed that the simulations converged. All the simulations were over 6 seconds simulation time which is adequate for the simulations of this nature. The data presented here are time averages which is a recommended way of presenting this data.

University of Cape Town

7.4 General flow fields

Typical flow fields at different planes (xy) of the interior portion for the conventional and three-product cyclone are shown in Figure 7-2. It was observed that the general flow structure of the three-product cyclone, regardless of variations in the length of inner vortex finder used, was similar to that of the conventional hydrocyclone. From this it can be concluded that the general flow structure in the hydrocyclone is preserved and the methods employed to analyse flow in the conventional hydrocyclone can be applied to the three-product cyclone. As presented in the rest of the chapter, upward swirl patterns are observed around the central core in both types of hydrocyclones. Despite the extra overflow product in the three-product cyclone, only one upward secondary spiral that results in the two overflow streams and a downward spiral which eventually leads to the underflow were present. For the three-product cyclone the highest velocities were observed at the tips of the inner and outer vortex finder with low velocities near the cyclone walls and no liquid was present in the air-core region.

7.5 Velocity vectors and profiles

The analysis of the tangential velocity profiles was performed for the entire cyclone but only the region where the influence of the dual vortex finder arrangement in the three-product cyclone was expected to be significant is discussed. This region begins at the position Z = 575mm located in the cylindrical section just above the tip of vortex finder (outer vortex finder for the three-product cyclone) and extends deep into the conical section to a position Z = 1075mm which is deep down into the conical section close to the spigot orifice. The position Z = 675mm locates the tip of the vortex finder for the conventional cyclone which is the outer vortex finder for the three-product cyclone. The positions Z = 775mm and Z = 1025mm correspond to the locations where the inner vortex finder terminate for the short and long inner vortex finder configurations of the three-product cyclone. The positions between Z =

University of Cape Town

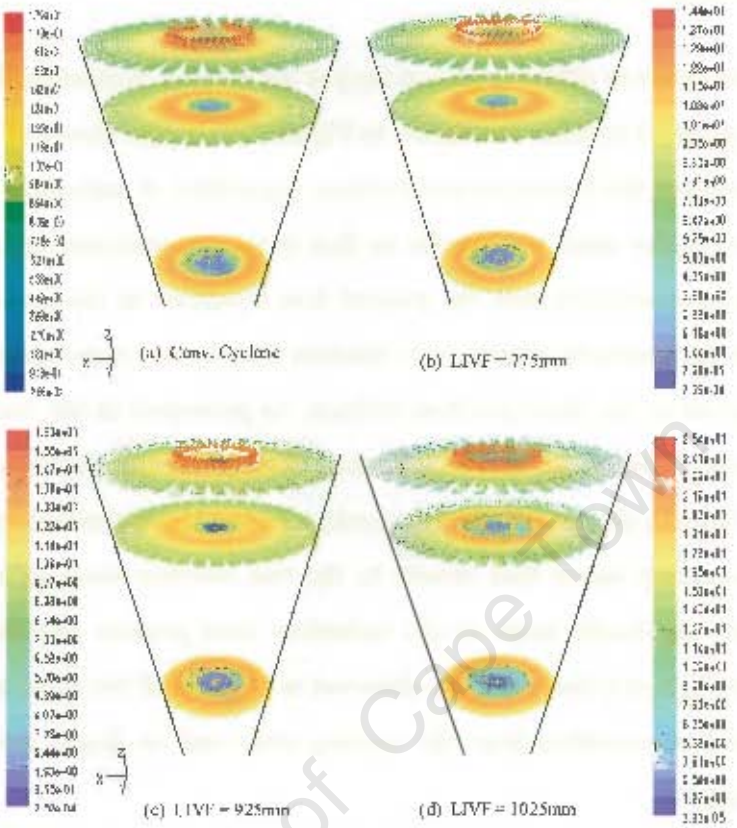


FIGURE 7-2. Typical flow fields in the planes (xy) at different Z positions of the interior portion of the conventional and three-product cyclones

875mm and 975mm correspond to the region identified as the 'cross-over region' for the three-product cyclone of this geometry. From the field experiments performed for the UG2 platinum ore application discussed in section 6.3.1, no significant differences were observed in the size distributions for the OFI and OFO streams when the inner vortex finder terminated in the 'cross-over region' [98].

7.5.1 Influence of the inner vortex finder length on the velocity profiles and velocity field vectors

The tangential velocity component is the dominant component of fluid flow in cyclones which results in centrifugal force for particle separation. Many authors have

University of Cape Town

indicated that the tangential and axial velocity components are the most significant velocities as they are responsible for particle separation (Hsieh and Rajamani, [86], Solero and Coghe [99], Ferrara and Bevilacqua [100]). Figure 7-3 shows tangential velocity profiles at six planes on the Z - axis for the three-product cyclone from simulations performed with different length inner vortex finders, and for the conventional hydrocyclone. The larger numbers on the y axis represent the position along y axis from the top plate where sampling was performed and the smaller numbers represent the magnitude of the measurement being analysed . The corresponding axial velocity distributions are presented in Figure 7-4. The radial positions from the central axis (marked zero), up to the outer wall of the hydrocyclone were analysed. The vertical axis on each sub plot is the tangential velocity in $m.s^{-1}$. Although the trends for the tangential velocity profiles from different cyclone configurations are similar, the magnitudes of local velocities are significantly different. It is generally accepted that higher tangential velocities result in higher separation efficiencies.

At Z = 675mm, a sharp rise was observed in the tangential velocity distribution for the conventional hydrocyclone from zero in the air-core region to a maximum near the vortex finder wall. A steady decline was observed with increasing radial position from the vortex finder wall prior to a sharp drop to zero at the cyclone wall (Figure 7-3). It should be noted that the zero velocity at the cyclone wall is a conventional boundary condition set by the CFD users. It applies to a relatively thin boundary layer and should not be interpreted as physically meaningful. A similar trend was exhibited by the tangential velocity distributions for the three-product cyclone with the exception of the zero velocities observed at the inner vortex finder wall - which is absent in the conventional hydrocyclone. The position of the zero velocity shows the location of the vortex finder. A comparison of the tangential velocities for different inner vortex finder length simulations showed that increasing the inner vortex finder length from 775mm to 1025mm resulted in a significant increase in the magnitudes of the local tangential velocities in the region between the cyclone wall and the inner

University of Cape Town

vortex finder wall for the three-product cyclone.

The three-product cyclone simulations for the inner vortex finder length of 1025mm had significantly higher local tangential velocities in this region compared to those performed using the inner vortex finder lengths of 775mm and 975mm, and the conventional hydrocyclones. It was observed that the local tangential velocities for the three-product cyclone with the inner vortex finder length of 775mm were identical to those for the conventional hydrocyclone in this region but lower than those for the three-product cyclones with the inner vortex finder lengths of 975mm and 1025mm. In the region between the inner vortex finder wall and the air-core higher local tangential velocities were observed for the conventional hydrocyclone than those for all the three-product cyclone configurations simulated. In the annular region, the three-product cyclone with the inner vortex finder length of 1025mm had the highest local tangential velocities and that with the inner vortex finder length of 775mm had the lowest.

The trends exhibited by the tangential velocity profile at Z = 775mm, Z = 875mm, 975mm, and Z = 1075mm were similar to those obtained at Z = 675mm, except that there is no outer vortex finder at these locations and the inner vortex finders from some of the three-product cyclones simulations had already terminated. For example at the plane Z = 875mm, only the three-product cyclones with inner vortex finder lengths of 925mm and 1025mm had zero tangential velocities at the inner vortex finder wall. It was observed that the tangential velocity distributions varied slightly with changes in the Z-axis implying that for each cyclone configuration the maximum velocities from one plane to another were similar. From the tangential velocity profiles, it can be concluded that inserting another vortex finder concentric to the existing one has an influence on the flow patterns and that the effect on the magnitude of the local tangential velocities is more pronounced with longer inner vortex finders. The high tangential velocities observed with long inner vortex finders suggest that the inner vortex finder can be exploited to improve separation efficiency

University of Cape Town

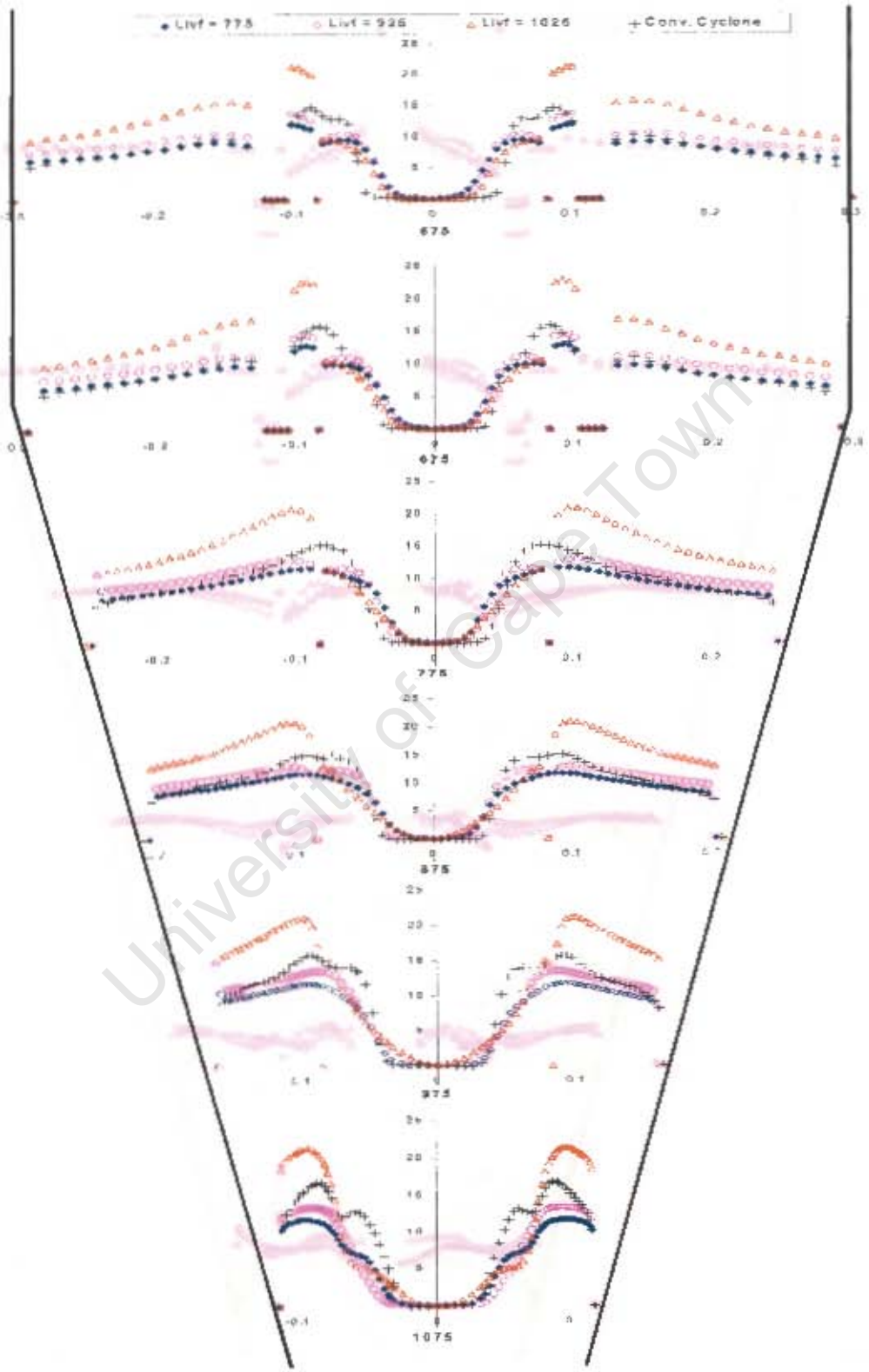


FIGURE 7-3. Tangential velocity distributions.

University of Cape Town

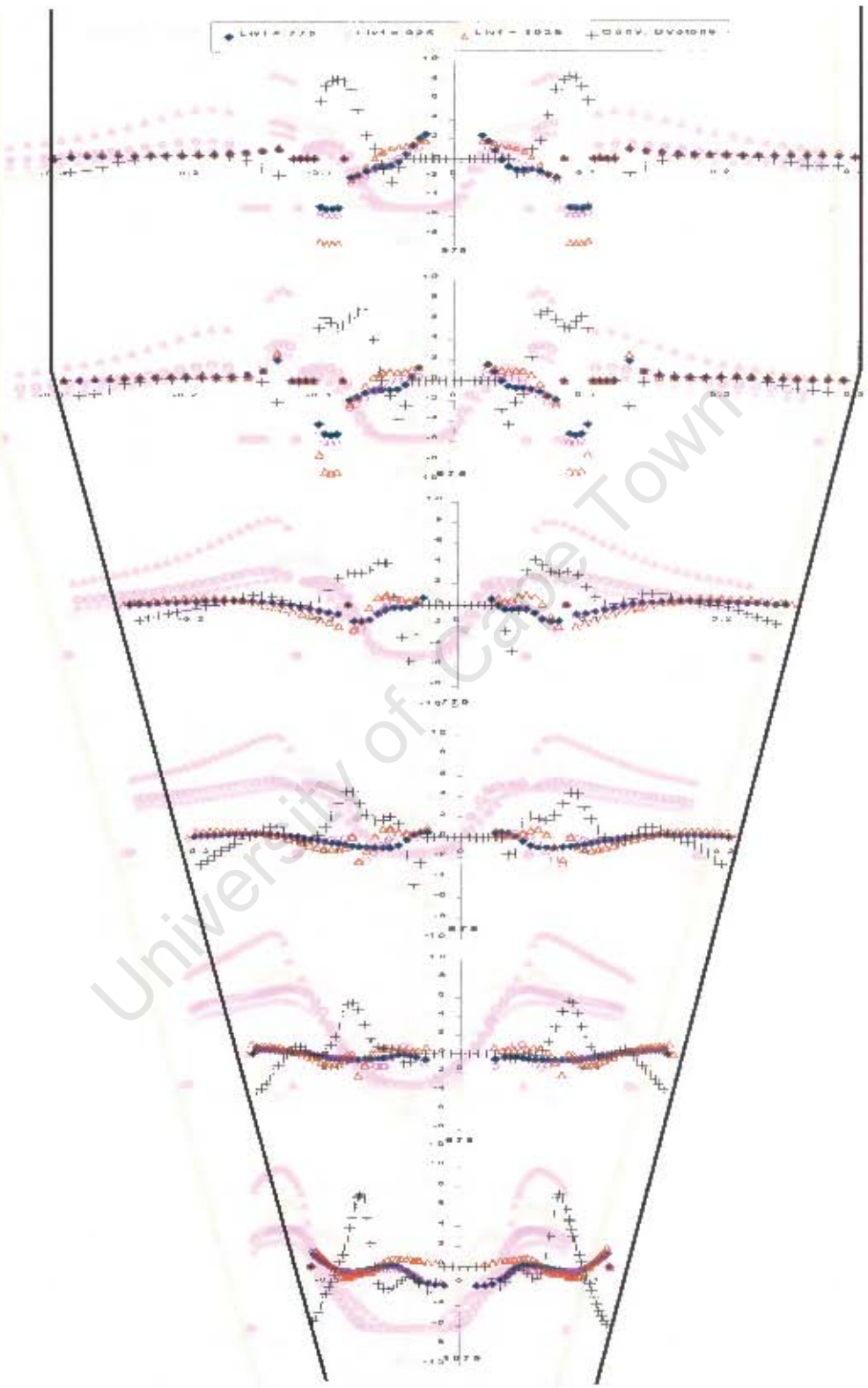


FIGURE 7-1. Axial velocity distributions.

University of Cape Town

in this dual vortex finder cyclone. The high pressure requirement at this inner vortex finder length discussed in section 6.3.6 also contribute to high tangential velocities.

The axial velocity distributions for the conventional hydrocyclone were significantly higher than those for the three-product cyclone in the region between the air-core and the radial position of 110mm for all planes along the Z-axis analysed (Figure 7-4). It was observed that the axial velocities for the conventional hydrocyclone were positive in this region as opposed to those for the three-product cyclone which were negative in the same region. However, the three-product cyclone had positive axial velocities outward while those for the conventional cyclone were negative. The axial velocity profiles for the three-product cyclone decreased with increasing inner vortex finder length which is the inverse of what was observed from the tangential velocity profiles.

7.5.2 Velocity field vectors

The velocity field vectors in the xz-plane for the three-product cyclones with short, and long inner vortex finders, and for the conventional hydrocyclone are presented in Figures 7-5, 7-6, and 7-7, respectively. From the velocity field vectors it was observed that flow reversals occur over the entire region for the conventional hydrocyclone and for the three-product cyclone. It was observed that inward flow for the three-product cyclone was split to that reporting to the inner vortex finder and to the annulus between the inner and outer vortex finders.

The major difference observed between the velocity field vectors for the three-product cyclone and for the conventional hydrocyclone is the splitting of the upward vectors to the inner vortex finder orifice, and to the annulus between the inner and outer vortex finders which results in the OFI and OFO products streams. Maximum velocities of 2.91 m/s and 1.71 m/s were observed at the vortex finder tips for the three-product cyclone with the inner vortex finder lengths of 1025mm and 775mm, respectively. The corresponding maximum velocity for the conventional hy-

University of Cape Town

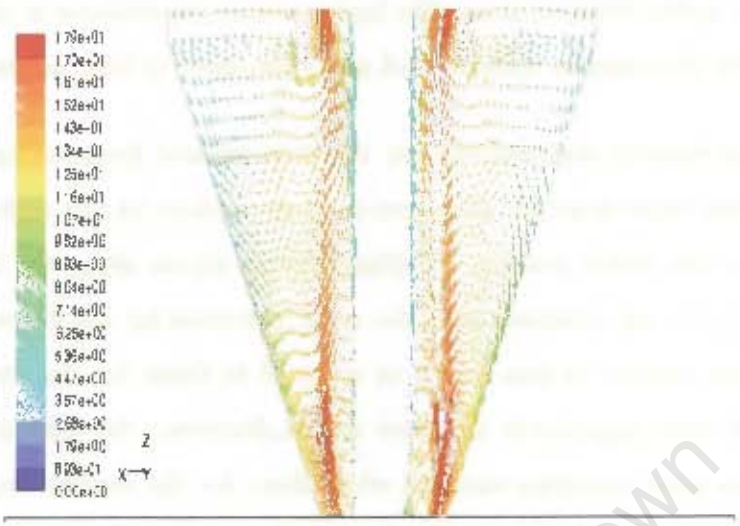


FIGURE 7-5. Velocity field vectors for the conventional hydrocyclone.

drocyclone was 1.79 m/s. A minimum velocity of zero was observed in the air-phase region for all the cases simulated.

This confirms the observations by Dabir and Petty [11], that the geometry of the vortex finder plays an important role in determining the flow patterns in the core region of the cyclone. In this dual vortex finder arrangement the effect of the inner vortex finder on flow patterns from CFD simulations in conjunction with data obtained from field experiments performed using the cyclone of the same geometry can be used to provide guidance on the optimal length for the inner vortex finder for specific applications (Mainza et al [98]).

7.6 Influence of the inner vortex finder length on the air-core

In section 6.3.3 it was found that the ratio of the annulus to the inner vortex finder openings had a significant influence on the flow split to the two overflow products of the three-product cyclone [98]. However, it was observed that only a portion of the inner vortex finder was active in allowing the slurry to flow through and a significantly large portion occupied by the air-core. Knowledge of the air-core be-

University of Cape Town

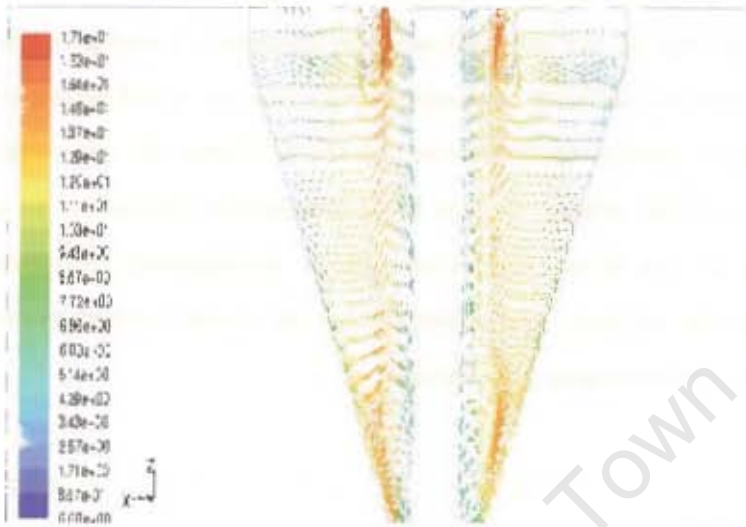


FIGURE 7-6. Velocity field vectors for the three-product cyclone - inner vortex finder length = 775mm.

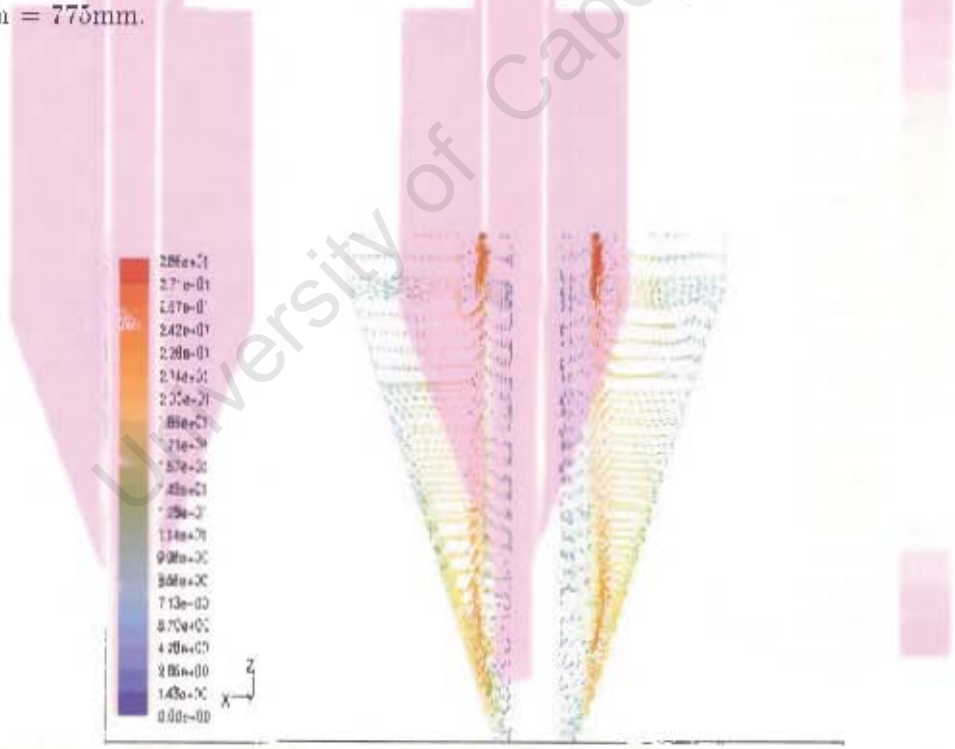


FIGURE 7-7. Velocity field vectors for the three-product cyclone - inner vortex finder length = 1025mm.

University of Cape Town

havior would assist in flow predictions (Steffens et al. [101]). The air-core diameter is critical in the three-product cyclone where the flow split to the inner overflow is adversely affected by the proportion of the diameter occupied by the air-core. Due to lack of practical methods of measuring the air-core in industrial cyclones, air-core measurements, though critical, were not made during the site experimental work. This motivated the author to have CFD simulations performed to study the influence of the air-core in this dual vortex finder arrangement. To enable comparisons to be made the air-core was generated for the three-product cyclone and for the conventional hydrocyclone simulations.

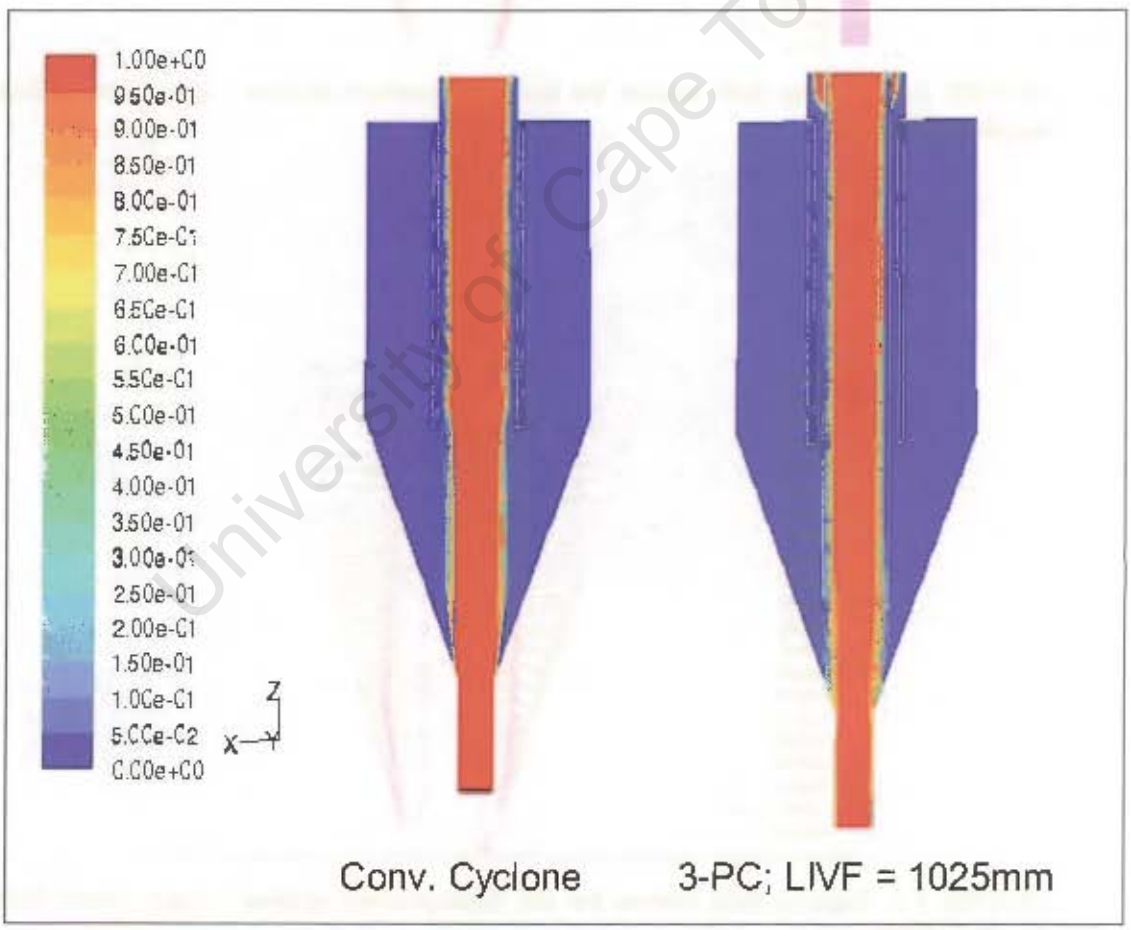


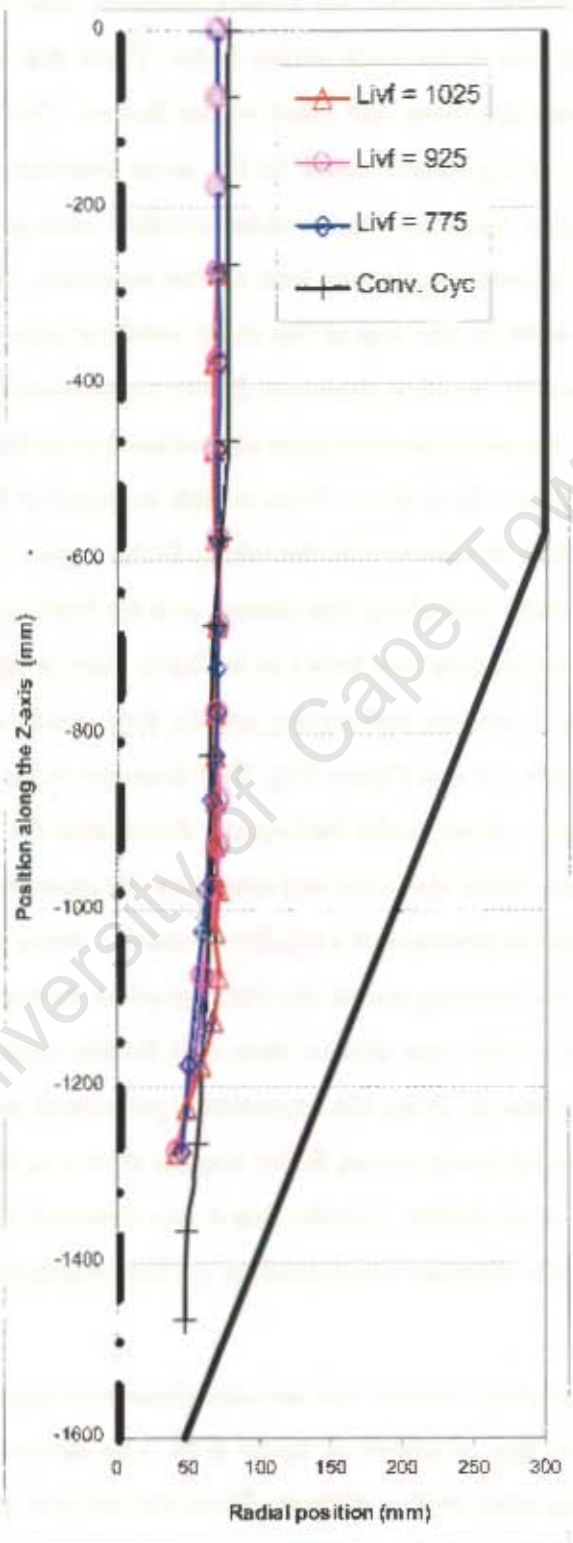
FIGURE 7-8. Cross sections of the conventional and three-product cyclones showing the shape of the aircore along the xz – plane.

University of Cape Town

For the three-product cyclone, the results indicated that the air-core is present only at the central core of the inner vortex finder. There was no air core observed in the annulus between the inner and outer vortex finders. This is expected otherwise there could be no slurry classification to the inner overflow. Experience of others with poorly designed three-product cyclone overflow arrangement has shown that an air-core in the annulus region can lead to this condition. However, there was air present near the walls at the top of the outer overflow pipe and is a consequence of a step change in the overflow diameter. In the experimental cyclone described in Chapters 3 and 4, the outer overflow pipe was reduced to avoid air being drawn from outside. This could have been drawn from outside as shown in Figure 7-8. Simulation results indicated that the air-core in the vortex finder region was generally found to be cylindrical in shape and along the central axis for both types of hydrocyclones. The diameter of the air core was found to be fairly even in the vortex finder region for the three-product cyclone and similar results were obtained for the conventional hydrocyclone (Figure 7-8 and Figure 7-9). The diameter of the air core seemed to be defined by the inner vortex finder and spigot dimensions for the three-product cyclone and the vortex finder diameter and spigot for the conventional cyclone (Fontein et al. [102]). Due to the presence of a smaller diameter - extra vortex finder - inserted concentrically to the existing one in the three-product cyclone, the air-core diameter in this type of cyclone was smaller than that for the conventional hydrocyclone resulting in high pressure. From the simulations performed using the three-product cyclones with different inner vortex finder lengths shown in Figure 7-9, the air-core diameters appear to be similar. Despite this it was observed that the air-core shapes were different for the different three-product cyclone configurations.

For the three-product cyclone the air-core diameters started tapering near the inner vortex finder tips as shown in figure 7-10. The air-core for the conventional cyclone started tapering at Z = 650mm. From the air-core profiles, it can be concluded that for a fixed spigot diameter the air-core diameter and shape is dependant

University of Cape Town



University of Cape Town

FIGURE 7-9. Comparison of the air-core dimensions in the conventional and three-product cyclone.

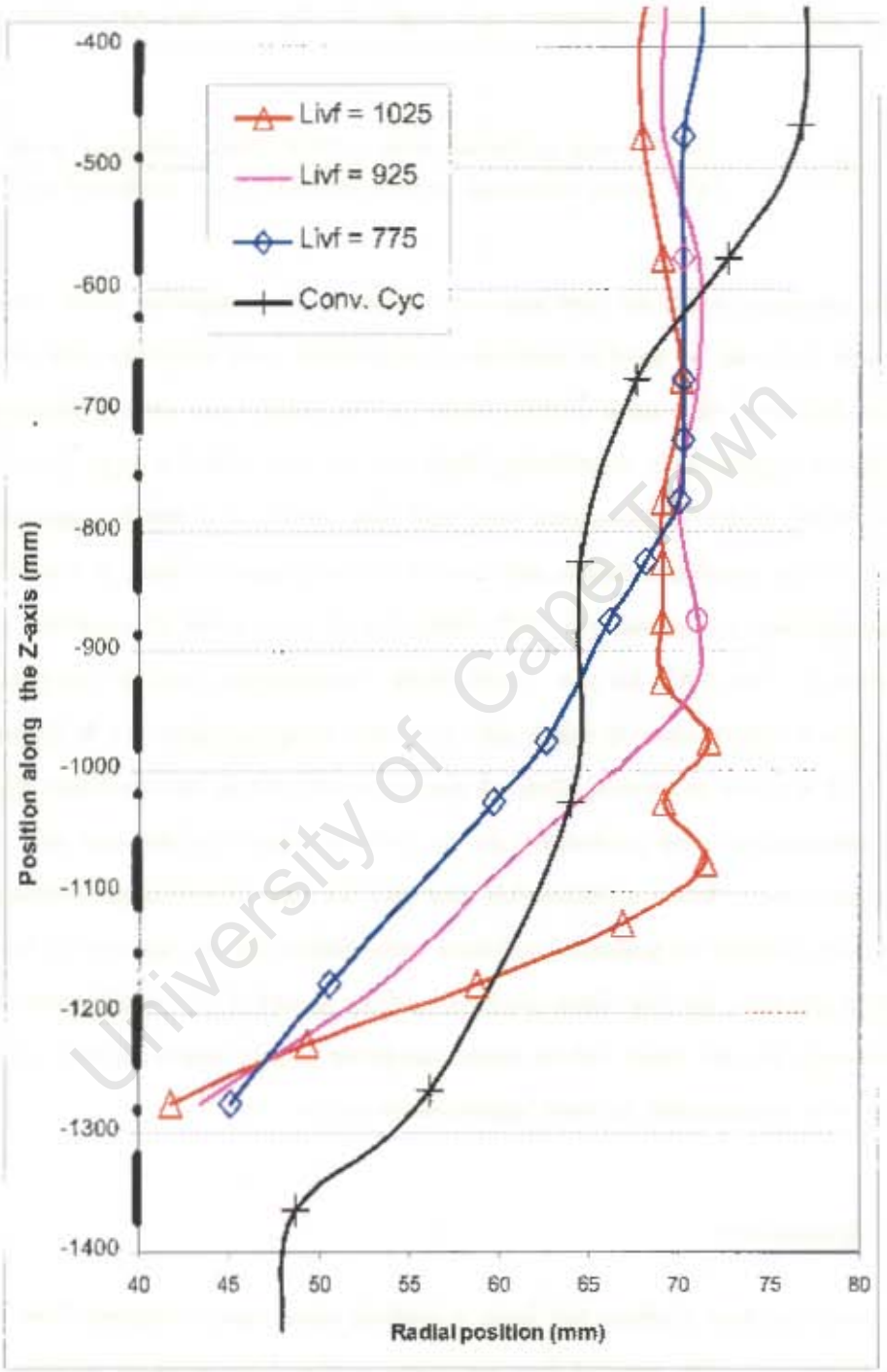


FIGURE 7-10. Magnified air-core profiles.

University of Cape Town

on the diameter and length of the inner vortex finder for the three-product cyclone, and on the vortex finder diameter and length for the conventional hydrocyclone.

$$SAR_{ef-ac} = \frac{OVF\ cross\ sectional\ area - IVF\ cross\ sectional\ area}{IVF\ cross\ sectional\ area - aircore\ cross\ sectional\ area} \tag{7.1}$$

The presence of the air core imposes a limit on the minimum inner vortex finder diameter that can be used to maintain a reasonable area active for flow in the inner vortex finder. If the inner vortex finder is too small, the area available for flow is reduced significantly considering that the air-core takes a large portion of the inner vortex finder cross-section area and this results in a much larger proportion of flow to the annulus which is not desired for most applications. It would therefore be appropriate to update the SAR definition to that given in equation 7.1. Using equation 6.1, the SAR for the vortex finder combination used in the simulation is 0.78, but if the air-core is taken into account using equation 7.1 it becomes 1.00. The SAR is more accurately defined when the air-core is incorporated. Only a few CFD simulations were performed on the three-product cyclone and only one inner and outer vortex finder combination was used for this. Simulations covering a wider range are required to generate sufficient information for the air-core to be included in the SAR term for the three-product cyclone model. CFD can be used to obtain information for the inner vortex finder diameter design limits so that a reasonable flow can be maintained to meet applications needs.

7.7 Summary

The three-product cyclone has been modelled using computational fluid dynamics code Fluent 6.0. The general flow structure in the three-product cyclone is similar to that of the conventional hydrocyclone where a downward primary spiral and an upward secondary spiral are present resulting in underflow and overflow products.

In the three-product cyclone, the upward secondary spiral splits in to the OFI and OFO products.

The inner vortex finder length has a significant influence on the magnitudes of the tangential and axial velocities at all profiles along the Z-axis. In general long inner vortex finders resulted in high tangential velocities and low axial velocities. Velocity field vectors indicate that flow reversals occur over the entire region extending from the tip of the vortex finder down into the region near the spigot indicating that classification takes place in the whole of this region.

The air-core is present only in the central core of the inner vortex finder and occupies a significantly large portion. For the fixed spigot diameter, the shape and size of the air-core appeared to be a function of the inner vortex finder diameter and length for the three-product cyclone and of the vortex finder diameter and length for the conventional hydrocyclone.

University of Cape Town

8

Pilot Plant Test Results

8.1 Introduction

This chapter discusses results from the pilot plant trials performed to assess the potential improvement that can be achieved by employing the three-product cyclone in conjunction with fine screening to prepare feed for the flotation of the UG2 platinum ore. A total of fourteen pilot plant tests were conducted. The pilot trials were extended to the flotation section for four of these tests with the aim of assessing the operability, and the flotation response for a circuit utilising this configuration. Due to the ease of changing cyclone parts at pilot scale, tests were performed using cyclones with different conical section lengths, and thus cone angle, to assess the influence of this design variable on the classification of the three-product cyclone. Fourteen trials to test the concept of the three-product cyclone at pilot plant scale required a big commitment from industry to avail the pilot plant facility and trained personnel to assist with the work. This chapter presents some findings which are of interest to the industry but by no means exhaustive to answer questions pertaining to the mechanisms causing the observed effects.

University of Cape Town

8.2 Effect of conical length

A summary of the cyclone dimensions used in the experimental work are given in Table 8.1. Six different conical section lengths were used in the experimental work to assess the influence of the cone angle on the performance of the three-product cyclone and the full data set is given in Appendix D.

From figure 8-1, for the tests performed at the same feed rate, the conical section length appears to have the same effect on particles reporting to the OFI, and to the

TABLE 8.1. A summary of the cyclone design variables for the cyclone used for the pilot plant trials.

Variable	Dimension
Cyclone diameter, mm	100
Equivalent inlet diameter, mm	30
Length of cylindrical part, mm	90
Outer vortex finder diameter, mm	35
Outer vortex finder length, mm	130
Inner vortex finder diameter, mm	18
Inner vortex finder length, mm	190
Spigot diameter, mm	12, 14
Vertical length of conical part, mm	190, 210, 250, 375, 475, 635

OFO streams as that of varying the LIVF discussed in section 6.3. The intermediate size particles reported to the OFO when the cyclone was operated with a long conical section, and to the OFI at short conical sections. Changing the length of the conical section while keeping the inner and outer vortex finder lengths of the three-product cyclone constant alters the position of the inner vortex finder in relation to the spigot as illustrated in figure 8-2, which is drawn to scale. For the cyclone configuration used in this work, the inner vortex finder is closer to the spigot when operated with a conical section length of 190 mm compared to the conical section length of 635mm. This is in agreement to the observations made by Mular and Jull who pointed out that small cone angles tend to decrease the separation size and increasing the cone angle tends to increase the separating size [28].

The cyclones with conical sections of 375, 475, and 635mm lengths were used to classify the feed for the flotation tests. At these conical section lengths, the finer overflow from the three-product cyclone discharged from the OFI and the intermediate size from the OFO stream - normal classification configuration. For the conical section lengths of 190, 210, and 250 mm, the finer overflow discharged from the OFO and the intermediate size product from the OFI - reverse classification configuration. It can be concluded that changing the conical section alters the position of the inner vortex finder tip relative to the spigot and has similar results to those obtained by

University of Cape Town

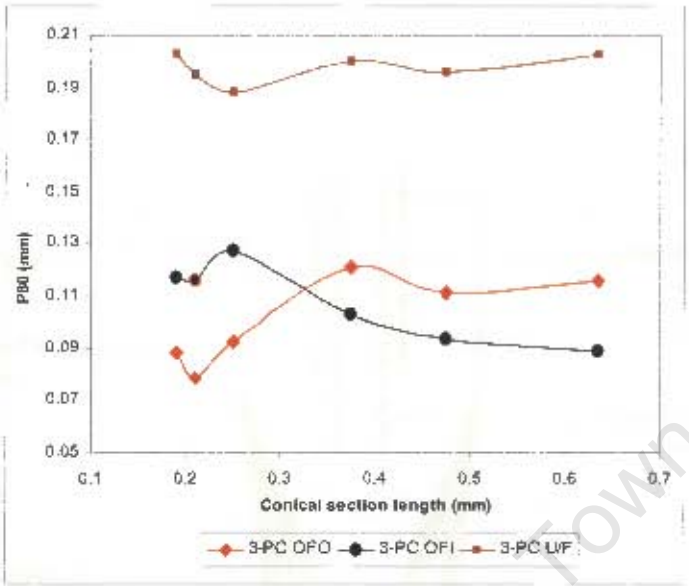


FIGURE 8-1. The effect of increasing the conical section length of the three-product cyclone on the P80 values.

altering the inner vortex finder length. However, the conical section can not be used for control purposes as cyclones are supplied with only one conical section.

8.3 Preparation of flotation feed

For all the tests involving the three-product cyclone, the intermediate size stream was screened on Pansep screens with 100μm apertures to obtain an undersize devoid of plus 100μm particles. A slightly oversized screen area was used in this work. This was done in order to attain high efficiencies on the Pansep screens and avoid the pitfall of inefficient screening clouding the overall circuit analysis. The finer overflow from the three-product cyclone and the Pansep screen undersize were then combined to form the final products from the comminution circuit.

The feed to the flotation circuit was classified using either the three-product cyclone - normal classification configuration - in conjunction with Pansep screens or the conventional cyclone only. A summary of stream data for these tests is given in

University of Cape Town

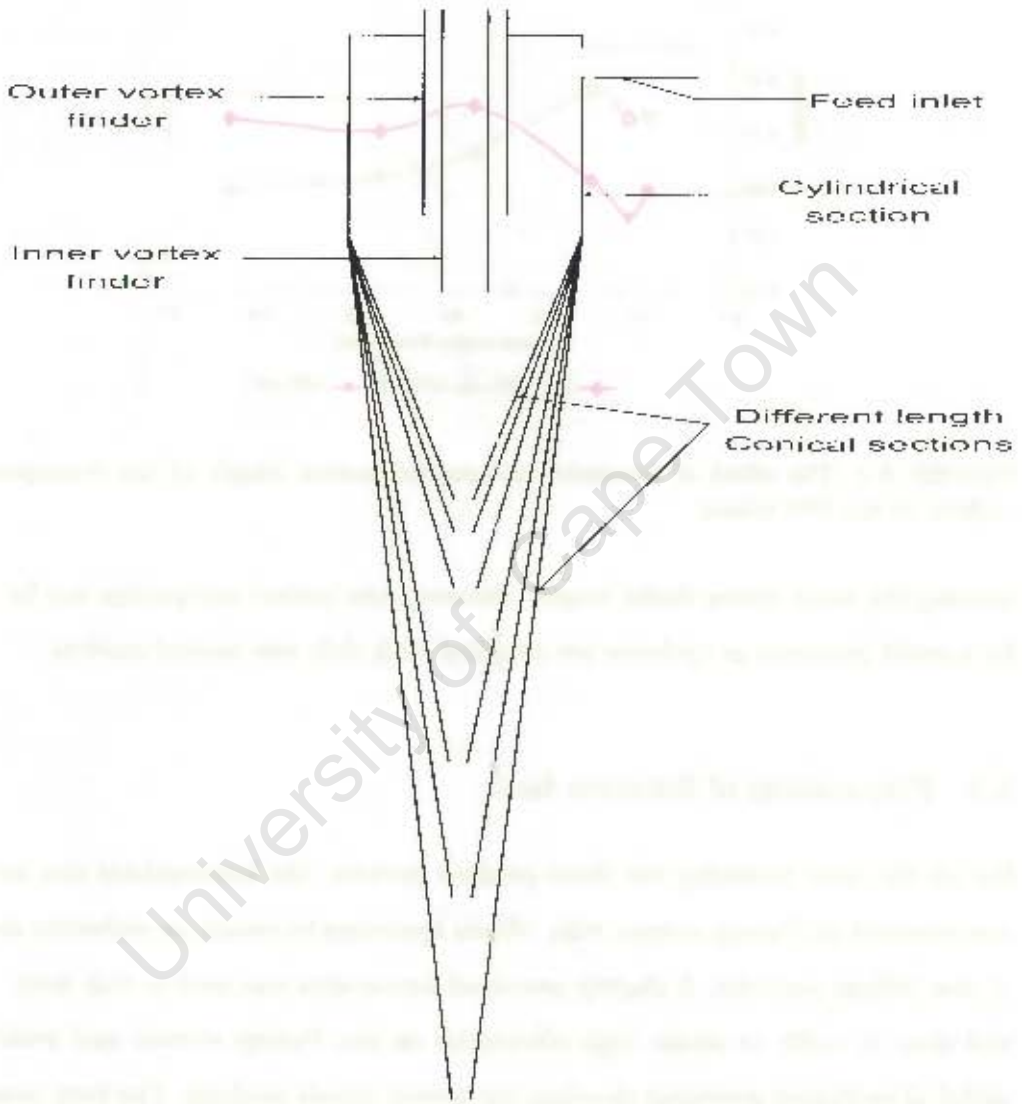


FIGURE 8-2. A schematic of the pilot plant cyclone showing the positions of the vortex finder in relation to the spigot for different conical section lengths.

University of Cape Town

TABLE 8.2. A summary of stream data for the pilot trials tests which included the flotation section.

	Conv. Cyc.	3-PC	3-PC	3-PC
Conical section length,mm	475	475	635	375
Crushed feed, tph	0.70	0.70	0.72	0.69
Crushed feed P80, mm	4.95	3.98	4.31	4.30
Cyclone feed, tph	3.56	3.2	3.0	3.5
Cyclone feed % solids	54.9	55.9	54.4	54.0
Cyclone feed, % sub-100μm	52.1	50.9	59.9	51.0
Cyclone feed P80, mm	0.162	0.143	0.159	0.164
Recycle load, %	440	400	340	425
OFO P80, mm	-	0.090	0.109	0.104
OFI P80, mm	-	0.060	0.073	0.083
Float feed, % sub-100μm	76.8	99.1	94.0	90
Float feed P80, mm	0.107	0.062	0.064	0.080
Float feed % solids	29.9	32.2	28.0	28.8

Table 8.2. The Floatability Characterisation Test Rig (FCTR) was used to perform pilot scale flotation tests (Coleman et al. [70]). A schematic and a photograph of the pilot plant circuit are shown figures 4-10 and 4-16, respectively. These tests were performed at 0.7 tph and the final product was floated using the FCTR. The feed rate of 0.7 tph is the optimum operating capacity for the FCTR facility at Karee concentrator. The pump imposed a constraint of a minimum pumping rate of 3.0 m^3/h slurry flow. This necessitated the use of a spigot size of 14mm to build up a relatively high recirculating load in order to match the minimum pump rate.

The remainder of the tests were performed with ~1.0 tph of crushed feed and a spigot size of 12mm. A summary of tests performed using the three-product cyclone - reverse classification configuration - and a conventional cyclone with short conical sections is given in Table 8.3. The final product from these tests were floated. For most of the tests, the cyclone feed solids concentration was maintained around 54% by weight. The final product from the comminution circuit feeds a flotation circuit that requires about 30% solids in the feed, and this dictated the high feed percent solids requirement for the cyclone. The per cent solids in the final product were within the required range.

University of Cape Town

TABLE 8.3. A summary of stream data for the tests conducted around the comminution and classification sections.

	Conv. Cyc.	3-PC	3-PC	3-PC
Conical section length, mm	210	210	190	250
Crushed feed, tph	1.02	1.00	1.05	1.00
Crushed feed P80, mm	4.12	4.34	4.13	4.21
Cyclone feed, tph	3.17	3.23	4.61	3.30
Cyclone feed % solids	52.3	55.9	47.8	55.27
Cyclone feed, % sub 100μm	50.3	51.3	43.4	50.0
Cyclone feed P80, mm	0.169	0.168	0.184	0.164
Recycle load, %	260	245	360	250
OFO P80, mm	-	0.079	0.088	0.093
OFI P80, mm	-	0.116	0.117	0.127
Float feed, % sub 100μm	76.0	93.2	91.0	89.1
Float feed P80, mm	0.108	0.078	0.082	0.084
Final product % solids	31.4	29.5	18.0	30.2

Significant differences were observed in the float feed P80 values between the circuit operated with the three-product cyclone in conjunction with fine screens (Pansep screens), and that operated with conventional cyclone only (Table 8.2). The circuit utilising the three-product cyclones and Pansep screens had a P80 value of 62μm in the float feed which was significantly finer compared to 107μm for the circuit operated with the conventional cyclone only at the same conical section length. Although the crushed feed and cyclone feed P80 values for the three-product cyclone were lower than those of the conventional cyclone, the difference between the P80 value in the final product is too big to be a consequence of the finer feed only. It was observed that the P80 values for the float feed for the circuits utilising the three-product cyclones with conical section lengths of 375mm and 635mm were significantly finer than those for the conventional cyclone with a conical section of 475mm. However, it must be noted that the P80 values for the circuit utilising the three-product cyclone are lower because the intermediate size overflow is screened to remove all the particles larger than 100μm.

Table 8.2 shows that the conventional cyclone circuit had a re-circulating load of 400% which was higher than the combined circulating load of 360% from the three-

University of Cape Town

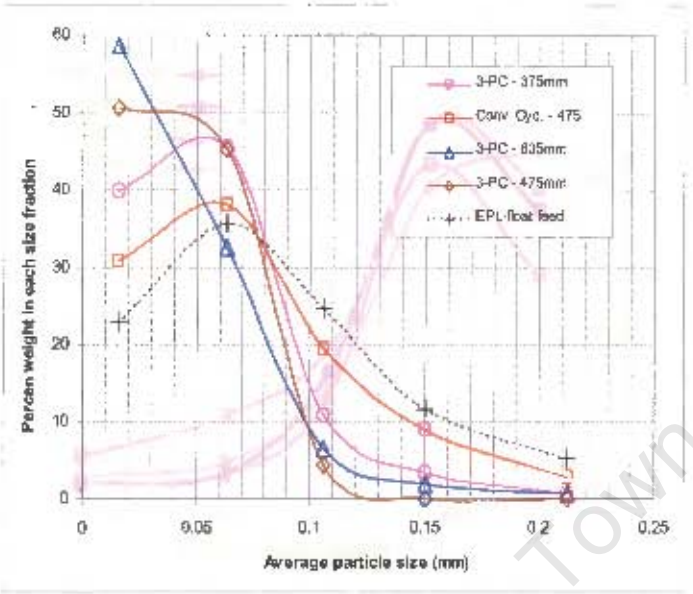


FIGURE 8-3. Comparison of the float feed size fractions from the classification systems ustilising the three-product cyclone with long conical sections and Pansep screens and the conventional hydrocyclone only.

product cyclone and Pansep screens. A significant reduction in the recirculating load for both the conventional and three-product cyclone was observed for circuits operated with cyclones fitted with shorter conical sections (Table 8.3).

The final product from the tests performed using shorter conical section lengths and thus inducing reverse classification, show that the product from the circuit utilising the three-product cyclone and fine screens was significantly finer compared to the circuit operated with the conventional cyclone only (Table 8.3). The final product for the circuits utilising the three-product cyclone with reverse classification are coarser than normal classification configuration. The conventional cyclone exhibited no change in the P80 value with the change in conical section length.

Figures 8-3 and 8-4 show the percentage weight of material in each size fraction of the final product for the circuit utilising the three-product cyclone and Pansep screens, and for the conventional cyclone only. It can be seen from figure 8-3 that

University of Cape Town

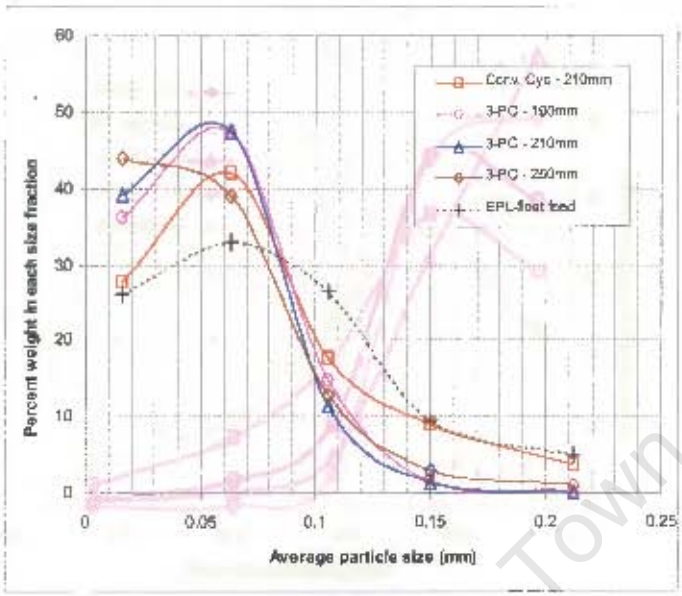


FIGURE 8-4. Comparison of the float feed size fractions from the classification systems ustilising the three-product cyclone with a short conical section and Pansep screens and the conventional hydrocyclone only.

the float feed from the circuit operated with the three-product cyclone has ~ 5% of material in plus 100μm size fraction range compared to 25% from the conventional cyclone circuit. A sample was obtained from the flotation feed at Eastern Platinum Limited - a concentrator owned by LONMIN - where a 600mm conventional cyclone is used in the classification circuit. It was observed that the float feed from both the 100mm pilot size, and 600mm industrial conventional cyclones had a significantly higher amount of plus 100μm compared to that from the three-product cyclone. The final products classified using three-product cyclones with shorter conical sections in the circuits had ~ 10% of material in the plus 100μm compared to 25% from the circuit utilising the conventional cyclone only (Figure 8-4).

The recycle streams for the cyclones with long conical sections are presented in figure 8-5. It was observed that the recycle streams from all the circuit configurations had a high amount of material in the plus 100μm. The recycle stream from the test performed using the three-product cyclone with a 635mm conical section had

University of Cape Town

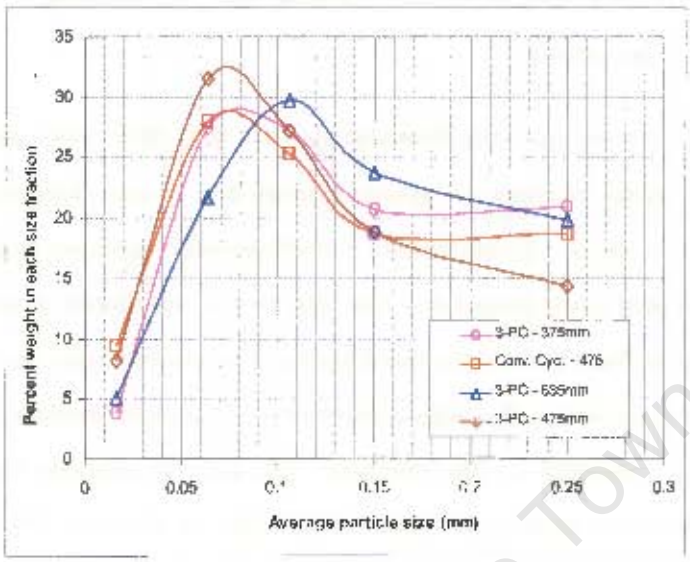


FIGURE 8-5. Distribution of particles in the recycle stream for cyclone configurations with longer conical sections - normal classification configuration.

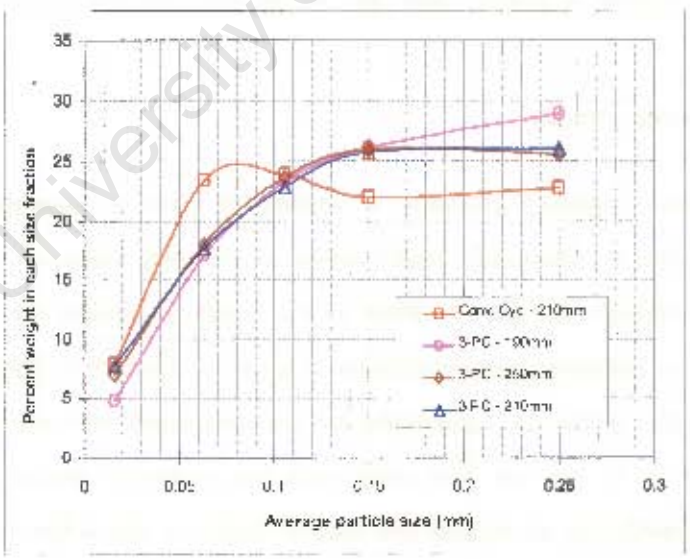


FIGURE 8-6. Distribution of particles in the recycle stream for cyclone configurations with shorter conical sections - reverse classification configuration.

University of Cape Town

the highest amount of material in the plus 100μm fraction. Despite having a significant amount of plus 100μm in the overflow, the conventional cyclone had similar proportions to the others.

The recycle stream size distributions for the test performed with cyclones fitted with shorter conical sections are given in figure 8-6. It was observed that the recycle stream from the circuit operated with a three-product cyclone fitted with a 190mm conical section had more material in the plus 100μm compared to the tests performed using 210, and 250mm conical section lengths. The conventional cyclone had the least plus 100μm compared to the others because a significant amount of the material in this size range reported to the overflow. The recycle streams from three-product cyclone circuits had similar amounts of material in the sub 100μm size fractions. The circuit operated with the conventional cyclone was shown to have a significantly high amount of material in the sub 100μm size fractions compared to those from the three-product cyclone circuits. This indicates that the quality of the recycle for the circuit utilising the three-product cyclone with short conical sections in conjunction with Pansep screens is higher than that of the conventional cyclone only.

8.4 Flotation results

In the platinum industry flotation is commonly used to upgrade the ore into a concentrate, with a reasonably high content of valuable minerals, prior to smelting. Standard conditions for the flotation of the UG2 platinum ore were adopted. A summary of the flotation test conditions is given in Table 8.4. The Platinum Group Elements (PGEs) in the UG2 platinum ore are associated with silica. Due to the high chromite content in this ore, low mass pulls are preferred during flotation to avoid recovering a significant amount of the barren chromite which has a detrimental effect in the smelting process (Ekmekci et al. [103]). Therefore the success of the three-product cyclone in the UG2 platinum ore application is dependant on sending the feed to the flotation circuit devoid of coarse silica particles and of very fine chromite

University of Cape Town

TABLE 8.4. A summary of the flotation test conditions.

$CuSO_4$	80 g/t
Xanthate - SIBX	100 g/t
Dow 250	10 g/t
Depressant (CMC)	30 g/t
Air in the cells	150 litres/min

– which is recovered by entrainment. Although the five element PGE assays were available for the purposes of this discussion, the flotation performance was assessed on the basis of silica recoveries which is an indirect measure of the PGE flotation performance in the UG2 platinum ore. Due to the problems encountered in smelting a chromite rich concentrate, it is critical to assess the recovery of the unwanted chromite which is barren of PGEs.

8.4.1 Recovery - grade curves

Silica and chromite grade-recovery curves for the circuits operated with three-product cyclones fitted with different length conical sections in conjunction with fine screens are compared to those for conventional cyclone circuit. Silica grade-recovery curves for the different circuits tested are presented in figure 8-7. The silica grade-recovery curves for the circuits which utilised the three-product cyclone in conjunction with fine screens were superior to that for the conventional cyclone only. This could be attributed to the absence of plus 100μm particles in the float feed for the three-product cyclone circuits. The curve for the feed prepared using a three-product cyclone with a 475mm long conical section had a significantly superior grade-recovery curve compared to those with other conical lengths. At present it is not clear why despite having little plus 100μm material in the float feed this is so.

Chromite grade-recovery curves for the different circuits are presented in figure 8-8. A higher amount of chromite was recovered into the concentrate for the feed prepared using the conventional cyclone compared to that obtained using the three-product cyclones with 635mm and 475mm long conical sections. However, the test with the conical section length of 375mm recovered a significantly higher amount of

University of Cape Town

chromite than all the other circuits tested in this work. The consistency of each individual grade recovery curve indicates a high degree of reliability in the assays, and indicates that the results are significant. Reproducibility in terms of duplicate tests were constrained by the costs to the sponsor of this work. Based on the outcomes of this thesis, the sponsor may well conduct further assays to test the significance of the outcomes.

The apparent anomaly of the short 375mm cone can be explained by the fact that with the short cylindrical section used in the pilot plant experiments this change in length of the inner vortex finder dramatically changes the location of the vortex finder relative to the spigot. It is concluded that this switched the operation of the cyclone between normal and reverse classification, and the measured change in the grade recovery curve is a consequence of this.The reasons for the deviations in the chromite recovered by the different circuits is at present not well understood and requires further investigation as a flotation-liberation study.

The grade-recovery curves for the valuable sulphide component for the different circuits are given in figure 8-9. A higher amount of the valuable sulphide component was recovered by the circuits utilising the three-product cyclones in combination with fine screens than that recovered by the conventional cyclone circuit. The three-product cyclone operated with a conical section of 475mm appear to give a superior flotation response compared to the others. The plant personnel verified that the results observed in this work fall within the range of their operation.

8.4.2 Recovery by size curves

The principal mineral components in each size fraction were estimated from the assay data. The assays were given in direct measures of Silica (SiO_2) and chromite (Cr_2O_3). The remainder of the minerals were lumped together and calculated by difference and were used for checking the component balances. This approach of analysing mineral processing performance using minerals in size fractions is not new

University of Cape Town

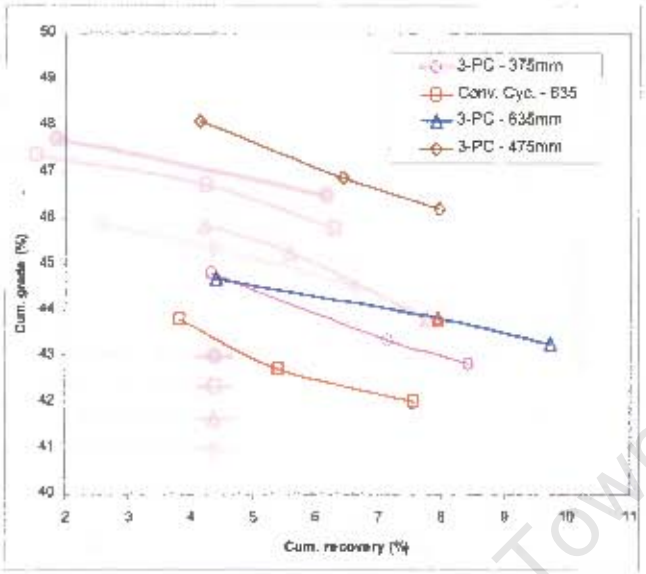


FIGURE 8-7. Silica grade - recovery curves for the three-product cyclone circuits and conventional hydrocyclone circuit.

(Gaudin et al. [104], Feng [105], and Johnson [106]).

Size by size assays were performed on the concentrates and tailings of the three-product cyclone circuit that produced a superior grade-recovery curve and of the conventional cyclone circuit. Recovery by size curves shown in figure 8-10 for the two circuits were then plotted and assessed. It can be seen that the recovery increases with reduction in particle size for the silica component, which is the expected trend in most ores (Trahar [107]). The recovery of the silica component for the three-product cyclone circuit was higher than that of the conventional cyclone circuit in all the size fractions considered. From figure 8-10, it was observed that despite major differences in the proportions of fractions in the float feed from the two circuit configurations, the concentrates produced had similar mass flow proportions in all the size fractions. Since the mass flow rates for the two circuits are similar, it is not clear why the silica recovery - size curves deviated.

The three-product cyclone circuit float feed shown in figure 8-3 had proportions

University of Cape Town

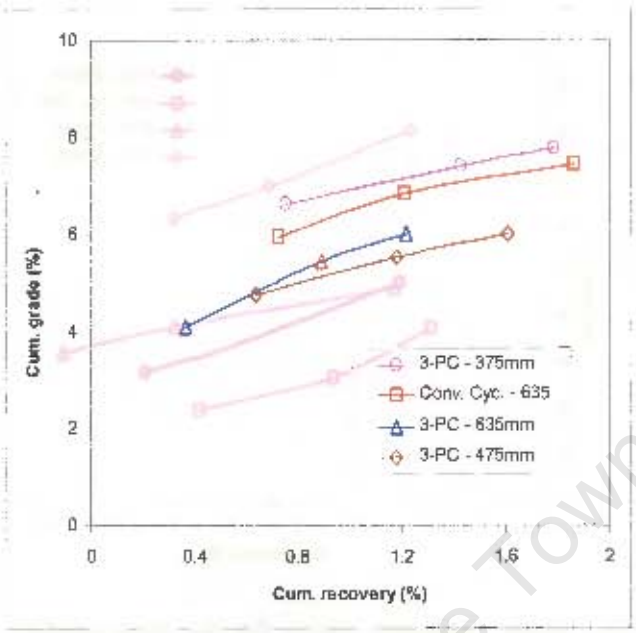


FIGURE 8-8. Chromite grade - recovery curves for the three-product cyclone circuits and conventional hydrocyclone circuit.

similar to that of the concentrates shown in figure 8-10 with less than 10% in the plus 90μm size fractions while the proportions in the fractions from the conventional cyclone circuit float feed deviated significantly with 25%, 18%, and 15% of the total mass flow in the 90 - 125μm, 125 - 180μm, and plus 180μm size ranges, respectively. These are significantly higher than the proportions in the respective size ranges of the float feed from the three-product cyclone circuit and the concentrate streams. Since higher recoveries of the silica component were achieved at finer sizes it can be concluded that utilising the three-product cyclone in conjunction with the fine screens provides the flotation circuit with a suitable feed for silica recovery.

From the recovery - size curve in figure 8-10, it was observed that for the three-product cyclone circuit 5% of chromite was recovered into the concentrate at the fine size fraction and the recovery decreased with increase in size before rising at plus 100μm size. The increase at the fine end could be a result of chromite being recovered into the concentrate by entrainment and that in the coarse fractions can

University of Cape Town

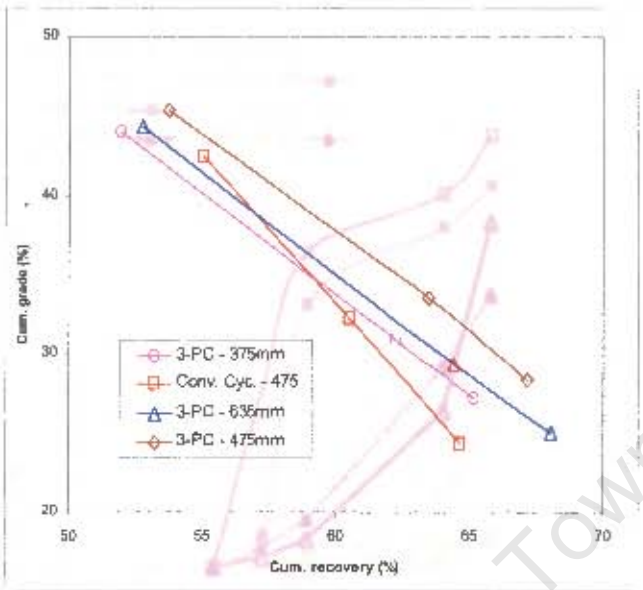


FIGURE 8-9. Valuable sulphide component grade - recovery curves for the three-product cyclone circuits and conventional hydrocyclone circuit.

be attributed to the presence of composites of silica and chromite (Wesseldijk et al. [108]). However, the fraction of mass flow into this size range was negligible so the amount of chromite at the coarse end is negligible. Due to the high mass flow of the sub 32μm size fractions in the concentrate, the amount of chromite in this size range can have a detrimental impact on the quality of the concentrate. The chromite content for the conventional cyclone circuit was significantly higher in the 30 – 90μm size range where the concentrate flow rate is high, resulting in a substantially more chromite reporting to the concentrate. The recovery by size curve for the valuable sulphide component for the three-product cyclone appeared to be superior to that of the conventional cyclone.

This work has shown that utilising the three-product cyclone in conjunction with Pansep screens provides a feed that has similar proportions material to that of the concentrate in most of the size fractions. If it is speculated that when the particles are presented in the preferred size range, that all the floatable particles are recovered. Then the three-product cyclone circuit will have a significantly higher recovery of

University of Cape Town

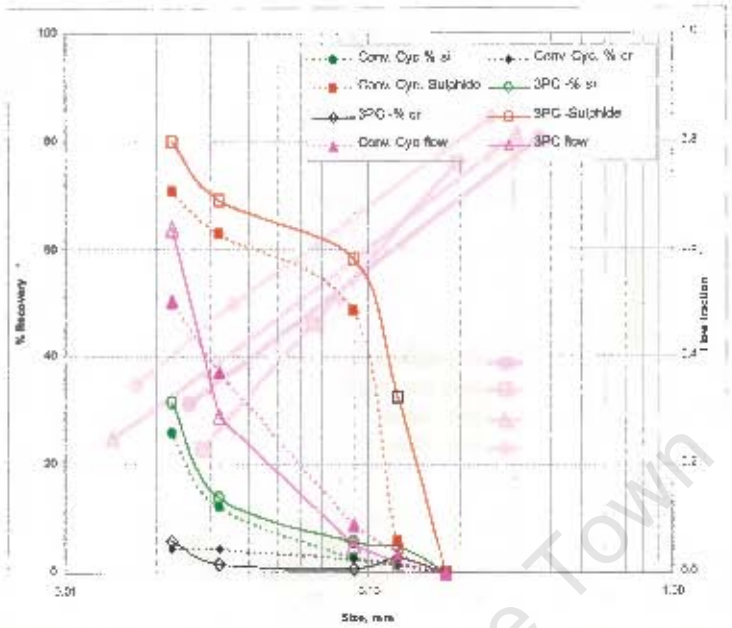


FIGURE 8-10. Recovery - size curves and mass flow rate in the concentrate for the three-product and conventional cyclone circuits.

the valuable mineral than the conventional cyclone circuit, as it provides a feed suitable for flotation. It can therefore be concluded that the combination of the three-product cyclone with fine screens in the processing of the UG2 platinum ore enhances flotation recovery of valuable minerals without diluting the grade.

The author expected to see similar recovery by size curves since the two different circuits were treating the same ore. However, detailed flotation and liberation studies are required to gain understanding into the mechanisms leading to differences observed in the recovery by size, and grade-recovery curves for the different circuit configurations. Liberation data is required to determine if the losses encountered in the coarse fractions when the conventional hydrocyclone is used are due to the presence of composites or unliberated material . Liberation data can also supply information on the mechanisms that lead to losses in the respective circuits and assist in pinpointing areas that may be further refined to maximise the recoveries of

University of Cape Town

this problematic ore. Liberation data together with assay by size data will provide insight on the manner in which free and composite particles in this ore are classified, and subsequently on their distribution in all key streams.

The utilisation of the three-product cyclone in the mineral industry is not limited to the application demonstrated in this chapter, where it is operated in conjunction with fine screens to provide feed for flotation. Other potential areas of application include using the middlings stream as feed to a flash flotation circuit, or the Knelson concentrator in the gold industry (Obeng and Morrell, [69]). It can also be used for desliming applications (Morrell [109]).

The findings in this chapter though by no means exhaustive provide an exciting area for the platinum industry to explore in the quest for improving the concentrator plant recoveries.

8.5 Summary

Classification challenges in the UG2 platinum ore can be reduced by using the three-product cyclone in combination with fine screens to produce a feed well suited for flotation.

The silica and chromite grade-recovery curves for the three-product cyclone circuits were shown to be superior to those of the conventional hydrocyclone circuit.

The recovery by size data has shown that the recovery of silica - the PGE carrying component - is significantly higher in fine size fractions and that the amount of sub 100μm particles in the concentrate mass flow rate is negligible. This suggests that flotation recovery of this ore is maximised in the sub 100μm particle size range.

The recovery of chromite was high in fine fractions for both circuit configurations which could be a result of entrainment. However, the three-product cyclone circuit had less chromite than the conventional cyclone circuit in fractions between 32μm

University of Cape Town

and 90μm and the increase in chromite in the plus 90μm can be attributed to the presence of composites.

The data from assay by size analyses was useful in analysing the performance of the circuit, but does not provide information on the manner in which minerals are classified and distributed in key streams. To understand the mechanisms that lead to the observed improvement in flotation recovery, liberation data and detailed flotation studies are required.

University of Cape Town

9

Model Development and Validation

9.1 Introduction

This chapter describes the model for the three-product cyclone which was developed in this thesis. The model was developed using the Whiten model building technique [110]. Expressions to describe the variations in operating pressure, volumetric flow and water split, and cut sizes for the U/F and OFI are given. Additional expressions for predicting the silica and chromite cut sizes are presented.

In a parallel project undertaken at the JKMRC, University of Queensland, Obeng [61], modelled the three-product cyclone as two cyclones in series. In this thesis, the three-product cyclone is modelled as a process unit producing 'three distinct products' from a single feed. The model building technique involves developing equations from the data by combining the known physical theory of the equipment and regression to obtain the unknown parameters for predicting the performance of the process unit.

University of Cape Town

9.2 Three-product cyclone model development

In most of the models developed for process units, quite often the underlying theory based on the physics of the unit is not fully understood. Most models are built by expressing the known physics analytically and then the unknown parts are expressed by some empirical parameters fitted from the data. The model for predicting the performance of the three-product cyclone based on this principle was developed using the automatic model builder developed by Whiten [111].

A general formulation of the automatic model building technique is completed by

the form indicated in equation 9.1.

$$y = f\left(x, P(c(x))\right) \tag{9.1}$$

where: y = vector of output variables

x = vector of input variables

c = vector of operating conditions

P = unknown parameter vector which is a function of c and needs to be determined from experimental data.

f = known vector function of x which is usually nonlinear.

This form of model building has been used successfully by other workers to develop models for predicting the performance for conventional hydrocyclones (Kojovic [82], and Xiao [63]).

The model building programs developed at JKMRC were extended by Whiten in conjunction with the author of this thesis to accommodate the nature of data obtained from the testwork. The author used the programs independently to develop the equations reported in this thesis for predicting the performance of the three-product cyclone. Details of the model building technique applied is described in detail by Petersen [112], Xiao[63], Kojovic [82] and Kojovic and Whiten [113].

University of Cape Town

9.3 Model equations

Matlab version 7.0 was used to perform all the regressions in this work. Variables that are physically meaningful were included and the terms with negligible contribution were then removed. The criterion for selecting equations for the model was accuracy, simplicity, and significance of parameter values. For each model the standard error of the residuals (se) and the adjusted coefficient of multiple determination (R^2adj). The former allows the calculation of approximate confidence limits on the predictions and the latter is a generally accepted goodness-of-fit criterion which is used to compare

regressions. Since regressions were performed by linearising the variables by taking the logs, the standard error included here was obtained directly from the regression. Where possible design variables have been normalised, for example orifice diameters are normalised as a fraction of the cyclone diameter to provide a dimensionless term. Flow rate and operating pressure are exceptions. Units are implicit in the constant terms of the equations and all the variables are SI units or as specified for each equation (Powell [114]). From the 82 tests performed using a 600mm three-product cyclone, sixty four tests were used for developing the model and the remainder for validation. As discussed in section 6.4, the efficiency curves used for modelling two product classifiers were extended to accommodate multiple splits in the three-product cyclone.

9.3.1 Pressure drop

In most conventional hydrocyclone models, pressure has been shown to depend on several variables (Lynch et al. [23], [115], Plitt et al. [116], Nageswararao [40]). The cardinal ones are volumetric feed flow rate, vortex finder diameter, spigot diameter, and fraction of feed solids. These, along with variables unique to the three-product cyclone such as the inner vortex finder diameter and length which have a significant effect on the pressure drop, were included in the regressions to obtain the expression for the operating pressure.

Equation 9.2 was selected which combines only variables that had a significant effect and represented the operating pressure for the three-product cyclone better than the other equations tested. Figure 9-1 shows the correlation between the observed, and predicted operating pressure for the three-product cyclone. Figure 9-2 shows the corresponding residuals plot. There is good agreement between the observed and predicted operating pressure. From equation 9.2, it can be seen that the LIVF and the Volumetric feed flow terms influence the operating pressure of the three-product cyclone more than the other terms.

University of Cape Town

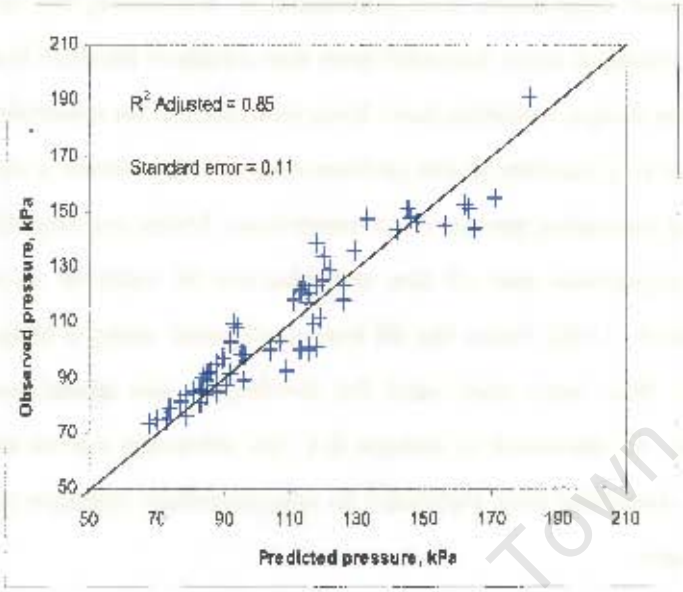


FIGURE 9-1. Correlation observed and predicted pressure drop for the three-product cyclone

$$P = \frac{0.513 \times \left(\frac{LIVF}{Dcyc}\right)^{1.445} Q_f{}^{0.726}}{\left(\frac{DIVF}{Dcyc}\right)^{0.235} \left(F_{fracSolids}\right)^{0.159}} \tag{9.2}$$

where: P - pressure drop, kPa,

$DIVF$, $LIVF$, inner vortex finder diameter, and length, mm,

D_{cyc} - cyclone and spigot diameters, mm,

Q_f - feed volumetric flow rate, m^3/h,

$F_{fracSolids}$ - feed solids concentration.

9.3.2 Flow split

Flow split is a critical factor in the operation of any hydrocyclone. For the three-product cyclone, the additional overflow product requires that the flow split to two products is known to specify its performance. Flow split to the U/F, and the OFI streams were chosen for this thesis. The choice was based on the assumption that the inner and outer overflow are influenced by the same variables since they originate

University of Cape Town

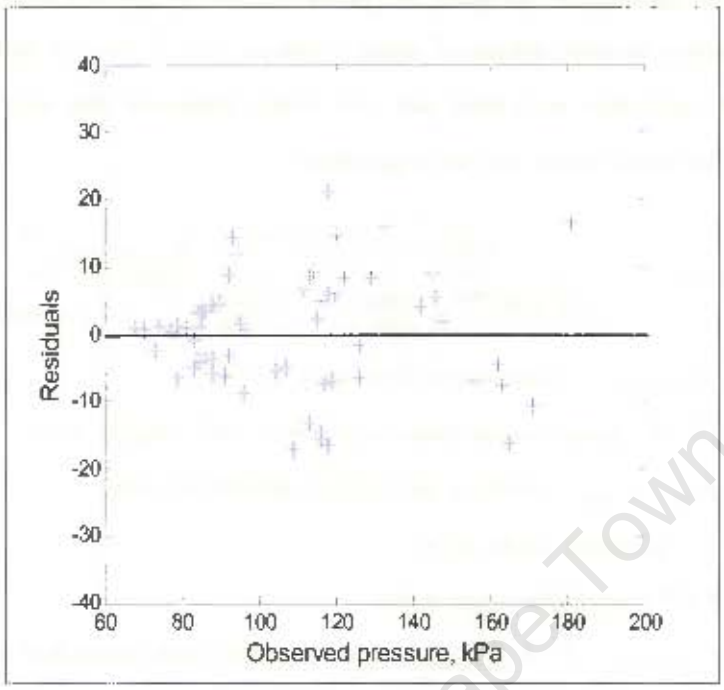


FIGURE 9-2. Residual plots for the operating pressure.

from the same upward swirl flow. Therefore, only one of the two should be specified while the other can be obtained by difference.

Equation 9.3 gave the best correlation between the observed and predicted flow fraction to the OFI among the equations tested. Figure 9-3 shows the correlation between the observed and predicted fraction of total flow split to the OFI stream and the corresponding residuals plot is given in figure 9-4. There is good agreement between the observed and predicted fraction of flow split to the OFI. From the flow split expressions, it can be seen that the per cent solids in the underflow and the feed influence the splits more than the other terms in the equation. Among the geometric variables in equation 9.3, the LIVF and SAR terms have higher influence on the split than the DIVF and spigot terms.

The volumetric flow split to the underflow for the three-product cyclone is represented by equation 9.4 and the correlation between the observed and predicted fraction is given in figure 9-5. The corresponding residuals plot is given in figure 9-6.

University of Cape Town

There is good agreement between the observed and predicted fraction of flow split to the underflow stream obtained using equation 9.4. It can be seen from equation 9.4 that the underflow and feed per cent solids influence the split to U/F stream more than the other terms in the expression.

$$Q_{OFI_{frac}} = \frac{6.67 \times 10^{-2} \left(P\right)^{0.232} \left(U/F_{frac Solids}\right)^{1.60}}{\left(SAR\right)^{0.643} \left(\frac{Dspig}{Dcyc}\right)^{0.164} \left(\frac{LIVF}{Dcyc}\right)^{0.860} \left(F_{frac Solids}\right)^{0.670}} \tag{9.3}$$

where: $Q_{OFI_{frac}}$ - Volumetric flow split to OFI,

$LIVF$, inner vortex finder diameter, and length, mm,

D_{cyc} , D_{spig} - cyclone and spigot diameters, mm,

$P-$ pressure drop, kPa,

SAR - selection area ratio,

$F_{frac Solids}$, $U/F_{frac Solids}$ - fraction feed and underflow solids concentration.

$$Q_{U/F_{frac}} = \frac{1.325 \times \left(\frac{DOVF}{Dcyc}\right)^{0.243} \left(\frac{Dspig}{Dcyc}\right)^{0.476} \left(F_{frac Solids}\right)^{1.796}}{\left(U/F_{frac Solids}\right)^{2.365}} \tag{9.4}$$

$Q_{U/F_{frac}}$ - fraction water split to U/F,

$DOVF$ - outer vortex finder diameter, mm,

D_{cyc} , D_{spig} - cyclone and spigot diameters, mm,

$F_{frac Solids}$, $U/F_{frac Solids}$ - fraction feed and underflow solids concentration.

9.3.3 Water split

Water split to the products of the cyclone is an important factor which affects the separation efficiency of any cyclone. Several equations exist for predicting water split in a conventional hydrocyclone: Lynch and Rao [23], [17], Brookes [117], and Vallebuona [118]. The common terms in their expressions along with variables unique to the three-product cyclone were included in the initial regressions. For the three-

University of Cape Town

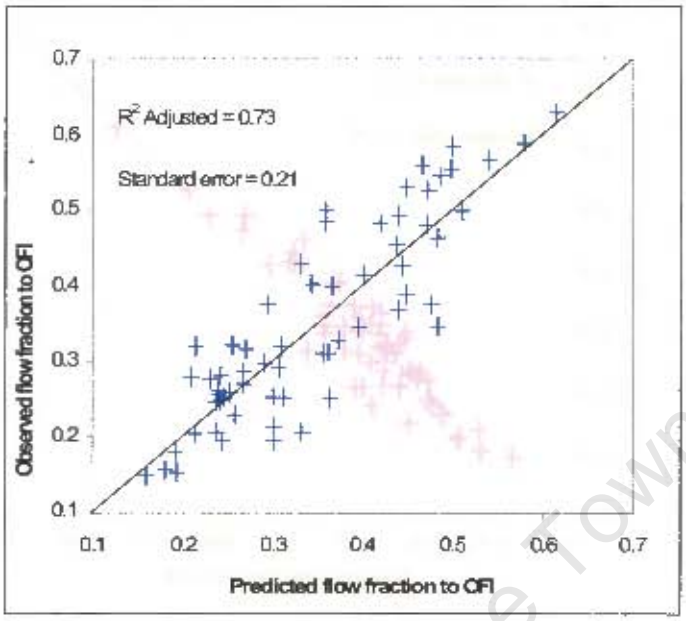


FIGURE 9-3. Comparison between observed and predicted fraction flow split to the OFI of the three-product cyclone

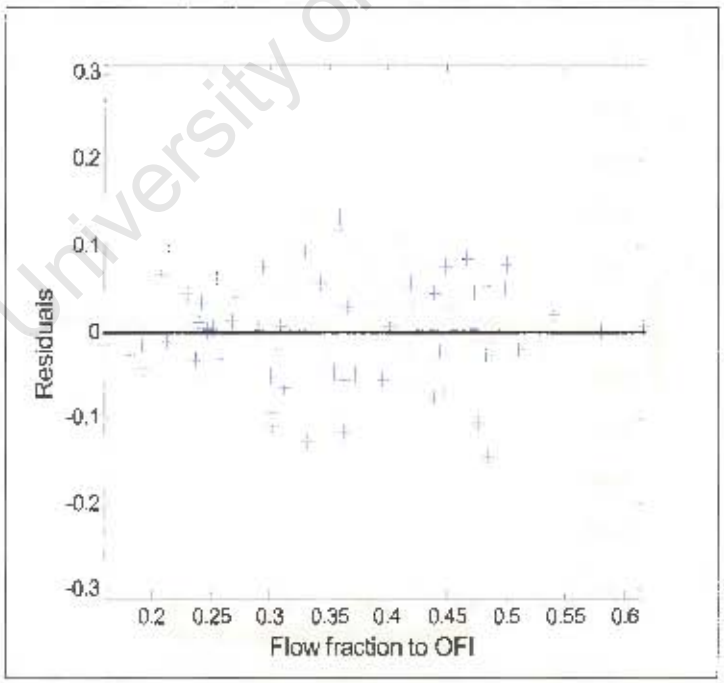


FIGURE 9-4. Residual plots for the flow fraction split to the OFI.

University of Cape Town

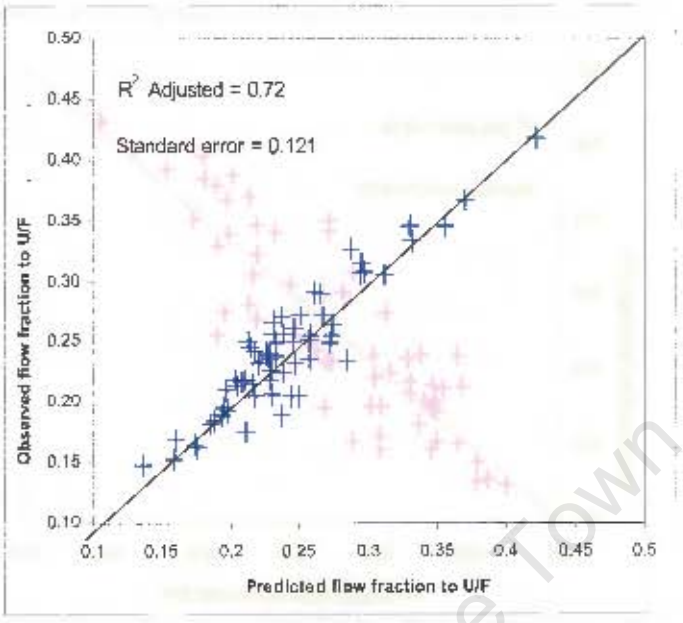


FIGURE 9-5. Comparison between observed and predicted fraction flow split to the U/F of the three-product cyclone

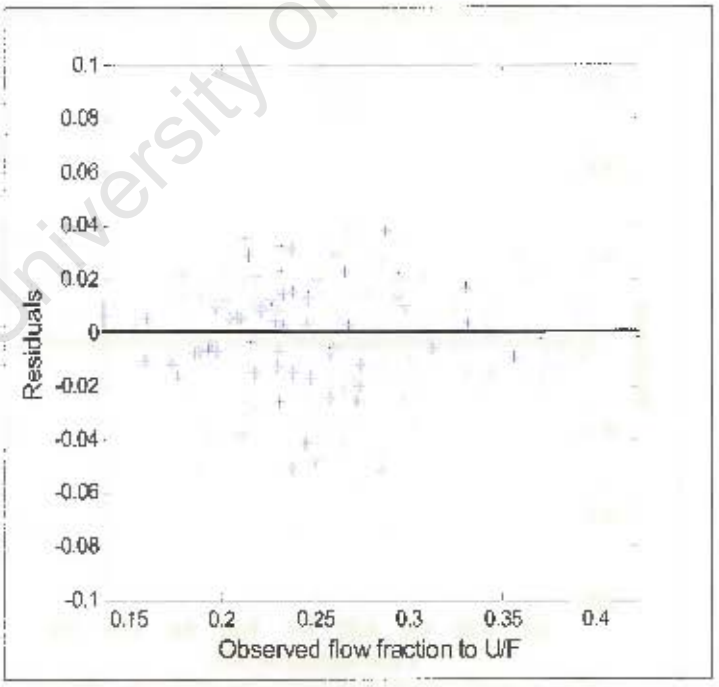


FIGURE 9-6. Residual plots for the flow fraction split to the U/F.

University of Cape Town

product cyclone, the additional overflow product requires splits to two products to be specified to assess the performance for this unit.

Equation 9.5 was developed for predicting the fraction of water split to the OFI stream of the three-product cyclone. The correlation between the observed and predicted fraction water split to the OFI is presented in figure 9-7 and the corresponding residuals plot is given in figure 9-8. There is a good match between the observed and predicted flow split to the OFI. It can be seen from equation 9.5 that the SAR and LIVF are the geometric variables that have the strongest influence.

Equation 9.6 represents the water split to the U/F stream of the three-product cyclone. The correlation between the observed and predicted fraction of water split to U/F stream is presented in figure 9-9 and the corresponding residuals plot in figure 9-10. There is a good agreement between the observed and predicted flow fraction to the underflow. Among the geometric variables, the term expressed as a ratio of the outer vortex finder diameter to the spigot diameter has a higher influence than the DIVF term. The water split relationships is principally driven by the fraction of solids in the underflow and feed streams.

$$W_{OFI_{frac}} = \frac{0.12 \times \left(U/F_{_{frac}Solids}\right)^{1.537}}{(SAR)^{0.678}\left(\frac{DIVF}{Dcyc}\right)^{0.312}\left(\frac{Dspig}{Dcyc}\right)^{0.165}\left(\frac{LIVF}{Dcyc}\right)^{0.638}\left(F_{_{frac}Solids}\right)^{0.764}} \tag{9.5}$$

where: $W_{OFI_{frac}}$ - fraction water split to OFI,

$F_{_{frac}Solids}$, $U/F_{_{frac}Solids}$ - fraction feed and underflow solids concentration.

SAR - selection area ratio,

$DIVF$, $LIVF$, inner vortex finder diameter, and length, mm,

D_{cyc} , D_{spig} - cyclone and spigot diameters, mm.

$$W_{U/F_{frac}} = \frac{0.404 \times \left(\frac{DIVF}{Dcyc}\right)^{0.157}\left(F_{_{frac}Solids}\right)^{2.077}}{\left(\frac{DOVF}{Dspig}\right)^{0.431}\left(U/F_{_{frac}Solids}\right)^{3.896}} \tag{9.6}$$

University of Cape Town

$W_{U/F_{frac}}$ - fraction water split to U/F,

$DIVF$, $LIVF$, inner vortex finder diameter, and length, mm,

D_{cyc} , D_{spig} - cyclone and spigot diameters, mm,

$DOVF$ - outer vortex finder diameter, mm, and

$F_{fracSolids}$, $U/F_{fracSolids}$ - fraction feed and underflow solids concentration.

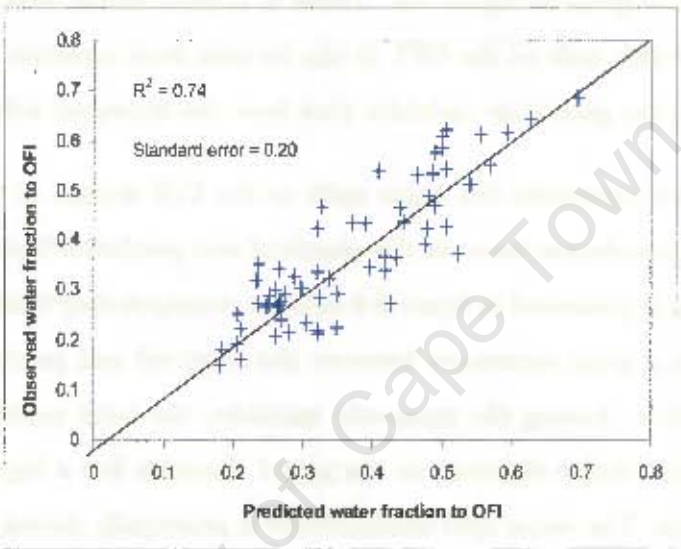


FIGURE 9-7. Comparison of observed and predicted fraction of water split to OFI

University of Cape Town

9.3.4 Corrected cut size

The separation size in the hydrocyclone is usually expressed in terms of the corrected cut size - $d50_c$. Many workers have shown that the $d50_c$ for the conventional cyclone depends on the vortex finder diameter, spigot diameter, pressure drop, volumetric feed flow rate or feed solids concentration, and overflow or underflow flow rate: Dahlstrom [13]; Lynch and Rao [23]; Plitt [24][119]; Nageswararao [40]; Asomah [35]; and Gupta [120], Svarovsky [121]. For the three-product cyclone, two separate ($d50_c$) expressions were developed - one for the OFI (d_{50_cOFI}), and the other for the U/F ($d_{50_cU/F}$).

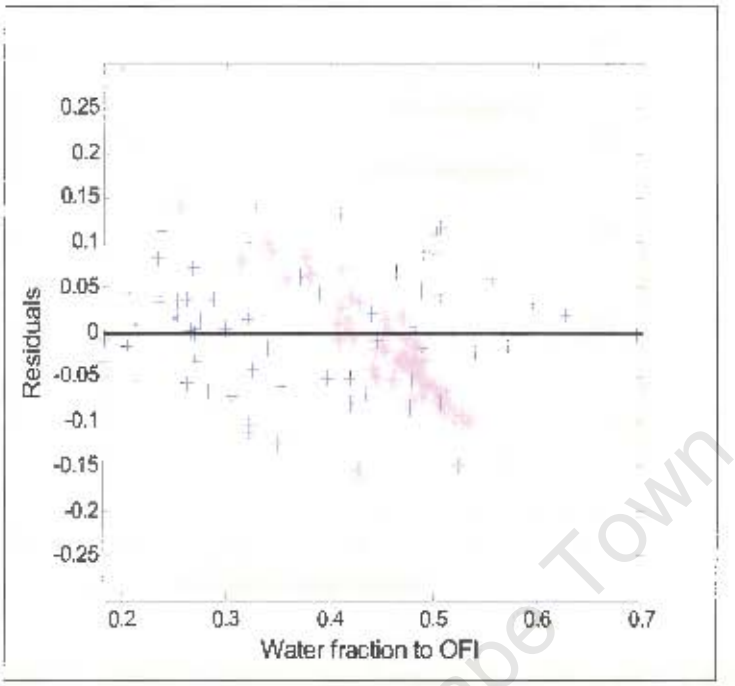


FIGURE 9-8. Residual plots for the water fraction split to the OFI.

The expressions for the d_{50_cOFI} is given in equation 9.7. The correlation between the observed and predicted d_{50_cOFI} is given in figure 9-11 and the corresponding residuals plot in figure 9-12. Although the d_{50_cOFI} values were from a narrow range, there was a good agreement between the observed and predicted. The term for the per cent solids in the underflow has the highest influence on the d_{50_cOFI} compared to the other terms in the expression. The LIVF term had a higher influence compared to the other terms representing geometric variables.

$$d_{50_cOFI} = \frac{0.1443 \times \left(\frac{DOVF}{Dcyc}\right)^{0.507} \left(\frac{DIVF}{Dcyc}\right)^{0.112} \left(\frac{LIVF}{Dcyc}\right)^{0.719} \left(OFI_{frac Solids}\right)^{1.218}}{\left(F_{frac Solids}\right)^{1.404} \left(U/F_{frac Solids}\right)^{0.162}} \quad (9.7)$$

where: d_{50_cOFI} - cut size for the OFI, mm,

$DOVF$ - outer vortex finder diameter, mm,

D_{cyc} , D_{spig} - cyclone and spigot diameters, mm,

University of Cape Town

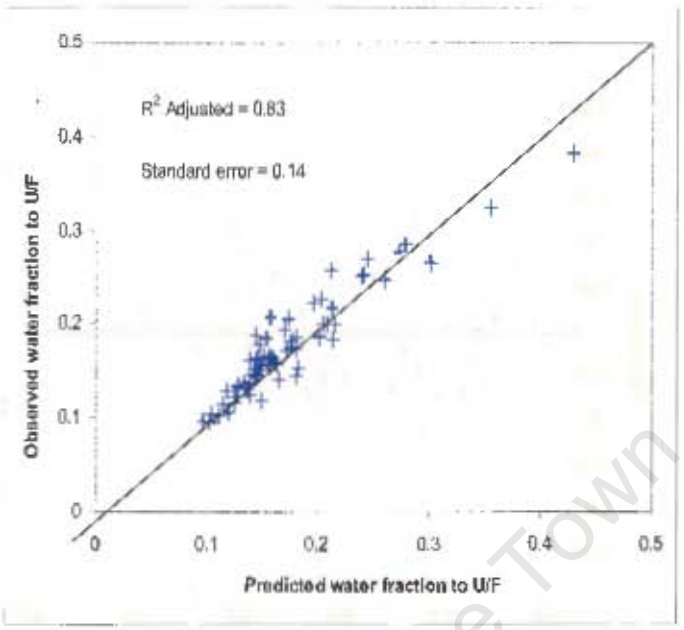


FIGURE 9-9. Comparison of observed and predicted fraction of water split to U/F

$DIVF$, $LIVF$, inner vortex finder diameter, and length, mm,

$F_{fracSolids}$, $U/F_{fracSolids}$ - fraction feed and underflow solids concentration.

The expressions for the $d_{50cU/F}$ is given in equation 9.8. The correlation between the observed and predicted $d_{50cU/F}$ is given in figure 9-13 and the corresponding residuals plot in figure 9-14. There was a good agreement between the observed and predicted cut size to the underflow stream.

$$d_{50cU/F} = \frac{2.72 \times 10^{-2} \left(\frac{DQVF}{D_{spig}}\right)^{0.124} \left(F_{fracSolids}\right)^{2.08}}{\left(\frac{DIVF}{D_{cyc}}\right)^{0.339} \left(U/F_{fracSolids}\right)^{3.556} \left(Q_{U/F_{frac}}\right)^{0.709}} \tag{9.8}$$

where: $d_{50cU/F}$ - cut size for the U/F, mm,

$DIVF$, $LIVF$, inner vortex finder diameter, and length, mm,

D_{cyc} , D_{spig} - cyclone and spigot diameters, mm,

$Q_{U/F_{frac}}$ - fraction water split to U/F,

University of Cape Town

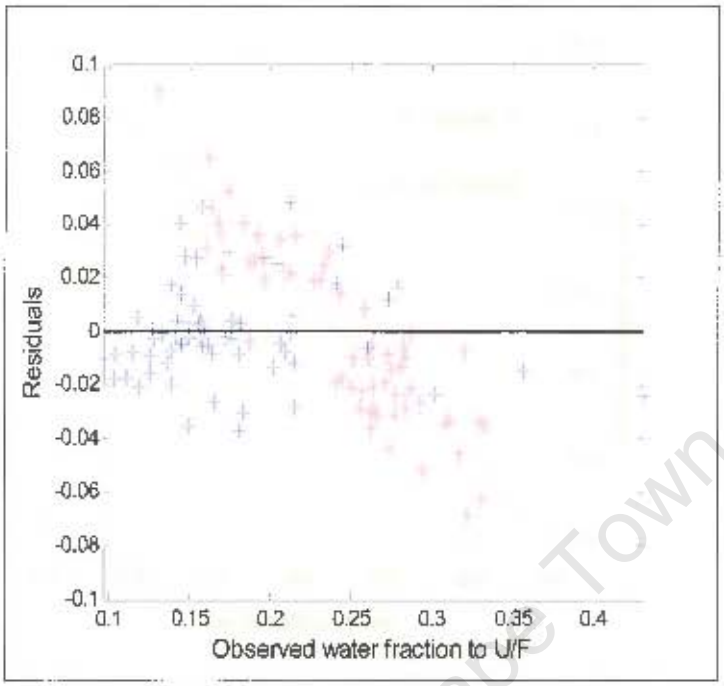


FIGURE 9-10. Residual plots for the water fraction split to the U/F.

$F_{frac Solids}$, $U/F_{frac Solids}$, - fraction feed and underflow solids concentration.

9.3.5 Corrected component cut size

The corrected cut size ($d50_c$) for components were obtained and separate equations for studying the influence of the silica (low density component), and chromite (high density component) were developed. The equations developed here relate the component cut sizes to the overall cut size for efficiency curves representing the OFI and U/F streams, and to the geometric and operating variables of the cyclone. This could enable prediction of the component cut size from information that can be obtained easily (Lynch and Rao [23]).

Equation 9.9 was developed for predicting the corrected cut size of the silica component to the OFI stream - $d_{50_cOFI(si)}$. The correlation between the observed and predicted $d_{50_cOFI(si)}$ is given in figure 9-15, and the corresponding residuals in

University of Cape Town

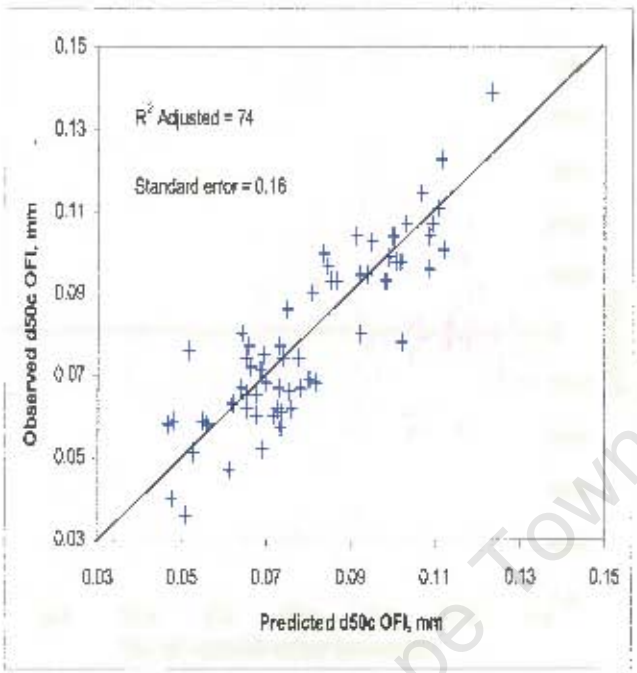


FIGURE 9-11. Comparison of the observed and predicted d_{50_cOFI} for the OFI of the three-product cyclone

figure 9-16. There is good agreement between the observed and predicted silica cut size to the inner overflow - $d_{50_cOFI(si)}$. The $d_{50_cOFI(si)}$ relationship is principally driven by the LIVF term.

$$d_{50_cOFI(si)} = \frac{1.59\left(d_{50_cOFI}\right)^{0.861}\left(\frac{LIVF}{Dcyc}\right)^{1.282}}{Q_f{}^{0.244}\left(\frac{DOVF}{Dcyc}\right)^{0.576}} \tag{9.9}$$

where: $d_{50_cOFI(si)}$ - silica cut size for the OFI, mm,

d_{50_cOFI} - overall cut size for the OFI, mm,

$DOVF$, Outer vortex finder diameter, mm,

$LIVF$, inner vortex finder length, mm

D_{cyc} - cyclone and spigot diameters, mm.

Q_f - Feed flow rate, m^3/h.

Equation 9.10 was developed for predicting the corrected cut size of the chromite

University of Cape Town

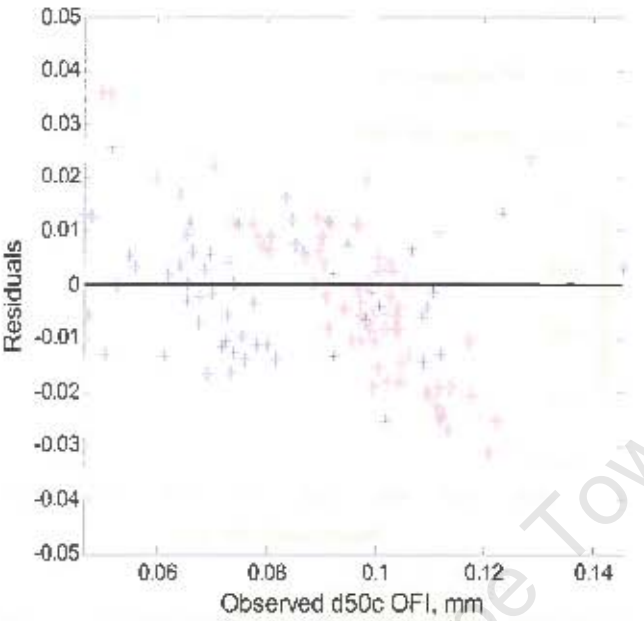


FIGURE 9-12. Residual plots for the $d50_cOFI$.

component to the OFI stream - $d_{50_cOFI(cr)}$. The correlation between the observed and predicted $d_{50_cOFI(cr)}$ is given in figure 9-21, and the corresponding residuals in figure 9-18. The $d_{50_cOFI(cr)}$ relationship appears to be driven by the overall cut size to the OFI stream than the terms from the geometric variables.

$$d_{50_cOFI(cr)} = 0.931 \times (d_{50_cOFI})^{0.900} \left(\frac{DOVF}{Dcyc}\right)^{0.109} \left(\frac{DIVF}{Dcyc}\right)^{0.214} \tag{9.10}$$

where: $d_{50_cOFI(cr)}$ - chromite cut size for the OFI, mm,

d_{50_cOFI} - overall cut size for the OFI, mm,

$DIVF$, $DOVF$, Outer, and inner vortex finder diameters, respectively, mm,

D_{cyc} - cyclone and spigot diameters, mm.

Equation 9.11 was developed for predicting the corrected cut size of the silica component to the U/F stream - $d_{50_cU/F(si)}$. The correlation between the observed

University of Cape Town

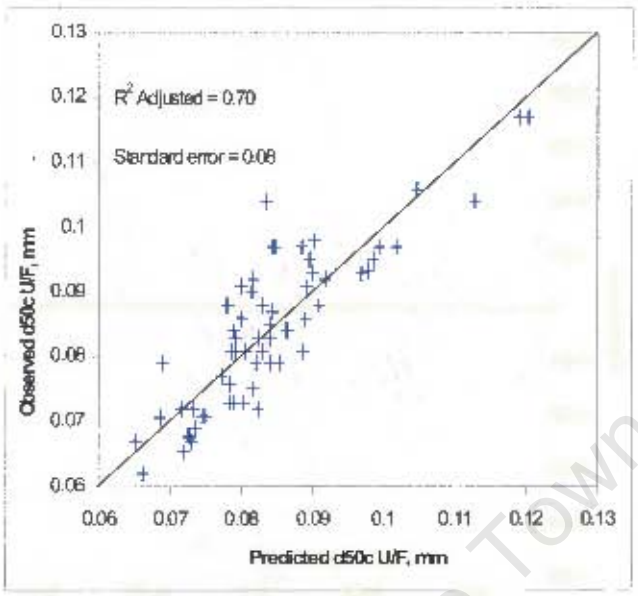


FIGURE 9-13. Comaparison of the observed and predicted $d_{50_cU/F}$ for the three-product cyclone

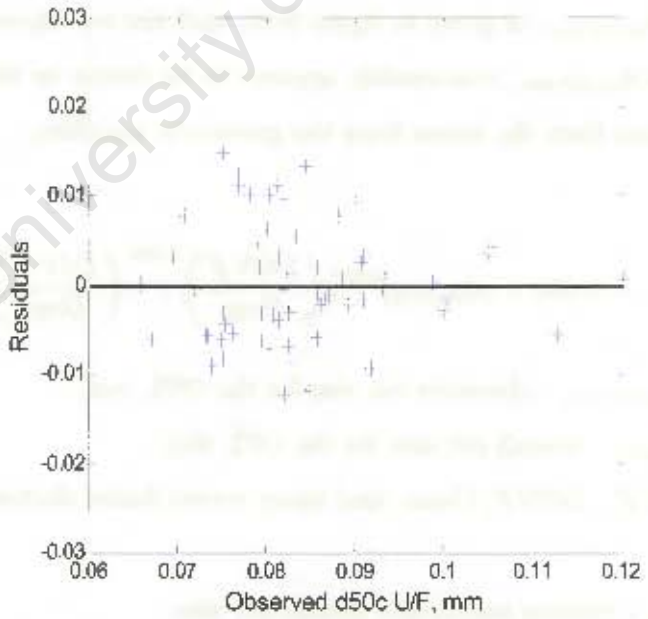


FIGURE 9-14. Residual plots for the $d50_cU/F$.

University of Cape Town

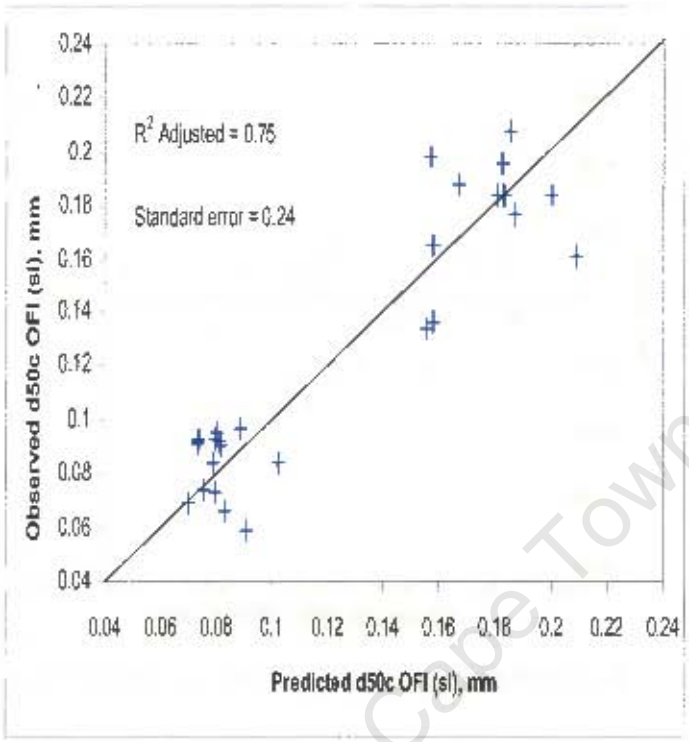


FIGURE 9-15. Comparison of the observed and predicted $d_{50_cOFI(si)}$ for the three-product cyclone

and predicted $d_{50_cU/F(si)}$ is given in figure 9-19, and the corresponding residuals in figure 9-20. The predicted appear to deviate from the measured at larger cut size values. The $d_{50_cU/F(si)}$ relationship is principally driven by the spigot size. However, from the expression in equation 9.11 it appears that a number of variables have an influence on the silica cut size to the U/F stream. Among these, the $d_{50_cU/F}$ and the DIVF terms have a higher influence.

$$d_{50_cU/F(si)} = \frac{0.40 \times \left(d_{50_cU/F}\right)^{0.764} \left(\frac{DOVF}{Dcyc}\right)^{1.500}}{\left(\frac{DIVF}{Dcyc}\right)^{0.688} \left(\frac{Dspig}{Dcyc}\right)^{0.757}} \tag{9.11}$$

where: $d_{50_cU/F(si)}$ - silica cut size for the U/F, mm,

$d_{50_cU/F}$ - overall cut size for the U/F, mm,

University of Cape Town

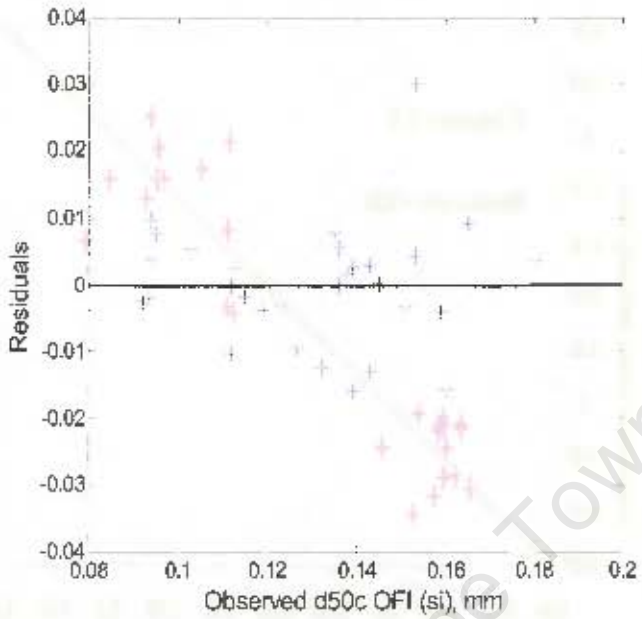


FIGURE 9-16. Residual plots for the $d50_c OFI(si)$.

$DIVF$, $DOVF$, inner, and outer vortex finder diameters, respectively, mm,

D_{cyc} , D_{spig} - cyclone and spigot diameters, mm.

Equation 9.12 was developed for predicting the corrected cut size of the chromite component to the U/F stream - $d_{50_c U/F(cr)}$. The correlation between the observed and predicted $d_{50_c U/F(cr)}$ is given in figure 9-21, and the corresponding residuals in figure 9-22. Like the $d_{50_c OFI(cr)}$, the $d_{50_c U/F(cr)}$ relationship is principally driven by the the overall cut size to the U/F stream - $d_{50_c U/F}$.

$$d_{50_c U/F(cr)} = 5.05 \times \left(d_{50_c U/F}\right)^{1.231} \left(\frac{DOVF}{Dcyc}\right)^{0.736} \left(\frac{DIVF}{Dcyc}\right)^{0.322} \tag{9.12}$$

where: $d_{50_c U/F(cr)}$ - chromite cut size for the U/F, mm,

$d_{50_c U/F}$ - overall cut size for the U/F, mm,

$DIVF$, $DOVF$, Outer, and inner vortex finder diameters, respectively, mm,

University of Cape Town

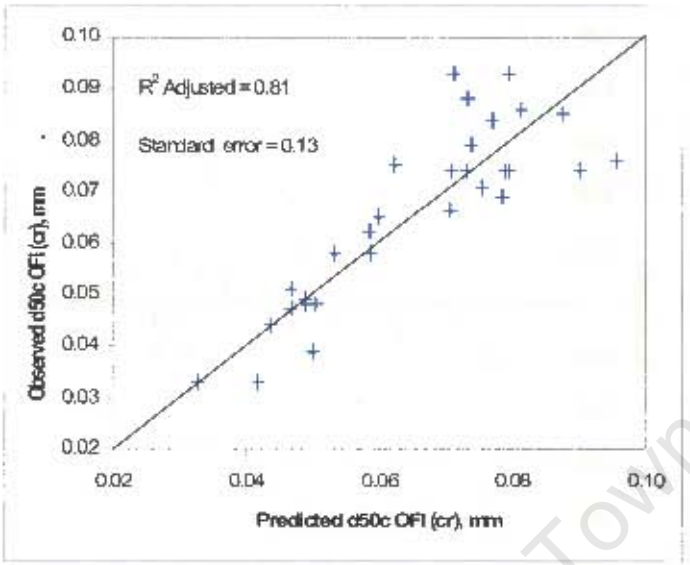


FIGURE 9-17. Comparison of the observed and predicted $d_{50,OFl(cr)}$ for the three-product cyclone

D_{cyc} - cyclone and spigot diameters, mm.

9.4 Validation

A sub section of the data which was not included in the regression was used to validate the model by comparing the model predictions to the observed results. A summary of the tests used for validation is given in Table 9.1. A complete data set is given in Appendix B. The comparisons between the observed and predicted results from figure 9-23 to figure 9-32, appear to be in agreement for almost all the equations developed. It can therefore, be concluded that the model is applicable to the classification of the UG2 platinum ore using the 600mm three-product cyclone. The model should be extended to apply to a range of cyclone diameters.

University of Cape Town

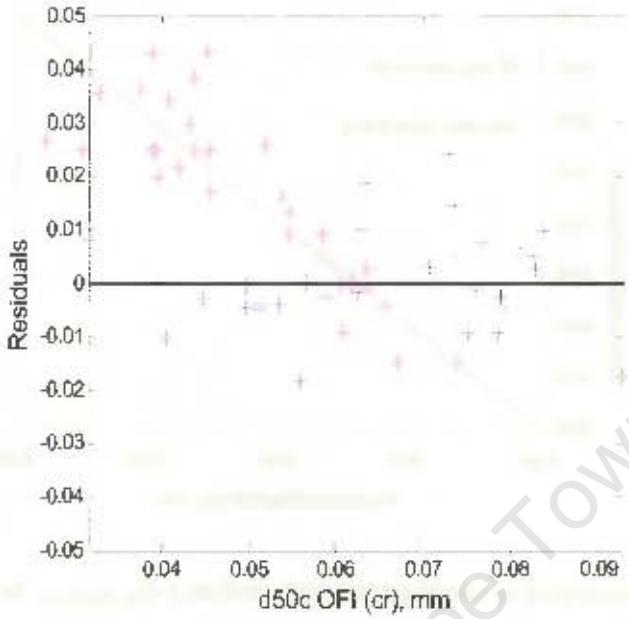


FIGURE 9-18. Residual plots for the $d50_c OFI(cr)$.

9.5 Model trends and sensitivity analysis

Sensitivity analysis using step changes in some of the variables was used to assess the capability of the model to predict the trends observed in the data. The data from test run no. 64 was used as the base case and details of this data set are given in Table 9.2.

The model responses to step changes in some of the key variables are shown in figure 9-33 to figure 9-36. The model response to changes in the volumetric feed flow rate on the cyclone operating pressure in figure 9-33 is similar to that given in section 6.3.6 for both the inner vortex finder length of 775mm and 1025mm, and this demonstrates that the model successfully predicts the observed experimental trends. The effect of the SAR on the volumetric flow split, and water split to the overflow products is given in figure 9-34 and figure 9-35 respectively. It can be seen that the model gives similar trends to the mass split trends presented in section 6.3.3 demonstrating that the model successfully predicts the observed experimen-

University of Cape Town

TABLE 9.1. A summary of the subsection of data used for model validation.

Test No.	DOVF mm	DIVF mm	Dspig mm	LIVF mm	Press kPa	$F_{frac Solids}$ -	$U/F_{frac Solids}$ -	$OFl_{frac Solids}$ -
3	220	190	100	750	62	0.42	0.59	0.35
7	210	165	95	775	81	0.52	0.79	0.27
8	220	165	95	775	68	0.52	0.68	0.33
14	230	192	95	925	120	0.49	0.69	0.35
29	210	150	95	775	85	0.43	0.71	0.27
33	230	209	95	925	124	0.46	0.68	0.36
36	220	198	95	925	107	0.49	0.76	0.38
44	210	177	95	825	82	0.51	0.71	0.37
49	210	177	95	775	79	0.52	0.77	0.37
51	220	184	95	1025	138	0.41	0.75	0.34
59	220	165	90	1025	165	0.41	0.78	0.33
62	210	184	95	775	81	0.53	0.78	0.37
66	220	192	70	775	83	0.48	0.78	0.36
71	220	184	85	775	80	0.50	0.77	0.35
79	220	177	95	875	93	0.48	0.73	0.32

TABLE 9.2. Details of the data set used as a base case for sensitivity analysis of model trends.

Variable	Dimension
Cyclone diameter, mm	600
Equivalent inlet diameter, mm	160
Length of cylindrical part, mm	655
Slanting length of conical part, mm	770
Cone angle	20°
Outer vortex finder internal diameter, mm	210
Inner vortex finder internal diameter, mm	184
Inner vortex finder length, mm	775
Outer vortex finder length, mm	675
Spigot diameter, mm	95
Volumetric flow rate, m^3/h	410.7
Cyclone feed % solids	50.1
Inner overflow % solids	35.6
Underflow % solids	80.0
Operating pressure, kPa	83

University of Cape Town

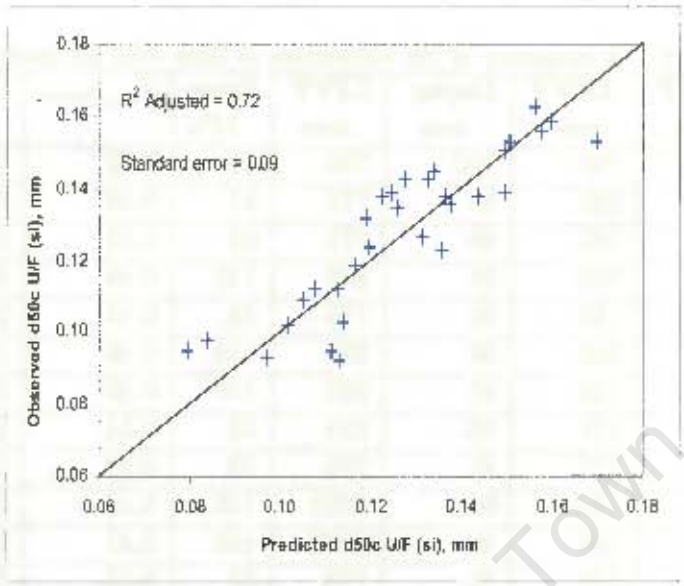


FIGURE 9-19. Comparison of the predicted and observed $d_{50_cU/F(si)}$ for the three-product cyclone

tal trends. Figure 9-36 shows the model predictions for the overall size, silica and chromite component cut sizes with variations in LIVF. The predicted trends show that increasing the length results in a significant increase in the silica component cut size which is in agreement with the observation made by Obeng [61]. It can be seen from figure 9-36 the model can be used to perform predictions for the three-product cyclone with a long inner vortex finder from a short inner vortex finder base case. This demonstrates that the model can successfully model trends for the inner vortex finder LIVF.

The model predictions shown in figures 9-36 indicate that operating the three-product cyclone with a long LIVF results in the OF1 that has a significantly coarse silica cut size in the intermediate product which is suitable for the screening application. The model prediction in figure 9-34 indicate that the SAR values above 0.6 provides a suitable flow split to the OF1 for the screening application.

University of Cape Town

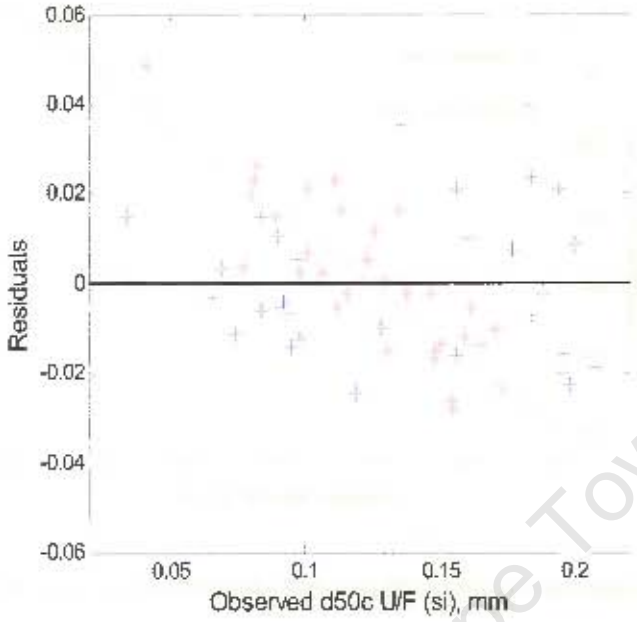


FIGURE 9-20. Residual plots for the $d50_c U/F(si)$.

9.6 Summary

Equations 9.2 to 9.6 represent the expressions for predicting the operating pressure, volume and water split for the three-product cyclone.

A model treating the three-product cyclone as a single unit was developed using a subsection of data obtained from the 600mm cyclone. The model comprises 7 equations for predicting operating pressure, flow and water splits to the OFI and U/F streams, and $d50_c$ for the OFI and U/F streams. Additional expressions for assessing the silica and chromite components $d50_c$ have been developed. The model equations were tested using a separate set of data which was not included in the model development.

In additional to the variables used in the conventional hydrocyclone models, the LIVF and SAR terms were included in the model. The per cent solids to the underflow were also included.

University of Cape Town

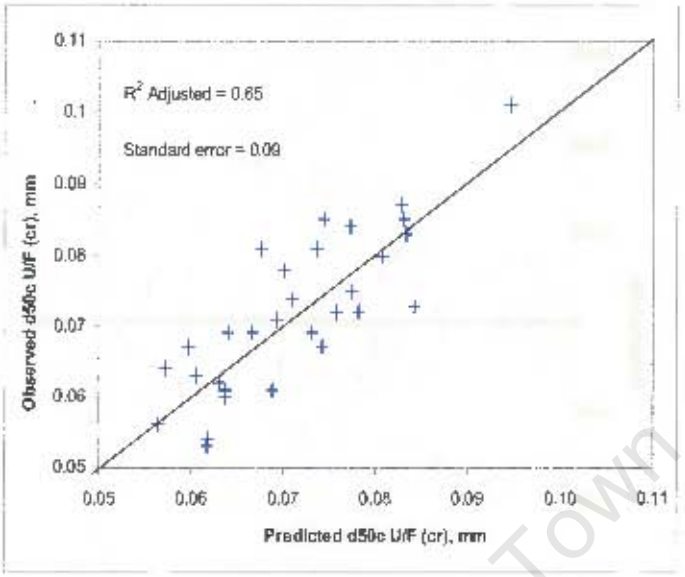


FIGURE 9-21. Comparison of the predicted and observed $d_{50_cU/F(cr)}$ for the three-product cyclone

The model presented was developed on a data set from one diameter cyclone treating a single ore type.

The model needs to be expanded to include different ore types and a wide range of feed size distribution for it to become of general applicability.

University of Cape Town

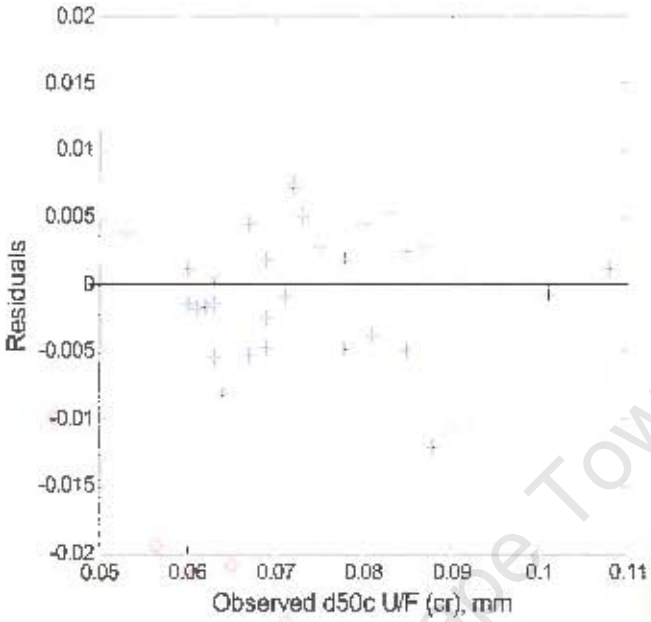


FIGURE 9-22. Residual plots for the $d50_c U/F(cr)$.

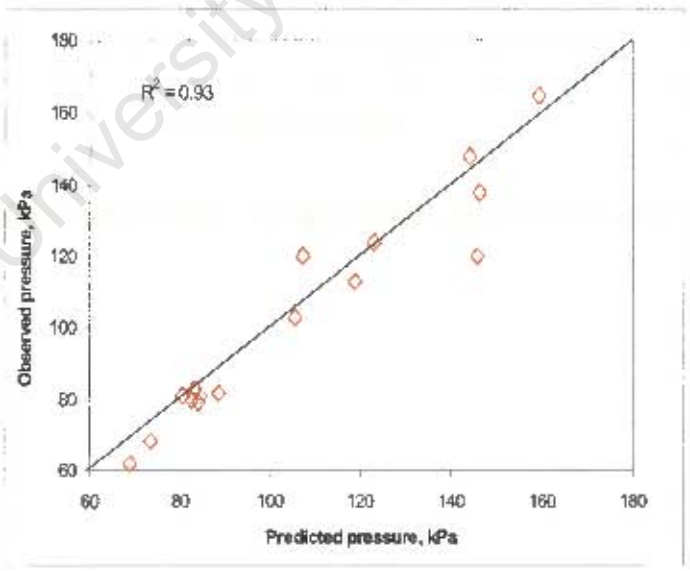


FIGURE 9-23. Comparison of the observed against predicted operating pressure.

University of Cape Town

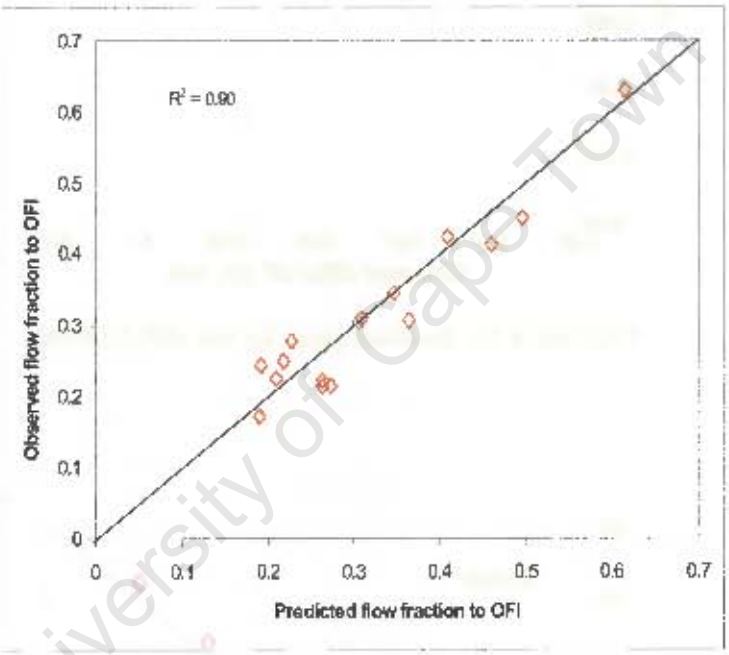


FIGURE 9-24. Comparison of the observed against predicted fraction flow split to the OFI stream.

University of Cape Town

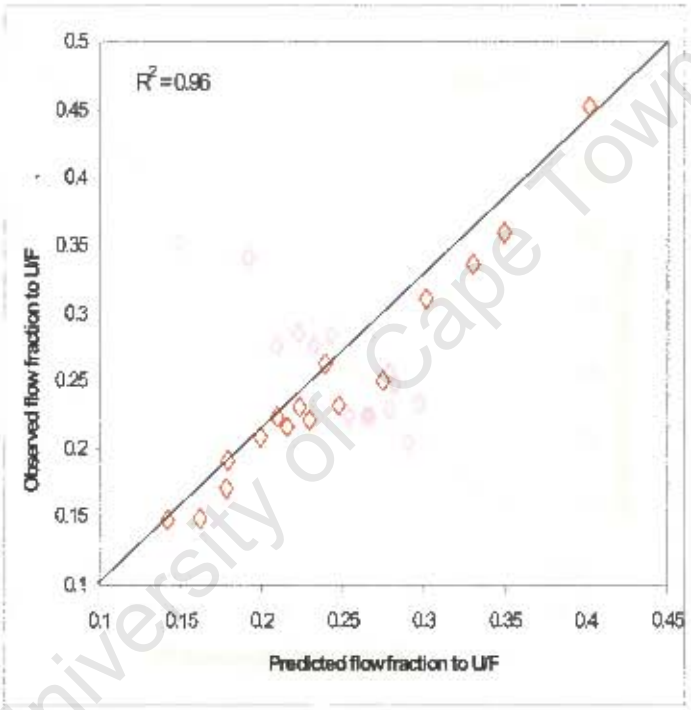


FIGURE 9-25. Comparison of the observed against predicted fraction flow split to the U/F

University of Cape Town

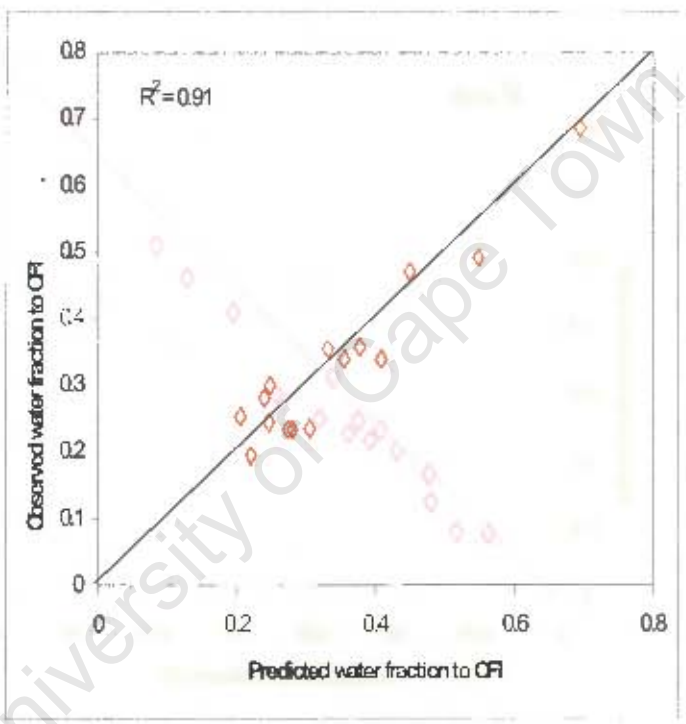


FIGURE 9-26. Comparison of the observed against predicted fraction water split to the OFI stream.

University of Cape Town

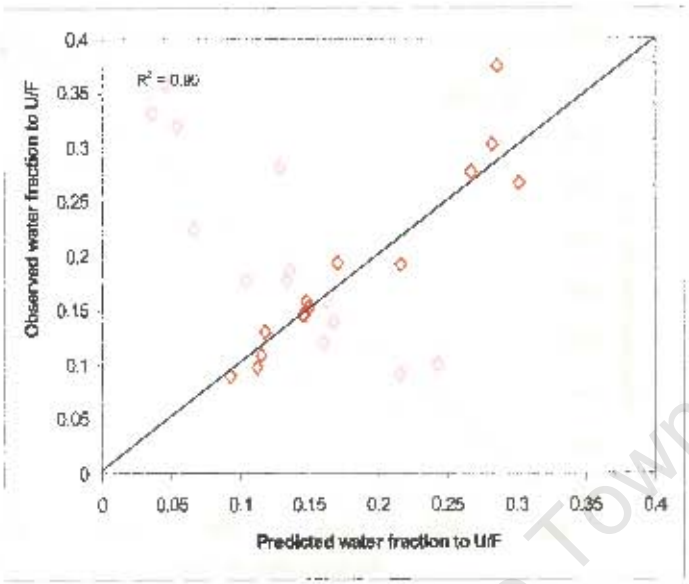


FIGURE 9-27. Comparison of the observed against predicted fraction water split to the U/F stream.

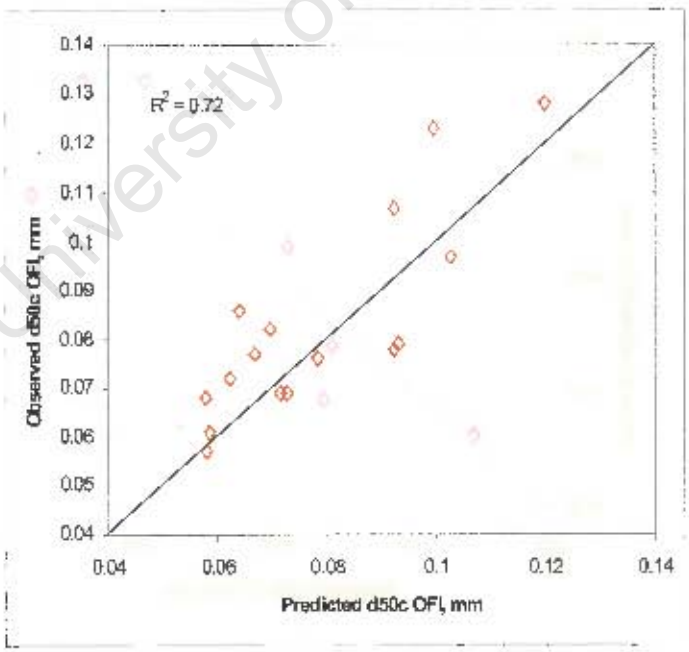


FIGURE 9-28. Comparison of the observed against predicted d_{50c} OFI.

University of Cape Town

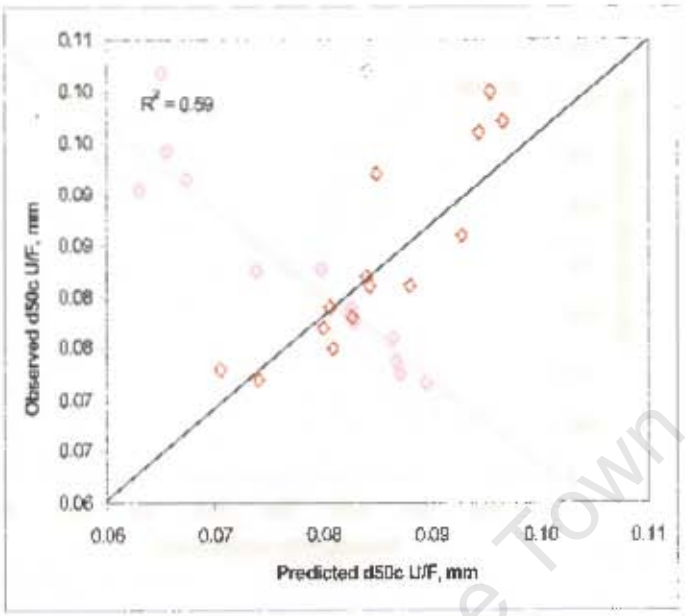


FIGURE 9-29. Comparison of the observed against predicted d_{50c} U/F.

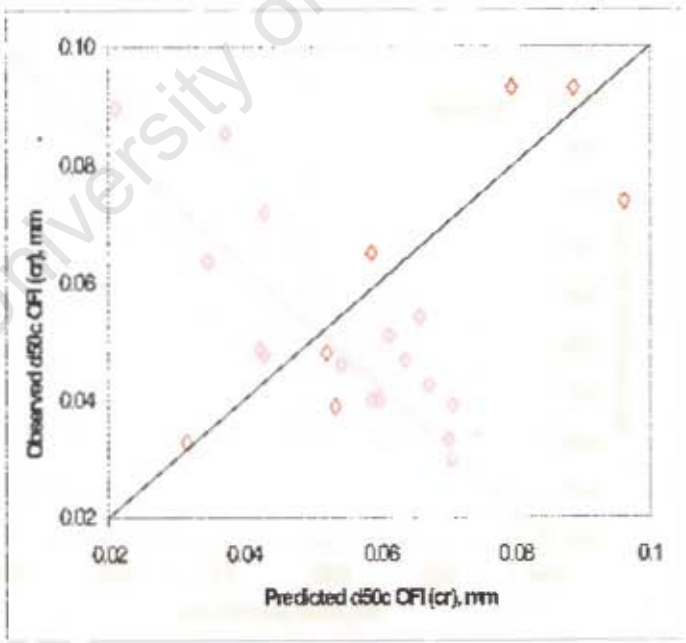


FIGURE 9-30. Comparison of the observed against predicted d_{50c} OFI (cr).

University of Cape Town

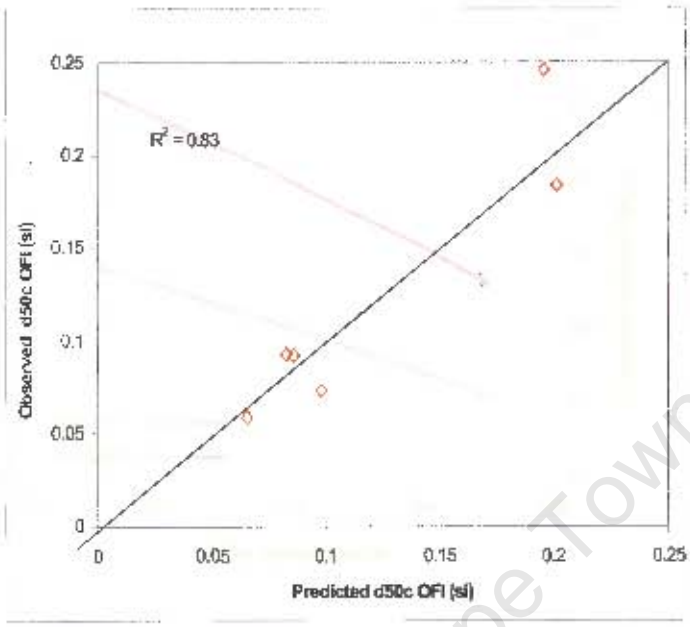


FIGURE 9-31. Comparison of the observed against predicted d_{50c} OFI (si).

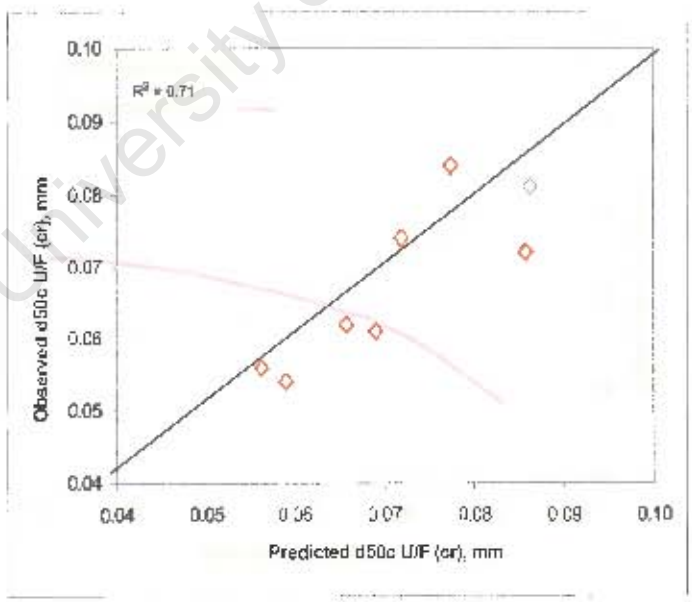


FIGURE 9-32. Comparison of the observed against predicted d_{50c} U/F (cr).

University of Cape Town

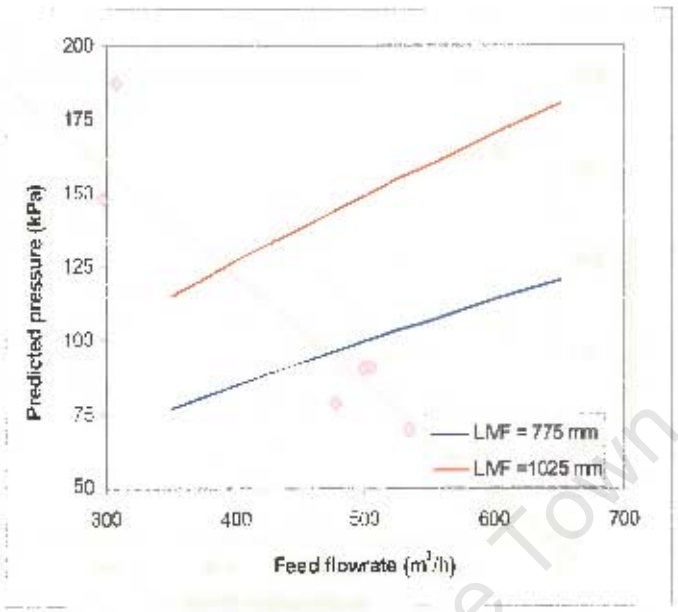


FIGURE 9-33. Model response to step changes in volumetric feed flow rate.

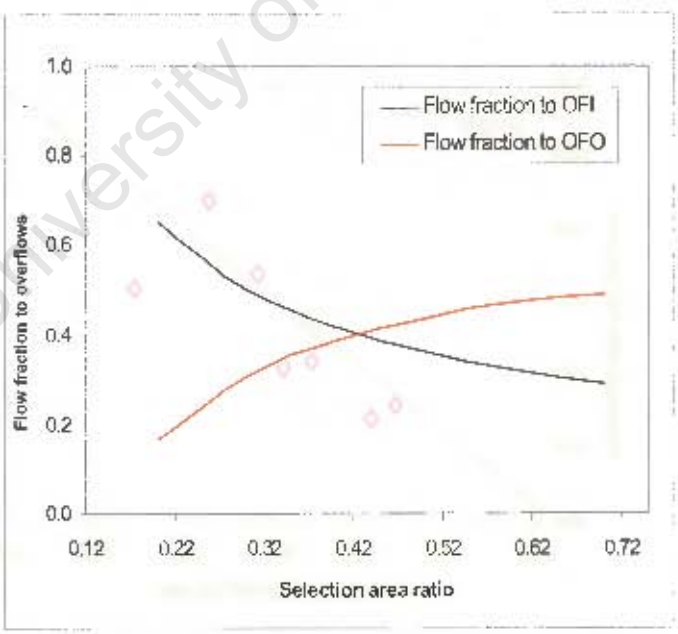


FIGURE 9-34. Model prediction of water fraction to the overflow products.

University of Cape Town

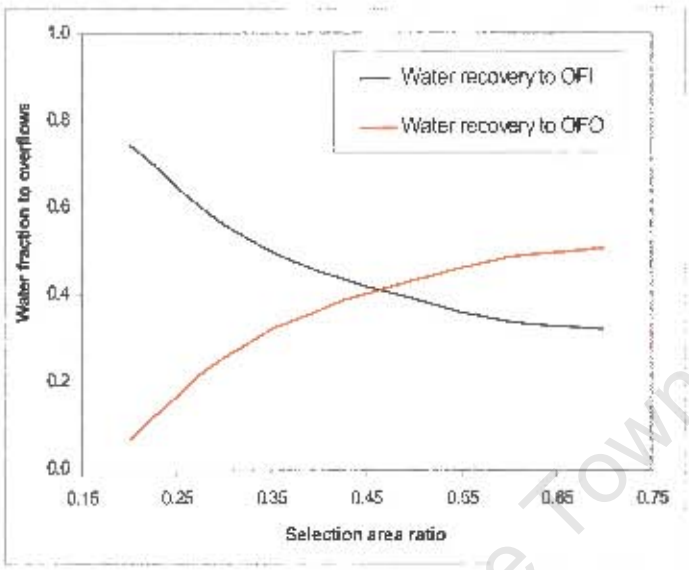


FIGURE 9-35. Model prediction of water fraction to the overflow products.

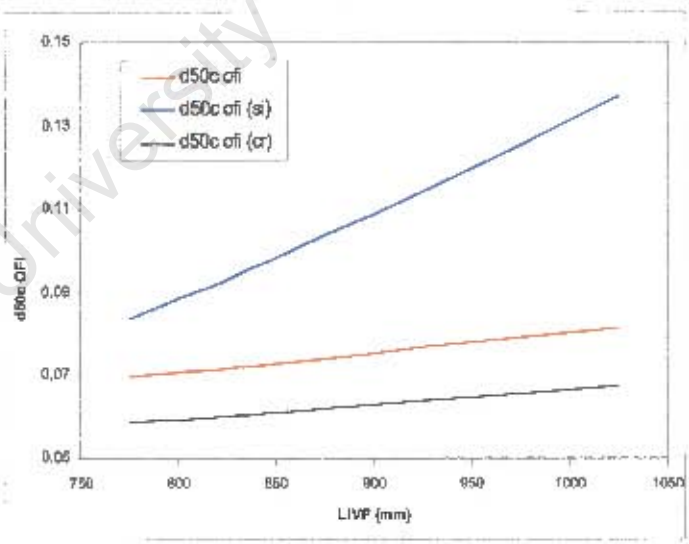


FIGURE 9-36. Model predictions for the variation of the overall and component cut sizes with step changes in LIVF.

University of Cape Town

University of Cape Town

10

Conclusions and Recommendations

This chapter presents the summary of the findings of this thesis, main conclusions drawn from the work, and recommendations.

10.1 Summary of findings

10.1.1 Experimental apparatus and methodology

Two separate test rigs were designed and constructed which allowed flow measurements to be taken for a cyclone operated with either a single or a dual vortex finder arrangement.

The reducer collar system was designed and fabricated which allowed a range of inner vortex finders with different diameters and lengths to be tested.

The test methodology for evaluating the performance of the three-product cyclone has been developed and used successfully to conduct 82 industrial and 14 pilot plant scale tests.

University of Cape Town

10.1.2 Effect of the operation and design variables

The response of the three-product cyclone is reasonably similar to the conventional cyclone. Only the features unique to the three-product cyclone are summarised here.

10.1.3 Operating pressure

The three-product cyclone requires a higher pressure than the conventional hydrocyclone. The reverse classification configuration is operated at a higher pressure than the normal classification configuration.

10.1.4 Length of the Inner Vortex Finder (LIVF)

Using a short LIVF results in the finer overflow discharging from the inner overflow stream, and the intermediate size from the outer overflow stream - normal classification configuration.

Using a long LIVF results in the finer overflow discharging from the outer overflow stream, and the intermediate size from the inner overflow stream - reverse classification configuration.

Positioning the LIVF in the transition zone between the normal and reverse classification configurations results in overflow products with similar size distributions.

The three-product cyclone successfully produces a finer overflow, intermediate size overflow, and a coarse underflow if properly operated.

The LIVF is found to be the principal design parameter for the three-product cyclone.

10.1.5 The Selection Area Ratio (SAR)

The SAR is the ratio between the cross section area of the annulus to the inner vortex finder, and influences the flow split between the inner and outer overflow streams.

The SAR can be used to control the flow split to the inner, and outer overflow streams if the cyclone design has provision which allows interchangeable inner and outer vortex finder diameters such as a reducer-collar system for the inner vortex finder.

This is the next most important design parameter for the three-product cyclone.

University of Cape Town

10.1.6 Cone angle

Varying the conical section length in the three-product cyclone changes the classification configuration. Using a longer conical section results in the normal classification configuration and shorter conical lengths in the reverse classification configuration.

10.1.7 Separation efficiency

The separation in the three-product cyclone can be described by two efficiency curves, with the third calculated from the other two. The same formulation used for the overall efficiency curves is applicable for component efficiency curves. Component efficiency curves have shown that the light component classifies at a coarser cut size while the denser component classifies at a finer cut size for all the product curves.

For the normal classification configuration, the underflow and the intermediate sized stream coarsened with decrease in spigot diameter for both the overall size curves, and the silica and chromite component curves. For the reverse classification configuration, the underflow and the outer overflow streams coarsened with decrease in spigot diameters for the overall size curves, while the inner overflow cut size decreased slightly.

University of Cape Town

10.1.8 Computational Fluid Dynamics (CFD)

The three-product cyclone has been modelled using computational fluid dynamics software Fluent version 6. The general flow structure in the three-product cyclone is similar to that of the conventional hydrocyclone where a downward primary spiral and an upward secondary spiral are present resulting in underflow and overflow products. In the three-product cyclone, the upward secondary spiral splits into the inner overflow and outer overflow products.

The inner vortex finder length has a significant influence on the magnitudes of

the tangential and axial velocities at all profiles along the vertical axis. In general long inner vortex finders resulted in higher tangential velocities and low axial velocities. Velocity field vectors indicate that flow reversals occur over the entire region extending from the tip of the vortex finder down into the region near the spigot, indicating that classification takes place in the whole of this region.

The air-core is present only in the central core of the inner vortex finder and occupies a significantly large portion of the cross section area. For a fixed spigot diameter, the shape and size of the air-core is a function of the inner vortex finder diameter and length for the three-product cyclone and of the vortex finder diameter and length for the conventional hydrocyclone.

10.1.9 Pilot plant trials

Using the three-product cyclone in combination with fine screens produces a feed devoid of plus 100μm which is well suited for flotation of the UG2 platinum ore.

The silica and chromite grade-recovery curves for the three-product cyclone circuits were shown to be superior to those of the conventional hydrocyclone circuit.

The recovery by size data has shown that the recovery of silica - the PGE carrying component - is significantly higher in fine size fractions and that the amount of plus 100μm particles in the concentrate mass flow rate is negligible. This suggests that flotation recovery of this ore is maximised in the sub 100μm particle size range.

The recovery of chromite was high in fine fractions for both circuit configurations which could be a result of entrainment. However, the three-product cyclone circuit had less chromite than the conventional cyclone circuit in fractions between 32μm and 90μm and the increase in chromite in the plus 90μm can be attributed to the presence of composites.

University of Cape Town

10.1.10 Three-product cyclone model

A model treating the three-product cyclone as a single unit producing three separate products has been developed using the Whiten model building technique (Whiten [111]). The model comprises 7 equations for predicting operating pressure, flow and water splits to the inner and U/F streams, and $d50_c$ for the inner and U/F streams. Additional expressions for assessing the silica and chromite components $d50_c$ have been developed.

In additional to the variables used in the conventional hydrocyclone model, the LIVF and SAR terms were included in the model. The per cent solids to the underflow were also included.

10.2 Conclusions

In addressing the hypotheses for this thesis the following conclusions were drawn:

1. Utilising the three-product cyclone with correctly inserted dual vortex finders results in the selection of particles from their region of concentration into a finer overflow, mid-sized overflow, and coarse underflow streams.

2. The three-product cyclone can be utilised to remove the mid-sized silica and fine chromite in a separate stream if the dual vortex finder arrangement is positioned in a manner that allows these particles to be selected from the region where they concentrate.

3. A model based on redefining the traditional efficiency curve to allow for multiple products to add up to unity makes it possible to use the traditional approach to modelling two product classifiers applicable to multiproduct classifiers.

4. A model based on efficiency curves was used to model the three-product cyclone by using the underflow and one of the overflow curves.

University of Cape Town

5. The pilot plant work demonstrated that by classifying appropriately for the recovery process, the recovery of values can be enhanced. The technique of tuning the size distribution of the feed to the recovery process to match the process natural selectivity has not been reported elsewhere, and may be a powerful design tool for classification systems.

The extension of the three-product cyclone work in this thesis to address new aspects is substantial. The main areas include:

- Due to the limitation of the cyclone diameter in his testwork, Obeng did not propose a way of controlling flow to the respective products which is critical in the operation of the three-product cyclone. This has been addressed in this thesis.
- The pilot plant work linking the three-product cyclone with micro screens or flash flotation units to test the application were not performed by Obeng who used simulations to assess the applications. In the present work experiments were done to assess these effects.
- To overcome some of the limitations in the previous work that are highlighted in the literature review, a new model has been built and is independent of the Obeng model.
- This model has the capability of predicting flow splits to the three products of the cyclone, and mineral components splits which are critical in the classification of different density minerals were included.
- A new definition of the partition curves was developed that enabled the model to address more that two splits from a single classifier. This is a novel contribution to classifier modelling.
- Utilising the partition curves without having to rearrange cyclones in series to accommodate any number of splits in a single unit is not reported in any previous work.
- The database for the application of the three-product cyclone has been substantially extended by the present author.

University of Cape Town

- Pilot tests linked to a full mini-flotation plant test rig (the FCTR), were used to demonstrate the beneficial effect of the improved classification on the flotation performance.

10.3 Recommendations

Testing the three-product cyclone for other applications will provide more data on the performance of this cyclone on different ore types, and the data can be used to refine the models developed in this thesis and ensure that they are generally applicable.

Computational fluid dynamics simulations should be performed to provide air-core profiles for a range of inner vortex finders and spigot diameters. The results will improve the definition of the selection area ratio which is critical in the design of the three-product cyclone.

A comparative pilot plant study of the three-product cyclone from the flotation and liberation aspect will shed more light on the differences observed from the pilot trials in this work.

It is proposed that work be carried out using classifier combinations to produce a feed that matches recovery processes and the influence on the final recovery is assessed.

It is proposed that the three-product cyclone model developed in this thesis be extended to incorporate the sharpness of separation which was not considered in the current work.

It is proposed that a common cyclone model that can accommodate the three-product cyclone and conventional cyclone can be developed based on the modelling methodology utilised in this work.

University of Cape Town

University of Cape Town

References

[1] Moder J. J. and Dahlstrom D. A., *Fine size, close-specific-gravity solid separation with the liquid-solid cyclone.*, Chemical Engineering Progress, Vol. 48, No. 2, pp 75-89., 1952.

[2] Pryor E. J., *Mineral processing.*, Applied science publishers limited., 1965.

[3] Wills B. A., *Mineral processing technology.*, Pergamon press., 1992.

[4] Mills C., *Process design and plant design for gravity concentration.*, Mineral processing design. 2 nd edition. Edited by Mular A. L. and Bhappu R. B. AIME., 1980.

[5] Coleman R. L., *Metallurgical testing procedure.*, Mineral processing design. 2 nd edition. Edited by Mular A. L. and Bhappu R. B. AIME., 1980.

[6] Bednarski S., *The three product hydrocyclone for simultaneous separation of solids, both heavier and lighter than liquid medium.*, Paper D5. 2nd International Conference on Hydrocyclones, England, pp 153-162., 1992.

[7] Kelsall D. F., *A study of the motion of solid particles in a hydraulic cyclone.*, Transactions of the Institution of Chemical Engineers, London, Vol 30, pp 87-107, 1952.

[8] Bradley D. and Pulling D. J, *Flow patterns in the hydraulic cyclone and their interpretation in terms of performance.*, Transactions for the Institute of Chemical Engineers., 1959.

[9] Hsieh K. T., *Phenomenological model of the hydrocyclone.*, PhD Thesis, The University of Utar, 1988.

University of Cape Town

[10] Lilge E. O., *Hydrocyclone fundamentals.*, Institution of Mining and Metallurgy, pp 285-335, 1962.

[11] Dabir B. and Petty C. A., *Laser doppler anemometry measurements of tangential an axial velocity in a hydrocyclone operating without an air core.*, Paper A2. 2nd International Conference on hydrocyclones, England, pp 15-40., 1984.

[12] Kelsall D. F., *A further study of the hydraulic cyclone.*, Transactions of the Institution of Chemical Engineers, London, Vol 30, pp 87-107., 1953.

[13] Dahlstrom D. A., *Cyclone operating factors and capacity on coal refuse slurries.*, Transactions for the American Institute of Mining Engineers., 1949.

[14] Fitch E. B. and Johnson E. C., *Transactions of the American Institute of Min. (Metall.) Engineers.*, 196, 304., 1953.

[15] Napier-Munn T. J. Morrell S. Morrison R. D. and Kojovic T., *Mineral Comminution Circuits - Their Operation and Optimisation.*, JKMRC Monograph series in Mining and Mineral Processing 2. JKMRC, University of Queensland., 1996.

[16] Dahlstrom D. A., *Fundamentals and applications of the liquid cyclone.*, Chemical Engineering Progress., Sympossium series No 15, 50., 1954.

[17] Lynch A. J. and Rao T. C., *Studies on the operating characteristics of hydrocyclone classifier.*, Department of Mining and Metallurgical engineering, Indian Institution of Technology, Kanpur, Vol. 6, pp 106-114., 1968.

[18] Trawinski H. F., *Practical aspects of the design and industrial applications of the hydrocyclone-part 1.*, Filtration and Separation, Loughbough University, pp 361-367., 1969.

[19] Yoshioka N. and Hotta Y., *Liquid cyclone as a hydraulic classifiers.*, Chemical engineering., Japan, 19, pp 632-640., 1955.

University of Cape Town

[20] Bradley D., *A theoretical study of the hydraulic cyclone.*, Indusrial Chemistry., 1958.

[21] Rietema K., *The performance and design of hydrocyclones, Parts I - IV.*, Chemical engineering science, 15, pp 298-302., 1960.

[22] Fahlstroom P. F., *Studies of the hydrocyclone as a classifier.*, Proceedings of the 6th Int. Mineral processing Congress, Cannes.,pp 87-114., 1963.

[23] Lynch A. and Rao T. C., *Modelling and scale-up of hydrocyclone classifiers.*, Proceedings of the IMPC (1975) conference. Cagliari., 1975.

[24] Plitt L. R., *A mathematical model of the hydrocyclone classifier.*, Canadian Mineral Processing Division of CIM, vol 69, No 776, pp 114-123., 1976.

[25] Bednarski S., *New designs of classifying hydrocyclones with high separation acuity.*, Paper D5. 2nd International Conference on Hydrocyclones, England, pp 153-162., 1984.

[26] Braun T. and Bohnet M., *Influence of feed solids concentration on the performance of the hydrocyclone.*, Chemical Engineering Technology., vol 13, pp 15-20., 1990.

[27] Tarjan G., *On the theory and use of the hydrocyclone.*, Institution of Mineral Dressing, Technical University, Sopron, pp 389-411., 1953.

[28] Mular A. L. and Jull N. A., *The selection of cyclone classifiers, pumps and pump boxes for grinding circuits.*, Krebs Engineers, Menlo Park, Califonia, pp 376-403., 1980.

[29] Trawinski H. F., *New hydrocyclone for classification and sorting.*, Technical Note, West Germany., 1982.

[30] Svarovsky L., *Hydrocyclones.*, Technomics., 1984.

University of Cape Town

[31] Schmidt M. P. and Turner P. A., *Flat bottom or horizontal cyclones - which is right for you?*, World mining equipment, September Isuue, pp 21-22., 1993.

[32] Dahlstrom D. A., *High-speed classification and de-sliming with the liquid-solid cyclone.*, Trans. AIME Min. Engng. Vol 190, pp 331-334., 1951.

[33] Yianatos J. B. Lisboa M. A. and Baeza D. R., *Grinding capacity enhancement by solid concentration control of hydrocyclone underflow.*, Minerals Engineeringes, vol 15, pp 317-323., 2002.

[34] Arterburn R. A., *The sizing and selection of hydrocyclones.*, Mineral processing design. 2 nd edition. Edited by Mular A. L. and Bhappu R. B. AIME., 1980.

[35] Asomah I., *Improved models of hydrocyclones.*, PhD thesis, JKMRC, University of Queensland, Australia., 1996.

[36] Nageswararao K., *Reduced efficiency curves of industrial hydrocyclones - an analysis for plant practice.*, Minerals Engineering. 12 (5), pp 517-544, 1999b.

[37] Svarovsky L., *Critical evaluation of the simple ways of determining the cut size.*, International conference on hydrocyclones. BHRA., 1980.

[38] Lynch A. J., *Mineral crushing circuits: their simulation, optimisation, design, and control.*, Elsevier., 1977.

[39] Nageswararao K., *Flow split and water split in Industrial hydrocyclones.*, American Filtration and separation society., 2001.

[40] Nageswararao K., *A generalised model for hydrocyclone classifiers.*, Proceedings for the Australasian Institute of Mining and Metallurgy., 1995.

[41] Asomah I. and Napier-Munn T. J., *An empirical model of hydrocyclones, incorporating angle of inclination.*, Minerals Engineering, 10 (3), 339-347., 1996.

University of Cape Town

[42] Nageswararao K. Wiseman D. M. and Napier-Munn T. J., *Two empirical hydrocyclone models revisited.*, Minerals Engineering, vol 17, pp 671-687., 2004.

[43] Cilliers J. J. and Hinde A. L., *An improved hydrocyclone model for backfill preparation.*, Minerals Engineering, Vol. 4, Nos 7-11, pp 683-693., 1991.

[44] Peterson R. D. and Herbst J. A., *The effects of two-stage hydrocyclone classification on mineral processing plant performance.*, Canadian Institution of Mining and Metallurgy, Vol. 23, No 4, pp 383-391., 1983.

[45] Neese T. Dallman W. and Espig D., *Effect of turbulence on the efficiency of separation in hydrocyclones at high feed solids concentrations.*, 2 nd International conference on hydrocyclones. BHRA., 1984.

[46] Monrendon T. C. Hsieh K. T. and Rajamani R. K., *Fluid flow model od the hydrocyclone: an investigation of device dimensions.*, International Journal of Mineral Processing, 35, pp 65-83., 1992.

[47] Colman D. A. and Thew M. T., *Hydrocyclone to give a highly concentrated sample of a lighter dispersed phase.*, International conference on hydrocyclones. BHRA Fluid Engineering., 1980.

[48] Kimber G. R. and Thew M. T., *Experiments on oil/water separation with hydrocyclones.*, European conference on mixing and centrifugal separation. Cambridge., 1974.

[49] Miller J. and Hupka J., *Water De-oiling in an air-sparged hydrocyclone.*, Filtration and separation, 1983.

[50] Goodall C. M., *The effect of flotation variables on the bubble size, mixing characteristics and froth behaviour in column cells.*, PhD Thesis. University of Cape Town., 1992.

University of Cape Town

[51] Breed W. A., *Beneficiation of fine coal using the air-sparged hydrocyclone.*, Masters Thesis. University of Cape Town., 1992.

[52] Kelsall D. F. and Holmes J. A., *Improvement of classification efficiency in hydraulic cyclones by water injection.*, Transactions of the Institution of Chemical Engineers, London, Vol 30, pp 150-170., 1963.

[53] Heiskanen K. Vesanto A. and H. Eronen, *A high performance hydrocyclone design - the twin vortex finder.*, Paper K2. 3rd International Conference on Hydrocyclones, England, pp 263-268., 1987.

[54] Dahlstrom D. A. and Kam W., *Potential savings in comminution by two-stage classification.*, International Journal of Mineral Processing, Vol 22, pp 239Ű250., 1988.

[55] Kelsall D. F. Stewart P. S. B. and Restarick C. J., *A practical multiple cyclone arrangement for improved classification.*, 1 st European conference on mixing and centrifugal separation, BHRA, Cambridge, pp 83-93., 1963.

[56] Rogers R. S. C. Hukki A. H. Steiner G.J. and Arterburn R. A., *An evaluation of the use of two vs one stage of hydrocyclones in a pilot scale ball mill circuit.*, Annual meeting, American Institute of Mining Engineers., 1981.

[57] Stratton C. R and Agar G. E., *Multistage hydrocyclone circuit optimisation by computer simulations.*, Canadian Mineral Processing, vol 11, pp 98-127., 1979.

[58] Bradley D., *The hydrocyclone.*, Pergamon press., 1965.

[59] Mizrahi J. and Cohen E., *Studies of some factors influencing the action of hydrocyclones.*, Institution of Mining and Metallurgy, pp 318-330., 1966.

University of Cape Town

[60] Lynch A. J. Rao T. C. and Prisbrey K. A, *The influence of hydrocyclone diameter on reduced efficiency curves.*, International Journal of Mineral Processing,Vol. 1, pp 173-181., 1974.

[61] Obeng D. P., *The three-product cyclone - separation performance, potential applications and modelling.*, PhD Thesis, University of Queensland., 2003.

[62] Morrell S., *Evaluation of the separation performance of a new design of hydrocyclone.*, chapter 9, Second progress report, JKMRC/AMIRA project P9L., 1996.

[63] Xiao J., *Extensions of the model building techniques and their applications in mineral processing.*, PhD Thesis, University of Queensland., 1997.

[64] Restarick C. J. and Krnic Z., *The effect of underflow/overflow ratio on dense medium cyclone operation.*, Minerals Engineering, Vol 4. No. 3/4, pp 263-270., 1991.

[65] Driessen M. G., *Theory of flow in a cyclone.*, Rev. Industrial Min. Special issue, (English), pp 449-461., 1951.

[66] Mainza A. Powell M. S. and Knopjes B., *A comparison of different cyclones in addressing challenges in the classification of the dual density UG2 platinum ore.*, J.SAIMM, vol. 105, pp 241-348., 2005.

[67] Trawinski H. F., *The application of hydrocyclones as versatile separators in chemical and mineral industries.*, International conference on hydrocyclones, BHRA, pp 179-188., 1980.

[68] Mainza A. Powell M. S. and Knopjes B., *Differential classification of dense material in a three-product cyclone.*, Minerals Engineering, Vol. 17, pp 573Ű579., 2004.

University of Cape Town

[69] Obeng D. P. and Morrell S., *The JK three-product cyclone - performance and potential applications.*, International journal of Mineral processing, 69, pp 129-142., 2003.

[70] Coleman R. L. Esvelt M. Franzidis J. P. and Manilapig E. V., *The floatability characterisation test rig as a pilot plant for flotation testing - an operaters view point.*, Proceedings of the 8th Mill Operaters Conference - Evolution and Survival in the Minerals Industry, Townsville, Qld., pp 22-23., 2003.

[71] Kojovic T., *Personal Communication.*, University of Queensland, Brisbane, Australia., 2000.

[72] Morrison R. D., *Personal Communication.*, JKMRC, Brasbane, Australia., 2005.

[73] Morrison R. D. and Richardson J. M., *JKMBal - The mass balancing system.*, Proceedings 2 nd Canadian Conference on Computer Applications for Mineral Industry (CAMI'91), Vol. II, Vancouver., 1991.

[74] JKTech., *JKSimMet steady state mineral processing simulator - User manual, Version 5.*, JKTech, JKMRC commercial division, University of Queensland, Australia., 1996.

[75] Wiegel R. L., *Advances in mineral processing material balances.*, Canadian Netallurgical Quarterly. Vol 11, 2. pp 413-424., 1972.

[76] Milin L. Hsieh K. T. and Rajamani R. K., *The leakage mechanisms in the hydrocyclone.*, Minerals Engineering, Vol 5, No. 7, pp 779-794., 1992.

[77] Bradley D., *Design and performance of cyclone thickeners.*, Pergamon press., 1965.

[78] Tromp K. F., *New methods of computing the washability of coal.*, Colliery guardian, CLIV., 1973.

University of Cape Town

[79] De Kok S. K., *Symposium on recent developments in use of hydrocyclones in mill operation.*, A review: Journal of Chem. Met. Mining Society of South Africa, vol 56, pp 281-294., 1956.

[80] Kutepov A. M., *Study and calculation of the separation efficiency of hydrocyclones.*, Zh. Prikl. Khim. Vol 51, pp 614-619., 1988.

[81] Whiten W. J., *Personal communication.*, University of Queensland, JKMRC, Brisbane., 2005.

[82] Kojovic T., *The development and application of model - an automated model builder for mineral processing.*, PhD Thesis, University of Queensland., 1988.

[83] Laplante A. R. and Finch J. A., *The origin of unusual cyclone performance curves*, International of mineral processing, Vol 13, 1984.

[84] Bazin C. and Hodouin D., *Processing assays of size fractions from sieve and cyclosizer analyses.*, Minerals Engineering, Vol. 9, No. 7, pp 753-763., 1996.

[85] Statie E. Salcudean M. Gartshore I. and Bibeau E., *A computational study of particle separation in hydrocyclones.*, Jounal of pulp and paper science, vol 28, No. 3, pp 84-92., 2002.

[86] Hsieh K. T. and Rajamani K., *Phenomenological model of the hydrocyclone based on the physics of fluid flow.*, American Institute of Chemical Engineers Journal, 37-5, pp 735-746, 1991.

[87] Bloor M. I. G. and Ingham D. B., *Turbulent spin in a cyclone.*, Transactions of the Institution of Chemical Engineers, London, Vol. 53, pp 1-11., 1975.

[88] Narasimha M. Sripriya R. and Banerjee P. K., *CFD modelling of hydrocyclone - prediction of cut size.*, International journal of Mineral Processing, vol 75, pp 53-68., 2005.

University of Cape Town

[89] Chakraborti N. and Miller J. D., *Fluid flow in hydrocyclones: A critical review.*, Mineral processing and extractive metallurgy (Trans Inst. Metall. C. Vol 11, pp 211-244., 1992.

[90] Fluent Software., *Fluent version 6.1.22 users' manual.*, February., 2003.

[91] Brennan M. S., *Multiphase CFD simulations of dense medium and classifying hydrocyclones.*, Third international conference on CFD in minerals and process industry, CSIRO, Melbourne, Australia., 2003.

[92] Slack M. D. Del Porte S. and Engelman M. S., *Designing automatic computational fluid dynamics modelling tools for hydrocyclone design.*, Minerals Engineering, vol 17, pp 705-711., 2003.

[93] Pericleous K. A. Rhodes N. and Cutting G. W., *A Mathematical model for predicting the flow field in a hydrocyclone classifier.*, International conference on hydrocyclones. BHRA., 1984.

[94] Cullivan J. C. and Williams R. A., *New insights into hydrocyclone operation.*, Particulate Science and technology, Vol. 21, pp 1-21., 2003.

[95] Cullivan J. C. Williams R. A. Dyakowski T. and Cross C. R., *New understanding of a hydrocyclone flow field and separation mechanism from computational fluid dynamics.*, Minerals Engineering, Vol. 17, pp 651-660., 2004.

[96] Cullivan J. C. Williams R. A. and Cross C. R., *Understanding the hydrocyclone separator through computational fluid dynamics.*, Trans. IChemE, vol 81, Part A, pp 455-466., 2003.

[97] Delgadillo J. A. and Rajamani K., *A comparative study of three turbulence-closure models for the hydrocyclone problem.*, International journal of Mineral Processing, vol 77, pp 217-230., 2005.

University of Cape Town

[98] Mainza A. and Powell M. S., *Use of the three-product cyclone in a dual density ore classification*, Proceedings of the IMPC 2003 conference. 28 September-3 October 2003. Cape Town. South Africa, 2003.

[99] Solero J. and Coghe A., *Experimental fluid dynamic characterisation of a cyclone chamber.*, Experimental Thermal and Fluid Science, Vol. 27, pp 87-96., 2002.

[100] Ferrara and Bevilacqua., *Particle segregation in hydrocyclones.*, Minerals and Metallurgical processing. pp 112-118., 1996.

[101] Steffens P. R. Whiten W. J. Appleby S. and Hitchins J., *Prediction of air core diameters for hydrocyclones.*, International Journal of Mineral Processing, vol 39, pp 61-74., 1979.

[102] Fontein F. J. Van Kooy J. G. and Leniger H. A., *The influence of some variables upon hydrocyclone performance.*, British Chemical Engineering, June vol 7, pp 410-421., 1962.

[103] Ekmekci Z. Bradshaw D. J. Allison S. A. and Harris P. J., *Effects of frother type and froth height on the flotation behaviour of chromite in UG2 ore.*, Minerals Engineering, vol 16, pp 941-949., 2003.

[104] Gaudin J. R. Schuhmann R. and Schlecten A., *The effect of size on the behaviour of galena particles*, Flotation Kinetics, II, Journal of Physical Chemistry. 46, pp 902-910, 1942.

[105] Feng D. and Aldrich C., *Effect of particle size on flotation performance of complex sulphide ores.*, Minerals Engineering, Vol 12, No 7., pp 721-731., 1999.

[106] Johnson N. W., *Personal Communication.*, Mineraluegy Pty Ltd, Australia., 2005.

University of Cape Town

[107] Trahar W. J., *A rational interpretation of the role of particle size in flotation.*, International journal of Mineral Processing, vol 8, pp 289-327., 1981.

[108] Wessldijk Q. I. Reuter M. A. Bradshaw D. J. and Harris P. J., *The flotation behaviour of chromite with respect to the beneficiation of UG2 ore.*, Minerals Engineering, Vol 12, 10. pp 1177-1184., 1999.

[109] Morrell S., *Personal communication.*, JKMRC, University of Queensland, Brisbane, Australia., 2005.

[110] Whiten W. J., *Model building techniques for mineral treatment processes.*, Automatic control systems in mineral processing plants, Brisbane, pp 129-148., 1971.

[111] Whiten W. J., *Determination of parameter Relations within Non-Linear models.*, Special interest group on numerical mathematics, Vol. 29, numbers 3 and 4., 1994.

[112] Petersen K. R. P., *Vortex chamber modelling for hydrocyclone simulation.*, MSc Thesis, JKMRC, University of Queensland., 1993.

[113] Kojovic T. and Whiten W. J., *Automated Model Building in Mineral Processing.*, Computational Techniques and Applications, CTAC - 89. Proceedings of the Computational Techniques and Applications, Grifith University, Australia., 1989.

[114] Powell M. S., *Personal communication.*, University of Cape Town, Cape Town, South Africa., 2006.

[115] Lynch A. J. Rao T. C. and Bailey C. W., *The influence of design and operating variables on the capacitis of hydrocyclone classifiers.*, International Journal of Mineral Processing,Vol. 2, pp 29-37., 1975.

University of Cape Town

[116] Flintoff B. C. Plitt L. R. and Turak A. A., *Cyclone modelling: a review of present technology.*, Canadian Mineral Processing Division of CIM, vol 80, No 905, pp 39-49., 1978.

[117] Brookes G. F. Miles N. J. and Clayton J. S., *Hydrocyclone performance related to velocity parameters.*, International conference on hydrocyclones. BHRA., 1984.

[118] Vallebuona G. Casali A. Ferrara G. Leal O. and Bevilacqua. P., *Modelling for small diameter hydrocyclones.*, Technical note . Minerals Engineering, Vol 8, No. 3, pp 321-327., 1995.

[119] Plitt L. R. and Kawatra S. K., *Estimating the cut (d50) size of classifiers without product particle-size measurement.*, International journal of Mineral Processing, vol 5, pp 369-378., 1978.

[120] Gupta A. and Eren H., *Mathematical modelling and on-line control of hydrocyclones.*, AusIMM Proceedings, No 1, pp 31-41., 1990.

[121] Svarovsky L., *Selection of hydrocyclone design and operation using dimensionless groups.*, International conference on hydrocyclones, BHRA, Paper A1, pp 1-5., 1987.

University of Cape Town

University of Cape Town

University of Cape Town

University of Cape Town

Appendix A

Mathematical Definitions

A.1 Derivation for Calculating the sump volume for flow rate measurements

Let L(0) = A_1, and B(0) = A_2, from geometry,

$$L(h) = (2h\tan\theta + A_1) \tag{A.1}$$

$$B(h) = (2h\tan\theta + A_2) \tag{A.2}$$

The expression for the volume is as follows:

$$Vol = \int_{ho}^{h} (L(h)B(h))\partial h \tag{A.3}$$

Substituting for L(h) and B(h) we get:

$$Vol = \int ((2h\tan\theta + A_1)(2h\tan\theta + A_2))\partial h \tag{A.4}$$

simplifying the above equation we have:

$$Vol = 4\tan^2\theta \int_0^h h^2\partial h + A^2 \int_0^h \partial h + 4A\tan\theta \int_0^h h\partial h \tag{A.5}$$

The volume was obtained by integrating the above equation to obtain:

$$Vol = 4\tan^2\theta \left[\frac{h^3}{3}\right]_0^h + A^2\left[h\right]_0^h + 4A\tan\theta \left[\frac{h^2}{2}\right]_0^h \tag{A.6}$$

The above formulae gave an exact volume calculation which was used in flow rate calculations.

University of Cape Town

University of Cape Town

University of Cape Town

University of Cape Town

B. Industrial Scale Three-Product Cyclone Data

Run1 Dcyc 600 Dovf 210 Divf 190 Lovf 675 Livf 750 Dspig 100 Press 70

Solids	Water	Cromite	Silica	SG
Feed	330.5	283.0	20.2	23.9	3.8
Ofi	58.6	77.4	23.9	20.2	3.8
Ofo	94.8	97.5	21.9	24.5	3.8
Uf	177.0	108.1	33.2	16.1	3.8

Size	Feed	Crmt	Silc	Ofi	Crmt	Silc	Ofo	Crmt	Silc	Uf	Crmt	Silc
0.710	0.1	0.0	0.0	0.0	0.0	0.0	0.0	0.0	0.0	0.1	0.0	0.0
0.500	0.0	0.0	0.0	0.0	0.0	0.0	0.0	0.0	0.0	0.0	0.0	0.0
0.355	0.1	0.0	0.0	0.0	0.0	0.0	0.0	0.0	0.0	0.1	0.0	0.0
0.250	0.3	0.0	0.0	0.0	0.0	0.0	0.1	0.0	0.0	0.5	0.0	0.0
0.180	2.2	31.0	15.0	0.6	44.3	3.4	0.9	40.1	7.9	3.4	22.8	28.0
0.125	7.6	19.6	26.1	2.8	38.4	6.1	3.8	33.1	11.6	11.2	33.6	15.9
0.090	16.5	16.8	20.2	8.4	32.1	14.6	11.9	23.9	22.1	21.7	35.9	12.4
0.063	18.9	16.4	28.4	16.2	22.6	14.3	18.9	19.9	25.5	19.9	15.0	15.0
0.045	12.0	18.0	27.4	12.0	22.9	22.3	11.8	20.4	24.4	12.1	33.1	16.5
0.032	6.7	19.4	24.5	9.8	20.7	22.2	8.5	20.2	25.0	4.7	31.3	18.0
0.000	35.6	24.6	22.0	50.2	22.8	23.2	44.2	21.7	26.1	26.3	32.0	18.4

Run2 Dcyc 600 Dovf 210 Divf 165 Lovf 675 Livf 1025 Dspig 100 Press 165

Solids	Water	Cromite	Silica	SG
Feed	263.1	370.2	24.6	17.3	3.8
Ofi	50.1	93.9	20.4	22.9	3.8
Ofo	70.5	177.5	26.7	19.2	3.8
Uf	142.5	98.8	28.8	13.6	3.8

Size	Feed	Crmt	Silc	Ofi	Crmt	Silc	Ofo	Crmt	Silc	Uf	Crmt	Silc
0.710	0.5	0.0	0.0	0.0	0.0	0.0	0.0	0.0	0.0	0.9	0.0	0.0
0.500	0.1	0.0	0.0	0.0	0.0	0.0	0.0	0.0	0.0	0.1	0.0	0.0
0.355	0.2	0.0	0.0	0.1	0.0	0.0	0.0	0.0	0.0	0.3	0.0	0.0
0.250	0.9	0.0	0.0	0.4	0.0	0.0	0.1	0.0	0.0	1.4	0.0	0.0
0.180	4.1	19.1	27.7	2.4	36.2	10.0	0.3	0.0	0.0	6.5	15.0	32.1
0.125	11.0	25.2	19.5	7.8	28.6	18.8	1.9	38.2	9.6	16.6	27.0	17.5
0.090	21.2	26.5	16.3	18.7	21.5	23.8	6.9	38.0	9.9	29.2	32.4	11.3
0.063	17.8	27.9	15.7	18.3	19.6	25.0	14.3	33.6	13.7	19.4	33.3	9.0
0.045	10.9	25.8	17.5	12.4	13.5	18.3	13.4	24.7	21.0	9.2	31.5	11.5
0.032	5.9	24.4	19.8	6.6	20.3	24.1	10.3	24.7	20.9	3.5	28.3	15.0
0.000	27.4	23.8	18.3	33.4	19.9	25.0	52.7	24.1	21.5	12.8	27.4	15.1

Run3 Dcyc 600 Dovf 220 Divf 190 Lovf 675 Livf 750 Dspig 100 Press 62

Solids	Water	Cromite	Silica	SG
Feed	265.8	254.7	14.8	34.3	3.8
Ofi	83.1	139.7	18.3	28.8	3.8
Ofo	51.5	66.8	24.1	43.1	3.8
Uf	131.2	48.1	12.5	31.0	3.8

Size	Feed	Crmt	Silc	Ofi	Crmt	Silc	Ofo	Crmt	Silc	Uf	Crmt	Silc
0.710	0.2	0.0	0.0	0.0	0.0	0.0	0.0	0.0	0.0	0.5	0.0	0.0
0.500	0.1	0.0	0.0	0.0	0.0	0.0	0.0	0.0	0.0	0.1	0.0	0.0
0.355	0.2	0.0	0.0	0.0	0.0	0.0	0.0	0.0	0.0	0.4	0.0	0.0
0.250	0.9	0.0	0.0	0.0	0.0	0.0	0.0	0.0	0.0	1.7	0.0	0.0
0.180	3.4	9.7	34.2	0.3	2.8	43.2	0.4	8.7	43.7	6.6	29.2	17.9
0.125	8.3	14.8	29.4	2.0	2.5	44.5	2.3	7.0	45.0	14.7	15.3	28.9
0.090	16.7	20.8	23.8	6.8	7.3	39.6	8.0	10.7	41.0	26.4	10.3	32.8
0.063	18.6	14.0	52.4	14.6	14.6	59.3	16.6	22.0	78.3	22.0	8.1	25.4
0.045	11.7	27.8	16.3	12.5	21.2	23.9	15.5	27.5	22.4	9.7	11.3	32.1
0.032	6.9	27.3	16.9	10.7	21.5	23.4	10.5	26.7	23.4	3.1	15.8	28.1
0.000	33.0	24.3	20.2	53.1	20.1	24.0	46.8	26.4	24.2	14.9	15.0	29.0

University of Cape Town

Run4 Dcyc 600 Dovf 210 Divf 165 Lovf 675 Livf 925 Dspig 95 Press 158

	Solids	Water	Cromite	Silica	SG
Feed	283.4	375.7			3.8
Ofi	42.2	102.7			3.8
Ofo	87.3	191.3			3.8
Uf	153.9	81.8			3.8

Size	Feed	Crmt	Silc	Ofi	Crmt	Silc	Ofo	Crmt	Silc	Uf	Crmt	Silc
0.710	1.1			0.0			0.0			2.1		
0.500	0.2			0.0			0.0			0.4		
0.355	0.5			0.0			0.0			0.9		
0.250	1.5			0.0			0.0			2.8		
0.180	4.8			0.1			0.4			8.7		
0.125	12.0			1.4			3.2			19.9		
0.090	20.9			5.9			12.5			29.7		
0.063	22.7			15.5			26.0			22.8		
0.045	8.0			13.8			10.8			4.8		
0.032	2.4			5.2			2.5			1.6		
0.000	25.9			58.1			44.7			6.3		

Run5 Dcyc 600 Dovf 210 Divf 165 Lovf 675 Livf 825 Dspig 95 Press 145

	Solids	Water	Cromite	Silica	SG
Feed	261.0	345.9			3.8
Ofi	39.4	100.9			3.8
Ofo	88.3	175.7			3.8
Uf	133.3	69.3			3.8

Size	Feed	Crmt	Silc	Ofi	Crmt	Silc	Ofo	Crmt	Silc	Uf	Crmt	Silc
0.710	0.7			0.0			0.0			1.4		
0.500	0.2			0.0			0.0			0.4		
0.355	0.4			0.0			0.0			0.8		
0.250	1.3			0.2			0.1			2.5		
0.180	4.4			0.6			0.7			8.0		
0.125	11.2			2.6			4.2			18.4		
0.090	18.6			8.5			12.1			25.8		
0.063	21.3			17.9			21.8			22.0		
0.045	10.3			12.8			12.6			8.0		
0.032	3.1			4.2			4.1			2.2		
0.000	28.5			53.2			44.4			10.6		

Run6 Dcyc 600 Dovf 210 Divf 165 Lovf 675 Livf 875 Dspig 95 Press 88

Solids	Water	Cromite	Silica	SG
Feed 231.1	285.9	27.4	17.6	3.8
Ofi 35.1	121.1	19.3	31.3	3.8
Ofo 72.5	126.1	22.0	25.7	3.8
Uf 123.5	38.6	26.5	14.4	3.8

Size	Feed	Crmt	Silc	Ofi	Crmt	Silc	Ofo	Crmt	Silc	Uf	Crmt	Silc
0.710	0.2	0.0	0.0	0.0	0.0	0.0	0.0	0.0	0.0	0.3	0.0	0.0
0.500	0.1	0.0	0.0	0.0	0.0	0.0	0.0	0.0	0.0	0.2	0.0	0.0
0.355	0.3	2.3	18.3	0.0	0.0	0.0	0.0	0.0	0.0	0.6	25.1	16.1
0.250	1.0	14.3	35.8	0.0	0.0	0.0	0.1	0.0	0.0	1.8	36.0	2.9
0.180	3.1	24.5	23.6	0.1	0.0	0.0	0.3	0.0	0.0	5.6	14.2	28.1
0.125	9.0	30.9	15.2	0.1	0.0	0.0	2.3	22.7	25.4	15.5	17.4	26.1
0.090	21.3	30.4	15.9	1.1	2.4	52.5	12.2	5.0	45.2	32.4	25.8	16.0
0.063	22.3	26.6	13.2	9.5	5.1	49.1	22.6	15.9	33.4	25.8	32.6	6.7
0.045	8.9	30.6	15.4	8.0	11.4	41.6	12.4	21.7	26.4	7.2	32.7	6.9
0.032	2.8	29.3	17.4	3.1	16.9	34.8	3.8	27.6	19.2	2.1	30.2	9.9
0.000	31.0	25.7	21.2	78.1	22.2	27.7	46.3	29.2	17.4	8.6	28.8	11.6

University of Cape Town

Run7 Dcyc 600 Dovf 210 Divf 165 Lovf 675 Livf 775 Dspig 95 Press 81

	Solids	Water	Cromite	Silica	SG
Feed	328.0	301.8			3.8
Ofi	40.5	107.5			3.8
Ofo	113.2	150.0			3.8
Uf	174.3	44.2			3.8

Size	Feed	Crmt	Silc	Ofi	Crmt	Silc	Ofo	Crmt	Silc	Uf	Crmt	Silc
0.710	0.4			0.0			0.0			0.7		
0.500	0.3			0.0			0.0			0.6		
0.355	0.5			0.0			0.0			0.9		
0.250	1.4			0.1			0.3			2.5		
0.180	5.3			0.4			2.1			8.6		
0.125	13.8			2.3			7.2			20.8		
0.090	27.1			8.7			24.2			33.2		
0.063	18.8			17.4			22.7			16.6		
0.045	5.9			9.7			7.7			3.9		
0.032	1.8			3.3			2.2			1.2		
0.000	24.6			58.3			33.5			11.1		

Run8 Dcyc 600 Dovf 220 Divf 165 Lovf 675 Livf 775 Dspig 95 Press 68

	Solids	Water	Cromite	Silica	SG
Feed	270.1	248.2	30.0	18.2	3.8
Ofi	24.1	48.2	19.7	29.7	3.8
Ofo	100.4	131.2	25.2	25.2	3.8
Uf	145.6	68.8	34.9	15.1	3.8

Size	Feed	Crmt	Silc	Ofi	Crmt	Silc	Ofo	Crmt	Silc	Uf	Crmt	Silc
0.710	0.3	0.0	0.0	0.0	0.0	0.0	0.0	0.0	0.0	0.5	0.0	0.0
0.500	0.1	0.0	0.0	0.0	0.0	0.0	0.0	0.0	0.0	0.3	15.2	28.4
0.355	0.3	2.3	18.3	0.1	0.0	0.0	0.1	0.0	0.0	0.6	16.5	31.4
0.250	1.2	14.3	35.8	0.0	0.0	0.0	0.1	0.0	0.0	2.1	17.7	32.6
0.180	4.4	24.5	23.6	0.1	0.0	0.0	0.9	5.6	46.4	7.5	27.7	22.5
0.125	12.1	30.9	15.2	0.8	3.8	48.0	4.9	6.7	45.7	18.9	34.5	15.3
0.090	26.3	30.4	15.9	6.9	2.8	48.7	18.9	18.9	31.5	34.6	39.2	10.2
0.063	20.2	26.5	13.1	18.2	10.4	40.5	23.9	28.2	21.4	18.0	38.8	9.5
0.045	7.0	30.6	15.4	12.7	18.7	31.2	9.7	29.2	20.1	4.2	36.4	12.5
0.032	2.3	29.3	17.4	4.8	23.1	26.9	2.6	28.5	20.4	1.7	34.4	16.0
0.000	25.9	25.7	21.2	56.3	24.9	23.4	39.0	28.0	23.0	11.9	26.7	28.9

Run9 Dcyc 600 Dovf 230 Divf 165 Lovf 675 Livf 775 Dspig 95 Press 79

	Solids	Water	Cromite	Silica	SG
Feed	328.0	301.1	27.9	17.2	3.8
Ofi	46.1	96.0	23.3	17.2	3.8
Ofo	143.1	162.4	23.3	19.5	3.8
Uf	138.8	42.7	28.8	9.8	3.8

Size	Feed	Crmt	Silc	Ofi	Crmt	Silc	Ofo	Crmt	Silc	Uf	Crmt	Silc
0.710	0.3	4.1	4.9	0.0	0.0	0.0	0.0	0.0	0.0	0.7	29.5	34.9
0.500	0.1	4.5	2.4	0.0	0.0	0.0	0.0	0.0	0.0	0.1	32.4	17.0
0.355	0.1	4.3	3.7	0.1	0.0	0.0	0.0	0.0	0.0	0.3	30.9	26.6
0.250	0.6	6.5	24.0	0.0	0.0	0.0	0.1	4.3	46.3	1.2	33.0	26.8
0.180	3.1	9.4	41.2	0.0	3.4	48.0	0.6	7.1	43.0	6.8	34.7	14.8
0.125	9.4	10.6	39.0	0.1	3.0	48.4	3.5	10.0	39.9	18.7	35.0	8.0
0.090	25.7	13.1	25.8	1.2	6.3	44.8	19.2	13.1	13.1	40.5	33.2	7.9
0.063	18.8	22.6	23.3	9.4	16.6	33.4	23.2	28.3	18.1	17.5	23.1	8.5
0.045	6.9	24.4	20.6	7.3	22.7	26.6	9.9	28.2	17.7	3.7	17.8	12.1
0.032	2.1	21.4	16.8	2.8	14.8	15.5	2.7	27.3	19.9	1.1	23.1	11.2
0.000	33.0	22.5	21.3	79.1	24.8	23.4	40.9	25.0	21.6	9.5	7.7	14.2

University of Cape Town

Run10 Dcyc 600 Dovf 230 Divf 192 Lovf 675 Livf 1025 Dspig 95 Press 171

Solids	Water	Cromite	Silica	SG
Feed	463.0	419.8	21.7	22.8	3.8
Ofi	134.0	114.8	23.9	24.4	3.8
Ofo	91.7	168.9	24.7	24.0	3.8
Uf	237.3	136.2	32.0	11.9	3.8

Size	Feed	Crmt	Silc	Ofi	Crmt	Silc	Ofo	Crmt	Silc	Uf	Crmt	Silc
0.710	0.3	0.0	0.0	0.0	0.0	0.0	0.1	0.0	0.0	0.5	0.0	0.0
0.500	0.2	0.0	0.0	0.0	0.0	0.0	0.1	0.0	0.0	0.3	0.0	0.0
0.355	0.3	2.5	22.7	0.1	0.0	0.0	0.2	4.4	45.9	0.4	5.8	47.2
0.250	0.8	10.3	45.3	0.4	8.6	50.2	0.8	11.0	41.2	1.0	12.9	39.5
0.180	3.3	16.7	35.1	2.3	9.2	44.0	3.1	23.1	25.3	4.0	25.6	26.0
0.125	10.1	22.9	27.3	7.6	15.4	36.5	8.5	29.8	18.8	12.2	31.6	16.8
0.090	24.9	28.2	21.3	28.4	24.2	25.9	19.8	27.7	21.2	24.9	35.7	13.2
0.063	20.8	28.9	20.1	19.7	28.7	20.3	16.7	26.7	22.8	23.1	30.9	17.9
0.045	7.0	29.1	20.4	6.6	28.8	20.2	9.3	26.7	22.0	6.3	31.4	19.6
0.032	2.0	26.6	23.0	1.5	26.6	23.2	2.4	23.7	25.1	2.1	28.8	21.2
0.000	30.3	23.2	24.1	33.4	22.9	21.8	38.9	21.5	27.1	25.3	24.8	26.4

Run11 Dcyc 600 Dovf 220 Divf 192 Lovf 675 Livf 1025 Dspig 95 Press 163

Solids	Water	Cromite	Silica	SG
Feed	444.3	403.4	21.7	23.0	3.8
Ofi	136.3	187.7	21.4	23.2	3.8
Ofo	62.6	100.2	18.8	25.8	3.8
Uf	245.4	115.4	28.7	15.9	3.8

Size	Feed	Crmt	Silc	Ofi	Crmt	Silc	Ofo	Crmt	Silc	Uf	Crmt	Silc
0.710	0.3	0.0	0.0	0.0	0.0	0.0	0.0	0.0	0.0	0.5	0.0	0.0
0.500	0.1	0.0	0.0	0.0	0.0	0.0	0.0	0.0	0.0	0.2	0.0	0.0
0.355	0.2	2.1	11.7	0.0	0.0	0.0	0.0	0.0	0.0	0.4	6.7	38.2
0.250	0.8	3.1	10.4	0.2	0.0	0.0	0.0	0.0	0.0	1.3	10.1	34.0
0.180	3.1	9.0	29.2	1.3	5.1	39.1	0.1	0.0	0.0	5.0	20.1	24.9
0.125	10.5	9.8	28.6	4.7	8.3	36.5	0.8	22.0	23.0	16.2	6.8	17.0
0.090	27.6	20.2	24.6	18.7	17.1	28.0	6.3	5.0	39.1	37.9	32.8	11.6
0.063	18.3	26.8	18.1	21.4	26.0	19.1	18.0	14.1	30.6	16.6	34.0	10.7
0.045	6.3	26.4	18.5	8.5	25.7	19.1	11.9	20.1	24.9	3.8	30.6	14.4
0.032	2.4	25.2	19.5	3.7	24.4	20.1	3.6	21.5	23.6	1.3	28.3	16.4
0.000	30.4	23.0	22.3	41.6	21.7	22.8	59.3	21.5	23.5	16.8	26.2	21.0

Run12 Dcyc 600 Dovf 210 Divf 192 Lovf 675 Livf 1025 Dspig 95 Press 148

Solids	Water	Cromite	Silica	SG
Feed	416.5	378.4			3.8
Ofi	90.7	177.8			3.8
Ofo	26.2	58.9			3.8
Uf	299.7	141.7			3.8

Size	Feed	Crmt	Silc	Ofi	Crmt	Silc	Ofo	Crmt	Silc	Uf	Crmt	Silc
0.710	0.7			0.0			0.0			0.9		
0.500	0.1			0.0			0.0			0.2		
0.355	0.2			0.0			0.0			0.3		
0.250	0.5			0.0			0.0			0.7		
0.180	1.9			0.1			0.0			2.6		
0.125	6.6			1.4			0.1			8.7		
0.090	28.7			6.8			1.6			37.7		
0.063	20.7			19.1			9.1			22.2		
0.045	8.3			9.4			11.6			7.7		
0.032	2.0			3.0			4.8			1.5		
0.000	30.3			60.2			72.8			17.5		

University of Cape Town

Run13 Dcyc 600 Dovf 230 Divf 192 Lovf 675 Livf 975 Dspig 95 Press 116

	Solids	Water	Cromite	Silica	SG
Feed	284.0	259.0			3.8
Ofi	57.2	71.3			3.8
Ofo	75.1	115.9			3.8
Uf	151.7	71.8			3.8

Size	Feed	Crmt	Silc	Ofi	Crmt	Silc	Ofo	Crmt	Silc	Uf	Crmt	Silc
0.710	0.5			0.0			0.0			1.0		
0.500	0.2			0.1			0.0			0.3		
0.355	0.3			0.1			0.0			0.4		
0.250	0.5			0.1			0.1			0.9		
0.180	2.1			0.8			0.1			3.6		
0.125	9.8			3.9			1.1			16.2		
0.090	17.5			11.1			6.2			25.4		
0.063	17.8			18.3			14.2			19.5		
0.045	11.3			13.4			13.9			9.1		
0.032	4.7			6.4			6.9			2.9		
0.000	35.4			45.8			57.4			20.6		

Run14 Dcyc 600 Dovf 230 Divf 192 Lovf 675 Livf 925 Dspig 95 Press 120

	Solids	Water	Cromite	Silica	SG
Feed	297.0	313.9			3.8
Ofi	39.2	73.3			3.8
Ofo	83.7	145.6			3.8
Uf	174.1	95.0			3.8

Size	Feed	Crmt	Silc	Ofi	Crmt	Silc	Ofo	Crmt	Silc	Uf	Crmt	Silc
0.710	0.2			0.0			0.0			0.3		
0.500	0.3			0.0			0.0			0.6		
0.355	0.5			0.0			0.0			0.8		
0.250	0.9			0.1			0.0			1.6		
0.180	2.4			0.3			0.2			4.0		
0.125	11.5			2.0			1.9			18.2		
0.090	18.8			8.8			7.8			26.3		
0.063	20.3			17.4			18.5			21.8		
0.045	11.4			14.4			16.1			8.4		
0.032	2.5			4.8			3.5			1.5		
0.000	31.4			52.3			52.1			16.7		

Run15 Dcyc 600 Dovf 230 Divf 192 Lovf 675 Livf 775 Dspig 95 Press 68

	Solids	Water	Cromite	Silica	SG
Feed	316.0	258.9	21.4	21.8	3.8
Ofi	42.0	75.2	21.4	22.7	3.8
Ofo	97.1	124.6	23.3	20.8	3.8
Uf	176.9	59.0	32.2	11.9	3.8

Size	Feed	Crmt	Silc	Ofi	Crmt	Silc	Ofo	Crmt	Silc	Uf	Crmt	Silc
0.710	1.8	0.0	0.0	0.0	0.0	0.0	0.0	0.0	0.0	3.2	0.0	0.0
0.500	0.1	0.4	6.5	0.0	0.0	0.0	0.0	0.0	0.0	0.2	2.5	42.2
0.355	0.2	1.1	5.7	0.0	0.0	0.0	0.0	0.0	0.0	0.4	7.5	37.2
0.250	0.8	1.9	5.0	0.1	0.0	0.0	0.1	0.0	0.0	1.3	12.2	32.3
0.180	3.6	7.6	37.0	0.3	4.7	40.2	1.0	4.9	39.3	5.8	23.5	21.2
0.125	11.1	9.3	34.7	2.0	4.4	39.2	4.0	6.9	37.2	17.1	31.4	13.4
0.090	25.9	16.2	27.4	8.9	10.2	33.4	18.9	17.7	25.8	33.8	34.8	9.2
0.063	20.1	23.7	21.7	17.8	23.2	24.9	23.4	25.8	19.4	18.9	21.6	14.4
0.045	7.6	26.3	17.8	14.1	24.5	19.5	8.5	26.6	17.8	5.5	32.1	11.9
0.032	2.2	26.2	18.5	4.7	25.3	19.7	2.4	25.9	18.8	1.5	30.1	13.8
0.000	26.7	24.2	18.1	52.1	23.8	19.7	41.8	23.9	20.0	12.3	26.2	8.8

University of Cape Town

Run16 Dcyc 600 Dovf 220 Divf 177 Lovf 675 Livf 1025 Dspig 95 Press 126

Solids	Water	Cromite	Silica	SG
Feed	272.7	304.7	32.0	12.5	3.8
Ofi	36.2	63.6	22.1	22.3	3.8
Ofo	76.9	173.2	22.1	22.5	3.8
Uf	159.6	67.8	32.0	11.9	3.8

Size	Feed	Crmt	Silc	Ofi	Crmt	Silc	Ofo	Crmt	Silc	Uf	Crmt	Silc
0.710	0.8	0.0	0.0	0.0	0.0	0.0	0.0	0.0	0.0	1.3	0.0	0.0
0.500	0.1	0.2	5.7	0.0	0.0	0.0	0.0	0.0	0.0	0.2	1.8	42.6
0.355	0.2	1.8	4.1	0.0	0.0	0.0	0.0	0.0	0.0	0.4	13.6	30.5
0.250	0.8	2.0	3.9	0.1	0.0	0.0	0.1	0.0	0.0	1.2	14.9	29.2
0.180	3.8	7.3	24.2	0.6	7.8	36.2	0.1	0.0	0.0	6.3	20.8	22.8
0.125	13.7	8.6	35.8	3.1	5.6	38.9	1.5	5.6	38.9	21.9	28.0	15.8
0.090	20.6	13.6	31.0	10.7	11.4	33.4	9.3	8.8	35.8	28.4	33.5	10.0
0.063	19.6	22.6	22.0	23.7	23.5	23.6	23.1	21.6	24.5	17.0	20.6	9.3
0.045	8.7	25.6	19.1	10.4	24.6	20.1	8.0	23.9	21.1	8.7	33.7	10.6
0.032	2.6	25.4	18.8	3.0	24.5	19.7	2.5	24.3	20.3	2.6	31.8	12.1
0.000	29.1	24.2	20.5	48.6	23.8	20.8	55.5	24.0	21.0	11.9	26.2	18.3

Run17 Dcyc 600 Dovf 220 Divf 177 Lovf 675 Livf 975 Dspig 95 Press 116

Solids	Water	Cromite	Silica	SG
Feed	261.8	249.1			3.8
Ofi	47.5	67.0			3.8
Ofo	85.8	132.3			3.8
Uf	128.5	49.8			3.8

Size	Feed	Crmt	Silc	Ofi	Crmt	Silc	Ofo	Crmt	Silc	Uf	Crmt	Silc
0.710	0.1			0.0			0.0			0.1		
0.500	0.1			0.0			0.0			0.3		
0.355	0.2			0.1			0.0			0.3		
0.250	0.6			0.1			0.0			1.3		
0.180	3.2			0.6			0.5			6.0		
0.125	12.4			4.4			2.5			21.9		
0.090	18.1			10.2			8.6			27.4		
0.063	17.5			19.5			16.7			17.4		
0.045	12.0			14.8			15.7			8.5		
0.032	2.9			3.4			5.1			1.3		
0.000	32.9			47.0			51.0			15.6		

Run18 Dcyc 600 Dovf 230 Divf 177 Lovf 675 Livf 975 Dspig 95 Press 113

Solids	Water	Cromite	Silica	SG
Feed	265.3	249.0	22.8	26.7	3.8
Ofi	31.8	40.4	24.3	27.3	3.8
Ofo	90.1	145.5	20.0	26.4	3.8
Uf	143.3	63.1	31.2	15.4	3.8

Size	Feed	Crmt	Silc	Ofi	Crmt	Silc	Ofo	Crmt	Silc	Uf	Crmt	Silc
0.710	0.1	0.0	0.0	0.0	0.0	0.0	0.0	0.0	0.0	0.1	0.0	0.0
0.500	0.2	0.8	4.6	0.0	0.0	0.0	0.0	0.0	0.0	0.3	6.9	38.4
0.355	0.2	0.7	5.4	0.1	0.0	0.0	0.0	0.0	0.0	0.4	5.8	45.1
0.250	1.0	6.0	27.5	0.2	7.9	42.9	0.0	0.0	0.0	1.7	14.1	36.3
0.180	4.1	7.5	43.3	1.3	5.2	49.1	0.5	5.4	40.5	7.0	24.1	24.9
0.125	11.1	10.6	41.1	5.7	10.5	42.3	2.8	3.8	47.7	17.6	30.3	17.5
0.090	22.5	17.0	32.2	13.2	18.4	31.8	10.1	8.6	40.7	32.5	34.2	9.9
0.063	19.1	23.8	24.9	19.4	23.6	26.2	17.8	19.8	28.0	19.9	35.7	10.6
0.045	10.1	26.2	21.4	14.2	26.2	22.7	16.3	23.5	22.1	5.2	34.1	13.9
0.032	2.7	24.8	23.5	3.3	24.9	25.3	4.5	22.0	23.0	1.3	32.4	16.7
0.000	28.9	25.8	24.5	42.7	28.2	25.5	47.9	22.3	23.2	13.9	24.8	24.1

University of Cape Town

Run19 Dcyc 600 Dovf 210 Divf 177 Lovf 675 Livf 975 Dspig 95 Press 109

Solids	Water	Cromite	Silica	SG
Feed	248.2	220.3	23.0	21.5	3.8
Ofi	54.4	67.2	20.4	23.8	3.8
Ofo	68.2	98.7	19.6	24.7	3.8
Uf	125.6	54.5	27.7	18.0	3.8

Size	Feed	Crmt	Silc	Ofi	Crmt	Silc	Ofo	Crmt	Silc	Uf	Crmt	Silc
0.710	0.1	0.0	0.0	0.0	0.0	0.0	0.0	0.0	0.0	0.1	0.0	0.0
0.500	0.2	2.8	8.3	0.0	0.0	0.0	0.0	0.0	0.0	0.3	12.6	37.7
0.355	0.5	4.4	6.4	0.0	0.0	0.0	0.0	0.0	0.0	0.9	20.1	29.3
0.250	0.9	5.5	3.4	0.1	0.0	0.0	0.0	0.0	0.0	1.7	25.2	15.6
0.180	2.8	9.2	27.1	0.7	3.2	48.6	0.2	0.0	0.0	5.2	34.7	11.4
0.125	8.5	11.3	39.2	3.5	5.5	47.1	1.7	4.5	48.0	14.4	33.2	9.7
0.090	19.3	16.0	34.5	13.5	12.6	39.8	7.4	8.6	43.1	28.3	33.0	11.6
0.063	20.5	24.9	25.1	21.9	26.1	25.6	18.9	18.9	31.0	20.9	29.5	16.5
0.045	10.6	24.1	24.0	9.7	24.9	23.4	14.4	23.5	25.1	8.9	22.8	24.1
0.032	2.9	21.3	26.7	3.9	24.3	23.9	4.5	23.3	25.7	1.7	12.1	34.4
0.000	33.6	20.3	27.7	46.7	21.9	26.2	52.8	21.4	26.0	17.6	15.3	33.0

Run20 Dcyc 600 Dovf 230 Divf 177 Lovf 675 Livf 875 Dspig 95 Press 92

Solids	Water	Cromite	Silica	SG
Feed	309.0	325.5			3.8
Ofi	57.1	114.6			3.8
Ofo	117.2	151.0			3.8
Uf	134.7	59.9			3.8

Size	Feed	Crmt	Silc	Ofi	Crmt	Silc	Ofo	Crmt	Silc	Uf	Crmt	Silc
0.710	0.1			0.0			0.0			0.3		
0.500	0.2			0.0			0.0			0.4		
0.355	0.2			0.0			0.0			0.5		
0.250	0.5			0.0			0.0			1.1		
0.180	1.5			0.0			0.3			3.2		
0.125	5.6			1.0			2.2			10.5		
0.090	16.6			5.7			11.6			25.7		
0.063	18.9			13.9			17.3			22.5		
0.045	13.9			14.5			16.0			11.8		
0.032	2.9			3.6			3.9			1.7		
0.000	39.5			61.3			48.8			22.3		

Run21 Dcyc 600 Dovf 220 Divf 177 Lovf 675 Livf 875 Dspig 95 Press 86

Solids	Water	Cromite	Silica	SG
Feed	226.4	281.6			3.8
Ofi	24.2	80.1			3.8
Ofo	54.6	148.1			3.8
Uf	147.7	53.3			3.8

Size	Feed	Crmt	Silc	Ofi	Crmt	Silc	Ofo	Crmt	Silc	Uf	Crmt	Silc
0.710	0.1			0.0			0.0			0.2		
0.500	0.2			0.0			0.0			0.3		
0.355	0.6			0.1			0.0			0.8		
0.250	1.4			0.1			0.0			2.1		
0.180	4.5			0.6			0.3			6.7		
0.125	11.6			2.3			2.0			16.6		
0.090	23.0			4.7			6.9			31.9		
0.063	19.7			9.6			16.3			22.6		
0.045	9.8			14.1			15.5			7.0		
0.032	2.6			4.4			5.2			1.4		
0.000	26.4			64.2			53.7			10.2		

University of Cape Town

Run22 Dcyc 600 Dovf 220 Divf 177 Lovf 675 Livf 775 Dspig 95 Press 85

	Solids	Water	Cromite	Silica	SG
Feed	295.3	339.5			3.8
Ofi	44.6	109.7			3.8
Ofo	105.3	176.9			3.8
Uf	145.3	52.9			3.8

Size	Feed	Crmt	Silc	Ofi	Crmt	Silc	Ofo	Crmt	Silc	Uf	Crmt	Silc
0.710	0.1			0.0			0.0			0.3		
0.500	0.2			0.0			0.0			0.3		
0.355	0.2			0.0			0.0			0.5		
0.250	0.9			0.0			0.1			1.9		
0.180	3.0			0.1			0.5			5.6		
0.125	9.2			1.2			3.6			15.6		
0.090	20.6			6.6			11.3			31.5		
0.063	19.6			13.6			20.8			20.6		
0.045	10.6			12.0			13.8			7.8		
0.032	2.7			3.8			4.3			1.3		
0.000	32.9			62.7			45.6			14.5		

Run23 Dcyc 600 Dovf 210 Divf 150 Lovf 675 Livf 1025 Dspig 95 Press 145

	Solids	Water	Cromite	Silica	SG
Feed	345.5	380.5			3.8
Ofi	48.0	57.5			3.8
Ofo	129.6	246.6			3.8
Uf	167.9	76.3			3.8

Size	Feed	Crmt	Silc	Ofi	Crmt	Silc	Ofo	Crmt	Silc	Uf	Crmt	Silc
0.710	0.1			0.0			0.0			0.1		
0.500	0.2			0.0			0.0			0.3		
0.355	0.3			0.1			0.0			0.7		
0.250	1.0			0.4			0.1			1.9		
0.180	3.7			2.1			0.6			6.6		
0.125	10.6			7.2			3.0			17.4		
0.090	23.1			17.6			11.0			33.9		
0.063	19.0			21.5			19.7			17.7		
0.045	11.0			12.8			13.8			8.4		
0.032	2.8			2.8			4.0			1.9		
0.000	28.3			35.5			47.9			11.1		

Run24 Dcyc 600 Dovf 210 Divf 150 Lovf 675 Livf 925 Dspig 95 Press 148

	Solids	Water	Cromite	Silica	SG
Feed	338.1	452.3			3.8
Ofi	37.2	87.1			3.8
Ofo	125.7	281.5			3.8
Uf	175.3	83.7			3.8

Size	Feed	Crmt	Silc	Ofi	Crmt	Silc	Ofo	Crmt	Silc	Uf	Crmt	Silc
0.710	0.1			0.0			0.0			0.3		
0.500	0.2			0.0			0.0			0.3		
0.355	0.2			0.0			0.0			0.4		
0.250	0.7			0.0			0.0			1.3		
0.180	3.6			0.3			0.2			6.7		
0.125	13.7			2.6			2.1			24.4		
0.090	19.1			7.3			13.4			25.6		
0.063	16.6			12.6			15.0			18.5		
0.045	12.7			16.2			17.5			8.4		
0.032	2.8			4.5			3.7			1.8		
0.000	30.5			56.4			48.0			12.4		

University of Cape Town

Run25 Dcyc 600 Dovf 210 Divf 150 Lovf 675 Livf 825 Dspig 95 Press 103

	Solids	Water	Cromite	Silica	SG
Feed	324.3	357.5			3.8
Ofi	39.1	100.5			3.8
Ofo	111.4	200.5			3.8
Uf	173.8	56.5			3.8

Size	Feed	Crmt	Silc	Ofi	Crmt	Silc	Ofo	Crmt	Silc	Uf	Crmt	Silc
0.710	0.1			0.0			0.0			0.3		
0.500	0.3			0.0			0.0			0.5		
0.355	0.6			0.0			0.0			1.0		
0.250	1.1			0.0			0.1			2.0		
0.180	3.8			0.2			0.5			6.8		
0.125	9.7			1.7			3.0			15.8		
0.090	19.8			7.0			9.7			29.1		
0.063	19.7			12.6			18.6			21.9		
0.045	12.3			14.2			17.8			8.3		
0.032	3.4			5.5			5.2			1.8		
0.000	29.3			58.8			45.2			12.5		

Run26 Dcyc 600 Dovf 210 Divf 150 Lovf 675 Livf 825 Dspig 95 Press 126

	Solids	Water	Cromite	Silica	SG
Feed	317.8	424.4			3.8
Ofi	39.1	122.8			3.8
Ofo	119.1	245.5			3.8
Uf	159.7	56.1			3.8

Size	Feed	Crmt	Silc	Ofi	Crmt	Silc	Ofo	Crmt	Silc	Uf	Crmt	Silc
0.710	0.1			0.0			0.0			0.2		
0.500	0.1			0.0			0.0			0.3		
0.355	0.4			0.0			0.0			0.7		
0.250	0.9			0.0			0.1			1.8		
0.180	3.6			0.1			0.4			6.9		
0.125	11.3			1.5			2.6			20.2		
0.090	20.0			4.3			10.0			31.3		
0.063	18.9			9.6			21.9			18.9		
0.045	11.2			13.3			15.7			7.4		
0.032	2.4			5.3			3.3			1.1		
0.000	31.1			66.0			46.1			11.3		

Run27 Dcyc 600 Dovf 220 Divf 150 Lovf 675 Livf 825 Dspig 95 Press 156

	Solids	Water	Cromite	Silica	SG
Feed	331.1	564.7			3.8
Ofi	29.1	126.3			3.8
Ofo	120.6	347.2			3.8
Uf	181.4	91.2			3.8

Size	Feed	Crmt	Silc	Ofi	Crmt	Silc	Ofo	Crmt	Silc	Uf	Crmt	Silc
0.710	0.0			0.0			0.0			0.1		
0.500	0.1			0.0			0.0			0.1		
0.355	0.2			0.0			0.0			0.3		
0.250	0.6			0.0			0.0			1.0		
0.180	1.9			0.1			0.1			3.5		
0.125	7.2			0.3			0.7			12.6		
0.090	21.7			1.6			6.9			34.7		
0.063	19.2			4.7			13.9			25.0		
0.045	11.5			9.6			15.6			9.1		
0.032	2.9			6.2			4.5			1.3		
0.000	34.8			77.5			58.3			12.3		

University of Cape Town

Run28 Dcyc 600 Dovf 230 Divf 150 Lovf 675 Livf 825 Dspig 95 Press 119

	Solids	Water	Cromite	Silica	SG
Feed	353.1	389.7			3.8
Ofi	20.8	70.1			3.8
Ofo	108.4	238.6			3.8
Uf	223.9	80.9			3.8

Size	Feed	Crmt	Silc	Ofi	Crmt	Silc	Ofo	Crmt	Silc	Uf	Crmt	Silc
0.710	0.1			0.0			0.0			0.1		
0.500	0.1			0.0			0.0			0.1		
0.355	0.2			0.0			0.0			0.3		
0.250	0.8			0.0			0.0			1.3		
0.180	3.5			0.3			0.4			5.3		
0.125	11.2			1.2			2.3			16.4		
0.090	25.3			6.8			10.3			34.3		
0.063	20.1			13.6			17.9			21.8		
0.045	10.5			9.4			17.2			7.3		
0.032	2.6			3.4			3.5			2.1		
0.000	25.7			65.3			48.4			11.1		

Run29 Dcyc 600 Dovf 210 Divf 150 Lovf 675 Livf 775 Dspig 95 Press 85

	Solids	Water	Cromite	Silica	SG
Feed	251.0	336.0	25.0	21.0	3.8
Ofi	29.9	82.1	23.0	23.7	3.8
Ofo	96.3	202.7	14.3	37.3	3.8
Uf	124.9	51.1	30.9	16.2	3.8

Size	Feed	Crmt	Silc	Ofi	Crmt	Silc	Ofo	Crmt	Silc	Uf	Crmt	Silc
0.710	0.1	0.0	0.0	0.0	0.0	0.0	0.0	0.0	0.0	0.1	0.0	0.0
0.500	0.2	0.0	0.0	0.0	0.0	0.0	0.0	0.0	0.0	0.4	0.0	0.0
0.355	0.5	5.2	41.2	0.0	0.0	0.0	0.0	0.0	0.0	1.0	20.8	21.2
0.250	1.0	10.4	37.7	0.0	0.0	0.0	0.0	0.0	0.0	2.0	19.9	24.5
0.180	3.3	16.7	30.6	0.0	4.0	0.0	0.3	3.4	44.5	6.4	15.4	32.0
0.125	9.0	23.2	23.7	0.2	6.4	0.0	2.8	2.2	47.2	15.8	19.9	27.7
0.090	18.2	28.6	17.5	1.4	13.1	36.1	8.8	3.9	46.0	29.5	24.9	21.3
0.063	19.2	25.2	20.4	6.2	19.9	28.1	19.2	6.1	42.7	22.3	32.4	13.4
0.045	12.2	27.5	18.8	7.8	23.9	21.1	17.2	11.6	37.0	9.4	36.9	8.4
0.032	3.0	25.2	20.3	3.2	25.0	22.0	4.8	13.3	33.5	1.4	35.7	9.7
0.000	33.4	23.5	22.4	81.1	23.3	23.5	46.8	21.1	25.7	11.7	34.8	11.0

Run30 Dcyc 600 Dovf 230 Divf 209 Lovf 675 Livf 1025 Dspig 95 Press 150

	Solids	Water	Cromite	Silica	SG
Feed	276.6	303.2	23.6	22.5	3.8
Ofi	113.2	175.3	23.3	23.4	3.8
Ofo	27.4	75.3	20.1	27.3	3.8
Uf	136.0	52.5	30.8	15.9	3.8

Size	Feed	Crmt	Silc	Ofi	Crmt	Silc	Ofo	Crmt	Silc	Uf	Crmt	Silc
0.710	0.1	0.0	0.0	0.0	0.0	0.0	0.0	0.0	0.0	0.1	0.0	0.0
0.500	0.1	0.0	0.0	0.1	0.0	0.0	0.0	0.0	0.0	0.1	0.0	0.0
0.355	0.2	0.0	0.0	0.0	0.0	0.0	0.0	0.0	0.0	0.4	0.0	0.0
0.250	0.9	5.2	41.2	0.2	0.0	0.0	0.0	0.0	0.0	1.7	8.5	34.2
0.180	3.3	10.4	37.7	1.1	8.4	0.0	0.0	0.0	0.0	5.8	14.2	30.5
0.125	9.9	16.7	30.6	4.5	13.9	34.6	0.1	0.0	0.0	16.3	17.7	28.1
0.090	22.5	23.2	23.7	16.1	16.8	32.0	1.6	2.9	46.4	32.0	26.3	17.9
0.063	21.4	26.0	19.7	24.0	24.3	23.0	8.4	7.3	41.8	21.9	32.2	10.9
0.045	9.5	27.5	18.8	10.3	27.9	19.5	13.2	15.6	32.8	8.0	32.2	10.7
0.032	2.1	25.2	20.3	1.9	26.6	20.6	5.7	19.7	28.1	1.5	31.5	10.7
0.000	30.0	23.5	22.4	41.8	25.4	20.9	71.1	22.9	24.1	11.9	31.5	11.8

University of Cape Town

Run31 Dcyc 600 Dovf 230 Divf 209 Lovf 675 Livf 975 Dspig 95 Press 166

	Solids	Water	Cromite	Silica	SG
Feed	308.1	410.2			3.8
Ofi	140.5	250.4			3.8
Ofo	40.9	100.1			3.8
Uf	126.7	59.6			3.8

Size	Feed	Crmt	Silc	Ofi	Crmt	Silc	Ofo	Crmt	Silc	Uf	Crmt	Silc
0.710	0.1			0.0			0.0			0.2		
0.500	0.2			0.0			0.0			0.4		
0.355	0.2			0.0			0.0			0.6		
0.250	0.6			0.0			0.0			1.4		
0.180	2.1			0.1			0.0			4.9		
0.125	8.3			0.0			0.4			20.0		
0.090	13.6			2.8			3.7			28.8		
0.063	13.8			11.1			12.9			17.0		
0.045	13.8			16.1			16.9			10.3		
0.032	4.2			5.7			4.0			2.5		
0.000	43.2			64.2			62.1			13.9		

Run32 Dcyc 600 Dovf 230 Divf 209 Lovf 675 Livf 975 Dspig 95 Press 118

	Solids	Water	Cromite	Silica	SG
Feed	315.2	262.1	22.8	23.0	3.8
Ofi	68.4	111.5	22.5	24.1	3.8
Ofo	49.8	82.9	20.3	26.4	3.8
Uf	197.0	67.7	31.5	15.1	3.8

Size	Feed	Crmt	Silc	Ofi	Crmt	Silc	Ofo	Crmt	Silc	Uf	Crmt	Silc
0.710	0.1	0.0	0.0	0.0	0.0	0.0	0.0	0.0	0.0	0.1	0.0	0.0
0.500	0.1	0.0	0.0	0.1	0.0	0.0	0.0	0.0	0.0	0.2	0.0	0.0
0.355	0.4	2.9	5.7	0.1	0.0	0.0	0.0	0.0	0.0	0.5	13.5	26.5
0.250	1.0	3.5	6.8	0.1	0.0	0.0	0.0	0.0	0.0	1.5	15.9	31.2
0.180	3.3	8.6	32.4	0.9	8.0	40.9	0.0	0.0	0.0	4.9	16.3	31.2
0.125	10.1	11.3	27.9	4.6	8.8	38.7	0.1	0.0	0.0	14.6	26.8	17.1
0.090	21.8	17.6	29.6	14.2	16.4	31.0	1.6	2.1	46.8	29.5	32.7	13.2
0.063	20.0	24.1	22.7	17.6	24.3	22.5	8.4	5.2	44.0	23.7	37.6	7.6
0.045	12.1	26.6	20.0	18.0	26.5	20.1	14.5	15.6	32.3	9.5	34.9	10.8
0.032	3.3	26.6	20.3	3.2	25.7	21.4	7.4	19.2	28.3	2.2	34.6	11.1
0.000	27.9	25.7	20.6	41.0	23.9	22.6	68.1	23.7	22.3	13.2	32.1	13.7

Run33 Dcyc 600 Dovf 230 Divf 209 Lovf 675 Livf 925 Dspig 95 Press 124

	Solids	Water	Cromite	Silica	SG
Feed	332.7	392.8	23.8	18.5	3.8
Ofi	122.8	220.7	24.5	21.8	3.8
Ofo	43.0	93.4	20.3	24.6	3.8
Uf	166.9	78.7	32.4	14.3	3.8

Size	Feed	Crmt	Silc	Ofi	Crmt	Silc	Ofo	Crmt	Silc	Uf	Crmt	Silc
0.710	0.4	0.0	0.0	0.0	0.0	0.0	0.0	0.0	0.0	0.8	0.0	0.0
0.500	0.5	0.0	0.0	0.0	0.0	0.0	0.0	0.0	0.0	1.0	0.0	0.0
0.355	0.8	5.7	8.2	0.1	0.0	0.0	0.0	0.0	0.0	1.4	15.6	22.3
0.250	1.5	10.7	9.3	0.4	8.6	0.0	0.0	0.0	0.0	2.6	17.4	25.2
0.180	3.8	11.8	29.7	1.9	10.5	38.6	0.0	0.0	0.0	6.1	17.8	27.8
0.125	12.2	13.9	25.4	6.3	15.2	30.8	0.4	0.0	0.0	19.6	16.8	26.9
0.090	18.8	20.8	19.0	17.0	24.1	22.8	3.3	2.3	0.0	24.2	22.6	20.4
0.063	18.5	27.0	17.8	20.1	29.6	17.0	14.9	9.6	30.9	18.2	29.3	14.3
0.045	11.8	28.4	17.3	14.0	27.4	19.3	12.8	19.0	29.7	10.0	33.2	10.2
0.032	3.3	28.9	16.4	4.3	25.7	21.0	6.3	24.4	23.2	1.8	34.9	8.0
0.000	28.5	27.0	18.0	35.9	23.2	22.8	62.3	23.8	23.6	14.3	33.3	9.5

University of Cape Town

Run34 Dcyc 600 Dovf 230 Divf 209 Lovf 675 Livf 875 Dspig 95 Press 94

	Solids	Water	Cromite	Silica	SG
Feed	311.9	368.4			3.8
Ofi	96.5	179.1			3.8
Ofo	40.1	96.7			3.8
Uf	175.3	92.5			3.8

Size	Feed	Crmt	Silc	Ofi	Crmt	Silc	Ofo	Crmt	Silc	Uf	Crmt	Silc
0.710	0.1			0.0			0.0			0.2		
0.500	0.2			0.0			0.0			0.4		
0.355	0.6			0.0			0.0			1.0		
0.250	1.1			0.2			0.0			1.9		
0.180	3.6			1.0			0.1			5.8		
0.125	10.9			5.0			0.4			16.6		
0.090	21.4			13.4			4.6			29.6		
0.063	20.1			19.3			15.2			21.7		
0.045	10.6			13.9			15.3			7.6		
0.032	2.9			3.5			4.8			2.2		
0.000	28.5			43.6			59.6			13.0		

Run35 Dcyc 600 Dovf 220 Divf 198 Lovf 675 Livf 975 Dspig 95 Press 114

	Solids	Water	Cromite	Silica	SG
Feed	295.5	349.7			3.8
Ofi	78.5	136.9			3.8
Ofo	88.5	159.0			3.8
Uf	128.6	53.8			3.8

Size	Feed	Crmt	Silc	Ofi	Crmt	Silc	Ofo	Crmt	Silc	Uf	Crmt	Silc
0.710	0.1			0.0			0.0			0.3		
0.500	0.3			0.0			0.0			0.8		
0.355	0.4			0.0			0.0			0.9		
0.250	0.7			0.1			0.1			1.5		
0.180	3.1			0.6			0.5			6.4		
0.125	12.1			3.4			2.9			23.6		
0.090	18.5			10.8			10.5			28.7		
0.063	17.6			18.5			19.7			15.7		
0.045	12.1			15.3			15.2			8.0		
0.032	3.3			4.8			4.9			1.4		
0.000	31.8			46.5			46.2			12.9		

Run36 Dcyc 600 Dovf 220 Divf 198 Lovf 675 Livf 925 Dspig 95 Press 107

	Solids	Water	Cromite	Silica	SG
Feed	286.8	299.6	25.3	19.9	3.8
Ofi	67.6	111.5	23.7	20.6	3.8
Ofo	66.8	139.0	22.1	22.3	3.8
Uf	152.5	49.0	32.8	11.7	3.8

Size	Feed	Crmt	Silc	Ofi	Crmt	Silc	Ofo	Crmt	Silc	Uf	Crmt	Silc
0.710	0.1	0.0	0.0	0.0	0.0	0.0	0.0	0.0	0.0	0.1	0.0	0.0
0.500	0.1	2.5	7.9	0.0	0.0	0.0	0.0	0.0	0.0	0.2	10.7	33.6
0.355	0.3	3.5	6.9	0.1	0.0	0.0	0.0	0.0	0.0	0.5	14.9	29.4
0.250	1.0	3.8	6.6	0.1	0.0	0.0	0.0	0.0	0.0	1.8	16.2	28.2
0.180	3.7	8.5	25.2	1.2	5.6	38.1	0.2	0.0	0.0	6.4	23.4	20.9
0.125	10.9	13.5	30.9	6.3	9.5	34.9	1.5	4.5	39.8	17.1	31.4	12.9
0.090	21.3	20.8	23.6	13.8	19.9	24.5	7.0	7.3	37.0	30.9	36.1	8.1
0.063	17.9	26.3	18.0	19.6	25.0	19.3	16.0	18.1	26.3	18.0	37.3	7.0
0.045	10.9	29.2	15.1	12.6	28.1	16.3	14.8	25.9	18.4	8.5	34.9	9.4
0.032	3.4	27.0	17.6	4.1	25.3	19.5	5.6	25.3	19.0	2.1	32.4	11.8
0.000	30.3	27.4	19.4	42.2	28.8	20.1	54.9	25.0	19.2	14.3	26.4	18.0

University of Cape Town

Run37 Dcyc 600 Dovf 230 Divf 177 Lovf 675 Livf 925 Dspig 95 Press 113

	Solids	Water	Cromite	Silica	SG
Feed	272.4	357.4			3.8
Ofi	47.4	107.1			3.8
Ofo	91.9	190.2			3.8
Uf	133.1	60.1			3.8

Size	Feed	Crmt	Silc	Ofi	Crmt	Silc	Ofo	Crmt	Silc	Uf	Crmt	Silc
0.710	0.1			0.0			0.0			0.2		
0.500	0.3			0.0			0.0			0.5		
0.355	0.5			0.0			0.0			1.1		
0.250	1.1			0.1			0.0			2.1		
0.180	4.0			0.7			0.1			7.8		
0.125	13.1			5.5			0.3			24.5		
0.090	16.9			12.6			3.0			27.9		
0.063	15.8			19.2			11.9			17.3		
0.045	12.2			18.1			16.7			7.0		
0.032	2.8			3.8			4.2			1.6		
0.000	33.4			40.0			63.8			10.0		

Run38 Dcyc 600 Dovf 220 Divf 177 Lovf 675 Livf 875 Dspig 95 Press 115

	Solids	Water	Cromite	Silica	SG
Feed	299.3	392.6			3.8
Ofi	33.4	83.4			3.8
Ofo	85.7	238.9			3.8
Uf	180.2	70.3			3.8

Size	Feed	Crmt	Silc	Ofi	Crmt	Silc	Ofo	Crmt	Silc	Uf	Crmt	Silc
0.710	0.1			0.0			0.0			0.2		
0.500	0.2			0.0			0.0			0.4		
0.355	0.5			0.0			0.0			0.9		
0.250	1.0			0.0			0.0			1.7		
0.180	3.3			0.4			0.1			5.4		
0.125	9.8			2.3			1.5			15.2		
0.090	23.6			9.0			7.3			34.0		
0.063	19.0			17.1			16.8			20.4		
0.045	11.7			14.3			15.6			9.4		
0.032	2.6			4.4			4.9			1.2		
0.000	27.9			52.5			53.7			11.2		

Run39 Dcyc 600 Dovf 230 Divf 192 Lovf 675 Livf 1025 Dspig 95 Press 142

	Solids	Water	Cromite	Silica	SG
Feed	296.6	389.5			3.8
Ofi	50.4	93.5			3.8
Ofo	66.3	190.6			3.8
Uf	179.9	105.4			3.8

Size	Feed	Crmt	Silc	Ofi	Crmt	Silc	Ofo	Crmt	Silc	Uf	Crmt	Silc
0.710	0.1			0.0			0.0			0.1		
0.500	0.2			0.0			0.0			0.3		
0.355	0.3			0.0			0.0			0.5		
0.250	0.6			0.1			0.0			0.9		
0.180	2.5			0.5			0.1			4.0		
0.125	11.8			3.5			0.5			18.3		
0.090	19.5			11.1			3.8			27.6		
0.063	16.9			19.5			11.1			18.4		
0.045	12.5			15.2			15.1			10.8		
0.032	2.5			4.1			4.8			1.3		
0.000	33.1			46.0			64.5			17.9		

University of Cape Town

Run40 Dcyc 600 Dovf 220 Divf 192 Lovf 675 Livf 1025 Dspig 95 Press 120

Solids	Water	Cromite	Silica	SG
Feed	329.1	395.0	24.3	19.9	3.8
Ofi	124.8	195.7	23.5	21.1	3.8
Ofo	57.2	138.5	21.8	22.5	3.8
Uf	147.1	60.8	31.9	12.7	3.8

Size	Feed	Crmt	Silc	Ofi	Crmt	Silc	Ofo	Crmt	Silc	Uf	Crmt	Silc
0.710	0.1	7.5	9.4	0.0	0.0	0.0	0.0	0.0	0.0	0.3	19.7	24.9
0.500	0.2	7.1	9.6	0.0	0.0	0.0	0.0	0.0	0.0	0.4	18.7	25.4
0.355	0.3	6.0	10.9	0.0	0.0	0.0	0.0	0.0	0.0	0.7	15.7	28.8
0.250	0.9	6.8	10.1	0.1	0.0	0.0	0.0	0.0	0.0	1.8	18.0	26.5
0.180	3.3	13.6	24.1	1.0	8.5	35.8	0.1	5.3	0.0	6.4	23.5	21.3
0.125	11.8	16.9	27.4	5.0	9.9	34.1	0.6	7.7	36.9	22.0	29.3	15.2
0.090	19.6	19.1	25.5	14.9	6.7	37.9	6.5	16.1	28.4	28.7	35.1	9.5
0.063	19.1	25.4	19.0	21.7	14.4	29.8	11.2	27.0	17.5	20.1	37.6	7.0
0.045	10.5	28.2	16.5	12.9	22.9	21.9	16.7	28.4	16.4	6.1	34.5	10.3
0.032	2.7	28.0	16.7	3.7	23.6	20.9	4.6	27.7	16.8	1.1	33.3	11.7
0.000	31.4	25.9	18.6	40.6	26.2	18.4	60.2	24.9	19.6	12.4	26.1	18.2

Run41 Dcyc 600 Dovf 220 Divf 192 Lovf 675 Livf 1025 Dspig 100 Press 118

Solids	Water	Cromite	Silica	SG
Feed	294.4	310.7		3.8
Ofi	84.2	134.5		3.8
Ofo	64.9	118.0		3.8
Uf	145.3	58.2		3.8

Size	Feed	Crmt	Silc	Ofi	Crmt	Silc	Ofo	Crmt	Silc	Uf	Crmt	Silc
0.710	0.1			0.0			0.0			0.1		
0.500	0.1			0.0			0.0			0.2		
0.355	0.2			0.0			0.0			0.4		
0.250	0.6			0.1			0.0			1.2		
0.180	2.6			0.5			0.1			4.9		
0.125	8.3			3.3			0.6			14.6		
0.090	18.8			10.2			4.5			30.2		
0.063	16.9			17.1			11.9			18.9		
0.045	12.4			13.7			14.5			10.8		
0.032	3.6			4.5			6.3			1.8		
0.000	36.5			50.6			62.1			16.9		

Run42 Dcyc 600 Dovf 220 Divf 192 Lovf 675 Livf 1025 Dspig 105 Press 118

Solids	Water	Cromite	Silica	SG
Feed	263.7	370.0		3.8
Ofi	58.3	160.4		3.8
Ofo	39.7	133.6		3.8
Uf	165.7	76.0		3.8

Size	Feed	Crmt	Silc	Ofi	Crmt	Silc	Ofo	Crmt	Silc	Uf	Crmt	Silc
0.710	0.1			0.0			0.0			0.1		
0.500	0.1			0.0			0.0			0.2		
0.355	0.2			0.0			0.0			0.3		
0.250	0.7			0.0			0.0			1.1		
0.180	2.9			0.1			0.0			4.5		
0.125	9.1			1.3			0.1			13.9		
0.090	20.0			5.5			1.5			29.6		
0.063	19.6			14.1			7.0			24.5		
0.045	10.8			13.0			12.7			9.6		
0.032	4.2			8.0			7.1			2.1		
0.000	32.4			58.0			71.5			14.1		

University of Cape Town

Run43 Dcyc 600 Dovf 210 Divf 184 Lovf 675 Livf 775 Dspig 95 Press 84

	Solids	Water	Cromite	Silica	SG
Feed	309.4	348.8			3.8
Ofi	90.2	204.5			3.8
Ofo	62.6	88.5			3.8
Uf	156.7	55.7			3.8

Size	Feed	Crmt	Silc	Ofi	Crmt	Silc	Ofo	Crmt	Silc	Uf	Crmt	Silc
0.710	1.2			0.0			0.0			2.4		
0.500	0.2			0.0			0.0			0.4		
0.355	0.6			0.0			0.1			1.2		
0.250	2.8			0.1			1.1			5.1		
0.180	8.2			0.7			4.6			14.0		
0.125	14.3			3.2			9.0			22.8		
0.090	13.3			3.0			12.8			19.5		
0.063	16.2			16.1			17.5			15.8		
0.045	8.7			12.3			10.2			6.0		
0.032	7.0			12.4			10.9			2.2		
0.000	27.4			52.2			33.7			10.6		

Run44 Dcyc 600 Dovf 210 Divf 177 Lovf 675 Livf 825 Dspig 95 Press 82

	Solids	Water	Cromite	Silica	SG
Feed	301.8	292.5			3.8
Ofi	58.6	99.4			3.8
Ofo	102.8	136.7			3.8
Uf	140.4	56.4			3.8

Size	Feed	Crmt	Silc	Ofi	Crmt	Silc	Ofo	Crmt	Silc	Uf	Crmt	Silc
0.710	1.0			0.0			0.0			2.1		
0.500	0.2			0.0			0.0			0.4		
0.355	0.4			0.0			0.0			0.8		
0.250	1.3			0.0			0.4			2.6		
0.180	5.1			1.2			2.2			8.8		
0.125	13.4			4.0			6.5			22.3		
0.090	19.0			9.1			14.1			26.8		
0.063	18.2			15.6			21.7			16.7		
0.045	8.5			13.7			9.5			5.6		
0.032	5.6			8.4			8.6			2.2		
0.000	27.4			48.0			37.0			11.7		

Run45 Dcyc 600 Dovf 210 Divf 192 Lovf 675 Livf 775 Dspig 95 Press 85

	Solids	Water	Cromite	Silica	SG
Feed	314.2	323.5	25.2	18.9	3.8
Ofi	129.6	221.9	22.1	22.3	3.8
Ofo	18.6	54.6	23.7	20.6	3.8
Uf	165.9	47.0	32.8	11.7	3.8

Size	Feed	Crmt	Silc	Ofi	Crmt	Silc	Ofo	Crmt	Silc	Uf	Crmt	Silc
0.710	0.0	0.0	0.0	0.0	0.0	0.0	0.0	0.0	0.0	0.1	0.0	0.0
0.500	0.1	0.0	0.0	0.0	0.0	0.0	0.0	0.0	0.0	0.1	0.0	0.0
0.355	0.3	4.4	13.9	0.0	0.0	0.0	0.0	0.0	0.0	0.5	10.7	33.6
0.250	1.1	6.1	12.1	0.1	0.0	0.0	0.4	0.0	0.0	1.9	14.9	29.4
0.180	4.7	6.7	11.6	1.3	0.0	0.0	2.4	0.0	0.0	7.6	16.2	28.2
0.125	12.4	12.4	31.9	4.5	4.5	39.8	6.6	5.6	38.1	19.3	23.4	20.9
0.090	19.6	17.4	26.9	11.9	7.3	37.0	13.6	9.5	34.9	26.3	31.4	12.9
0.063	19.4	30.4	13.9	18.0	25.9	18.4	21.6	25.2	19.0	20.3	36.9	7.4
0.045	13.5	29.4	14.9	17.8	25.3	19.0	14.8	28.1	16.3	10.0	34.9	9.4
0.032	3.2	28.1	16.2	3.8	25.0	19.2	3.3	25.3	19.5	2.7	32.4	11.8
0.000	25.8	25.2	19.6	42.6	23.8	20.8	37.3	28.8	20.1	11.3	26.4	18.0

University of Cape Town

Run46 Dcyc 600 Dovf 220 Divf 198 Lovf 675 Livf 775 Dspig 95 Press 96

	Solids	Water	Cromite	Silica	SG
Feed	327.4	350.9			3.8
Ofi	120.6	225.5			3.8
Ofo	29.3	76.8			3.8
Uf	177.5	48.6			3.8

Size	Feed	Crmt	Silc	Ofi	Crmt	Silc	Ofo	Crmt	Silc	Uf	Crmt	Silc
0.710	0.0			0.0			0.0			0.0		
0.500	0.0			0.0			0.0			0.1		
0.355	0.2			0.0			0.0			0.3		
0.250	0.8			0.1			0.0			1.4		
0.180	3.9			0.3			0.3			6.9		
0.125	10.5			1.5			2.5			17.9		
0.090	18.4			5.2			8.2			29.2		
0.063	19.8			12.4			20.8			24.6		
0.045	13.2			15.3			16.6			11.3		
0.032	2.7			4.5			4.1			1.3		
0.000	30.5			60.8			47.6			7.0		

Run47 Dcyc 600 Dovf 220 Divf 198 Lovf 675 Livf 775 Dspig 95 Press 91

	Solids	Water	Cromite	Silica	SG
Feed	310.6	340.4			3.8
Ofi	112.4	210.2			3.8
Ofo	25.4	73.8			3.8
Uf	172.7	56.4			3.8

Size	Feed	Crmt	Silc	Ofi	Crmt	Silc	Ofo	Crmt	Silc	Uf	Crmt	Silc
0.710	0.0			0.0			0.0			0.1		
0.500	0.0			0.0			0.0			0.1		
0.355	0.2			0.0			0.0			0.3		
0.250	0.7			0.0			0.0			1.3		
0.180	3.5			0.3			0.7			6.0		
0.125	9.9			1.9			2.9			16.1		
0.090	18.7			6.1			8.2			28.4		
0.063	19.6			12.6			18.6			24.3		
0.045	14.7			19.2			16.4			11.6		
0.032	3.7			5.6			3.7			2.4		
0.000	29.0			54.4			49.5			9.5		

Run48 Dcyc 600 Dovf 220 Divf 198 Lovf 675 Livf 775 Dspig 95 Press 88

	Solids	Water	Cromite	Silica	SG
Feed	336.7	323.5			3.8
Ofi	148.7	281.9			3.8
Ofo	19.7	33.1			3.8
Uf	168.3	51.3			3.8

Size	Feed	Crmt	Silc	Ofi	Crmt	Silc	Ofo	Crmt	Silc	Uf	Crmt	Silc
0.710	0.1			0.0			0.0			0.1		
0.500	0.0			0.0			0.0			0.1		
0.355	0.1			0.0			0.0			0.2		
0.250	0.8			0.1			0.1			1.5		
0.180	4.1			0.1			0.7			8.0		
0.125	9.3			0.4			3.5			17.8		
0.090	15.8			2.7			12.1			27.8		
0.063	16.8			10.9			21.6			21.5		
0.045	11.9			13.3			16.1			10.2		
0.032	2.5			3.2			3.5			1.8		
0.000	38.6			69.3			42.4			11.1		

University of Cape Town

Run49 Dcyc 600 Dovf 210 Divf 177 Lovf 675 Livf 775 Dspig 95 Press 79

Solids	Water	Cromite	Silica	SG
Feed	330.9	306.5	23.1	22.2	3.8
Ofi	69.8	119.5	13.0	33.9	3.8
Ofo	84.9	135.4	20.7	25.9	3.8
Uf	176.3	51.6	27.8	13.9	3.8

Size	Feed	Crmt	Silc	Ofi	Crmt	Silc	Ofo	Crmt	Silc	Uf	Crmt	Silc
0.710	0.0	0.0	0.0	0.0	0.0	0.0	0.0	0.0	0.0	0.1	0.0	0.0
0.500	0.0	0.0	0.0	0.0	0.0	0.0	0.0	0.0	0.0	0.1	0.0	0.0
0.355	0.1	0.0	0.0	0.0	0.0	0.0	0.0	0.0	0.0	0.2	0.0	0.0
0.250	0.6	0.0	0.0	0.0	0.0	0.0	0.0	0.0	0.0	1.2	14.3	27.3
0.180	3.2	11.1	32.3	0.0	0.0	0.0	0.2	0.0	0.0	5.9	14.9	29.4
0.125	9.2	16.6	31.5	0.2	0.0	0.0	2.2	5.8	41.3	16.0	18.9	29.0
0.090	17.6	24.4	21.8	2.0	8.5	38.4	9.1	3.6	43.4	27.9	26.4	20.8
0.063	19.3	26.6	19.8	9.3	4.3	45.8	22.3	20.3	27.4	21.8	33.9	11.1
0.045	12.9	23.1	21.8	12.7	14.2	33.7	15.8	24.4	22.8	11.6	31.3	12.7
0.032	2.3	25.2	21.1	3.1	15.7	31.6	2.5	23.8	21.7	1.8	29.4	13.0
0.000	34.7	21.1	25.6	72.7	14.8	33.6	48.0	22.9	23.1	13.3	26.5	18.5

Run50 Dcyc 600 Dovf 210 Divf 177 Lovf 675 Livf 775 Dspig 95 Press 81

Solids	Water	Cromite	Silica	SG
Feed	321.8	314.2	18.0	28.3	3.8
Ofi	67.3	106.4	16.0	31.6	3.8
Ofo	78.9	156.0	20.6	27.6	3.8
Uf	175.6	51.8	29.3	11.5	3.8

Size	Feed	Crmt	Silc	Ofi	Crmt	Silc	Ofo	Crmt	Silc	Uf	Crmt	Silc
0.710	0.1	0.0	0.0	0.0	0.0	0.0	0.0	0.0	0.0	0.1	0.0	0.0
0.500	0.1	0.0	0.0	0.0	0.0	0.0	0.0	0.0	0.0	0.2	0.0	0.0
0.355	0.3	0.0	0.0	0.0	0.0	0.0	0.0	0.0	0.0	0.7	22.1	19.3
0.250	1.1	14.8	30.7	0.0	0.0	0.0	0.1	0.0	0.0	2.0	17.7	28.7
0.180	3.9	25.3	20.2	0.1	0.0	0.0	0.8	4.7	44.1	6.8	24.2	22.4
0.125	10.8	21.0	25.9	1.1	10.2	35.0	3.3	3.7	45.4	17.8	29.4	16.6
0.090	18.4	24.4	21.1	4.5	1.3	48.0	10.2	15.4	58.3	27.3	35.1	10.1
0.063	19.4	23.9	23.0	13.1	1.5	47.1	23.8	21.9	23.8	19.9	35.0	8.3
0.045	12.8	25.5	20.5	15.0	13.9	53.4	14.9	24.5	20.6	11.1	31.9	11.3
0.032	2.5	27.2	19.0	4.8	18.8	28.2	2.7	26.4	19.9	1.5	30.7	12.6
0.000	30.6	8.1	42.0	61.4	22.0	24.1	44.2	21.2	24.4	12.7	27.6	17.6

Run51 Dcyc 600 Dovf 220 Divf 184 Lovf 675 Livf 1025 Dspig 95 Press 138

Solids	Water	Cromite	Silica	SG
Feed	273.7	394.3			3.8
Ofi	73.3	141.5			3.8
Ofo	83.5	214.3			3.8
Uf	116.9	38.6			3.8

Size	Feed	Crmt	Silc	Ofi	Crmt	Silc	Ofo	Crmt	Silc	Uf	Crmt	Silc
0.710	0.3			0.0			0.0			0.7		
0.500	0.1			0.0			0.0			0.2		
0.355	0.3			0.0			0.0			0.6		
0.250	1.4			0.8			0.0			2.7		
0.180	4.8			3.6			0.0			9.1		
0.125	11.4			6.6			1.2			21.7		
0.090	17.2			8.2			6.6			30.4		
0.063	17.0			17.9			11.7			20.3		
0.045	10.8			14.4			16.3			4.6		
0.032	7.0			8.7			11.7			2.6		
0.000	29.7			39.8			52.5			7.1		

University of Cape Town

Run52 Dcyc 600 Dovf 210 Divf 184 Lovf 675 Livf 1025 Dspig 95 Press 122

	Solids	Water	Cromite	Silica	SG
Feed	295.3	329.2			3.8
Ofi	78.1	119.9			3.8
Ofo	94.8	191.3			3.8
Uf	122.5	39.1			3.8

Size	Feed	Crmt	Silc	Ofi	Crmt	Silc	Ofo	Crmt	Silc	Uf	Crmt	Silc
0.710	0.9			0.0			0.0			2.1		
0.500	0.1			0.0			0.0			0.3		
0.355	0.4			0.3			0.0			0.8		
0.250	1.9			2.1			0.0			3.1		
0.180	5.4			4.5			0.1			10.0		
0.125	12.4			7.0			3.5			22.8		
0.090	18.5			13.3			6.9			30.8		
0.063	15.3			19.4			12.3			15.1		
0.045	9.6			11.0			14.4			5.0		
0.032	5.5			8.4			8.4			1.4		
0.000	30.1			34.1			54.3			8.7		

Run53 Dcyc 600 Dovf 230 Divf 184 Lovf 675 Livf 1025 Dspig 95 Press 120

	Solids	Water	Cromite	Silica	SG
Feed	286.5	349.2			3.8
Ofi	83.6	114.6			3.8
Ofo	75.5	191.1			3.8
Uf	127.4	43.4			3.8

Size	Feed	Crmt	Silc	Ofi	Crmt	Silc	Ofo	Crmt	Silc	Uf	Crmt	Silc
0.710	0.6			0.0			0.0			1.4		
0.500	0.1			0.0			0.0			0.3		
0.355	0.5			0.3			0.0			0.9		
0.250	2.1			1.9			0.0			3.4		
0.180	6.3			5.9			0.0			10.4		
0.125	13.1			7.9			1.7			23.4		
0.090	18.6			16.5			10.0			25.1		
0.063	16.3			18.7			14.9			15.6		
0.045	10.5			12.2			17.1			5.6		
0.032	5.5			5.8			10.4			2.3		
0.000	26.3			30.9			45.9			11.7		

Run54 Dcyc 600 Dovf 230 Divf 192 Lovf 675 Livf 925 Dspig 95 Press 117

	Solids	Water	Cromite	Silica	SG
Feed	296.9	325.5	22.4	19.1	3.8
Ofi	38.8	73.6	22.9	24.6	3.8
Ofo	78.8	191.7	25.1	22.1	3.8
Uf	179.2	60.2	36.0	10.3	3.8

Size	Feed	Crmt	Silc	Ofi	Crmt	Silc	Ofo	Crmt	Silc	Uf	Crmt	Silc
0.710	0.2	0.0	0.0	0.0	0.0	0.0	0.0	0.0	0.0	0.3	0.0	0.0
0.500	0.4	2.5	2.0	0.0	0.0	0.0	0.0	0.0	0.0	0.7	18.9	15.2
0.355	0.6	3.3	2.6	0.2	0.0	0.0	0.0	0.0	0.0	0.9	24.9	19.7
0.250	0.8	3.4	2.6	0.1	0.0	0.0	0.0	0.0	0.0	1.3	26.1	19.9
0.180	3.0	8.4	39.5	0.6	5.4	42.6	0.3	6.5	41.6	4.8	26.6	20.7
0.125	11.7	8.6	40.6	3.6	3.7	45.9	2.7	7.4	42.1	17.4	33.5	12.9
0.090	19.0	13.8	35.6	11.9	8.1	41.8	9.8	14.6	34.9	24.6	38.4	8.0
0.063	21.4	22.8	24.9	19.8	18.9	29.2	17.4	23.2	24.4	23.6	40.1	6.6
0.045	11.9	28.8	18.3	16.5	26.3	21.1	16.1	28.9	18.0	9.2	40.5	5.9
0.032	3.0	28.7	18.5	4.8	26.3	20.9	6.5	28.6	18.7	1.1	39.8	7.2
0.000	27.9	29.1	17.7	42.7	29.3	17.7	47.3	27.4	19.3	16.1	31.9	14.9

University of Cape Town

Run55 Dcyc 600 Dovf 220 Divf 165 Lovf 675 Livf 1025 Dspig 90 Press 133

Solids	Water	Cromite	Silica	SG
Feed	316.1	383.8	20.4	27.1	3.8
Ofi	60.0	115.5	20.8	27.9	3.8
Ofo	111.9	229.2	23.8	24.9	3.8
Uf	144.2	39.1	33.1	12.6	3.8

Size	Feed	Crmt	Silc	Ofi	Crmt	Silc	Ofo	Crmt	Silc	Uf	Crmt	Silc
0.710	0.3	0.0	0.0	0.0	0.0	0.0	0.0	0.0	0.0	0.6	0.0	0.0
0.500	0.1	0.0	0.0	0.0	0.0	0.0	0.0	0.0	0.0	0.1	0.0	0.0
0.355	0.2	0.7	9.0	0.0	0.0	0.0	0.0	0.0	0.0	0.4	3.7	47.2
0.250	1.2	2.8	6.4	0.5	0.0	0.0	0.0	0.0	0.0	2.4	14.6	33.8
0.180	4.0	5.7	27.4	0.8	2.5	50.3	0.0	0.0	0.0	8.4	24.2	23.6
0.125	9.4	8.8	41.1	3.5	2.4	47.2	2.6	5.2	47.2	17.2	31.3	14.9
0.090	19.2	14.6	36.1	11.8	6.5	46.2	4.7	13.1	37.9	33.5	36.6	8.9
0.063	16.1	22.4	26.6	16.1	17.7	31.4	10.1	19.8	30.6	20.6	38.3	7.8
0.045	13.0	26.6	21.1	18.2	24.8	23.3	17.9	24.2	24.1	7.1	35.1	10.5
0.032	7.3	28.4	19.3	9.8	27.1	21.3	12.6	27.0	21.0	2.3	34.1	11.4
0.000	29.3	25.5	22.4	39.4	25.1	23.1	52.0	25.4	22.8	7.4	26.8	19.9

Run56 Dcyc 600 Dovf 220 Divf 165 Lovf 675 Livf 1025 Dspig 80 Press 113

Solids	Water	Cromite	Silica	SG
Feed	238.6	298.0	24.5	22.9	3.8
Ofi	43.5	80.5	24.8	23.6	3.8
Ofo	92.8	189.4	25.8	24.8	3.8
Uf	102.3	28.1	36.5	10.6	3.8

Size	Feed	Crmt	Silc	Ofi	Crmt	Silc	Ofo	Crmt	Silc	Uf	Crmt	Silc
0.710	0.1	0.0	0.0	0.0	0.0	0.0	0.0	0.0	0.0	0.2	0.0	0.0
0.500	0.1	0.0	0.0	0.0	0.0	0.0	0.0	0.0	0.0	0.1	0.0	0.0
0.355	0.3	1.2	7.5	0.0	0.0	0.0	0.0	0.0	0.0	0.6	6.4	41.3
0.250	1.5	2.7	6.2	0.0	0.0	0.0	0.0	0.0	0.0	3.6	14.6	34.0
0.180	4.4	6.7	24.6	1.5	2.9	50.9	0.0	0.0	0.0	9.6	29.6	15.5
0.125	10.0	16.0	37.6	4.5	13.1	40.3	3.6	7.2	46.6	18.2	41.6	11.9
0.090	20.1	25.4	24.1	11.9	25.2	24.4	7.6	18.6	32.4	35.0	40.0	5.8
0.063	15.8	28.5	19.4	17.7	26.2	21.2	13.2	25.8	23.6	17.3	39.5	6.3
0.045	11.5	27.8	20.3	16.5	26.4	21.9	14.4	26.1	23.1	6.9	34.7	10.4
0.032	5.8	27.8	20.5	8.4	27.1	22.2	9.0	26.0	22.7	1.9	33.5	11.9
0.000	30.4	26.4	22.2	39.5	25.0	22.4	52.1	28.1	23.2	6.7	26.1	19.6

Run57 Dcyc 600 Dovf 220 Divf 165 Lovf 675 Livf 1025 Dspig 95 Press 146

Solids	Water	Cromite	Silica	SG
Feed	339.9	383.5	22.8	24.8	3.8
Ofi	56.3	102.4	23.4	25.1	3.8
Ofo	113.1	234.0	24.6	24.3	3.8
Uf	170.5	47.2	34.1	10.7	3.8

Size	Feed	Crmt	Silc	Ofi	Crmt	Silc	Ofo	Crmt	Silc	Uf	Crmt	Silc
0.710	0.5	0.0	0.0	1.3	0.0	0.0	0.0	0.0	0.0	0.5	0.0	0.0
0.500	0.1	0.0	0.0	0.0	0.0	0.0	0.0	0.0	0.0	0.2	0.0	0.0
0.355	0.3	0.8	7.3	0.0	0.0	0.0	0.0	0.0	0.0	0.6	5.0	44.2
0.250	1.6	3.1	4.6	0.3	0.0	0.0	0.0	0.0	0.0	3.2	18.8	27.8
0.180	4.5	6.1	28.7	1.0	3.2	51.0	0.0	0.0	0.0	8.6	27.1	18.9
0.125	11.2	11.7	41.0	4.5	6.6	49.1	3.6	8.1	44.0	18.5	34.2	10.8
0.090	21.0	20.2	30.0	11.2	17.7	34.1	8.1	14.6	35.8	32.9	38.8	6.0
0.063	16.2	31.7	20.0	16.8	26.9	22.4	14.7	35.5	23.4	17.1	38.8	6.2
0.045	10.9	27.6	20.7	14.9	27.0	21.7	15.2	24.9	24.4	6.7	35.3	10.1
0.032	6.0	25.2	18.1	9.4	26.8	21.7	10.1	18.8	15.9	2.1	32.9	11.3
0.000	27.8	25.0	22.5	40.6	24.8	23.3	48.5	25.2	22.9	9.8	25.1	19.7

University of Cape Town

Run58 Dcyc 600 Dovf 220 Divf 165 Lovf 675 Livf 1025 Dspig 70 Press 162

Solids	Water	Cromite	Silica	SG
Feed	326.9	409.8	21.8	25.1	3.8
Ofi	60.4	140.2	23.2	25.5	3.8
Ofo	123.0	226.8	23.6	24.8	3.8
Uf	143.5	42.8	34.1	10.7	3.8

Size	Feed	Crmt	Silc	Ofi	Crmt	Silc	Ofo	Crmt	Silc	Uf	Crmt	Silc
0.710	0.3	0.0	0.0	0.0	0.0	0.0	0.0	0.0	0.0	0.7	0.0	0.0
0.500	0.1	0.0	0.0	0.0	0.0	0.0	0.0	0.0	0.0	0.2	0.0	0.0
0.355	0.3	0.8	8.4	0.0	0.0	0.0	0.0	0.0	0.0	0.6	4.3	45.5
0.250	1.3	3.2	5.7	0.0	0.0	0.0	0.0	0.0	0.0	3.0	17.2	30.9
0.180	4.5	5.2	26.1	1.0	2.3	49.4	0.0	0.0	0.0	9.7	22.7	24.1
0.125	10.3	9.8	42.1	4.3	2.5	52.3	2.4	6.7	45.4	19.6	33.6	11.5
0.090	19.2	18.9	31.3	10.8	13.5	38.8	6.7	14.8	35.8	33.4	40.0	4.7
0.063	16.4	25.3	22.9	17.7	24.0	25.3	13.7	20.5	28.3	18.3	38.2	6.4
0.045	11.4	28.1	19.6	16.2	27.8	20.2	15.2	25.2	23.8	6.1	34.8	9.4
0.032	6.3	28.5	19.6	9.0	27.1	20.8	10.5	27.1	22.6	1.6	34.5	10.6
0.000	29.9	25.4	21.6	41.0	25.3	21.8	51.6	25.1	22.3	6.8	25.8	19.6

Run59 Dcyc 600 Dovf 220 Divf 165 Lovf 675 Livf 1025 Dspig 90 Press 165

Solids	Water	Cromite	Silica	SG
Feed	295.1	429.7	20.8	26.6	3.8
Ofi	49.0	100.6	22.7	26.8	3.8
Ofo	109.1	290.4	22.6	26.2	3.8
Uf	136.9	38.6	32.6	12.2	3.8

Size	Feed	Crmt	Silc	Ofi	Crmt	Silc	Ofo	Crmt	Silc	Uf	Crmt	Silc
0.710	0.1	0.0	0.0	0.0	0.0	0.0	0.0	0.0	0.0	0.3	0.0	0.0
0.500	0.1	0.0	0.0	0.0	0.0	0.0	0.0	0.0	0.0	0.2	0.0	0.0
0.355	0.3	0.9	7.8	0.0	0.0	0.0	0.0	0.0	0.0	0.7	5.6	46.7
0.250	1.6	2.8	5.4	0.0	0.0	0.0	0.0	0.0	0.0	3.5	17.0	32.7
0.180	4.7	5.8	27.5	1.2	2.5	51.3	0.0	0.0	0.0	9.7	27.6	22.6
0.125	10.0	9.8	43.3	5.2	3.0	52.4	1.9	8.0	45.6	18.2	32.6	13.0
0.090	19.8	18.2	32.4	12.8	14.4	37.9	6.6	14.9	36.9	32.9	36.1	7.2
0.063	16.0	24.5	24.2	17.2	24.0	25.5	11.9	19.8	30.5	18.8	36.4	6.8
0.045	11.8	27.4	20.8	16.6	28.8	20.2	16.3	22.8	26.0	6.6	33.7	10.7
0.032	6.2	26.5	21.6	8.9	27.0	21.8	9.5	24.7	23.8	2.5	29.4	15.9
0.000	29.4	24.5	23.2	38.1	24.6	23.4	53.9	24.3	23.8	6.7	24.6	21.4

Run60 Dcyc 600 Dovf 210 Divf 165 Lovf 675 Livf 1025 Dspig 95 Press 181

Solids	Water	Cromite	Silica	SG
Feed	331.1	550.4	17.1	24.6	3.8
Ofi	54.9	120.7	17.6	25.0	3.8
Ofo	120.9	376.8	21.5	24.8	3.8
Uf	155.3	52.9	29.2	14.6	3.8

Size	Feed	Crmt	Silc	Ofi	Crmt	Silc	Ofo	Crmt	Silc	Uf	Crmt	Silc
0.710	0.3	0.0	0.0	0.0	0.0	0.0	0.0	0.0	0.0	0.6	0.0	0.0
0.500	0.1	0.0	0.0	0.0	0.0	0.0	0.0	0.0	0.0	0.1	0.0	0.0
0.355	0.2	0.7	8.0	0.0	0.0	0.0	0.0	0.0	0.0	0.5	4.1	48.3
0.250	1.3	2.2	6.1	0.2	0.0	0.0	0.0	0.0	0.0	2.6	13.1	36.5
0.180	4.5	3.3	5.7	2.0	0.0	0.0	0.0	0.0	0.0	8.8	19.6	34.6
0.125	9.9	7.2	20.9	7.8	1.7	4.8	1.7	5.3	42.9	17.0	26.8	17.9
0.090	19.5	11.7	37.9	12.5	4.4	46.4	6.7	12.1	38.9	32.0	31.0	11.8
0.063	17.2	18.7	27.9	13.8	13.6	34.4	11.7	17.9	29.1	22.7	34.7	7.3
0.045	12.4	24.2	22.0	16.4	22.6	23.8	16.7	22.2	25.3	7.6	32.9	9.6
0.032	6.6	26.0	19.6	10.1	25.2	20.6	10.7	24.5	22.1	2.2	31.6	11.1
0.000	28.1	23.5	21.4	37.2	23.4	21.8	52.5	23.1	22.0	5.9	24.4	19.2

University of Cape Town

Run61 Dcyc 600 Dovf 210 Divf 184 Lovf 675 Livf 775 Dspig 70 Press 79

Solids	Water	Cromite	Silica	SG
Feed	314.8	273.6	29.9	16.9	3.8
Ofi	101.6	151.0	33.5	11.9	3.8
Ofo	73.5	93.8	20.6	26.6	3.8
Uf	139.7	28.9	36.1	9.8	3.8

Size	Feed	Crmt	Silc	Ofi	Crmt	Silc	Ofo	Crmt	Silc	Uf	Crmt	Silc
0.710	0.1	0.0	0.0	0.0	0.0	0.0	0.0	0.0	0.0	0.2	0.0	0.0
0.500	0.1	0.0	0.0	0.0	0.0	0.0	0.0	0.0	0.0	0.2	3.2	46.4
0.355	0.4	6.9	43.7	0.0	0.0	0.0	0.0	0.0	0.0	0.9	8.1	41.0
0.250	1.9	20.7	27.1	0.0	0.0	0.0	0.5	0.0	0.0	4.1	18.8	28.9
0.180	5.5	27.8	19.8	0.8	14.9	33.9	2.8	25.2	22.1	10.3	30.6	16.2
0.125	13.4	31.7	13.9	4.1	26.3	19.6	7.2	27.7	18.5	23.3	38.5	6.3
0.090	22.0	35.9	12.2	10.2	33.6	12.3	15.0	29.8	13.8	34.2	40.3	5.2
0.063	14.2	31.2	13.2	9.8	37.2	7.3	20.8	28.1	17.6	13.9	39.8	6.3
0.045	10.7	28.0	17.5	16.7	37.3	6.6	13.6	26.1	19.6	4.9	34.1	11.6
0.032	5.6	27.4	19.2	9.9	34.8	10.7	7.1	24.7	21.8	1.7	31.4	14.4
0.000	26.3	25.5	22.2	48.5	32.0	13.8	33.1	6.6	43.8	6.4	26.4	20.7

Run62 Dcyc 600 Dovf 210 Divf 184 Lovf 675 Livf 775 Dspig 95 Press 81

Solids	Water	Cromite	Silica	SG
Feed	325.9	291.3	28.1	17.6	3.8
Ofi	84.3	144.4	19.9	28.2	3.8
Ofo	63.7	95.3	23.2	24.3	3.8
Uf	177.9	51.6	33.7	11.3	3.8

Size	Feed	Crmt	Silc	Ofi	Crmt	Silc	Ofo	Crmt	Silc	Uf	Crmt	Silc
0.710	0.2	0.0	0.0	0.0	0.0	0.0	0.0	0.0	0.0	0.3	0.0	0.0
0.500	0.1	0.0	0.0	0.0	0.0	0.0	0.0	0.0	0.0	0.2	0.0	0.0
0.355	0.3	7.7	41.1	0.0	0.0	0.0	0.0	0.0	0.0	0.6	6.7	43.9
0.250	1.7	14.5	33.5	0.0	0.0	0.0	0.0	0.0	0.0	3.0	15.0	33.5
0.180	4.6	25.5	22.0	0.0	0.0	0.0	1.0	5.5	44.8	8.0	26.3	19.4
0.125	12.2	28.1	18.3	0.6	2.3	46.5	5.2	8.0	42.9	20.3	33.8	12.2
0.090	22.0	32.3	12.8	3.4	0.9	51.1	12.0	14.2	34.4	34.5	37.3	7.2
0.063	16.3	30.3	13.7	12.7	5.3	45.0	18.3	26.0	22.3	17.4	37.4	6.5
0.045	10.4	28.6	17.5	13.0	17.4	31.4	16.4	28.8	18.8	7.0	35.1	10.6
0.032	6.0	26.5	19.5	11.0	22.9	24.1	9.6	26.6	19.6	2.3	32.4	13.6
0.000	26.3	25.1	21.7	59.4	24.2	23.1	37.5	23.9	22.6	6.6	27.0	19.0

Run63 Dcyc 600 Dovf 210 Divf 184 Lovf 675 Livf 775 Dspig 85 Press 83

Solids	Water	Cromite	Silica	SG
Feed	339.3	295.7	27.0	19.6	3.8
Ofi	99.7	152.2	20.3	27.6	3.8
Ofo	68.6	105.0	25.4	23.9	3.8
Uf	171.1	38.5	32.8	12.8	3.8

Size	Feed	Crmt	Silc	Ofi	Crmt	Silc	Ofo	Crmt	Silc	Uf	Crmt	Silc
0.710	0.2	0.0	0.0	0.0	0.0	0.0	0.0	0.0	0.0	0.5	0.0	0.0
0.500	0.1	0.0	0.0	0.0	0.0	0.0	0.0	0.0	0.0	0.2	27.9	18.1
0.355	0.4	8.8	40.0	0.0	0.0	0.0	0.0	0.0	0.0	0.7	25.1	21.7
0.250	1.6	19.5	30.9	0.0	0.0	0.0	0.0	0.0	0.0	3.2	7.8	41.3
0.180	4.6	22.7	26.4	0.0	0.0	0.0	1.0	4.9	46.6	8.7	21.6	25.9
0.125	11.3	14.1	34.4	0.7	1.4	50.5	4.8	6.9	44.4	20.2	29.8	16.6
0.090	20.2	25.5	21.3	4.0	1.1	50.5	11.9	14.2	34.9	33.0	35.5	9.7
0.063	15.7	31.5	15.0	9.4	5.0	46.8	17.0	36.6	22.3	18.8	39.8	5.4
0.045	10.5	34.6	11.9	12.8	16.2	31.9	16.7	28.1	18.5	6.6	38.5	6.3
0.032	6.4	32.0	13.9	11.8	22.3	25.4	9.0	27.5	19.4	2.2	35.9	10.7
0.000	29.1	28.1	17.5	61.4	24.4	22.6	39.7	25.1	21.6	6.0	33.3	12.0

University of Cape Town

Run64 Dcyc 600 Dovf 210 Divf 184 Lovf 675 Livf 775 Dspig 80 Press 83

Solids	Water	Cromite	Silica	SG
Feed	325.9	324.9	21.4	25.2	3.8
Ofi	110.3	199.0	29.2	17.7	3.8
Ofo	63.9	88.1	18.3	28.6	3.8
Uf	151.7	37.9	35.0	9.9	3.8

Size	Feed	Crmt	Silc	Ofi	Crmt	Silc	Ofo	Crmt	Silc	Uf	Crmt	Silc
0.710	0.3	0.0	0.0	0.0	0.0	0.0	0.0	0.0	0.0	0.6	0.0	0.0
0.500	0.1	0.0	0.0	0.0	0.0	0.0	0.0	0.0	0.0	0.1	0.0	0.0
0.355	0.3	0.0	0.0	0.0	0.0	0.0	0.0	0.0	0.0	0.7	18.3	30.0
0.250	1.7	31.2	13.6	0.0	0.0	0.0	0.3	0.0	0.0	3.5	22.7	24.5
0.180	4.7	31.6	14.2	0.5	0.0	0.0	2.4	23.5	23.6	8.7	33.0	12.4
0.125	12.7	30.4	15.4	3.0	16.8	30.8	7.2	28.3	15.3	21.9	38.6	7.8
0.090	21.4	27.6	17.8	8.6	23.4	22.2	14.6	27.7	17.3	33.6	38.1	6.0
0.063	16.5	27.0	20.8	14.4	27.7	19.1	19.7	28.3	17.6	16.7	35.4	9.8
0.045	10.9	23.2	22.6	15.6	25.8	19.0	15.5	24.5	20.1	5.5	31.6	13.5
0.032	5.9	4.3	43.3	10.6	50.7	6.8	7.4	2.3	47.7	1.8	31.9	13.6
0.000	25.6	10.1	37.9	47.3	28.2	17.8	32.9	6.5	43.5	6.8	27.2	19.9

Run65 Dcyc 600 Dovf 210 Divf 184 Lovf 675 Livf 775 Dspig 90 Press 92

Solids	Water	Cromite	Silica	SG
Feed	319.3	354.9	28.3	16.5	3.8
Ofi	98.9	189.8	20.6	26.0	3.8
Ofo	60.0	104.1	24.3	21.4	3.8
Uf	160.4	61.0	33.0	9.3	3.8

Size	Feed	Crmt	Silc	Ofi	Crmt	Silc	Ofo	Crmt	Silc	Uf	Crmt	Silc
0.710	0.5	0.0	0.0	0.0	0.0	0.0	0.0	0.0	0.0	1.0	0.0	0.0
0.500	0.1	0.0	0.0	0.0	0.0	0.0	0.0	0.0	0.0	0.2	6.2	38.0
0.355	0.4	8.9	38.5	0.0	0.0	0.0	0.0	0.0	0.0	0.7	12.8	35.0
0.250	1.6	18.0	28.2	0.0	0.0	0.0	0.0	0.0	0.0	3.3	18.6	27.8
0.180	5.1	28.0	17.9	0.0	0.0	0.0	1.9	6.1	43.8	9.4	34.8	7.4
0.125	13.0	32.7	12.8	2.2	2.1	50.0	6.0	11.1	39.2	22.2	34.9	8.1
0.090	20.1	31.8	12.9	6.8	4.3	47.1	14.3	21.7	24.2	30.4	36.0	6.7
0.063	15.3	30.7	14.4	10.8	13.1	36.0	18.9	28.3	16.6	16.8	36.3	6.7
0.045	10.0	28.0	17.1	14.0	21.6	26.1	15.1	27.9	17.4	5.6	33.0	10.4
0.032	6.3	26.5	17.8	10.9	23.8	22.1	8.3	27.1	19.1	2.8	31.1	14.8
0.000	27.6	24.1	20.4	55.3	23.9	21.2	35.6	24.2	20.7	7.7	25.6	19.2

Run66 Dcyc 600 Dovf 220 Divf 192 Lovf 675 Livf 775 Dspig 70 Press 83

Solids	Water	Cromite	Silica	SG
Feed	298.0	322.2	27.3	19.0	3.8
Ofi	87.8	158.2	20.1	27.6	3.8
Ofo	82.6	128.9	21.6	23.3	3.8
Uf	127.5	35.2	34.6	10.4	3.8

Size	Feed	Crmt	Silc	Ofi	Crmt	Silc	Ofo	Crmt	Silc	Uf	Crmt	Silc
0.710	0.2	0.0	0.0	0.0	0.0	0.0	0.0	0.0	0.0	0.5	0.0	0.0
0.500	0.1	0.0	0.0	0.0	0.0	0.0	0.0	0.0	0.0	0.1	0.0	0.0
0.355	0.2	4.8	46.0	0.0	0.0	0.0	0.0	0.0	0.0	0.5	5.8	42.2
0.250	1.4	12.7	38.1	0.0	0.0	0.0	0.0	0.0	0.0	3.2	15.7	31.4
0.180	4.6	21.5	26.3	0.0	0.0	0.0	1.6	4.5	47.0	9.6	27.6	18.3
0.125	10.2	28.2	18.3	0.5	3.2	48.5	5.8	8.6	45.9	19.7	34.2	11.6
0.090	19.1	30.7	14.4	2.4	2.9	49.9	12.2	16.8	32.6	35.0	39.9	5.0
0.063	14.1	31.2	15.1	7.0	5.3	46.7	17.4	25.4	22.5	16.8	38.9	6.0
0.045	11.4	28.3	18.2	12.4	14.2	34.3	18.9	27.9	19.0	5.8	35.3	9.4
0.032	6.3	26.2	19.7	11.4	22.3	27.7	8.1	27.2	20.1	1.6	31.4	13.9
0.000	32.6	24.6	22.7	66.4	23.1	23.4	35.9	19.8	18.9	7.1	25.3	20.2

University of Cape Town

Run67 Dcyc 600 Dovf 220 Divf 192 Lovf 675 Livf 775 Dspig 95 Press 88

Solids	Water	Cromite	Silica	SG
Feed	322.2	335.1	18.3	24.2	3.8
Ofi	99.1	208.5	16.1	29.9	3.8
Ofo	46.2	75.7	21.6	25.1	3.8
Uf	177.0	50.9	34.4	12.4	3.8

Size	Feed	Crmt	Silc	Ofi	Crmt	Silc	Ofo	Crmt	Silc	Uf	Crmt	Silc
0.710	0.2	0.0	0.0	0.0	0.0	0.0	0.0	0.0	0.0	0.3	0.0	0.0
0.500	0.1	0.0	0.0	0.0	0.0	0.0	0.0	0.0	0.0	0.1	0.0	0.0
0.355	0.3	1.3	14.0	0.0	0.0	0.0	0.0	0.0	0.0	0.6	4.3	45.4
0.250	1.9	5.3	9.5	0.0	0.0	0.0	0.2	0.0	0.0	3.4	17.1	30.8
0.180	5.3	8.7	12.7	0.3	0.0	0.0	0.9	5.6	46.3	9.3	25.5	19.8
0.125	10.9	10.3	11.3	1.7	0.0	0.0	3.6	4.1	47.1	18.0	31.5	14.6
0.090	21.7	17.2	29.7	6.4	8.0	39.2	10.8	11.6	39.7	33.1	36.2	8.2
0.063	15.6	20.6	30.5	9.2	6.6	44.0	15.6	19.4	26.0	19.1	46.1	8.4
0.045	10.8	18.0	30.7	14.1	7.8	44.8	18.5	22.2	19.4	6.9	34.2	10.7
0.032	5.6	20.2	26.2	9.6	11.6	34.7	10.0	28.5	19.6	2.2	31.7	14.2
0.000	27.8	23.5	21.8	58.7	21.8	23.2	40.4	25.1	22.5	7.1	25.9	18.8

Run68 Dcyc 600 Dovf 220 Divf 192 Lovf 675 Livf 775 Dspig 85 Press 85

Solids	Water	Cromite	Silica	SG
Feed	356.3	315.9	18.1	28.1	3.8
Ofi	94.3	172.2	17.5	31.2	3.8
Ofo	58.7	92.2	23.2	25.7	3.8
Uf	203.3	51.5	35.3	10.4	3.8

Size	Feed	Crmt	Silc	Ofi	Crmt	Silc	Ofo	Crmt	Silc	Uf	Crmt	Silc
0.710	0.2	0.0	0.0	0.0	0.0	0.0	0.0	0.0	0.0	0.4	0.0	0.0
0.500	0.1	0.0	0.0	0.0	0.0	0.0	0.0	0.0	0.0	0.1	0.0	0.0
0.355	0.3	46.0	6.6	0.0	0.0	0.0	0.0	0.0	0.0	0.6	5.8	42.8
0.250	1.8	31.4	16.6	0.0	0.0	0.0	0.1	0.0	0.0	3.1	16.1	32.2
0.180	5.8	26.8	21.4	0.0	0.0	0.0	1.2	5.7	45.5	9.8	28.2	18.7
0.125	12.1	18.4	28.3	1.1	0.0	0.0	4.8	7.6	44.0	19.3	34.6	11.7
0.090	22.0	12.4	32.9	3.6	6.3	45.0	11.9	14.1	36.9	33.5	40.1	5.1
0.063	16.0	15.0	31.8	9.7	4.4	47.4	15.9	23.0	26.1	18.9	39.6	6.1
0.045	10.6	18.4	27.7	17.8	8.7	42.2	17.5	27.9	20.7	5.3	36.2	9.4
0.032	5.4	20.9	25.6	9.2	15.7	34.4	10.4	28.1	20.6	2.3	31.4	14.0
0.000	25.7	21.0	25.3	58.6	23.7	24.4	38.3	25.4	22.9	6.8	25.8	20.6

Run69 Dcyc 600 Dovf 220 Divf 192 Lovf 675 Livf 775 Dspig 80 Press 74

Solids	Water	Cromite	Silica	SG
Feed	297.1	295.7	21.8	24.9	3.8
Ofi	71.6	125.9	18.8	29.8	3.8
Ofo	79.4	126.6	22.5	25.9	3.8
Uf	146.1	43.1	34.4	12.4	3.8

Size	Feed	Crmt	Silc	Ofi	Crmt	Silc	Ofo	Crmt	Silc	Uf	Crmt	Silc
0.710	0.6	0.0	0.0	0.0	0.0	0.0	0.0	0.0	0.0	1.2	0.0	0.0
0.500	0.1	0.0	0.0	0.0	0.0	0.0	0.0	0.0	0.0	0.2	0.0	0.0
0.355	0.3	44.9	4.4	0.0	0.0	0.0	0.0	0.0	0.0	0.6	4.3	45.6
0.250	1.4	39.2	10.5	0.0	0.0	0.0	0.0	0.0	0.0	2.8	17.1	30.7
0.180	4.2	38.5	19.5	0.0	0.0	0.0	1.2	4.8	49.0	7.9	25.7	19.8
0.125	9.0	24.6	23.5	0.9	1.3	48.6	5.3	5.2	42.5	15.1	31.6	14.6
0.090	18.9	19.2	27.0	5.2	1.0	51.0	11.2	14.1	42.0	29.9	36.3	8.2
0.063	17.4	15.8	30.4	10.7	5.0	43.8	16.2	27.7	20.3	21.4	46.9	8.5
0.045	12.5	20.8	26.1	13.1	18.5	31.7	19.0	22.7	20.2	8.6	34.1	10.7
0.032	6.2	21.4	25.2	12.0	22.0	23.9	7.8	22.9	24.4	2.6	32.2	14.4
0.000	29.3	24.3	22.3	58.2	22.6	25.9	39.3	25.5	23.6	9.7	26.0	18.8

University of Cape Town

Run70 Dcyc 600 Dovf 220 Divf 192 Lovf 675 Livf 775 Dspig 90 Press 85

Solids	Water	Cromite	Silica	SG
Feed	319.3	316.8	28.9	17.6	3.8
Ofi	83.5	149.0	20.8	28.7	3.8
Ofo	68.8	116.3	23.8	24.4	3.8
Uf	166.9	51.5	34.8	10.6	3.8

Size	Feed	Crmt	Silc	Ofi	Crmt	Silc	Ofo	Crmt	Silc	Uf	Crmt	Silc
0.710	0.5	0.0	0.0	0.0	0.0	0.0	0.0	0.0	0.0	0.9	0.0	0.0
0.500	0.1	0.0	0.0	0.0	0.0	0.0	0.0	0.0	0.0	0.2	0.0	0.0
0.355	0.4	7.5	41.8	0.0	0.0	0.0	0.0	0.0	0.0	0.8	5.3	45.0
0.250	1.7	14.1	34.6	0.0	0.0	0.0	0.0	0.0	0.0	3.2	18.9	27.9
0.180	5.6	23.5	23.5	0.0	0.0	0.0	1.5	5.1	45.9	10.1	27.8	19.3
0.125	12.3	32.2	14.2	1.3	1.3	50.3	5.3	7.1	44.5	20.6	34.4	10.8
0.090	21.3	31.4	15.2	5.3	1.1	52.6	13.8	15.9	35.0	32.5	39.6	6.2
0.063	15.9	30.4	15.6	11.1	6.5	46.2	16.1	25.7	22.3	18.3	39.4	6.3
0.045	11.6	30.8	16.3	15.9	20.1	29.7	18.1	29.2	18.1	6.8	35.3	10.2
0.032	5.5	31.8	14.5	10.4	25.7	28.3	8.2	27.8	20.3	1.8	33.3	11.2
0.000	25.1	25.6	21.1	56.0	25.1	22.4	36.9	25.4	21.6	4.7	25.4	20.0

Run71 Dcyc 600 Dovf 220 Divf 184 Lovf 675 Livf 775 Dspig 85 Press 80

Solids	Water	Cromite	Silica	SG
Feed	308.2	307.0			3.8
Ofi	56.8	104.1			3.8
Ofo	101.8	158.2			3.8
Uf	149.6	44.7			3.8

Size	Feed	Crmt	Silc	Ofi	Crmt	Silc	Ofo	Crmt	Silc	Uf	Crmt	Silc
0.710	0.1			0.0			0.0			0.2		
0.500	0.1			0.0			0.0			0.1		
0.355	0.4			0.0			0.1			0.8		
0.250	1.9			0.1			1.1			3.1		
0.180	5.7			0.6			4.5			8.4		
0.125	13.4			3.6			8.6			20.5		
0.090	19.5			8.8			12.6			28.2		
0.063	18.6			18.8			17.3			19.3		
0.045	8.4			10.7			10.8			5.9		
0.032	7.1			11.8			10.5			3.0		
0.000	24.9			45.7			34.5			10.4		

Run72 Dcyc 600 Dovf 220 Divf 184 Lovf 675 Livf 775 Dspig 80 Press 96

Solids	Water	Cromite	Silica	SG
Feed	303.3	402.5			3.8
Ofi	71.6	185.9			3.8
Ofo	79.3	164.3			3.8
Uf	152.4	52.3			3.8

Size	Feed	Crmt	Silc	Ofi	Crmt	Silc	Ofo	Crmt	Silc	Uf	Crmt	Silc
0.710	0.1			0.0			0.0			0.3		
0.500	0.1			0.0			0.0			0.2		
0.355	0.3			0.0			0.0			0.6		
0.250	1.4			0.1			0.1			2.7		
0.180	5.4			0.4			1.2			10.0		
0.125	13.3			2.5			4.8			22.8		
0.090	20.2			7.0			14.7			29.3		
0.063	18.2			17.7			19.6			17.7		
0.045	8.1			9.2			12.4			5.3		
0.032	6.8			12.9			11.2			1.7		
0.000	26.1			50.3			36.0			9.5		

University of Cape Town

Run73 Dcyc 600 Dovf 220 Divf 184 Lovf 675 Livf 775 Dspig 70 Press 95

	Solids	Water	Cromite	Silica	SG
Feed	317.9	405.3			3.8
Ofi	96.2	177.1			3.8
Ofo	84.4	181.7			3.8
Uf	137.4	46.4			3.8

Size	Feed	Crmt	Silc	Ofi	Crmt	Silc	Ofo	Crmt	Silc	Uf	Crmt	Silc
0.710	0.1			0.0			0.0			0.1		
0.500	0.1			0.0			0.0			0.1		
0.355	0.2			0.0			0.0			0.5		
0.250	1.4			0.1			1.1			2.7		
0.180	5.1			0.7			3.7			9.1		
0.125	13.5			3.6			9.2			23.1		
0.090	18.8			9.2			15.3			27.8		
0.063	15.4			19.2			15.1			13.0		
0.045	9.0			11.1			10.4			6.7		
0.032	8.4			9.8			9.8			6.5		
0.000	28.0			46.5			35.3			10.6		

Run74 Dcyc 600 Dovf 220 Divf 184 Lovf 675 Livf 775 Dspig 90 Press 73

	Solids	Water	Cromite	Silica	SG
Feed	271.2	268.1			3.8
Ofi	73.7	145.0			3.8
Ofo	54.0	81.7			3.8
Uf	143.5	41.4			3.8

Size	Feed	Crmt	Silc	Ofi	Crmt	Silc	Ofo	Crmt	Silc	Uf	Crmt	Silc
0.710	0.0			0.0			0.0			0.0		
0.500	0.2			0.0			0.0			0.3		
0.355	0.5			0.0			0.0			1.0		
0.250	1.1			0.0			0.5			1.9		
0.180	4.9			0.0			4.1			7.8		
0.125	12.8			3.1			6.8			20.1		
0.090	16.6			6.1			12.1			23.7		
0.063	18.2			14.2			14.5			21.6		
0.045	9.4			12.8			12.1			6.6		
0.032	5.5			9.1			8.5			2.6		
0.000	30.8			54.6			41.4			14.5		

Run75 Dcyc 600 Dovf 220 Divf 184 Lovf 675 Livf 775 Dspig 95 Press 77

	Solids	Water	Cromite	Silica	SG
Feed	299.7	299.8			3.8
Ofi	53.3	110.2			3.8
Ofo	92.6	148.7			3.8
Uf	153.9	40.9			3.8

Size	Feed	Crmt	Silc	Ofi	Crmt	Silc	Ofo	Crmt	Silc	Uf	Crmt	Silc
0.710	0.1			0.0			0.0			0.1		
0.500	0.0			0.0			0.0			0.1		
0.355	0.2			0.0			0.0			0.3		
0.250	1.3			0.0			0.0			2.5		
0.180	5.0			0.0			3.3			7.6		
0.125	11.9			2.1			6.5			18.5		
0.090	18.6			4.5			9.9			28.8		
0.063	18.2			13.9			14.1			22.2		
0.045	8.9			11.2			12.0			6.3		
0.032	6.8			11.6			9.7			3.4		
0.000	29.0			56.6			44.5			10.1		

University of Cape Town

Run76 Dcyc 600 Dovf 220 Divf 177 Lovf 675 Livf 975 Dspig 95 Press 85

	Solids	Water	Cromite	Silica	SG
Feed	306.8	325.8			3.8
Ofi	50.2	70.9			3.8
Ofo	101.4	196.8			3.8
Uf	155.2	57.0			3.8

Size	Feed	Crmt	Silc	Ofi	Crmt	Silc	Ofo	Crmt	Silc	Uf	Crmt	Silc
0.710	0.1			0.0			0.0			0.2		
0.500	0.3			0.1			0.0			0.5		
0.355	0.3			0.1			0.0			0.6		
0.250	1.0			0.6			0.1			1.6		
0.180	4.1			0.7			0.5			7.6		
0.125	13.3			5.7			2.2			22.9		
0.090	17.5			12.5			9.0			24.7		
0.063	18.5			22.4			18.1			17.5		
0.045	12.1			14.9			17.0			7.9		
0.032	2.9			2.9			5.8			1.1		
0.000	30.0			40.0			47.4			15.4		

Run77 Dcyc 600 Dovf 210 Divf 165 Lovf 675 Livf 775 Dspig 95 Press 83

	Solids	Water	Cromite	Silica	SG
Feed	282.7	312.5			3.8
Ofi	37.4	105.3			3.8
Ofo	101.3	159.8			3.8
Uf	144.0	49.1			3.8

Size	Feed	Crmt	Silc	Ofi	Crmt	Silc	Ofo	Crmt	Silc	Uf	Crmt	Silc
0.710	0.4			0.0			0.0			0.9		
0.500	0.6			0.0			0.0			1.1		
0.355	0.9			0.0			0.1			1.6		
0.250	1.9			0.0			1.1			3.0		
0.180	5.9			0.2			4.2			8.6		
0.125	14.0			2.3			10.5			19.6		
0.090	22.2			9.3			20.3			26.9		
0.063	20.6			19.9			18.5			22.3		
0.045	5.0			11.3			5.1			3.3		
0.032	2.5			4.8			3.0			1.6		
0.000	25.9			52.2			37.2			11.1		

Run78 Dcyc 600 Dovf 210 Divf 184 Lovf 675 Livf 825 Dspig 95 Press 90

	Solids	Water	Cromite	Silica	SG
Feed	309.6	339.5			3.8
Ofi	85.8	180.5			3.8
Ofo	58.7	96.6			3.8
Uf	165.2	61.8			3.8

Size	Feed	Crmt	Silc	Ofi	Crmt	Silc	Ofo	Crmt	Silc	Uf	Crmt	Silc
0.710	0.2			0.0			0.0			0.3		
0.500	0.1			0.0			0.0			0.2		
0.355	0.5			0.0			0.1			0.8		
0.250	2.0			0.0			0.4			3.6		
0.180	4.7			0.1			1.0			8.4		
0.125	12.3			0.7			6.4			20.5		
0.090	19.9			3.3			12.5			31.2		
0.063	16.1			13.6			18.9			16.5		
0.045	10.3			13.9			15.0			6.8		
0.032	6.3			12.0			8.4			2.5		
0.000	27.5			56.5			37.3			9.0		

University of Cape Town

Run79 Dcyc 600 Dovf 220 Divf 177 Lovf 675 Livf 875 Dspig 95 Press 93

	Solids	Water	Cromite	Silica	SG
Feed	302.7	355.4			3.8
Ofi	36.5	83.3			3.8
Ofo	92.7	223.5			3.8
Uf	173.6	68.8			3.8

Size	Feed	Crmt	Silc	Ofi	Crmt	Silc	Ofo	Crmt	Silc	Uf	Crmt	Silc
0.710	0.1			0.0			0.0			0.2		
0.500	0.3			0.0			0.0			0.5		
0.355	0.6			0.0			0.0			1.0		
0.250	1.2			0.1			0.1			2.0		
0.180	3.5			0.3			0.4			5.9		
0.125	9.7			2.1			1.6			15.7		
0.090	24.5			9.3			10.0			35.4		
0.063	19.1			17.2			18.5			19.8		
0.045	12.2			14.5			15.8			9.8		
0.032	2.7			4.4			5.2			1.0		
0.000	26.1			52.1			48.4			8.7		

Run80 Dcyc 600 Dovf 210 Divf 165 Lovf 675 Livf 675 Dspig 95 Press 80

	Solids	Water	Cromite	Silica	SG
Feed	278.7	319.0			3.8
Ofi	40.6	114.8			3.8
Ofo	153.5	208.2			3.8
Uf	84.6	31.5			3.8

Size	Feed	Crmt	Silc	Ofi	Crmt	Silc	Ofo	Crmt	Silc	Uf	Crmt	Silc
0.710	0.1			0.0			0.0			0.2		
0.500	0.1			0.0			0.0			0.2		
0.355	0.3			0.0			0.0			0.8		
0.250	1.0			0.0			0.2			2.9		
0.180	4.5			0.4			2.1			10.7		
0.125	10.7			1.8			6.0			23.5		
0.090	18.2			7.5			14.3			30.3		
0.063	19.5			10.4			23.7			16.4		
0.045	11.9			13.3			14.9			5.8		
0.032	2.4			4.3			2.9			0.8		
0.000	31.4			62.4			35.9			8.4		

Run81 Dcyc 600 Dovf 210 Divf 165 Lovf 675 Livf 575 Dspig 95 Press 78

	Solids	Water	Cromite	Silica	SG
Feed	320.8	378.4	22.1	21.8	3.8
Ofi	50.1	131.4	23.7	20.6	3.8
Ofo	111.4	207.5	22.1	22.3	3.8
Uf	159.3	55.0	32.8	11.7	3.8

Size	Feed	Crmt	Silc	Ofi	Crmt	Silc	Ofo	Crmt	Silc	Uf	Crmt	Silc
0.710	0.1	0.0	0.0	0.0	0.0	0.0	0.0	0.0	0.0	0.1	0.0	0.0
0.500	0.1	1.7	5.3	0.0	0.0	0.0	0.0	0.0	0.0	0.1	10.7	33.6
0.355	0.3	2.3	4.6	0.0	0.0	0.0	0.0	0.0	0.0	0.6	14.9	29.4
0.250	0.9	2.5	4.4	0.0	0.0	0.0	0.1	0.0	0.0	1.7	16.2	28.2
0.180	3.5	6.5	22.2	0.2	5.6	38.1	0.4	0.0	0.0	6.8	23.4	20.9
0.125	9.5	11.2	33.2	1.4	9.5	34.9	2.7	4.5	39.8	16.8	31.4	12.9
0.090	18.9	18.1	26.3	5.0	19.9	24.5	10.9	7.3	37.0	28.8	36.1	8.1
0.063	19.4	25.7	18.6	11.2	25.2	19.0	20.4	21.3	23.0	21.3	36.9	7.4
0.045	12.9	28.4	15.9	14.5	28.1	16.3	15.8	25.9	18.4	10.3	34.9	9.4
0.032	3.6	26.4	18.1	4.5	25.3	19.5	5.0	25.3	19.0	2.4	32.4	11.8
0.000	30.9	27.1	19.5	63.1	28.8	20.1	44.6	25.0	19.2	11.1	26.4	18.0

University of Cape Town

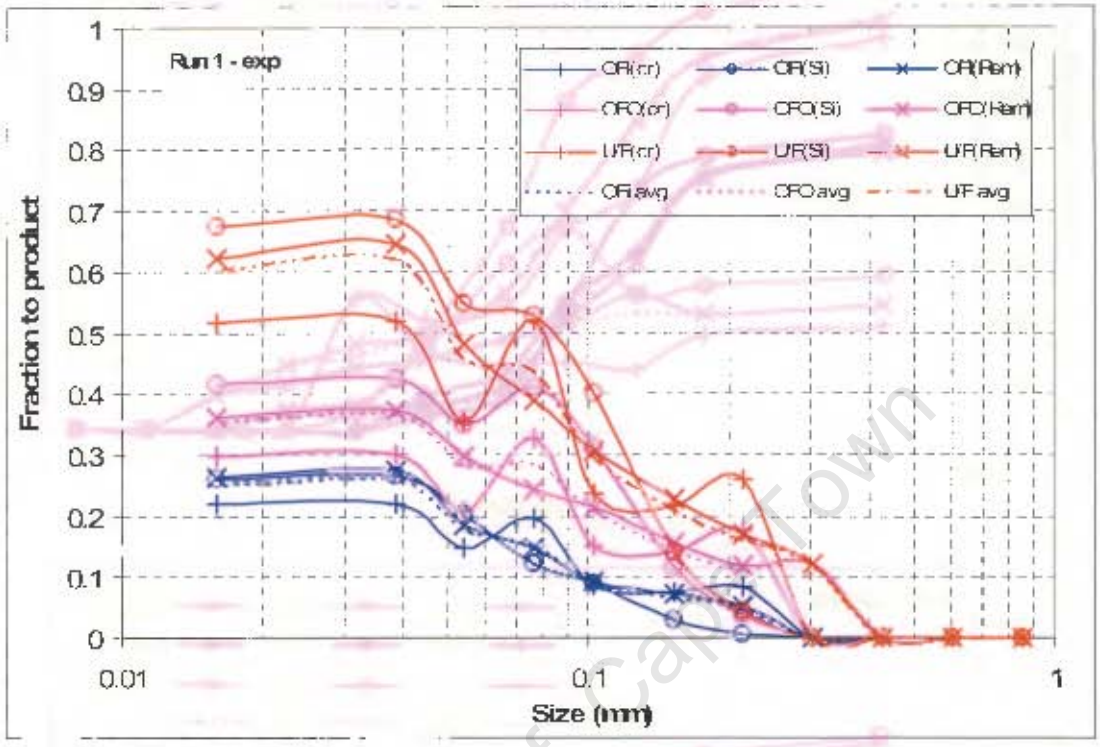
Run82 Dcyc 600 Dovf 210 Divf 0 Lovf 675 Livf 0 Dspig 95 Press 55

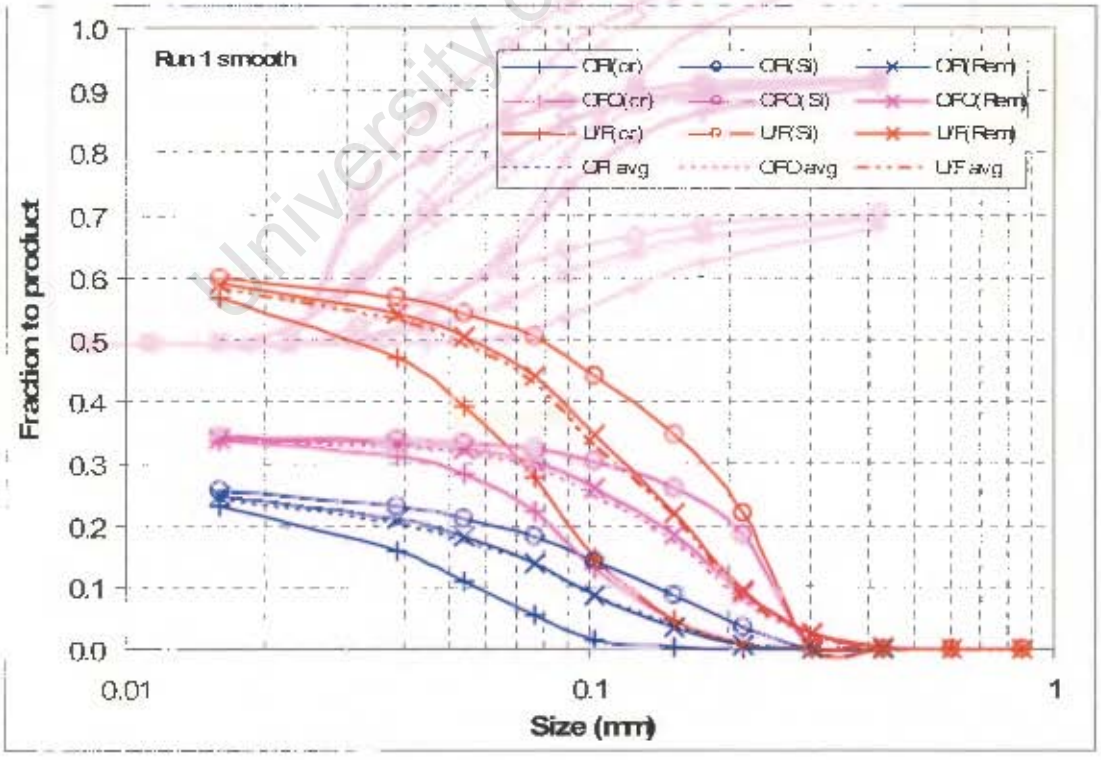
Solids	Water	Cromite	Silica	SG
Feed	286.2	294.9	18.8	26.9	3.8
Ofi	21.6	48.1	18.0	26.6	3.8
Ofo	118.3	177.6	20.3	25.9	3.8
Uf	146.3	41.9	29.7	8.9	3.8

Size	Feed	Crmt	Silc	Ofi	Crmt	Silc	Ofo	Crmt	Silc	Uf	Crmt	Silc
0.710	0.1	0.0	0.0	0.0	0.0	0.0	0.0	0.0	0.0	0.2	0.0	0.0
0.500	0.1	0.0	0.0	0.0	0.0	0.0	0.0	0.0	0.0	0.1	0.0	0.0
0.355	0.2	1.1	2.0	0.0	0.0	0.0	0.0	0.0	0.0	0.5	14.7	25.9
0.250	1.2	1.3	2.1	0.2	0.0	0.0	0.2	0.0	0.0	2.2	17.8	27.7
0.180	5.2	14.9	30.9	0.9	4.2	41.6	1.5	26.6	19.3	8.8	24.2	22.0
0.125	12.9	15.8	30.9	3.3	6.1	42.2	5.0	25.1	20.7	20.6	30.7	10.4
0.090	21.6	11.3	36.2	8.4	13.0	33.4	14.1	4.5	44.9	29.7	36.5	7.2
0.063	21.4	24.3	23.1	18.2	21.7	28.3	25.5	25.6	19.7	18.6	34.4	6.5
0.045	10.7	20.2	25.9	14.3	22.0	23.7	13.3	15.7	31.1	8.1	31.9	11.9
0.032	2.1	21.3	23.6	3.2	22.5	20.9	1.8	17.9	29.3	2.2	31.4	10.9
0.000	24.4	21.0	23.9	51.6	18.4	26.1	38.6	23.1	22.7	9.0	26.8	16.6

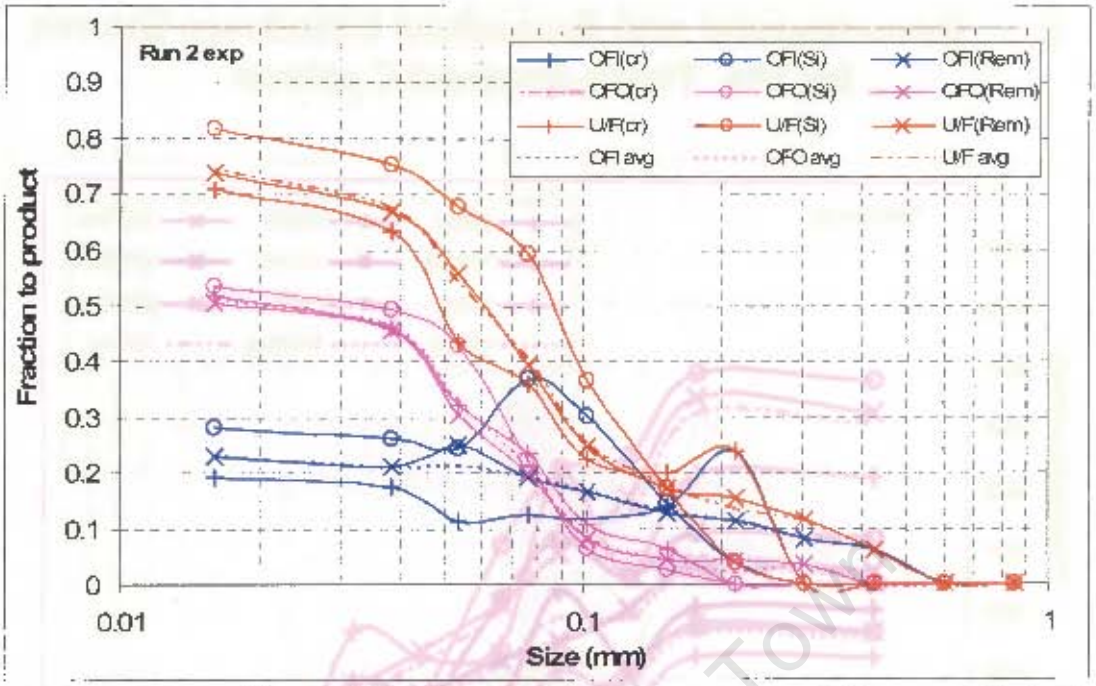
University of Cape Town

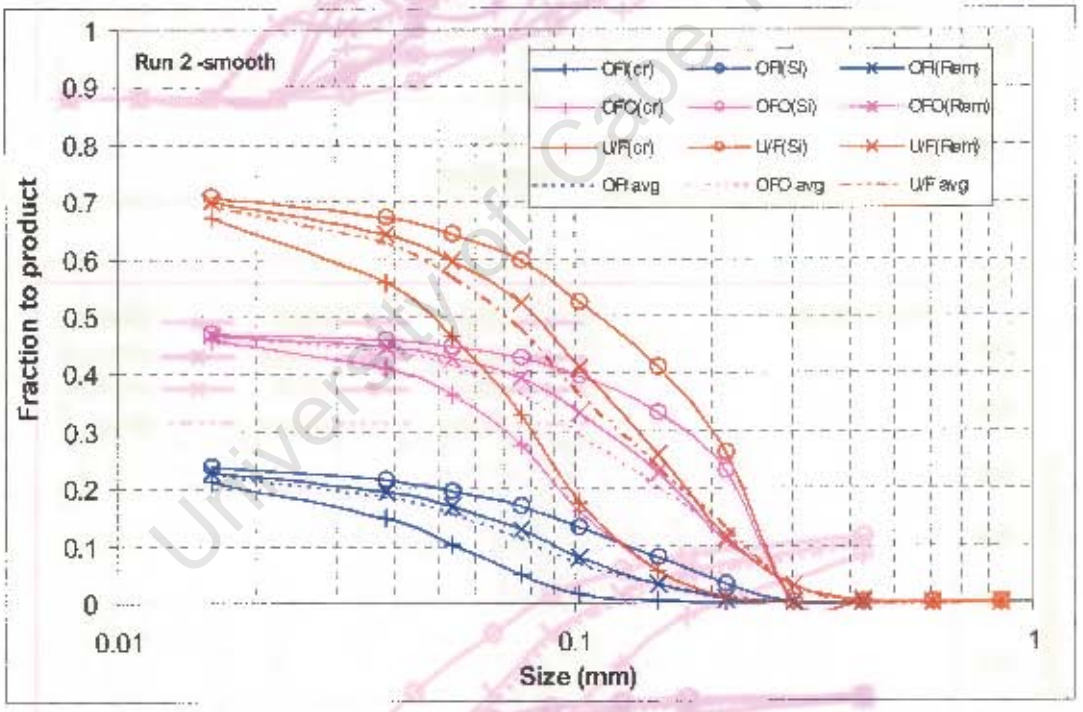
C. Experimental and Smoothed Efficiency Curves for the Three-Product Cyclone



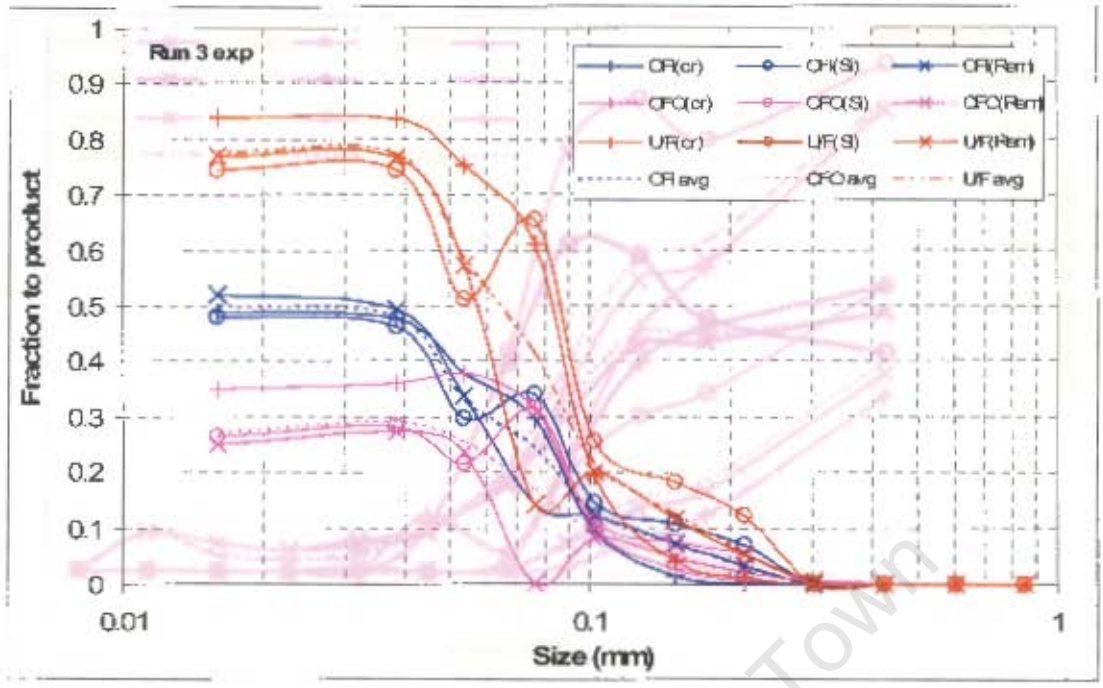


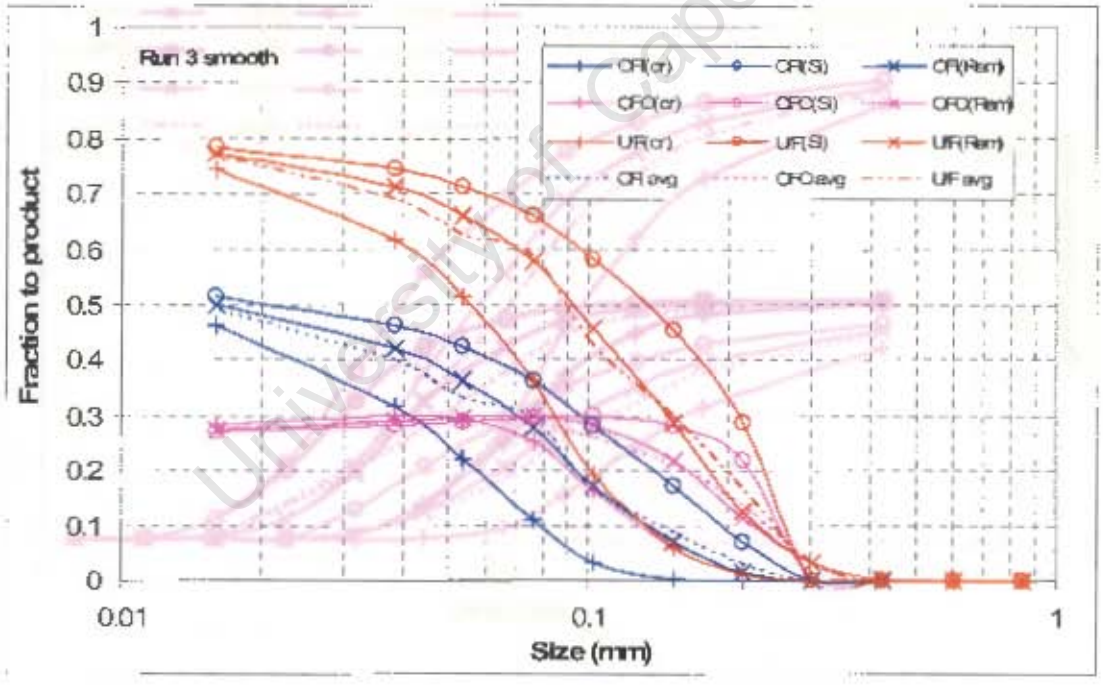
University of Cape Town



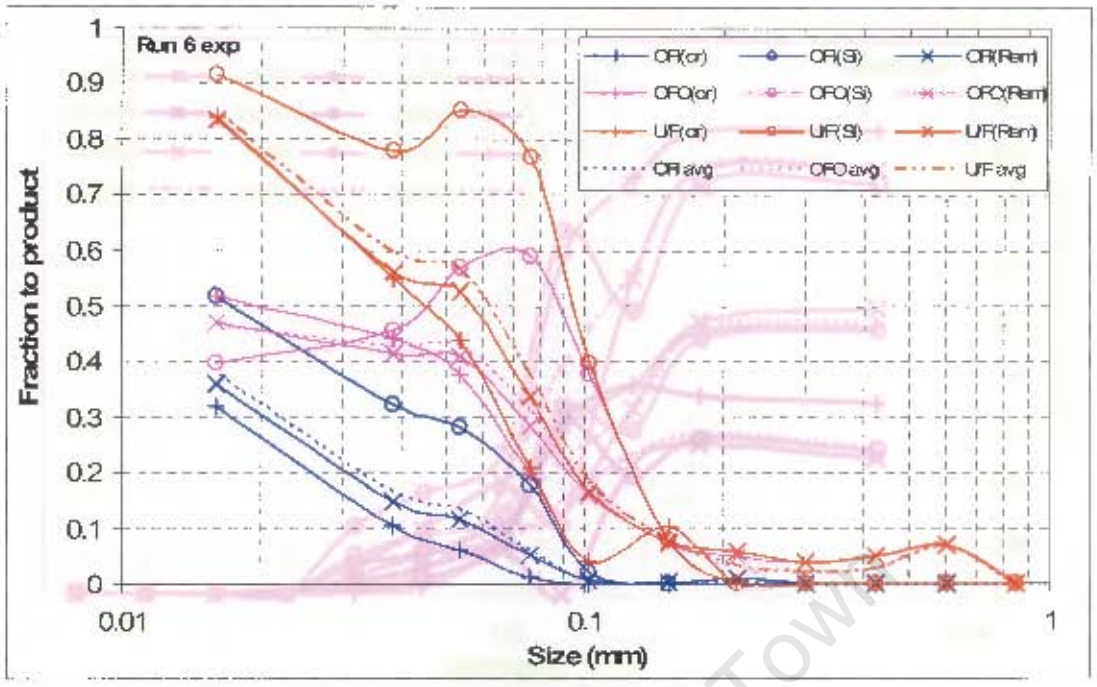


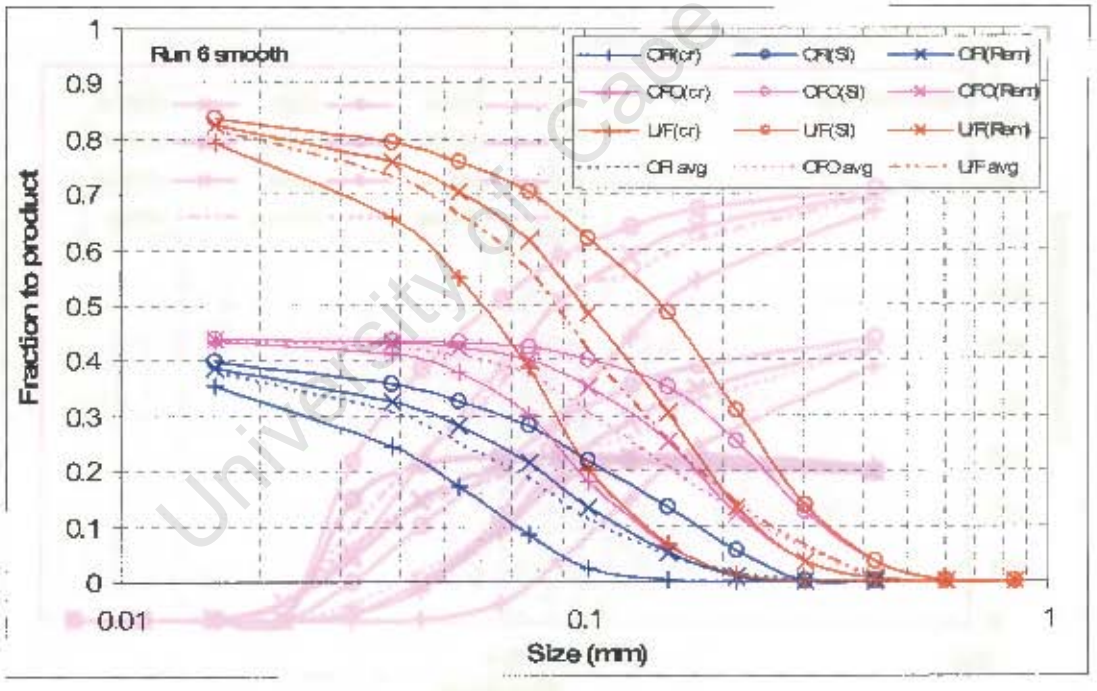
University of Cape Town



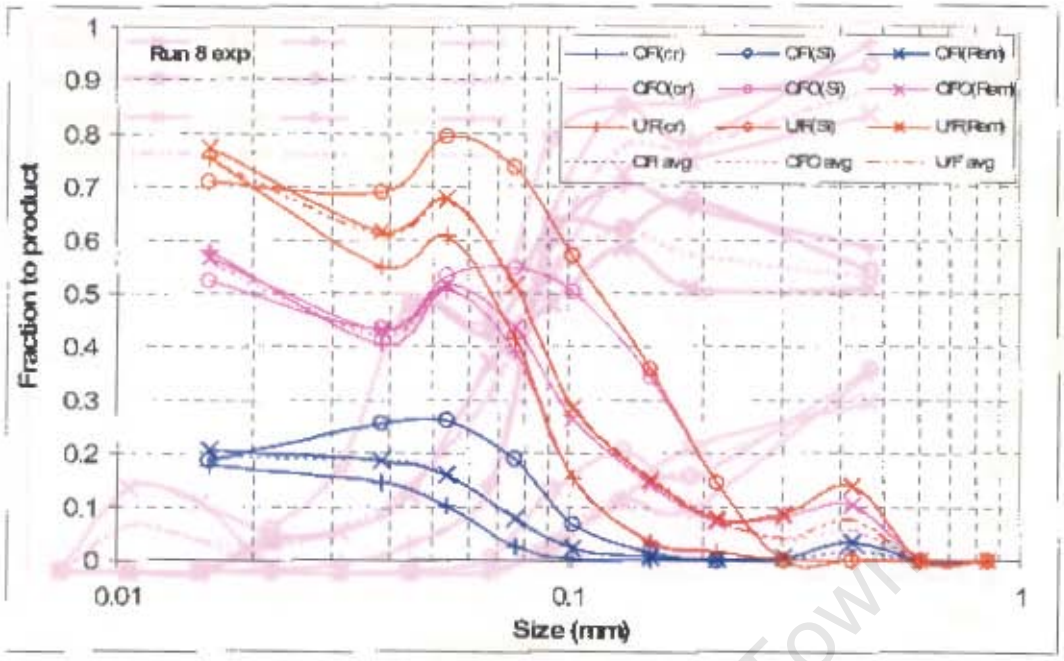


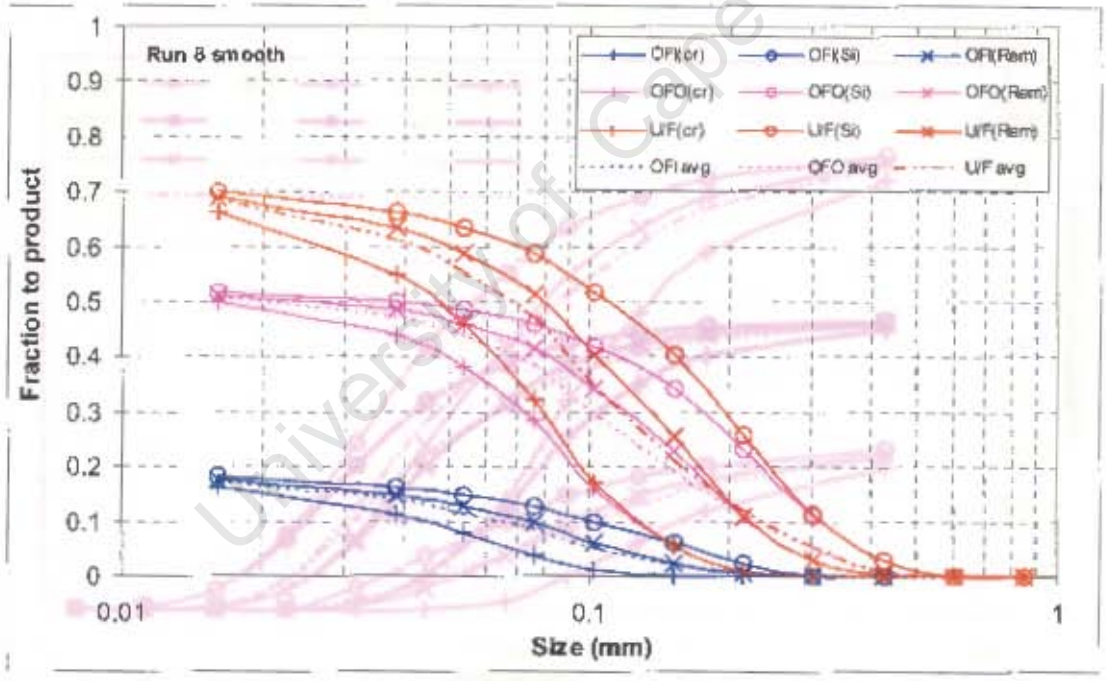
University of Cape Town



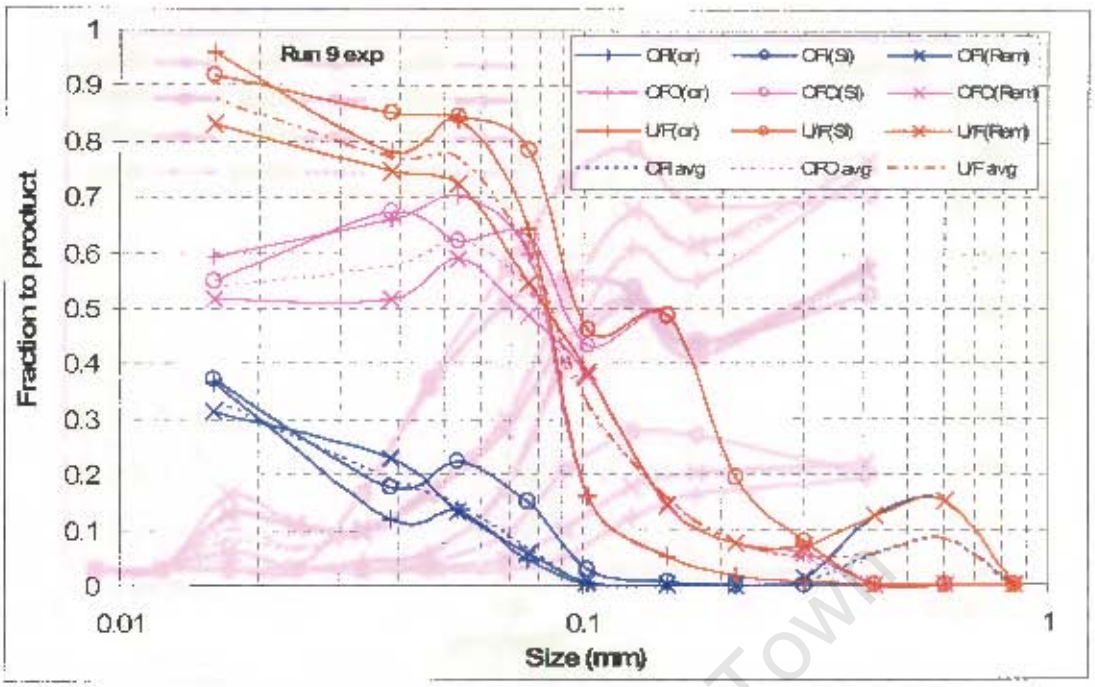


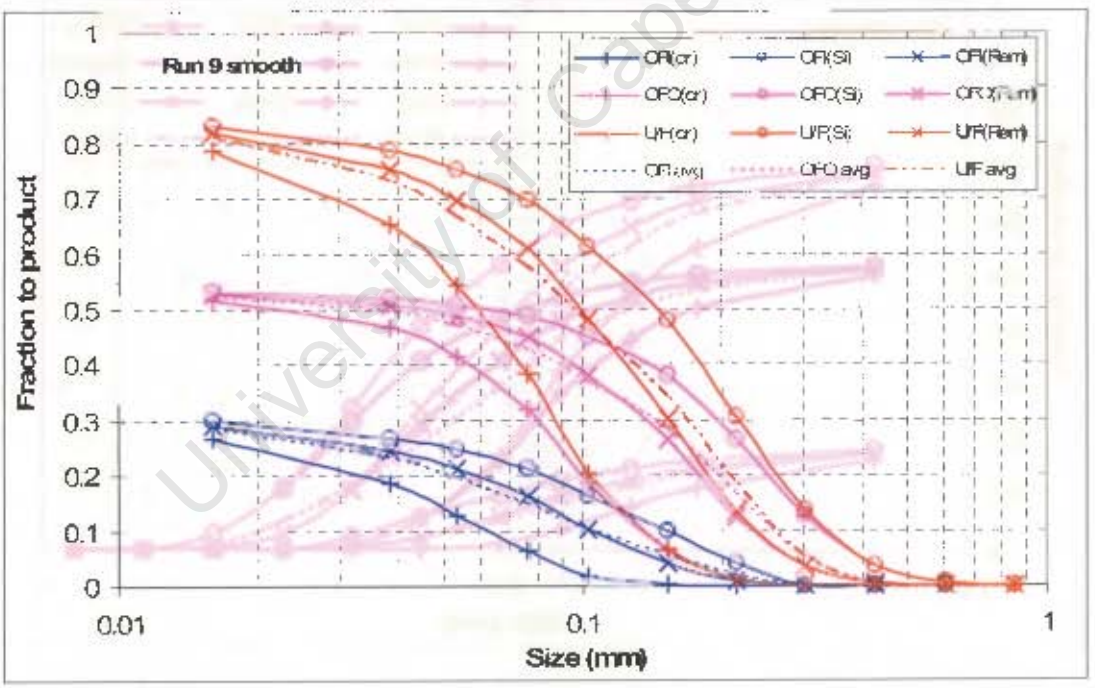
University of Cape Town



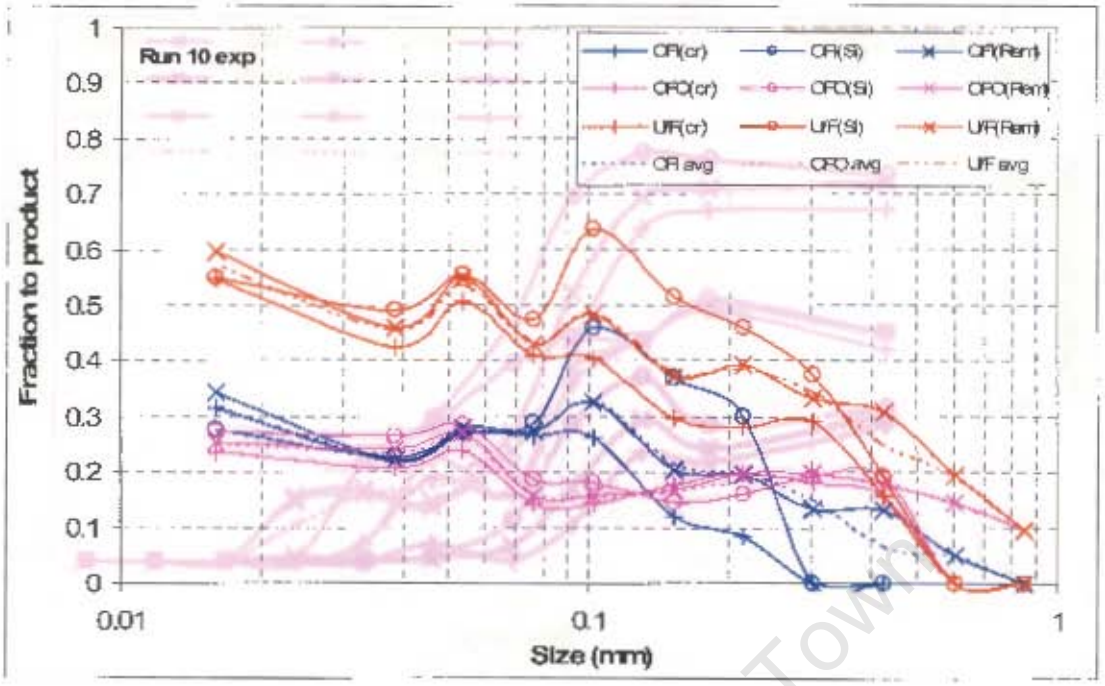


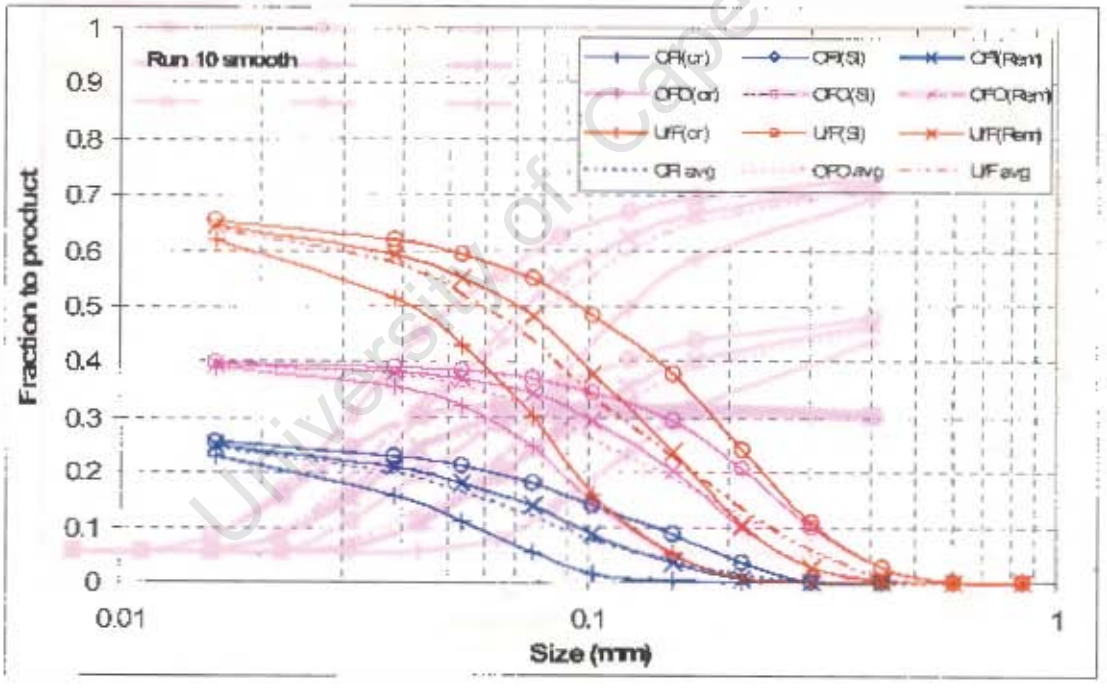
University of Cape Town



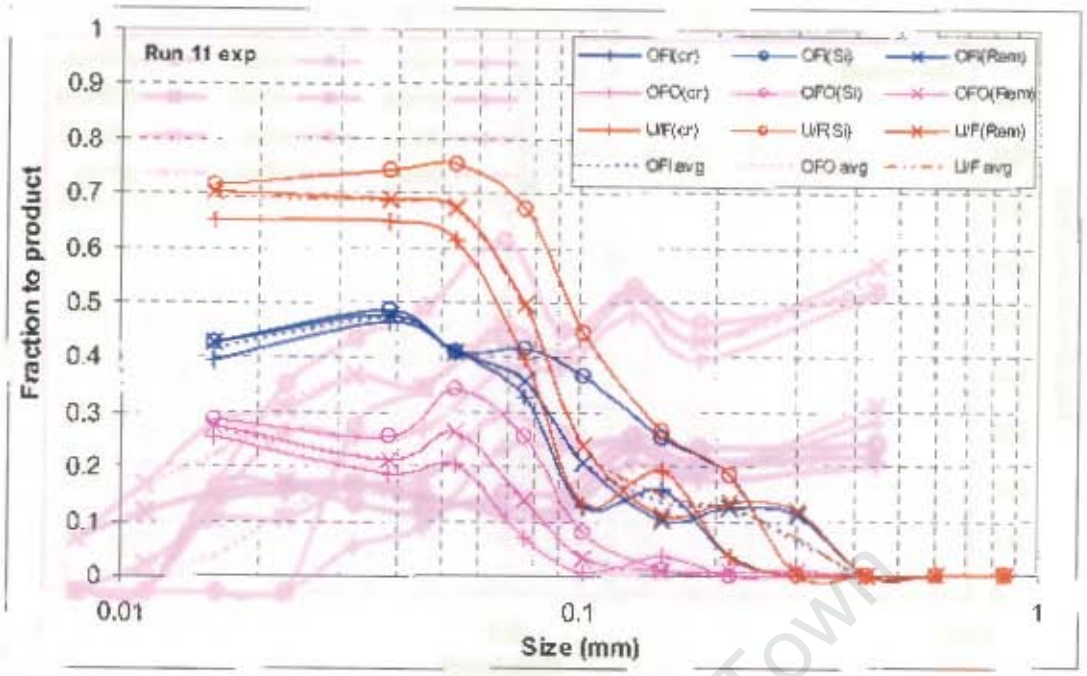


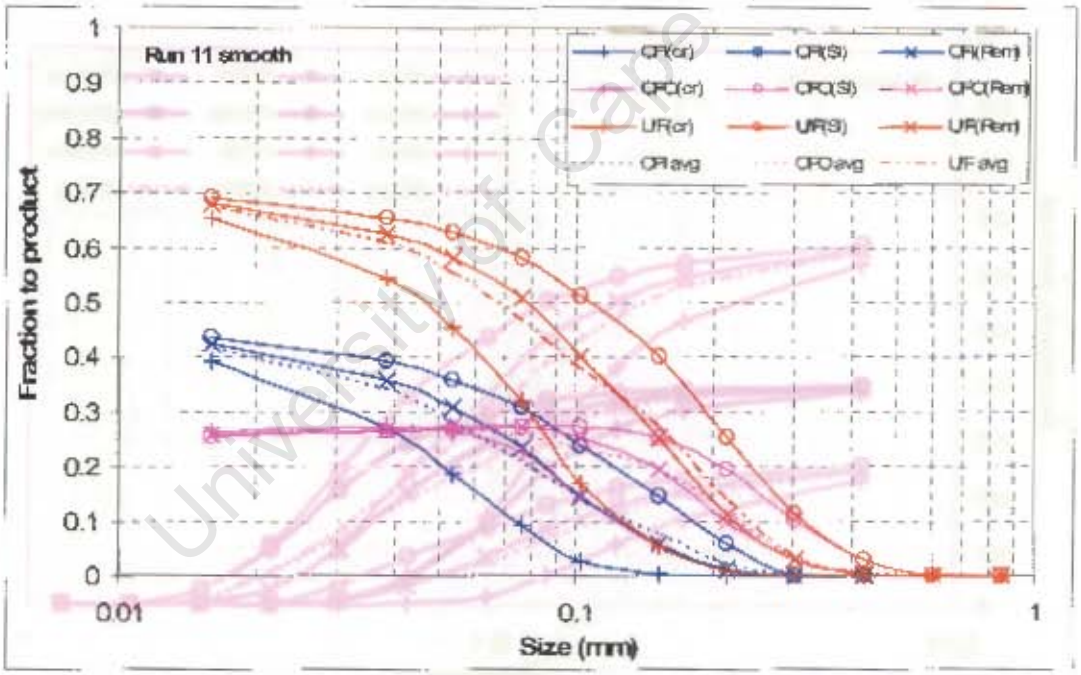
University of Cape Town



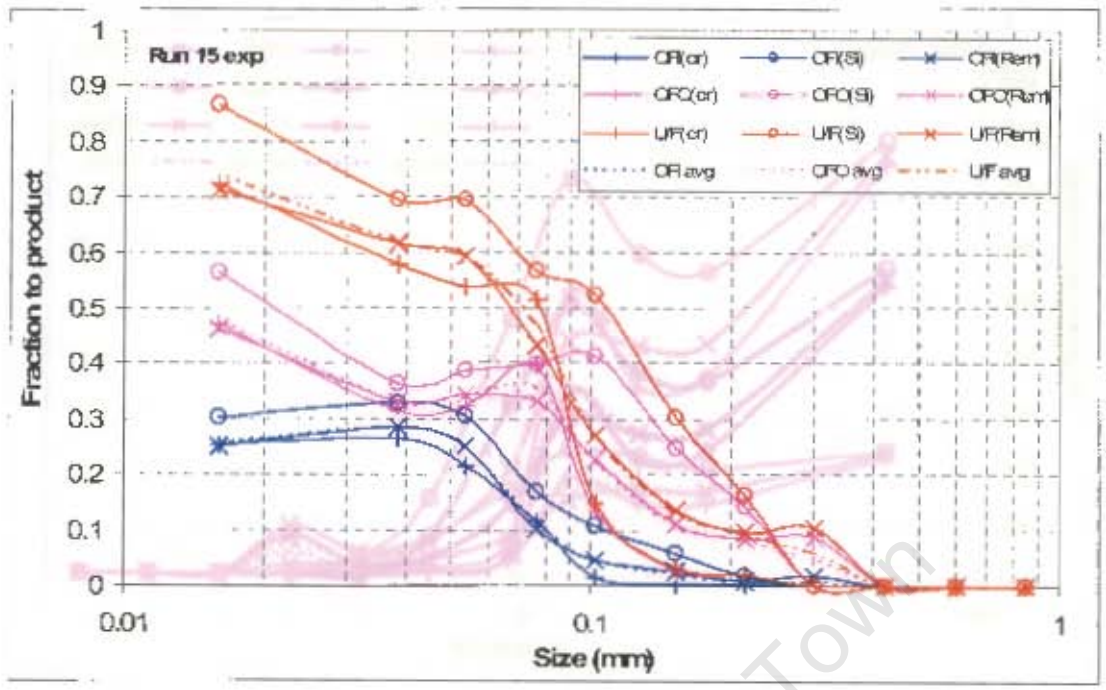


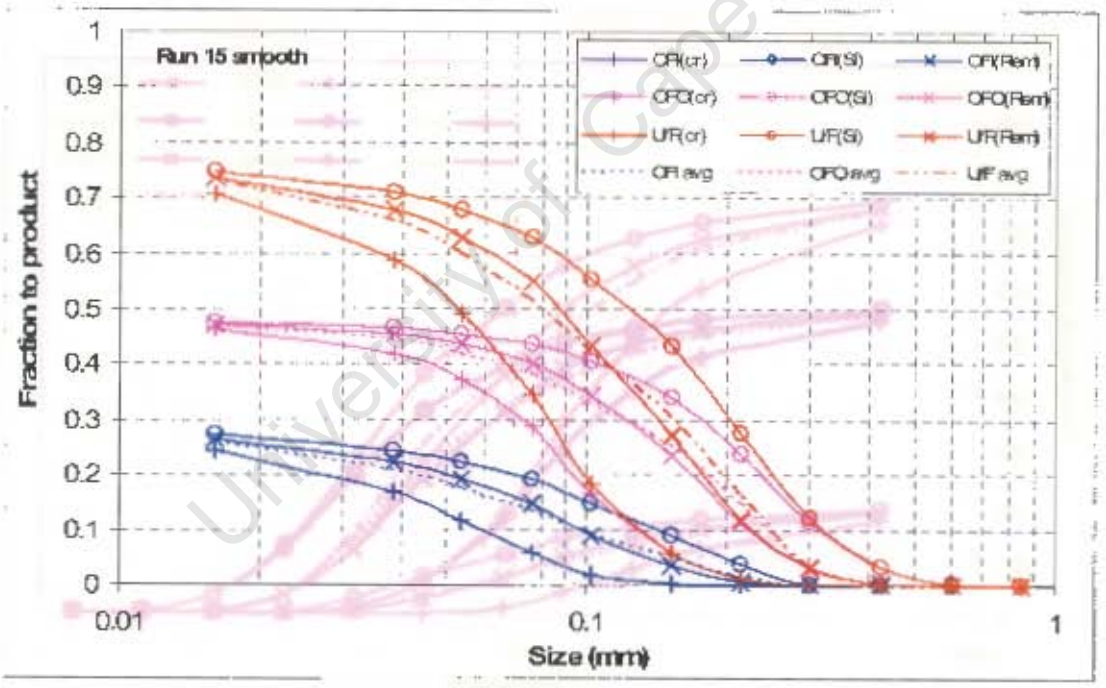
University of Cape Town



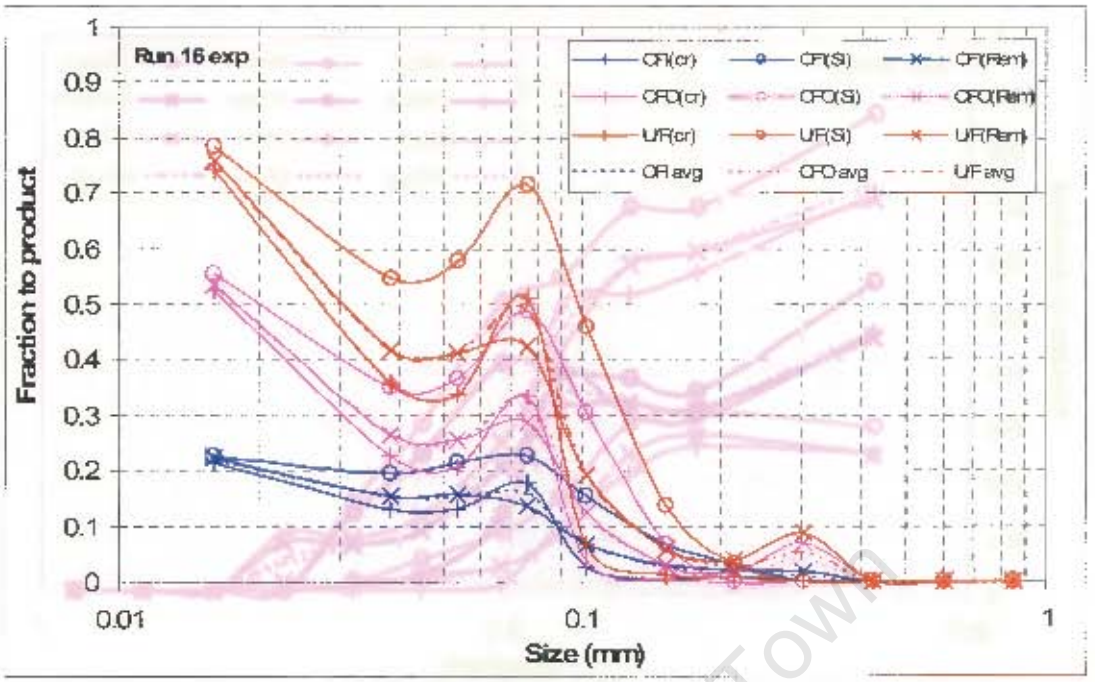


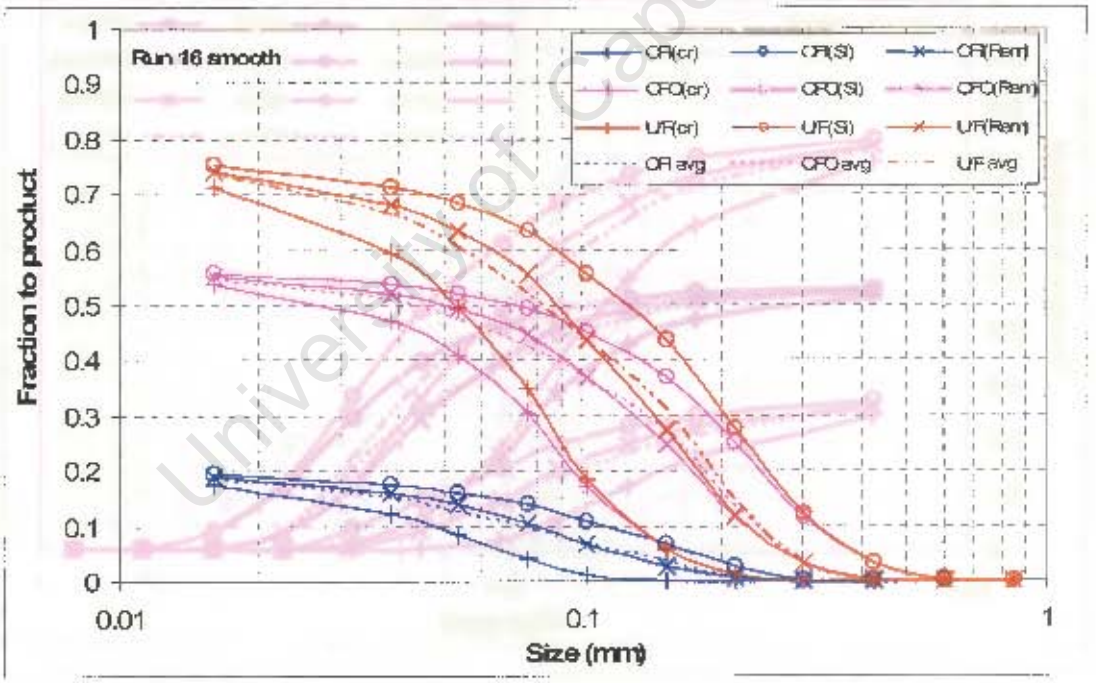
University of Cape Town



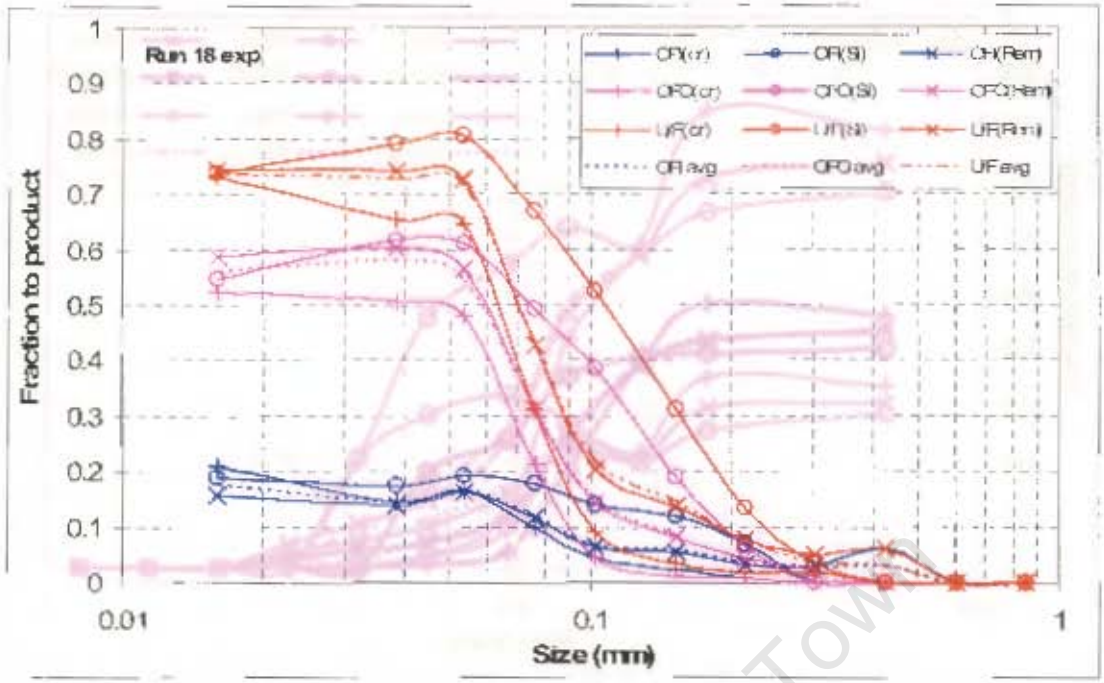


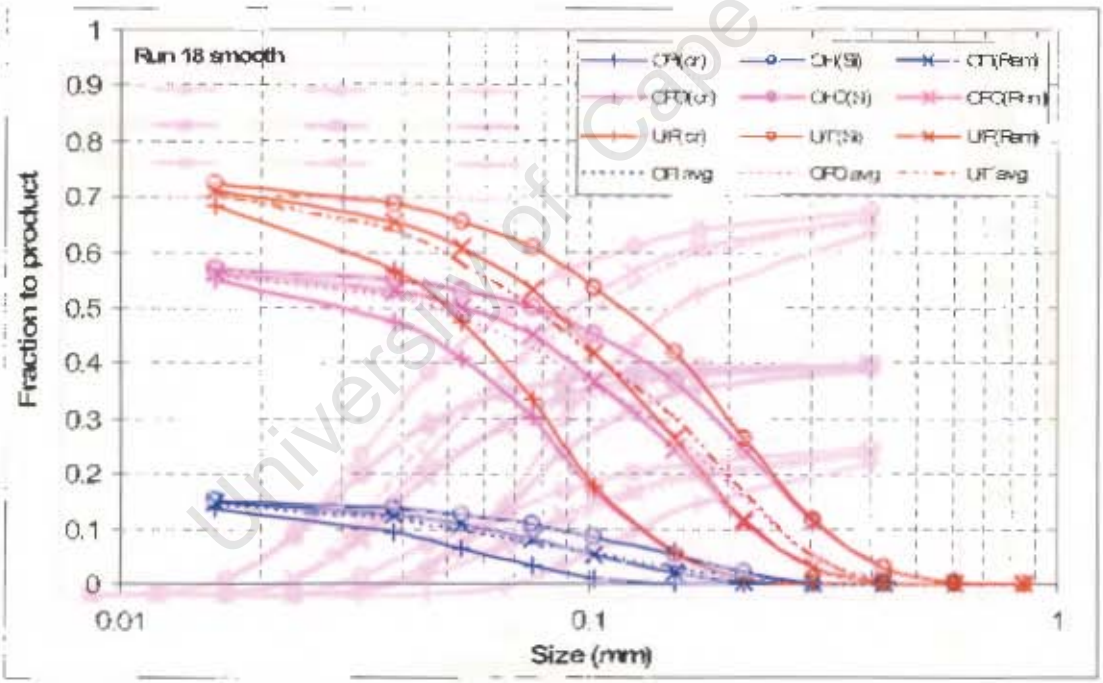
University of Cape Town



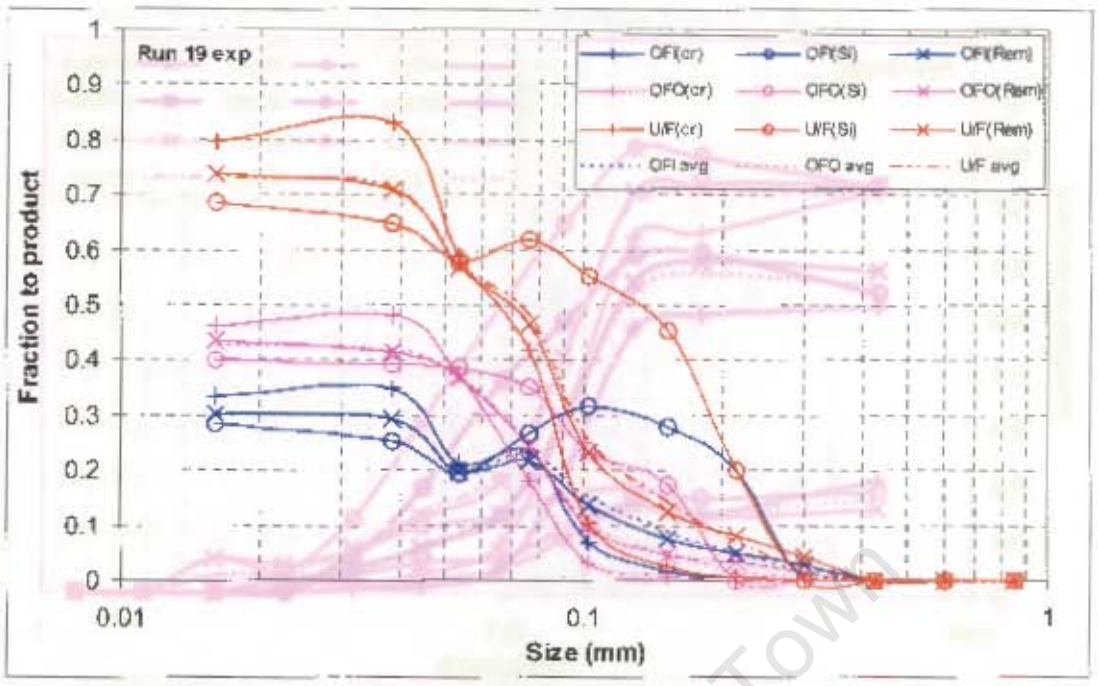


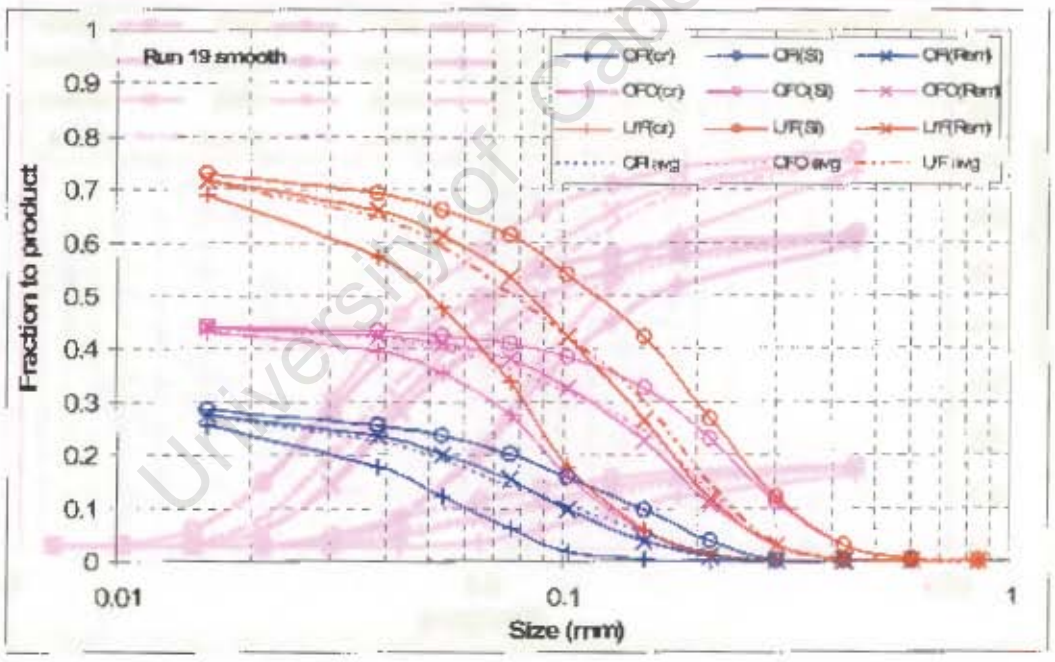
University of Cape Town



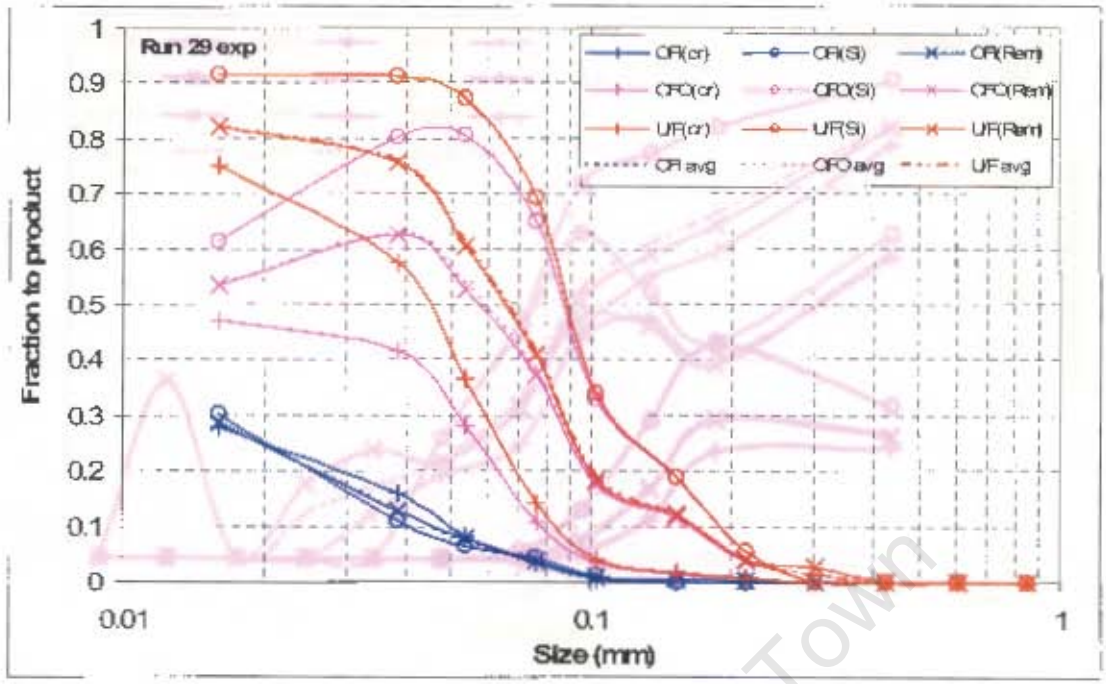


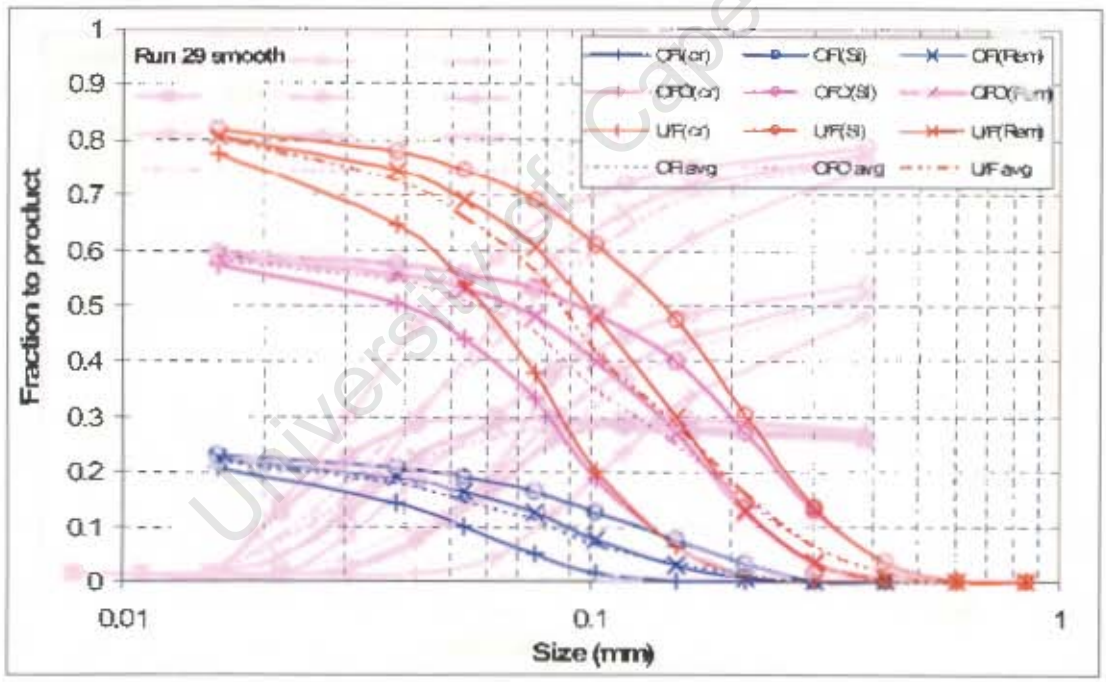
University of Cape Town



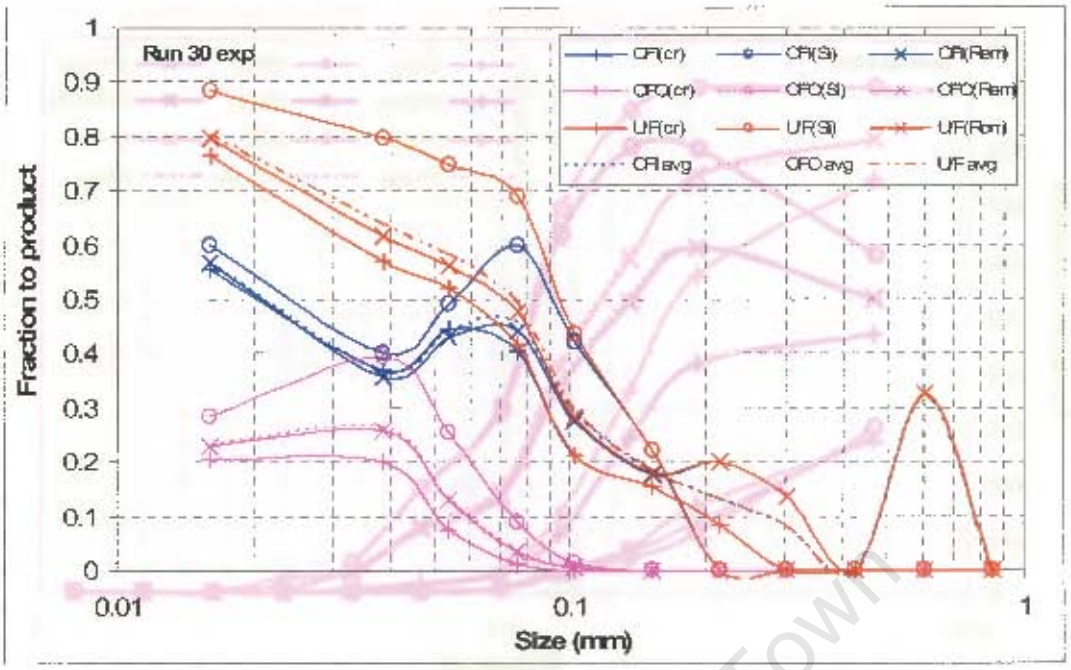


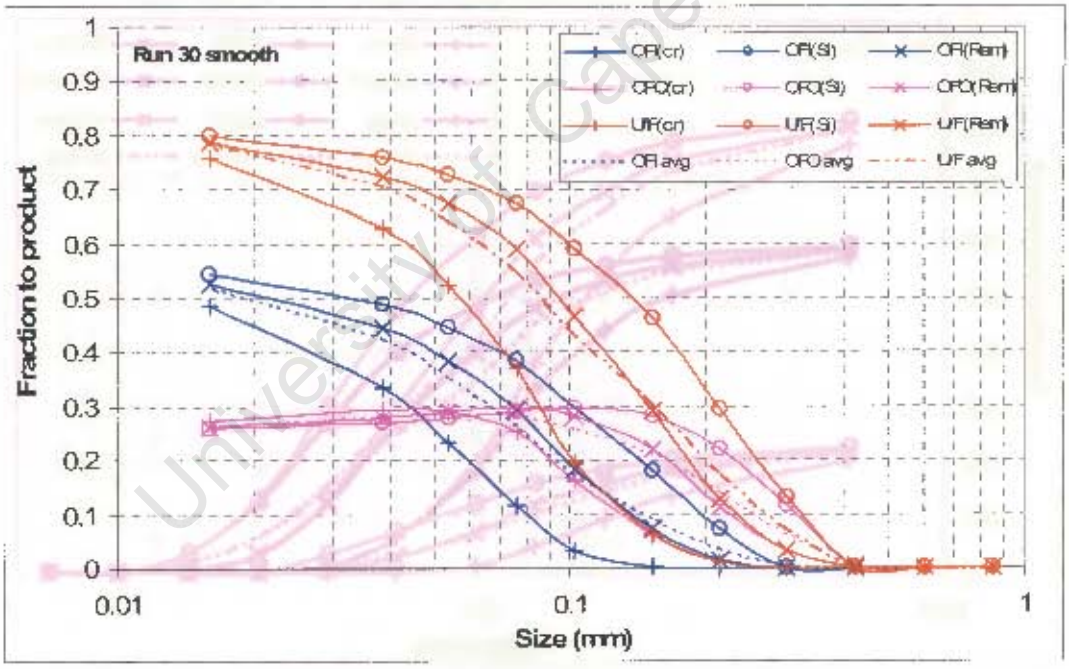
University of Cape Town



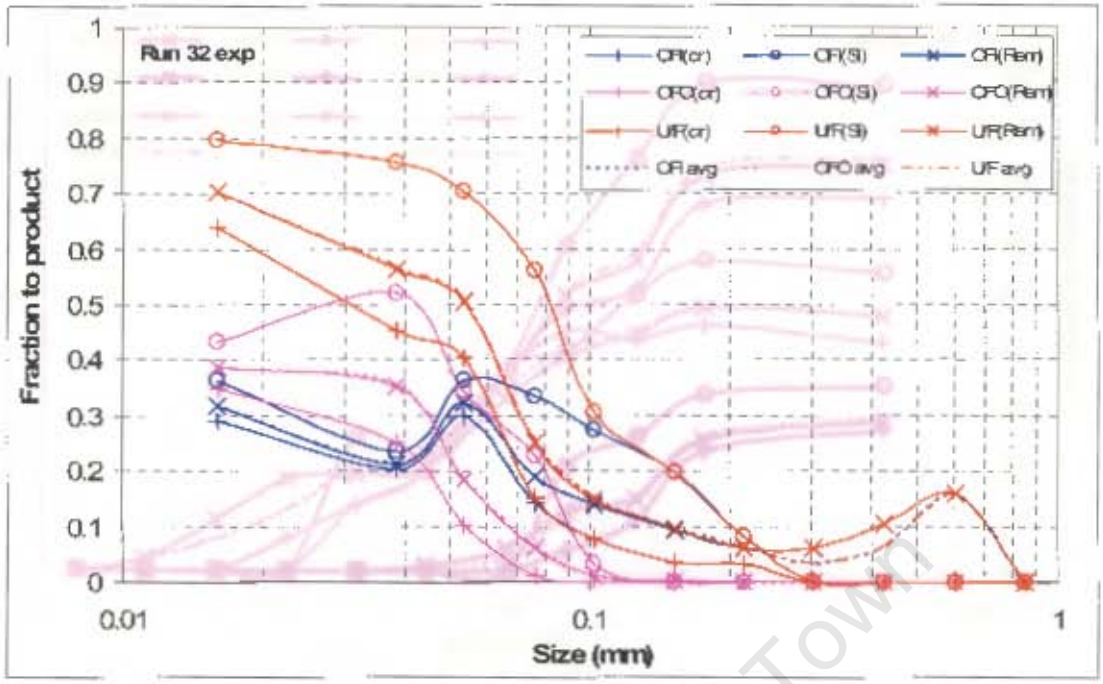


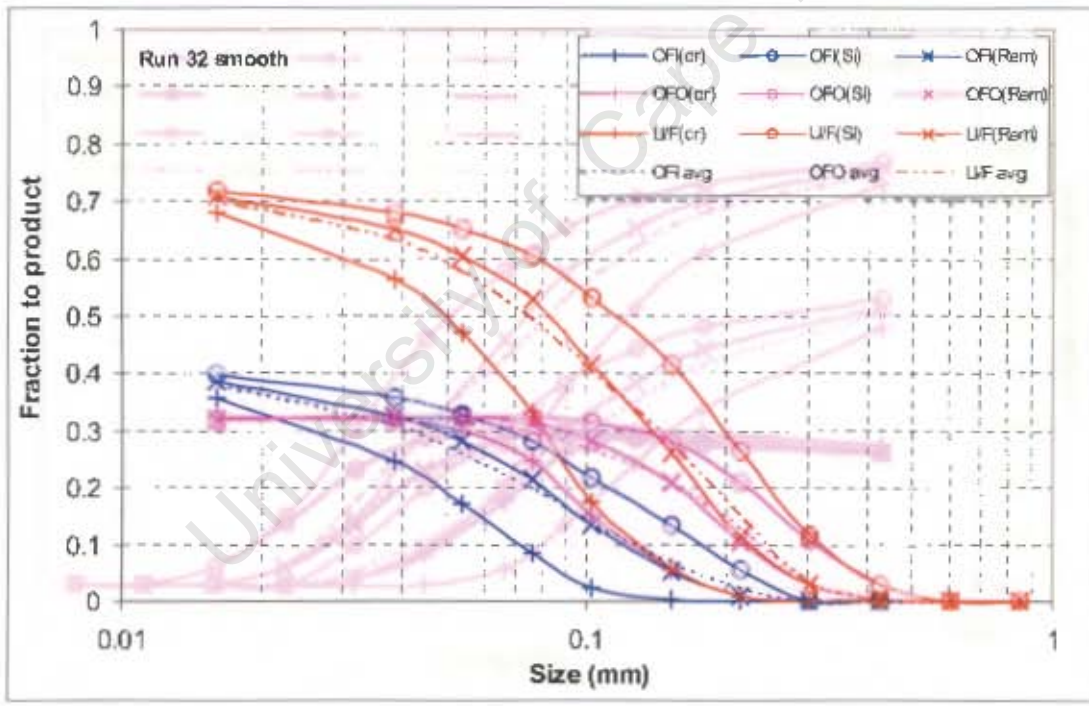
University of Cape Town



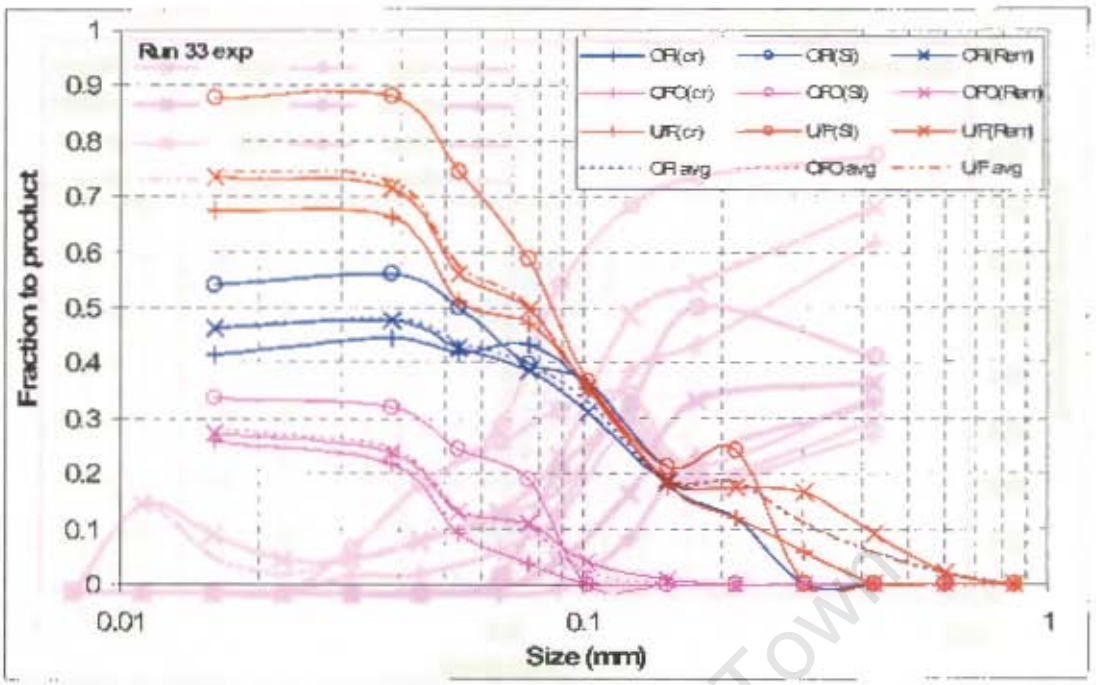


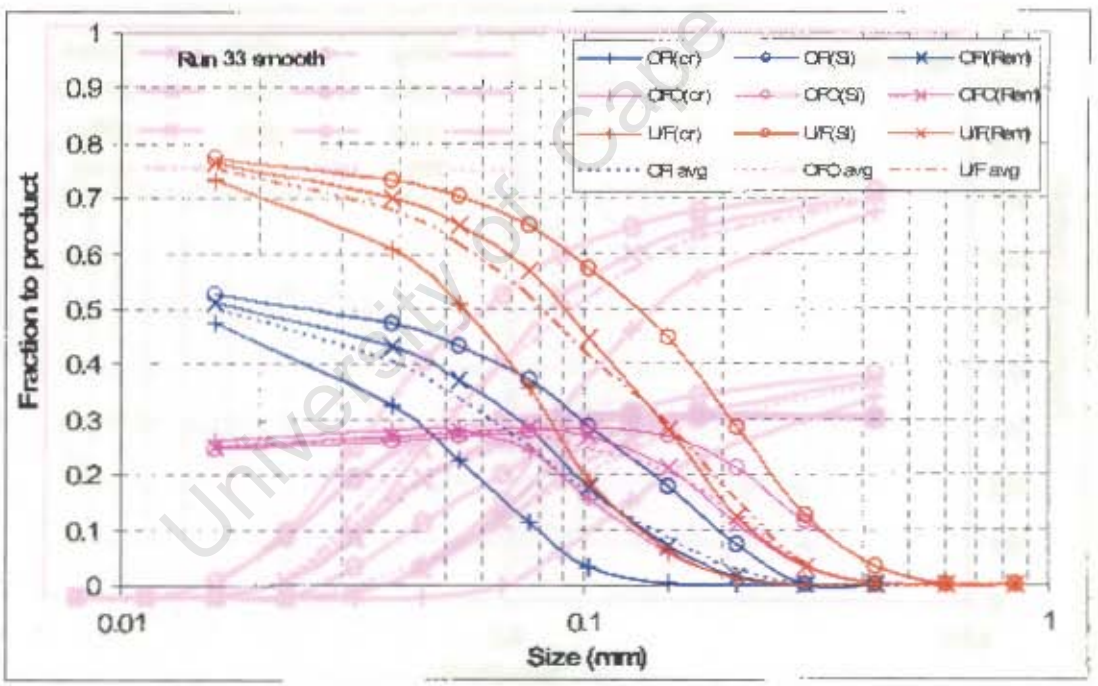
University of Cape Town



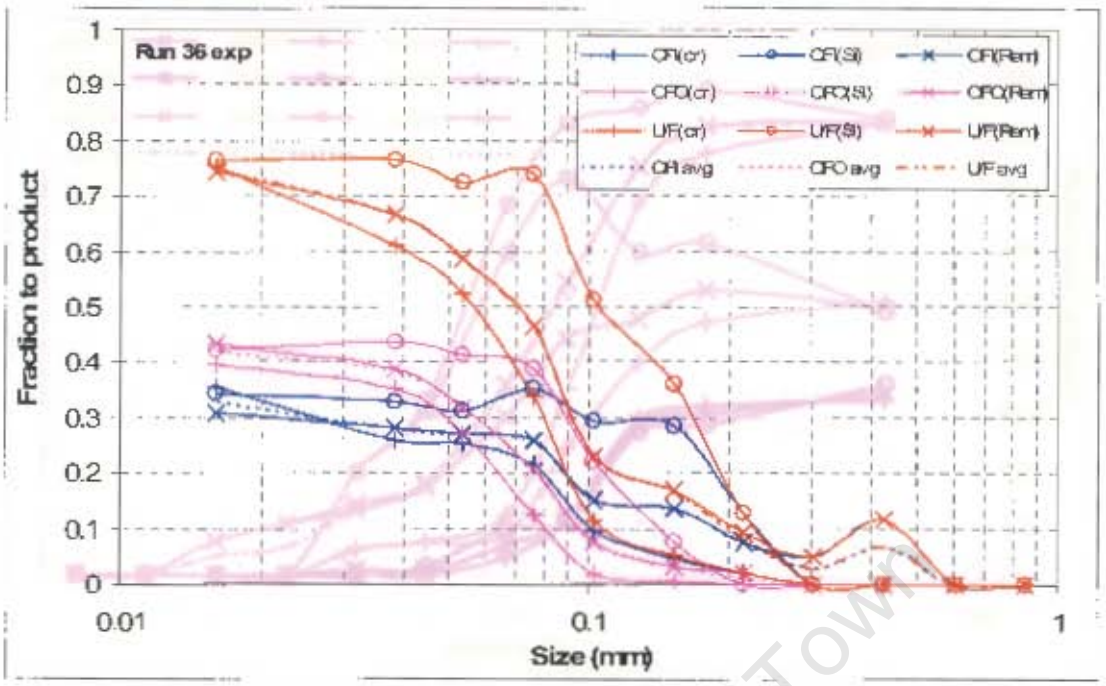


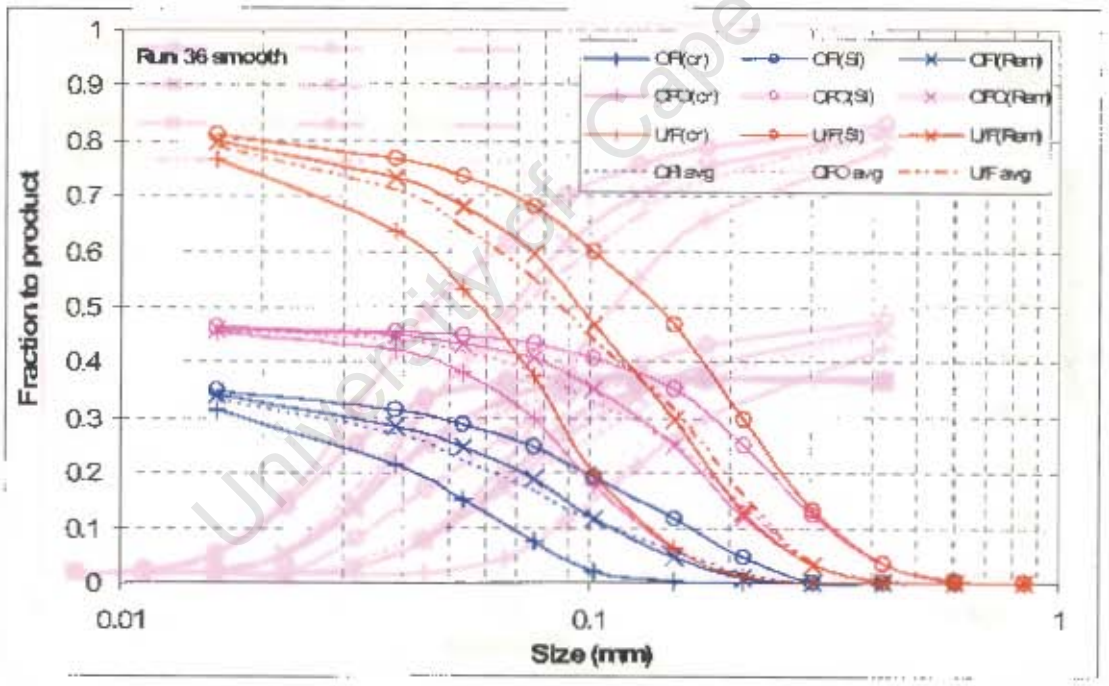
University of Cape Town



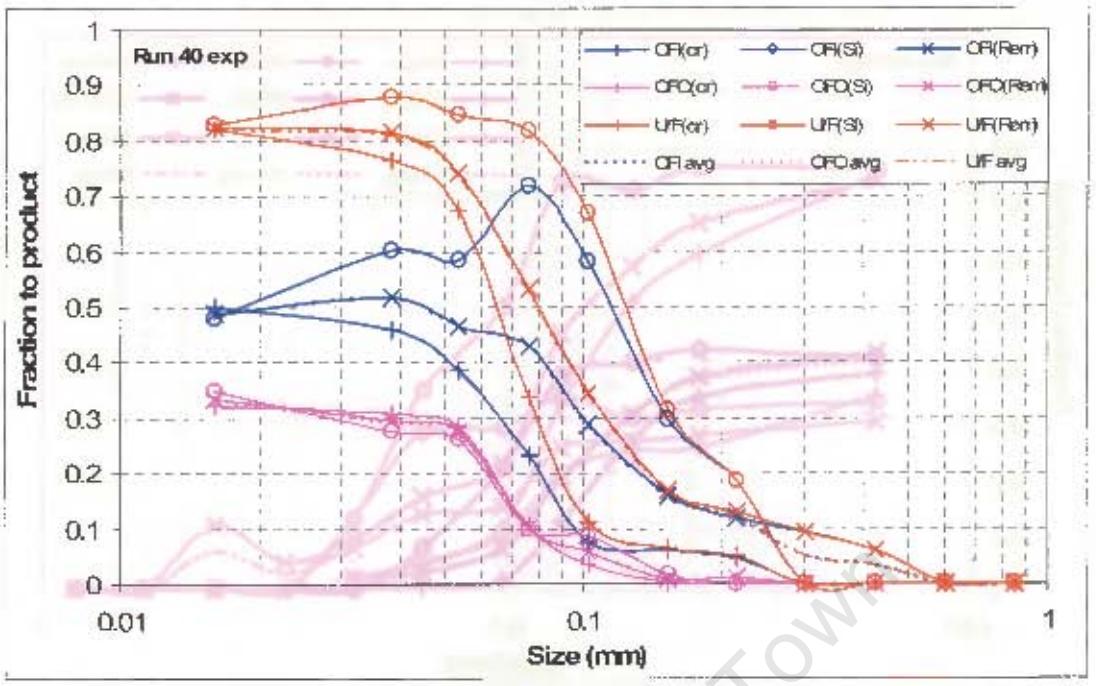


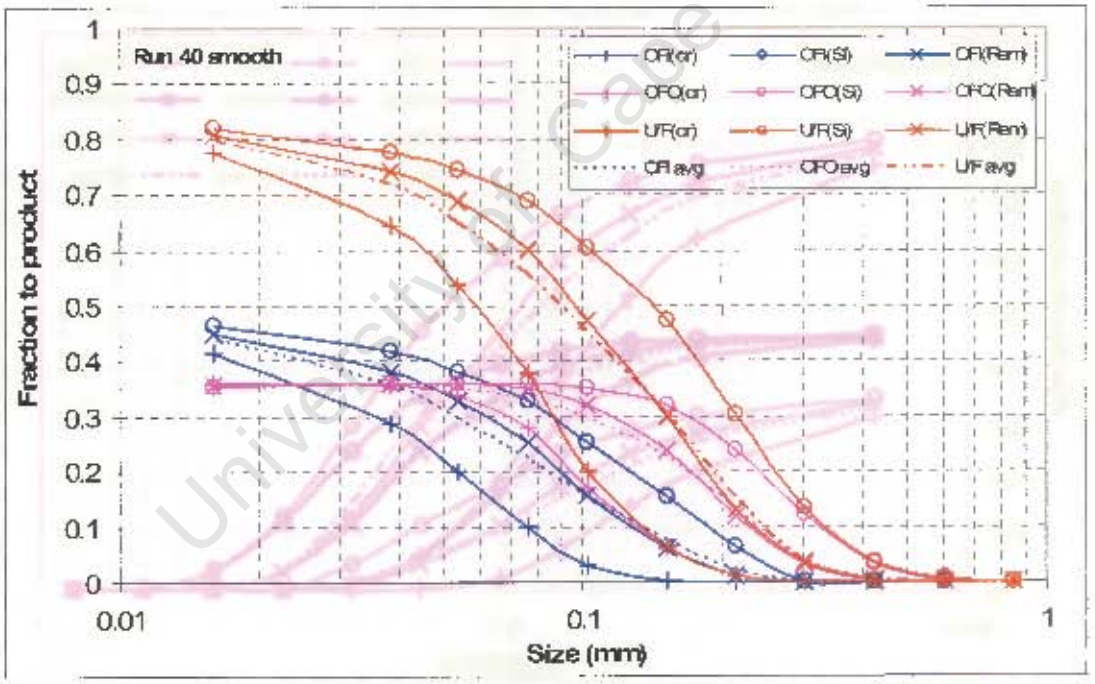
University of Cape Town



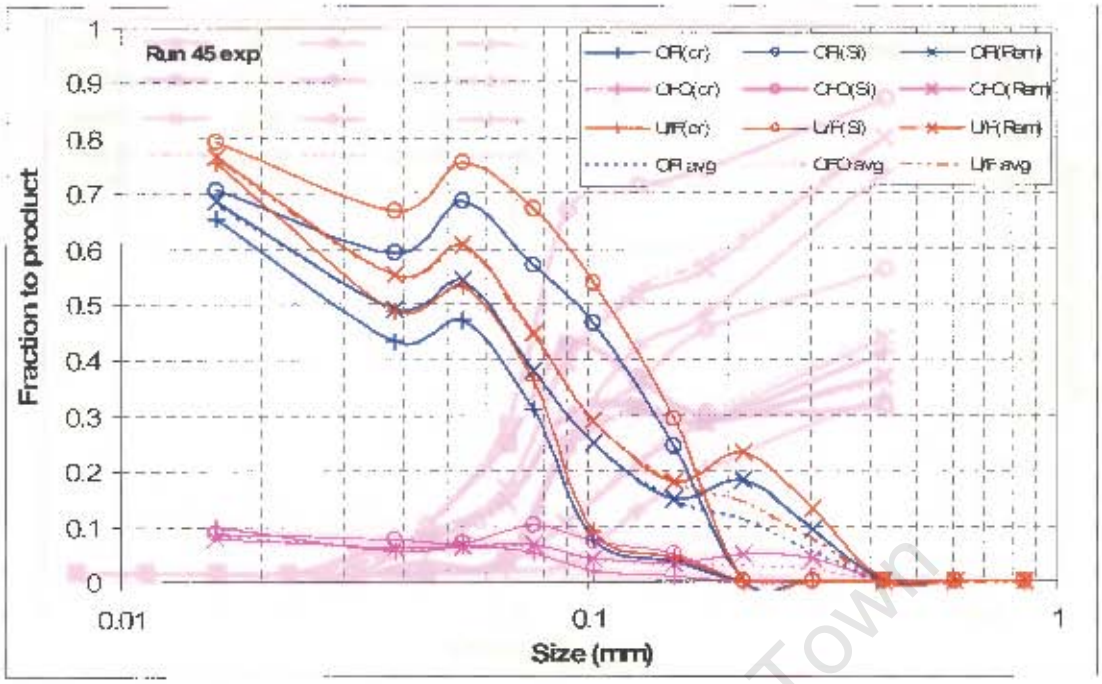


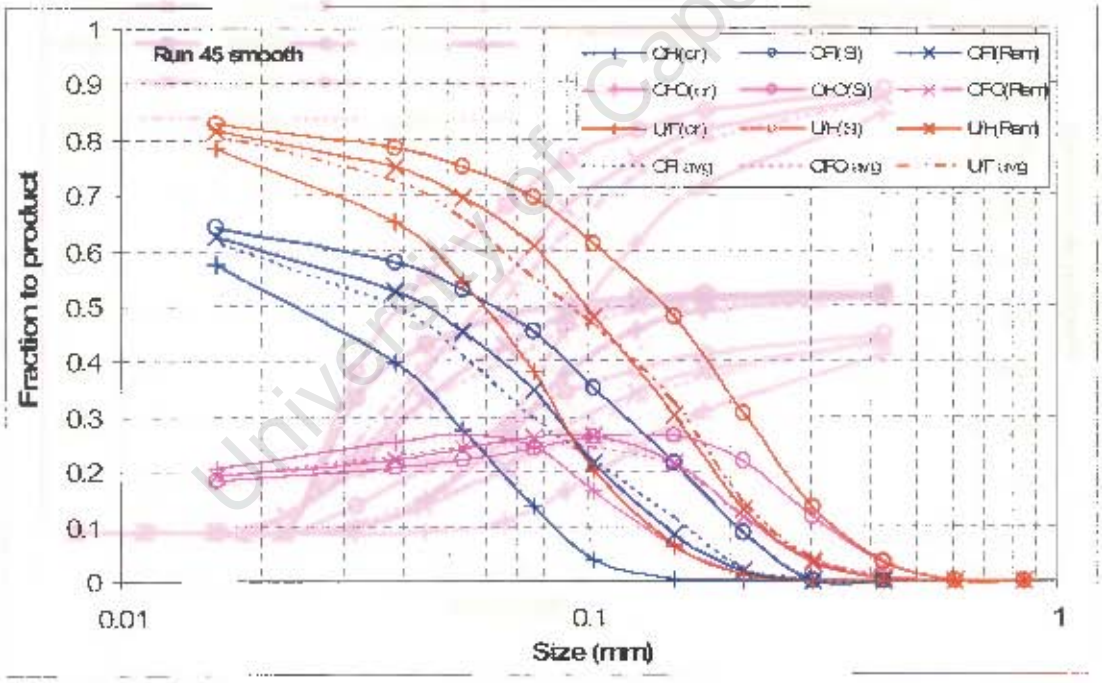
University of Cape Town



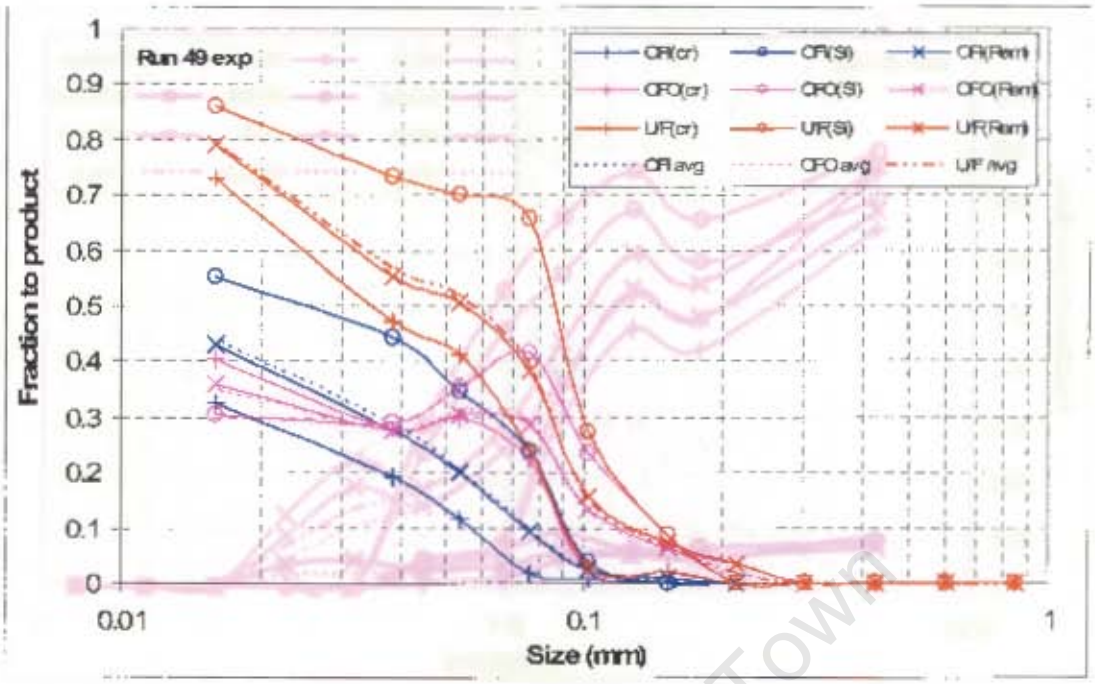


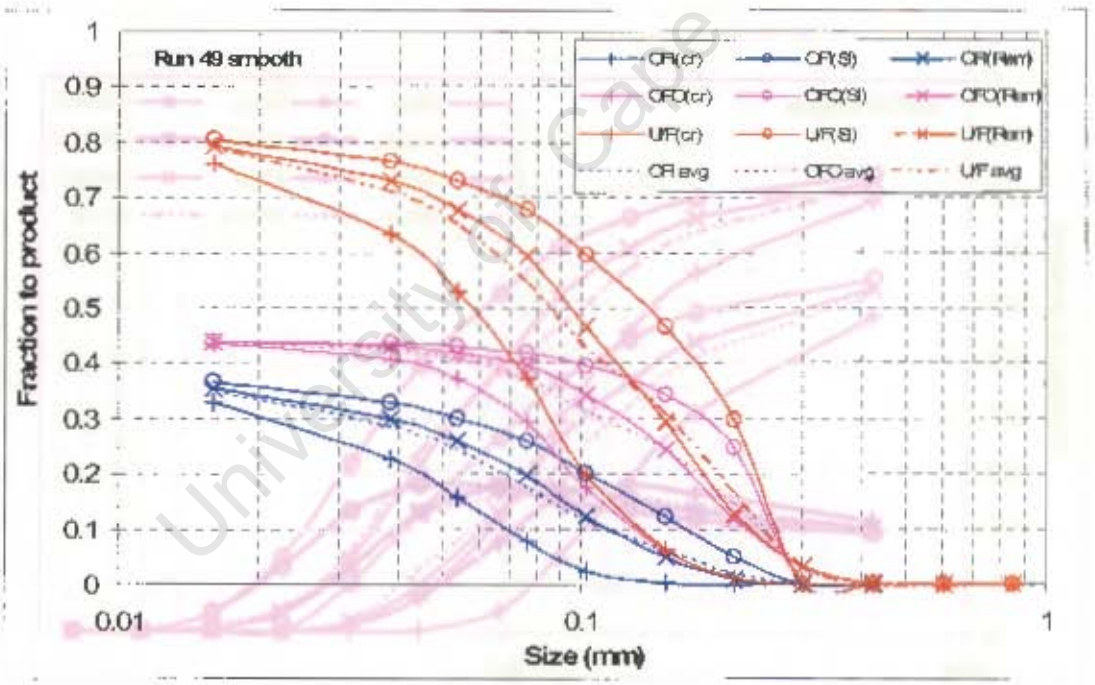
University of Cape Town



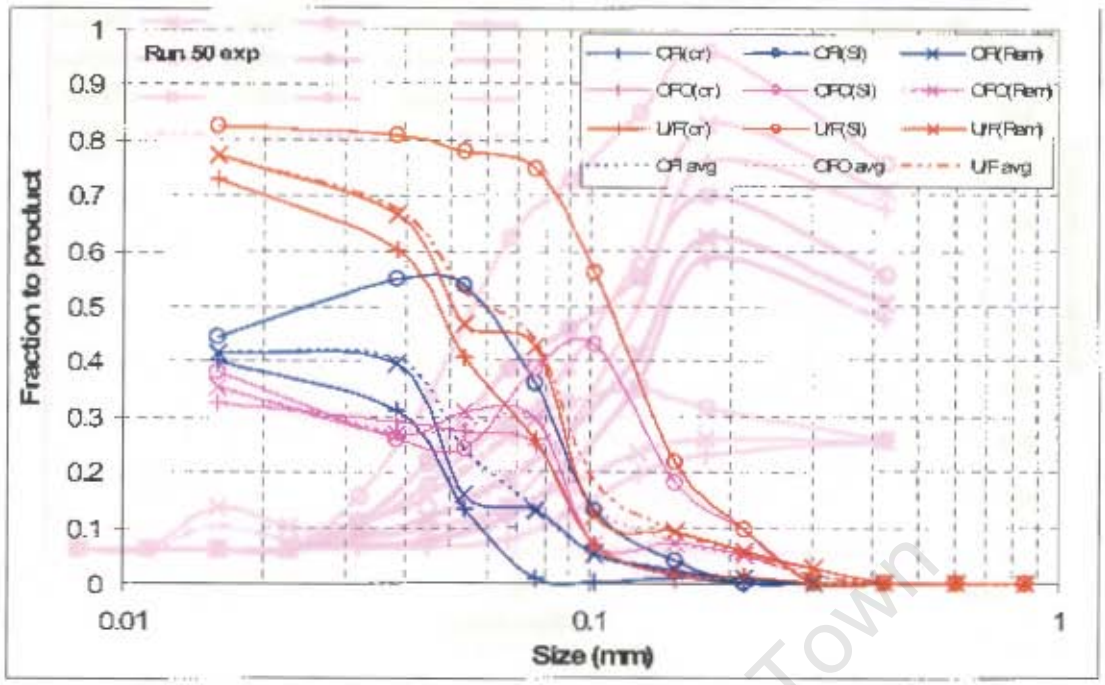


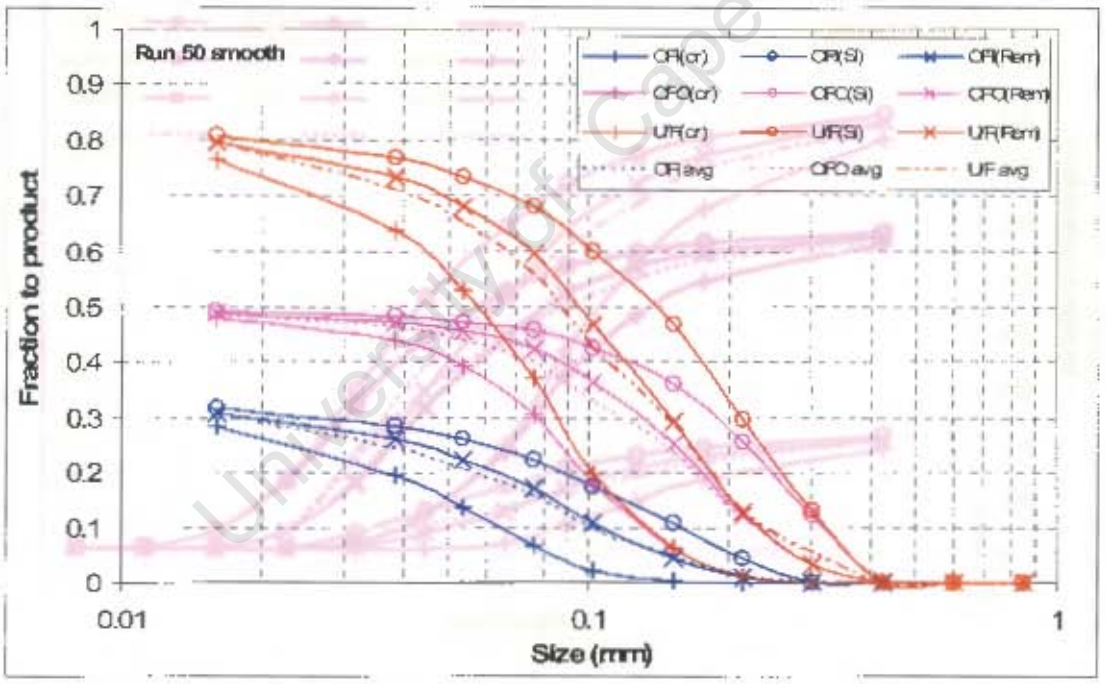
University of Cape Town



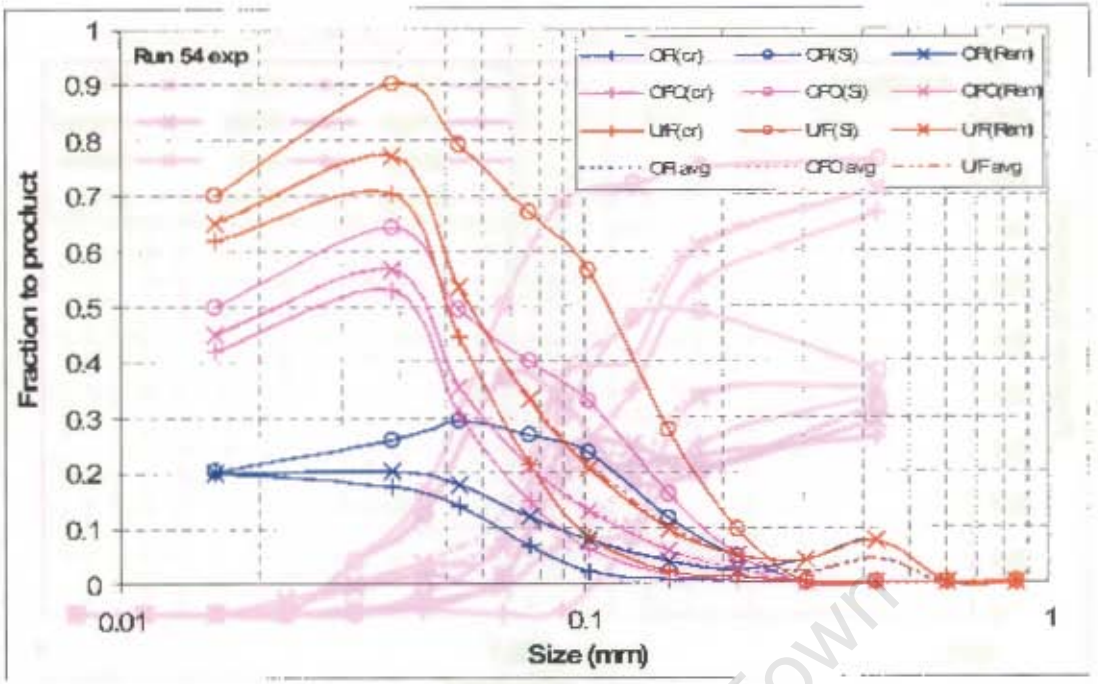


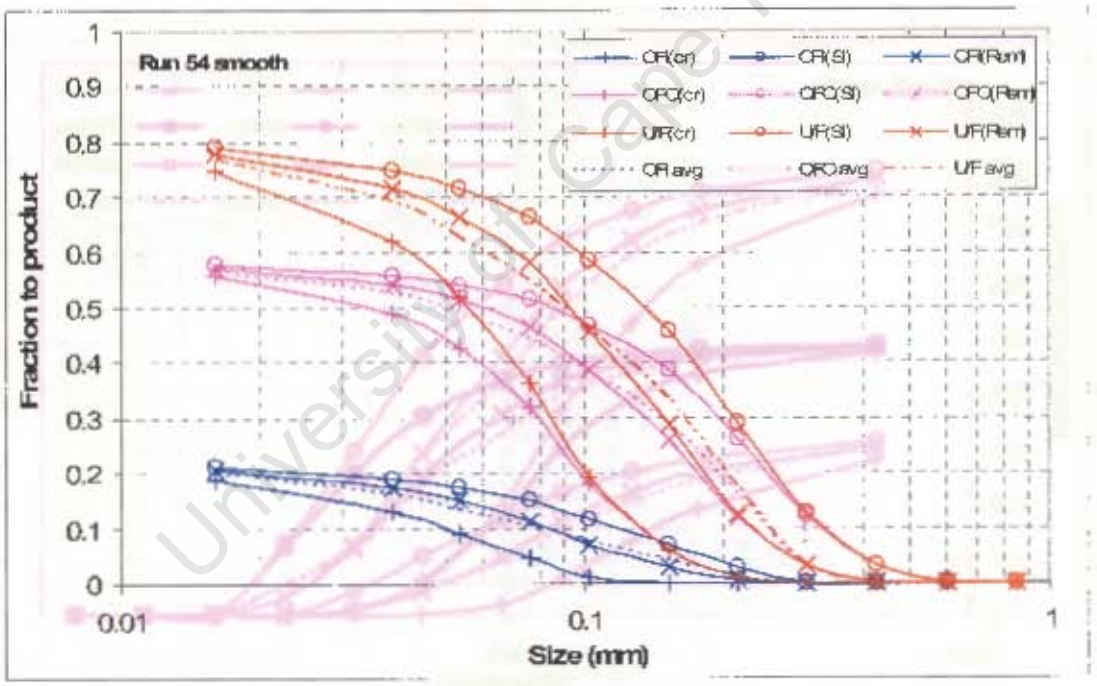
University of Cape Town



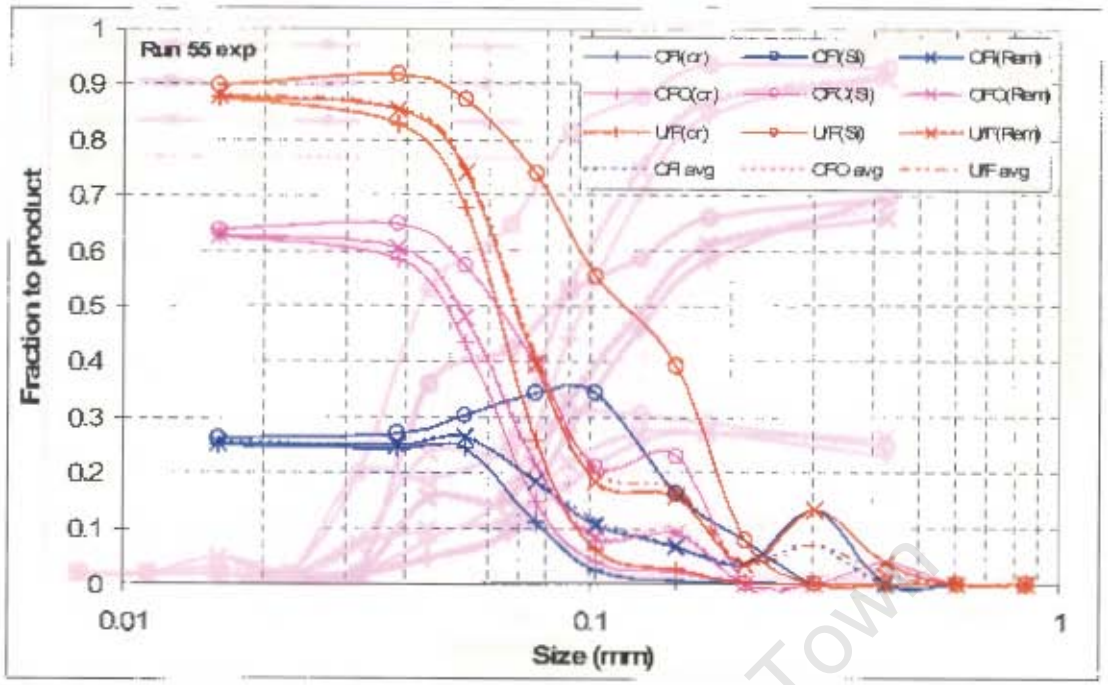


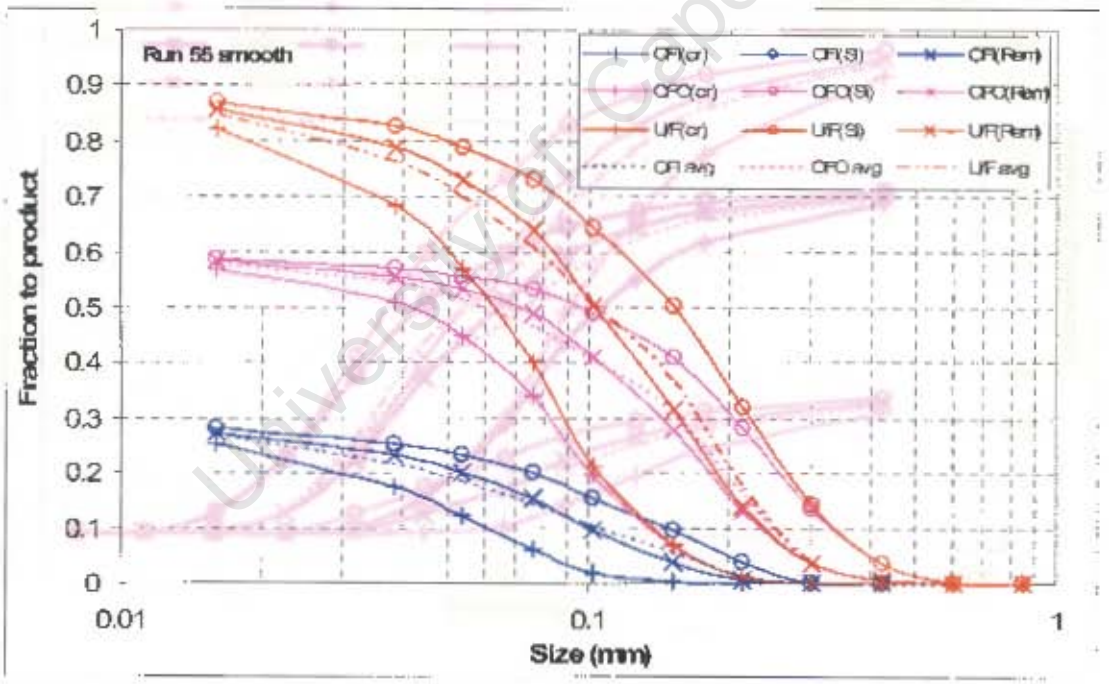
University of Cape Town



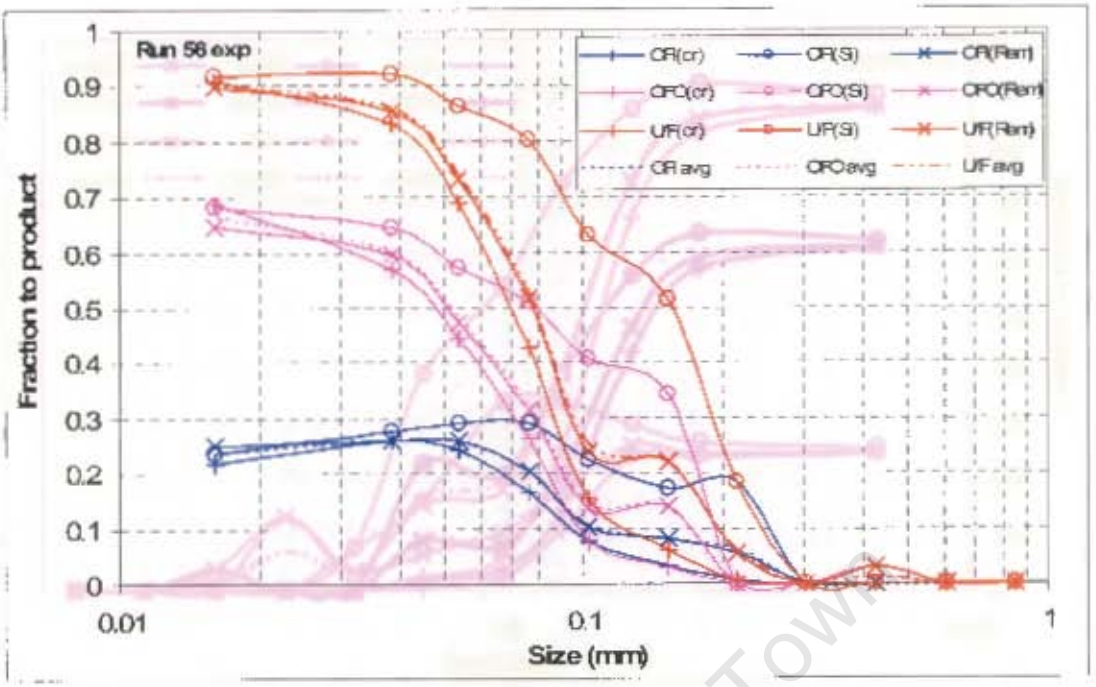


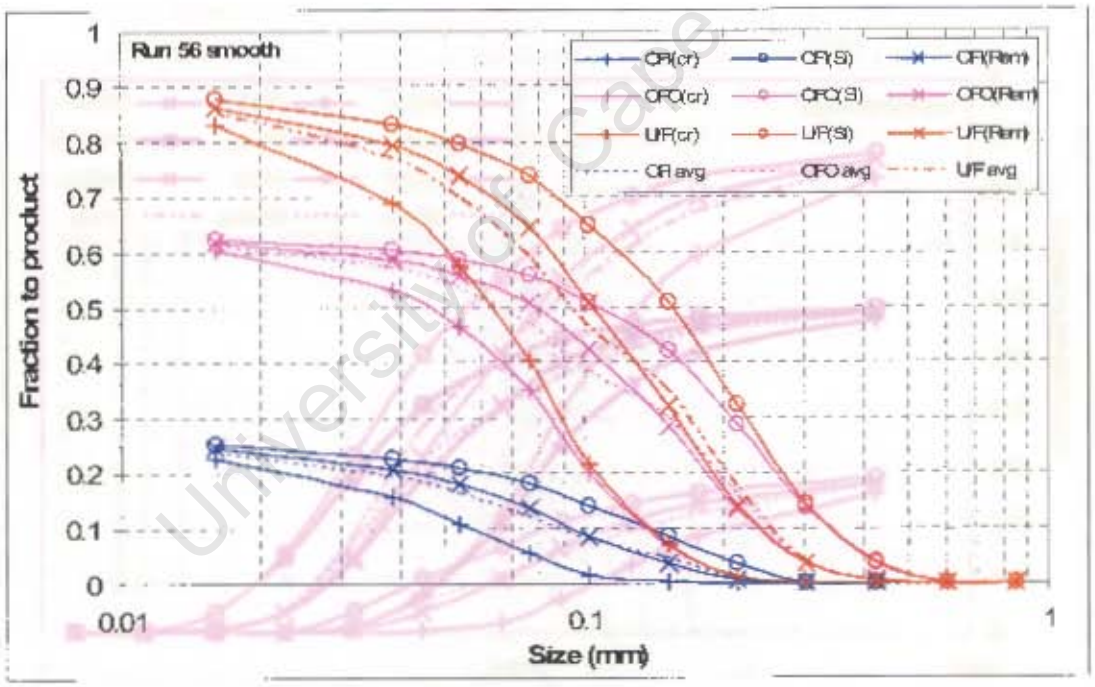
University of Cape Town



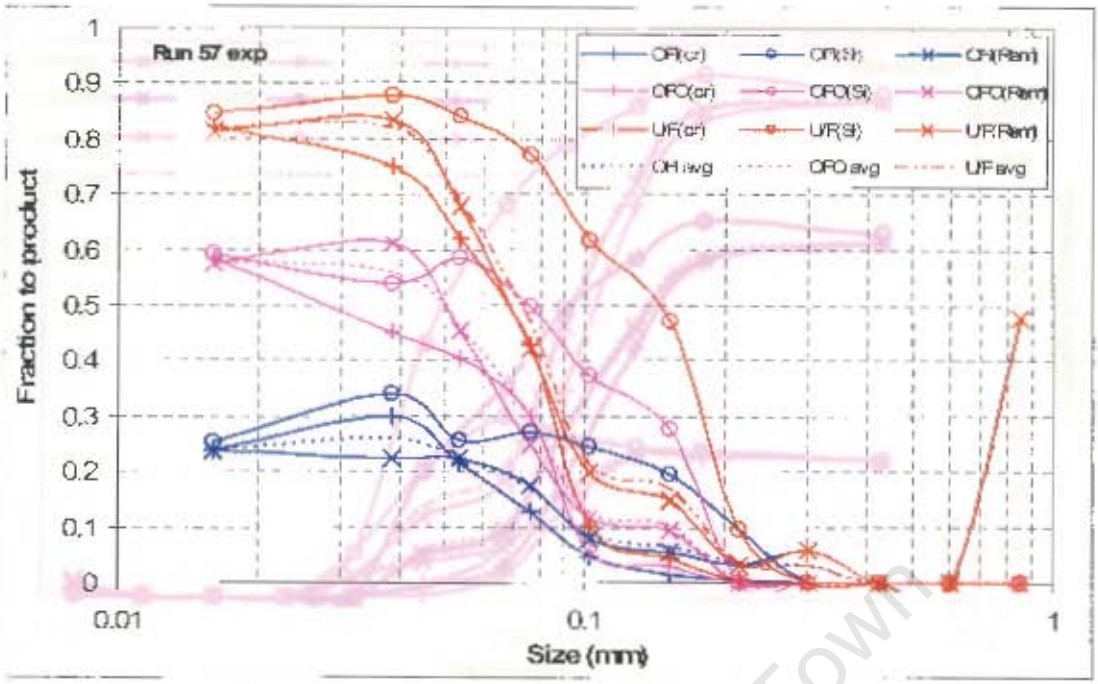


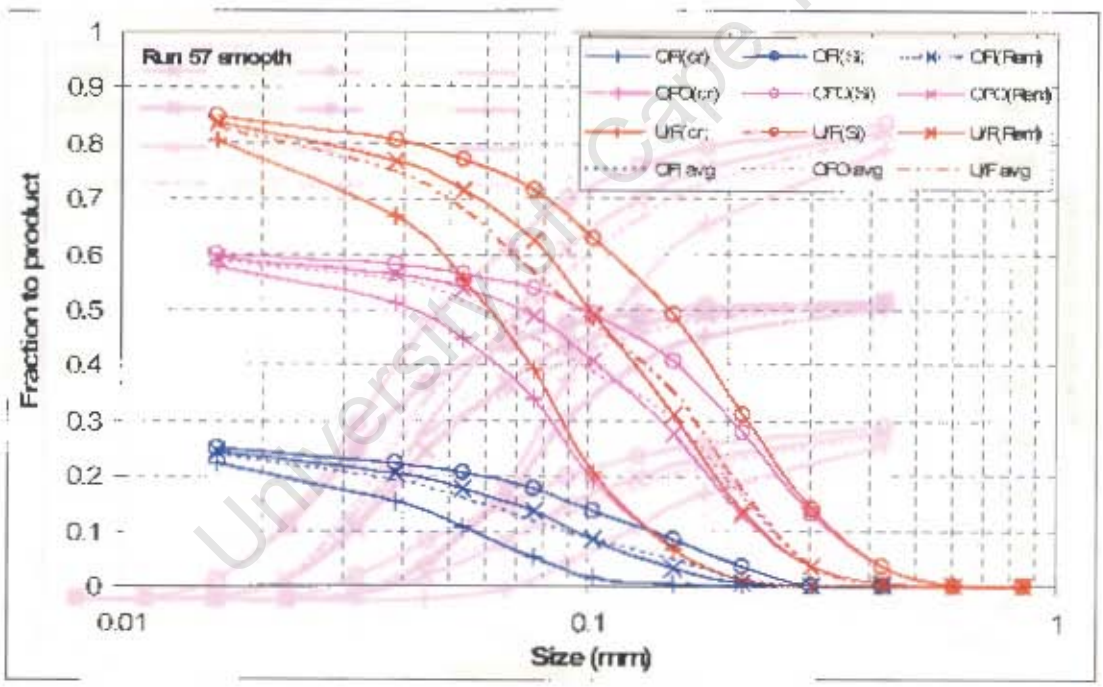
University of Cape Town



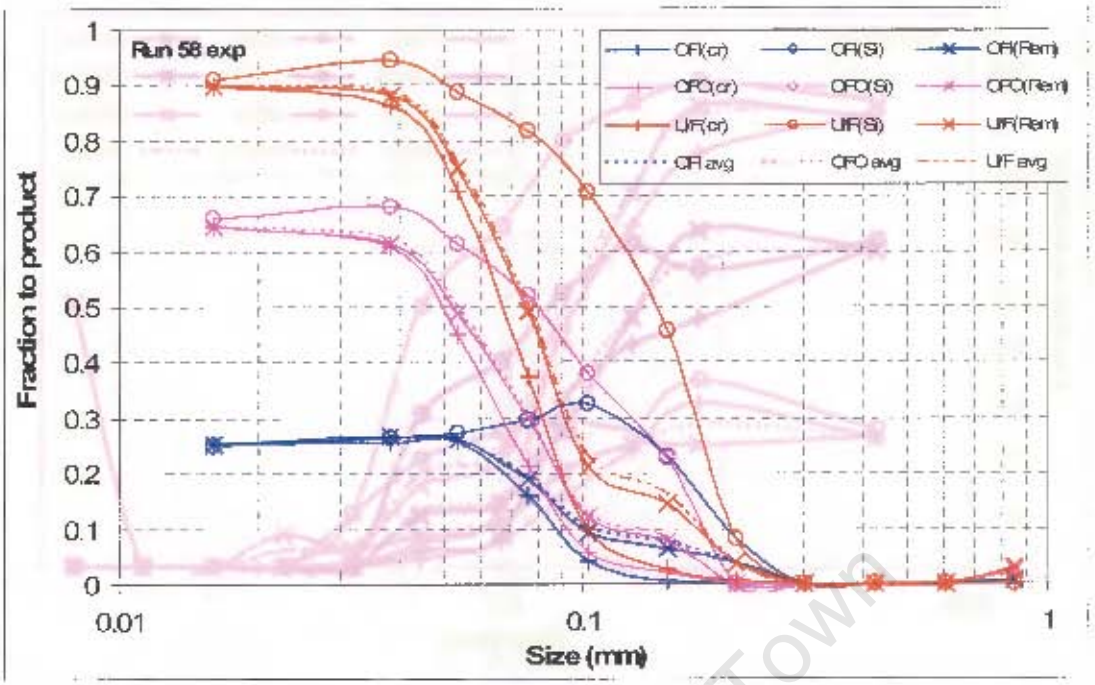


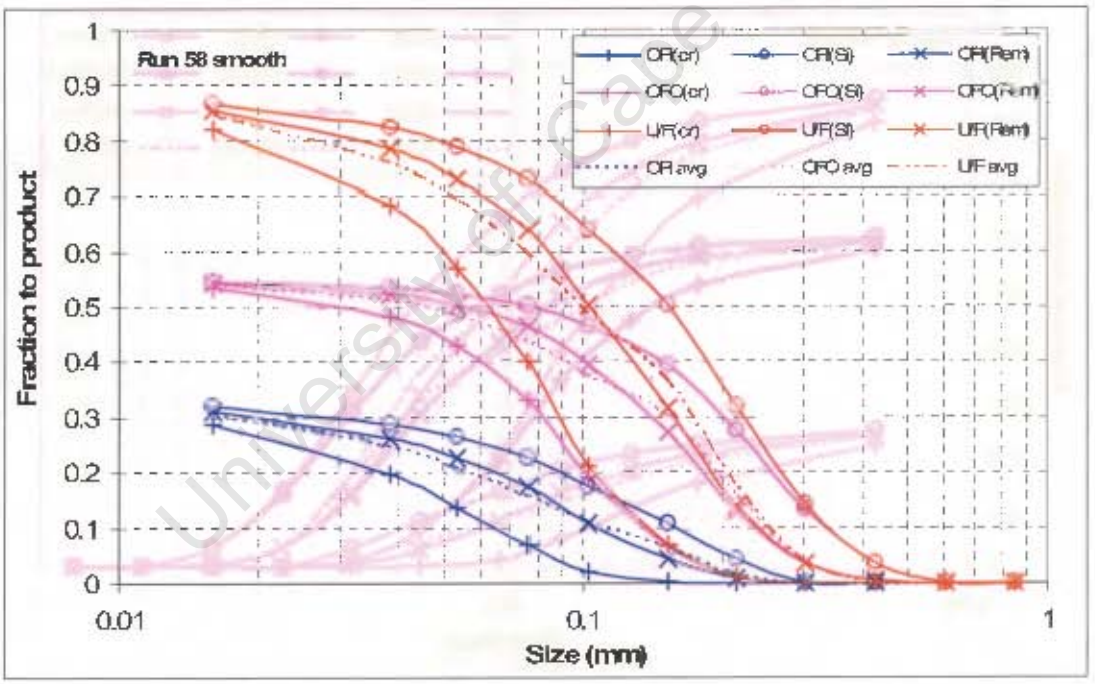
University of Cape Town



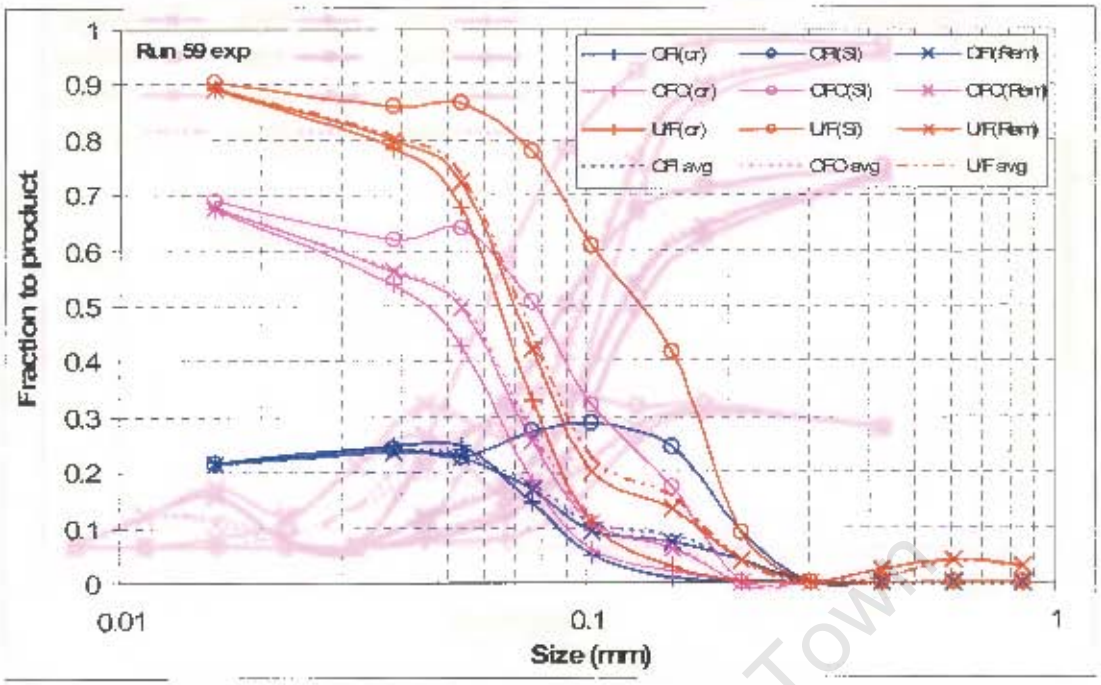


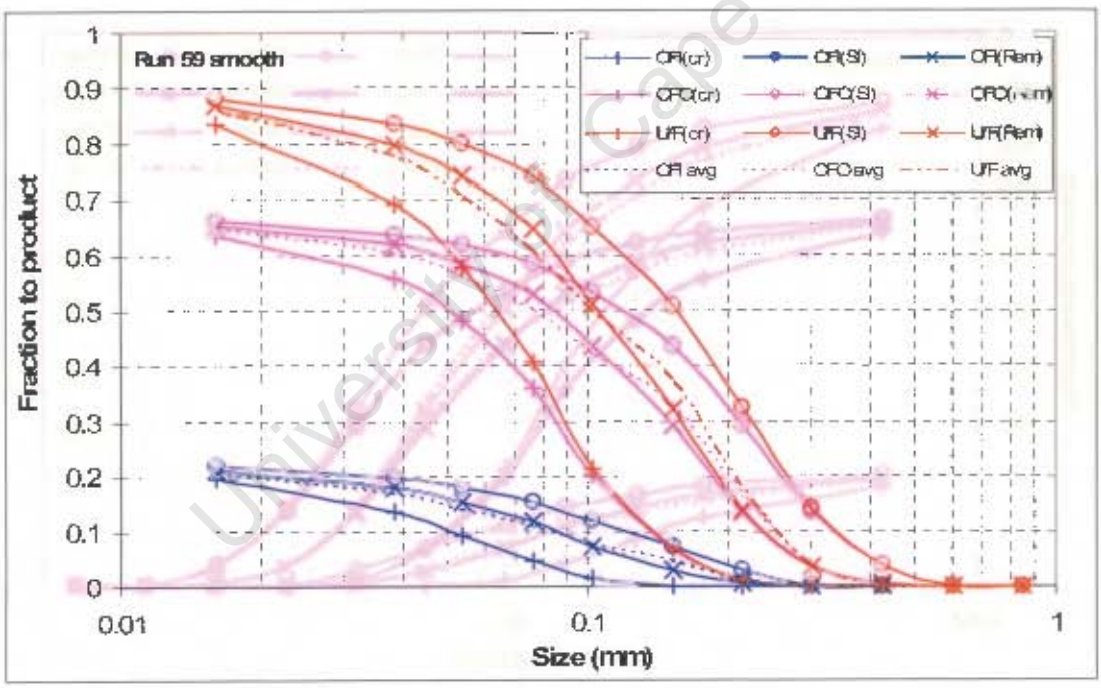
University of Cape Town



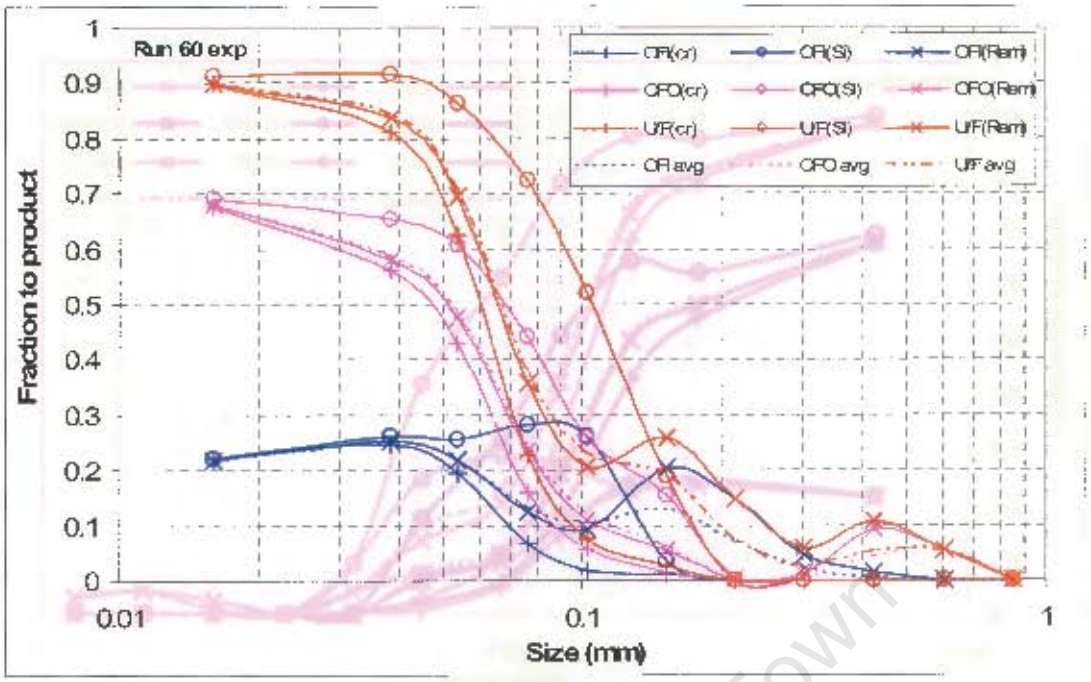


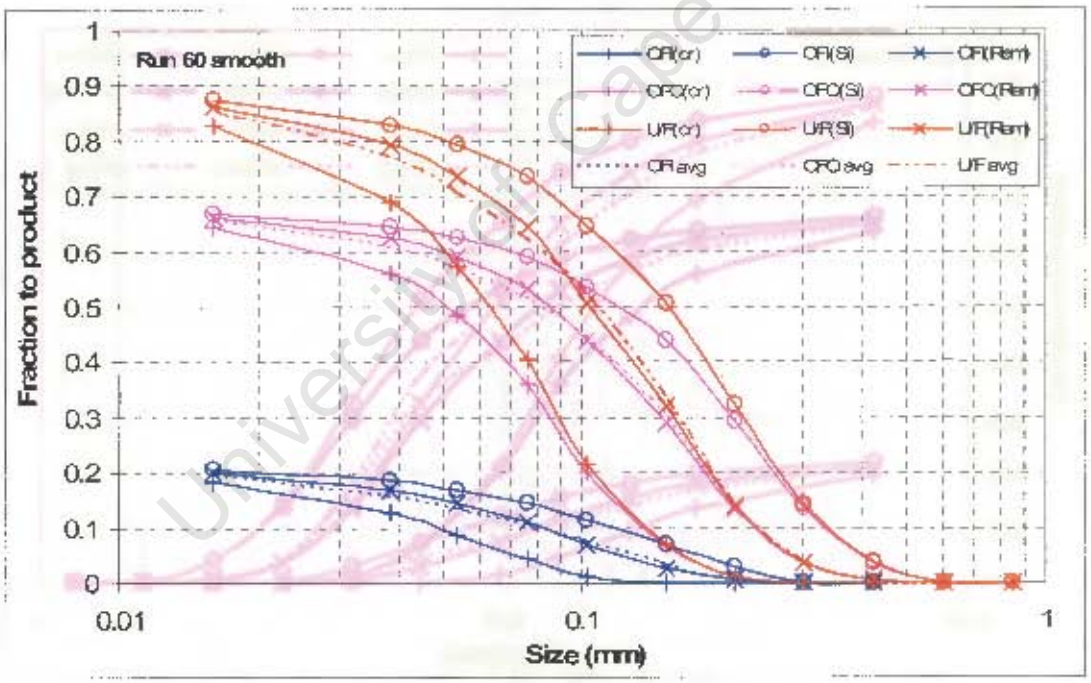
University of Cape Town



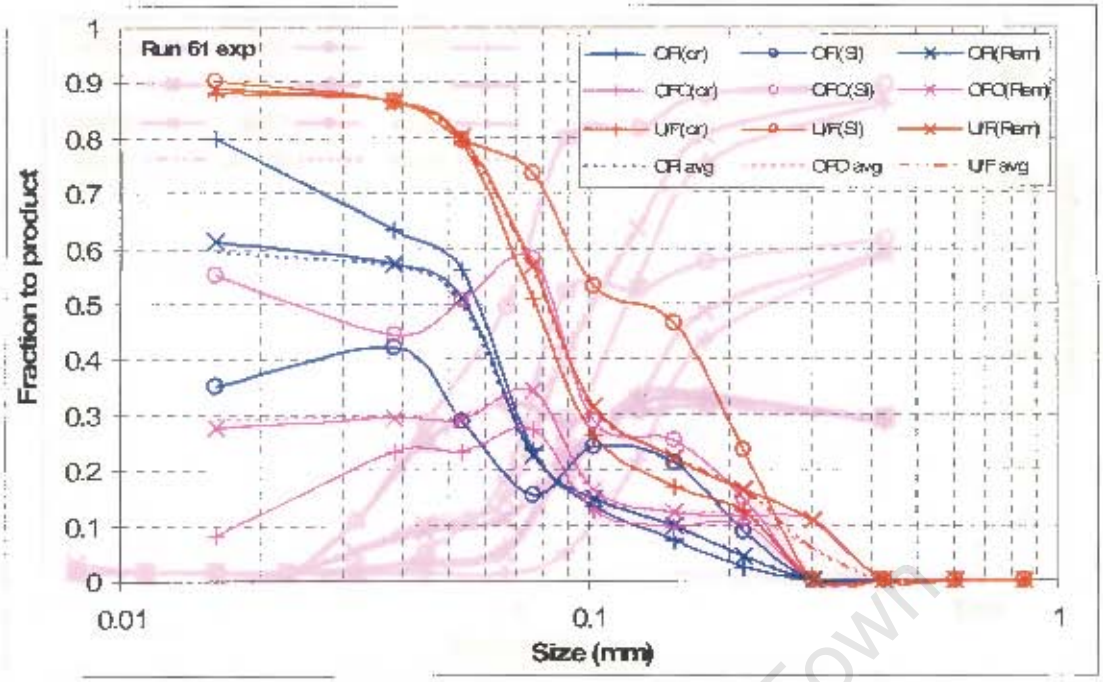


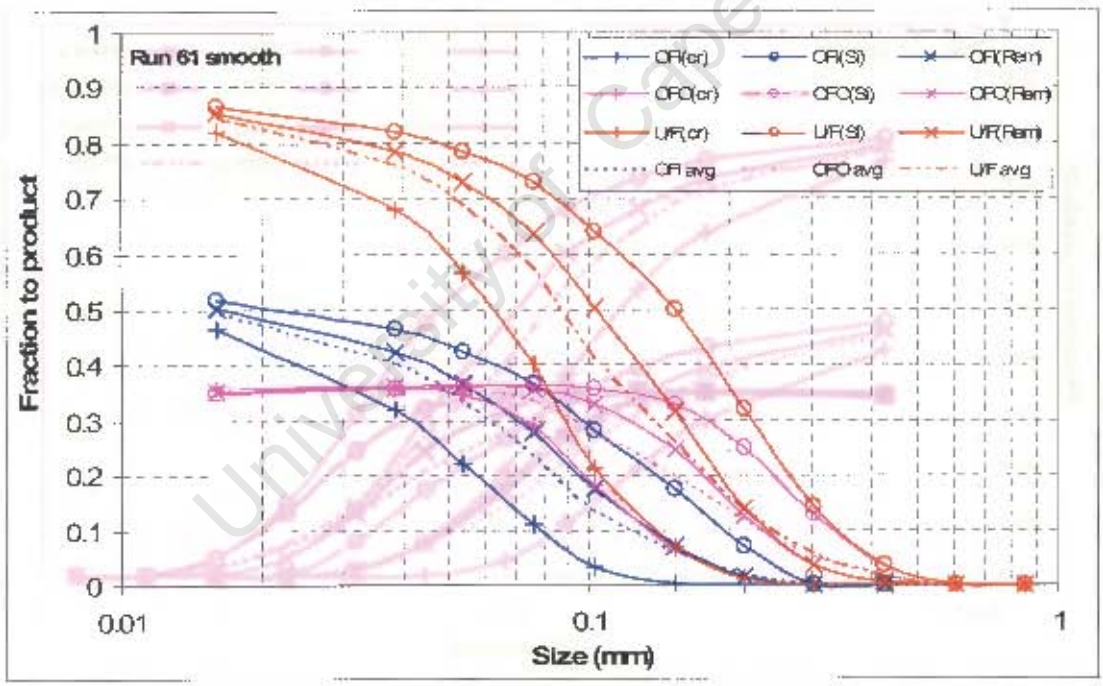
University of Cape Town



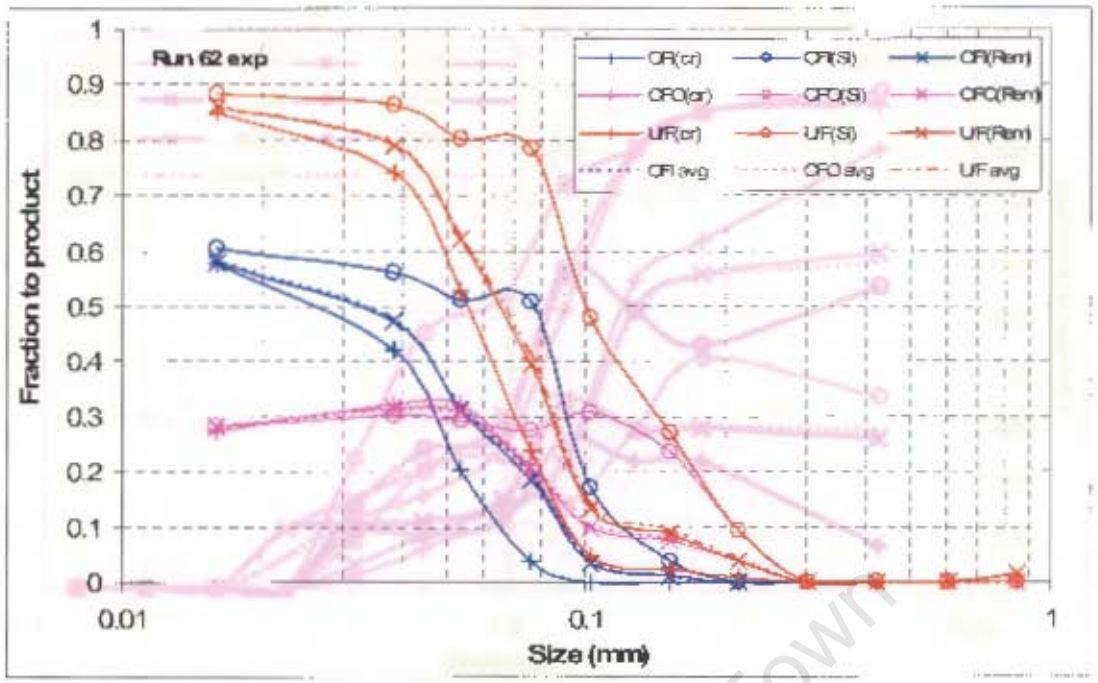


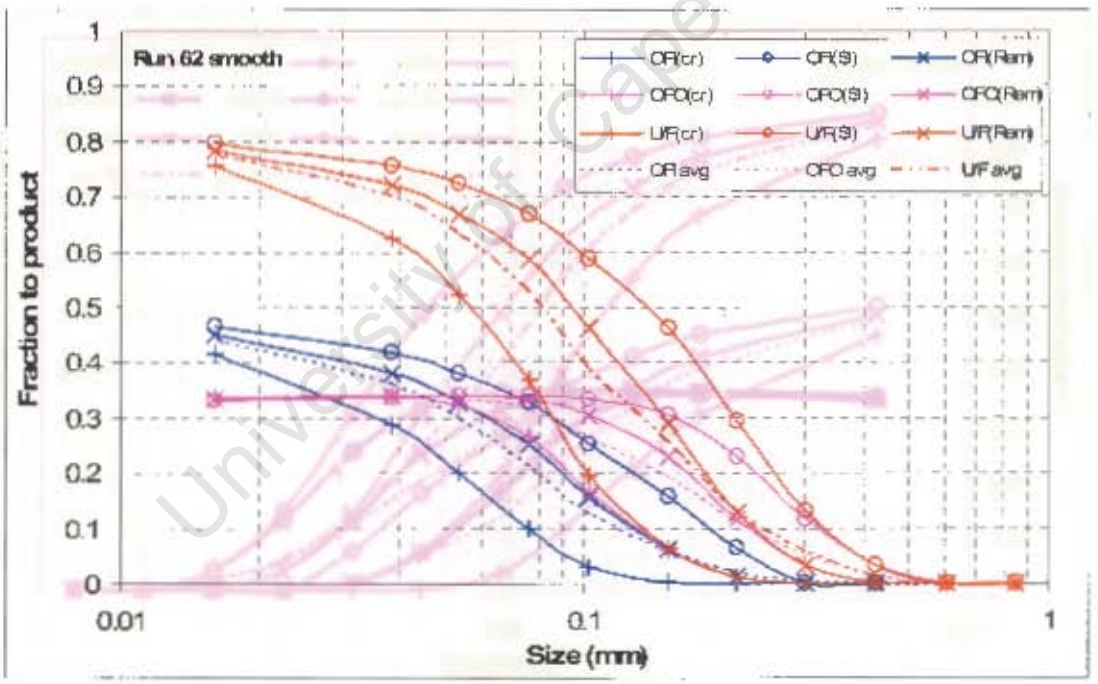
University of Cape Town



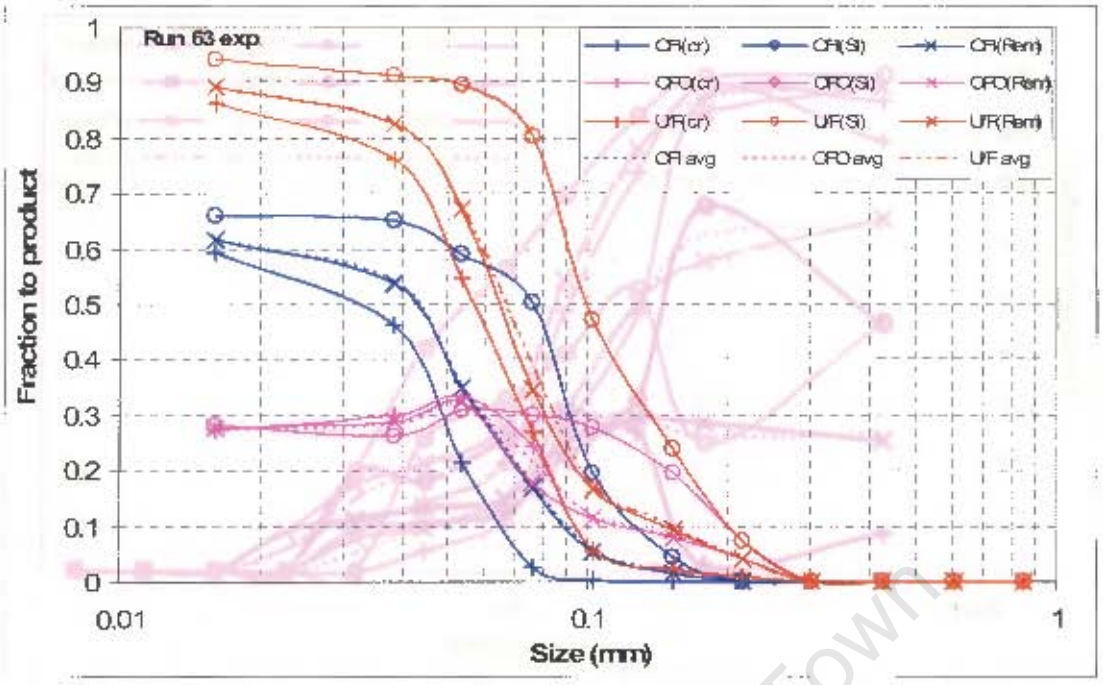


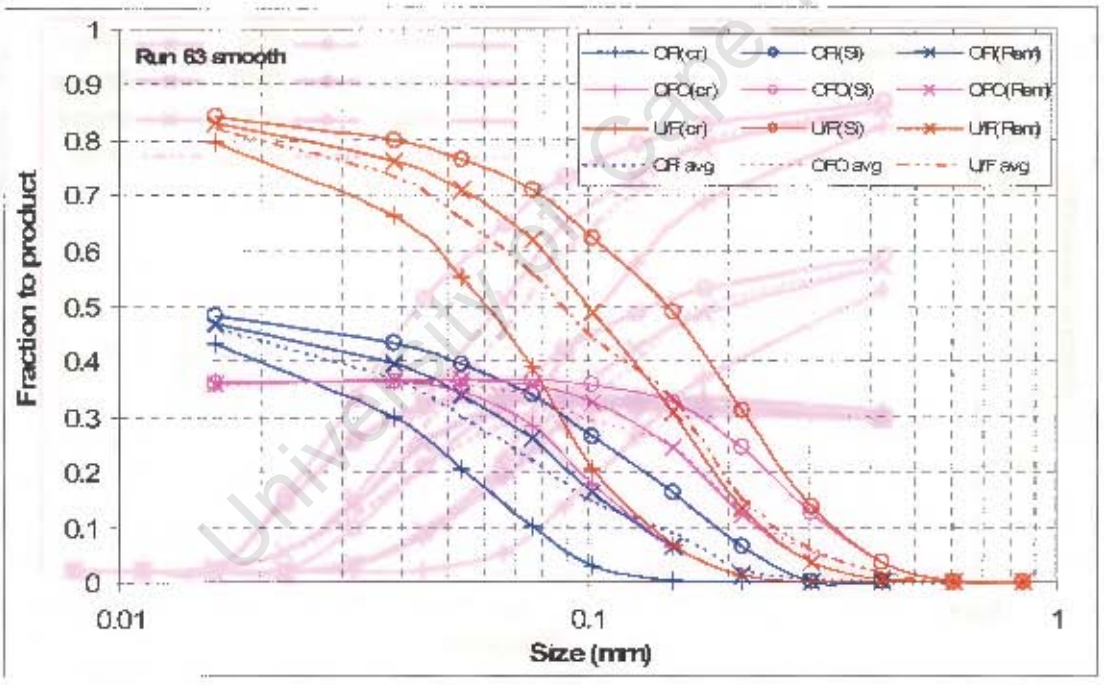
University of Cape Town



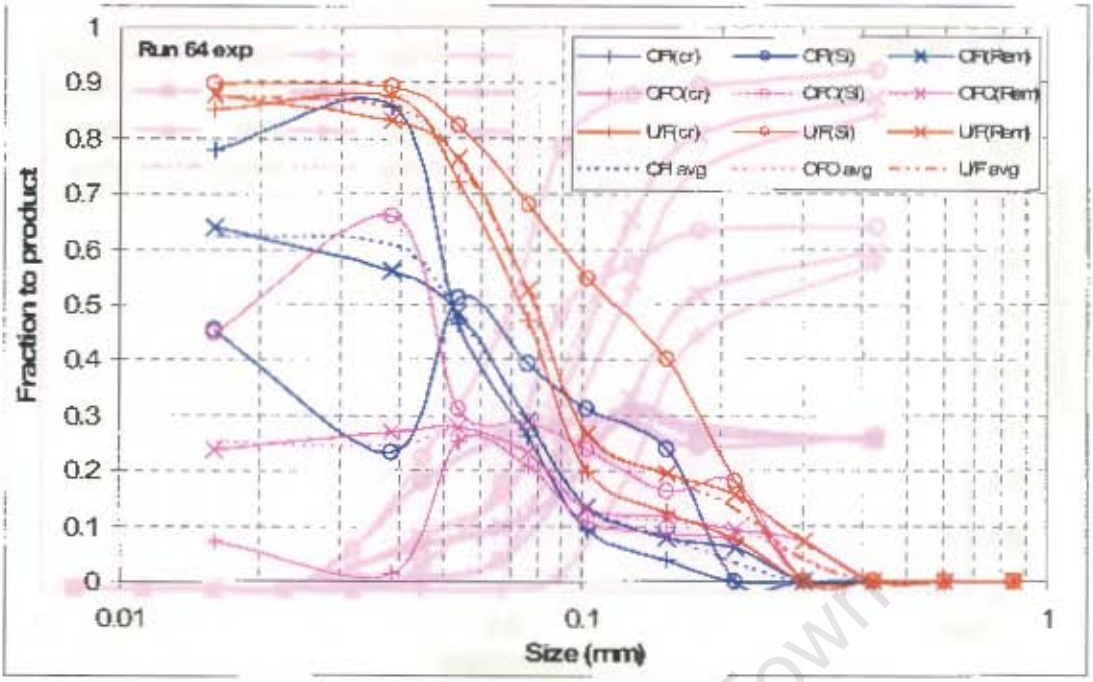


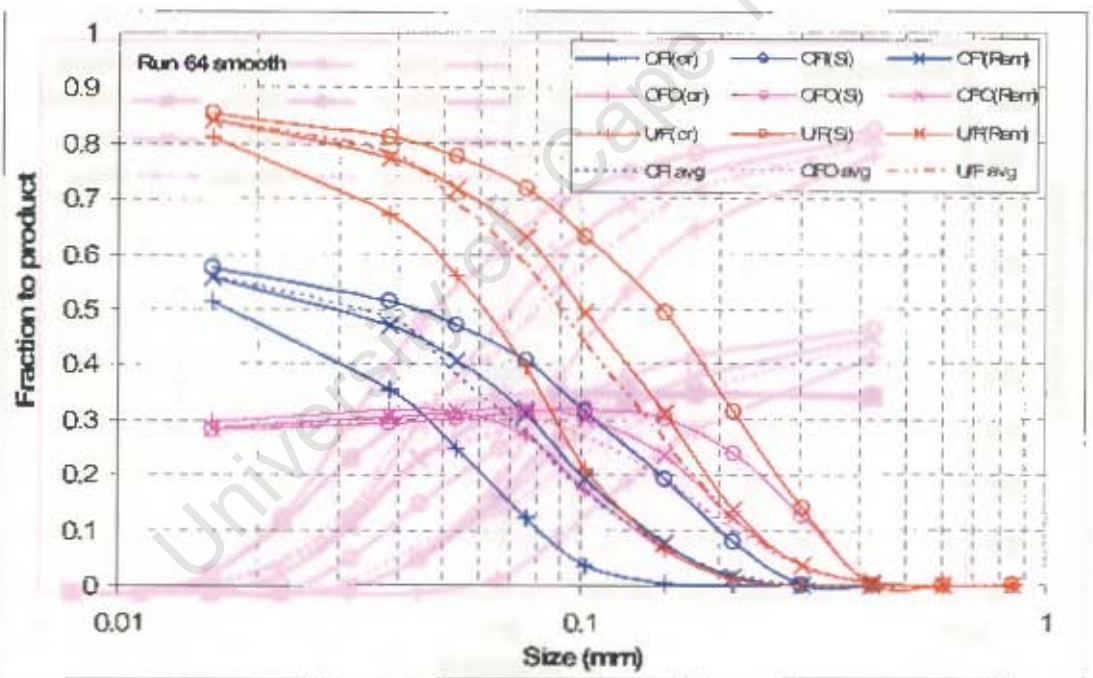
University of Cape Town



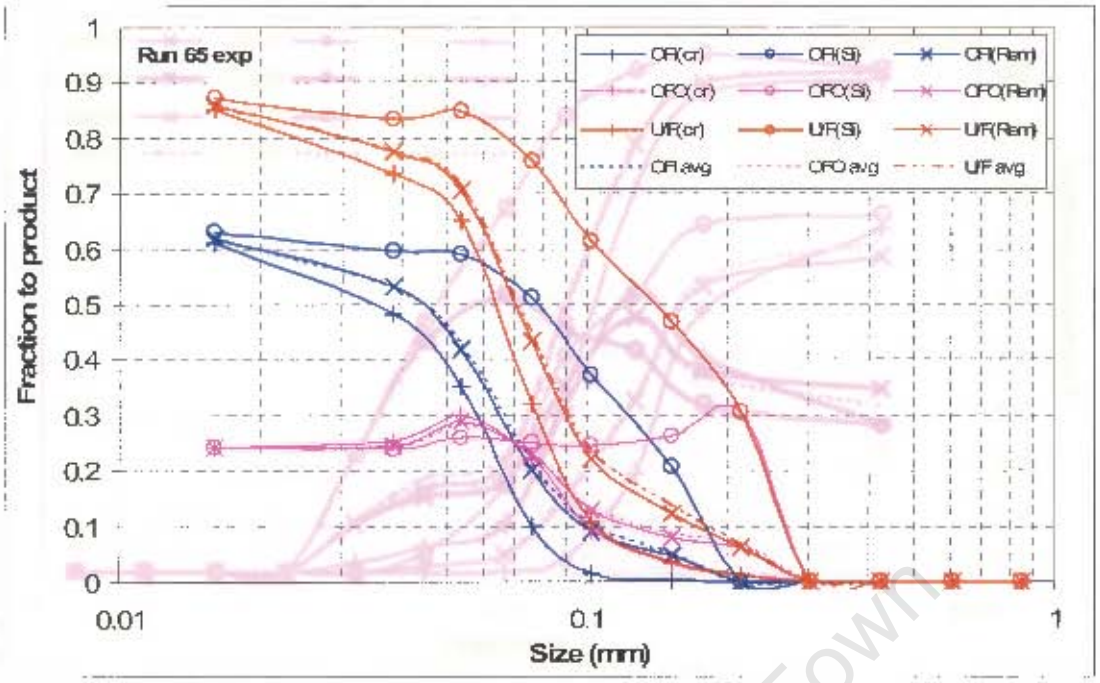


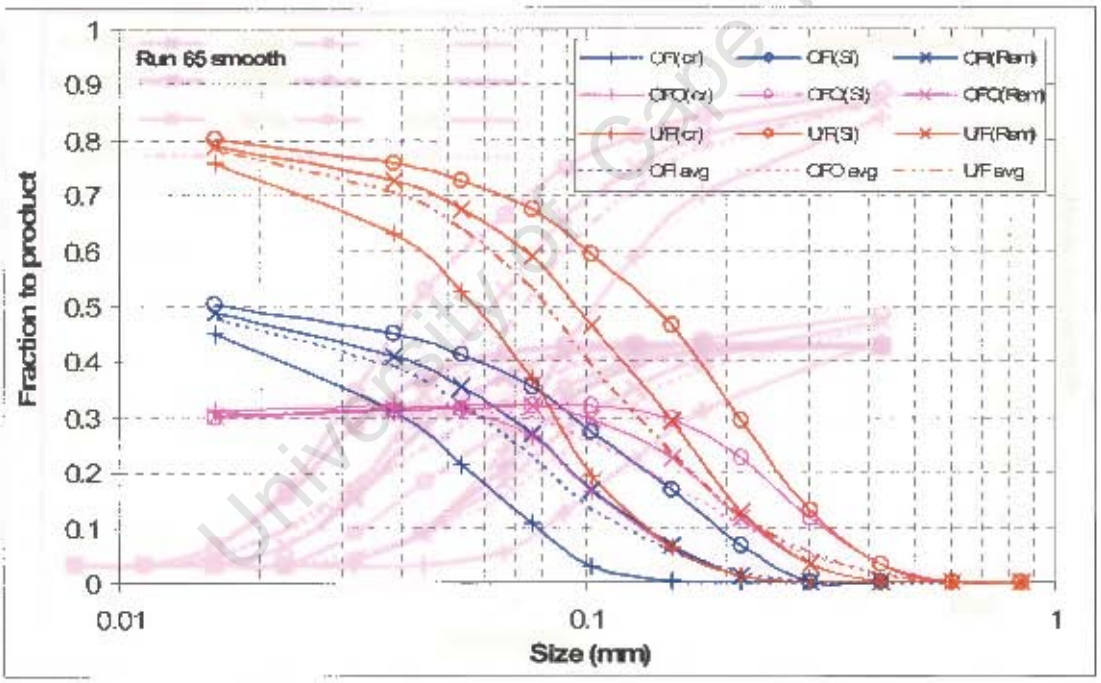
University of Cape Town



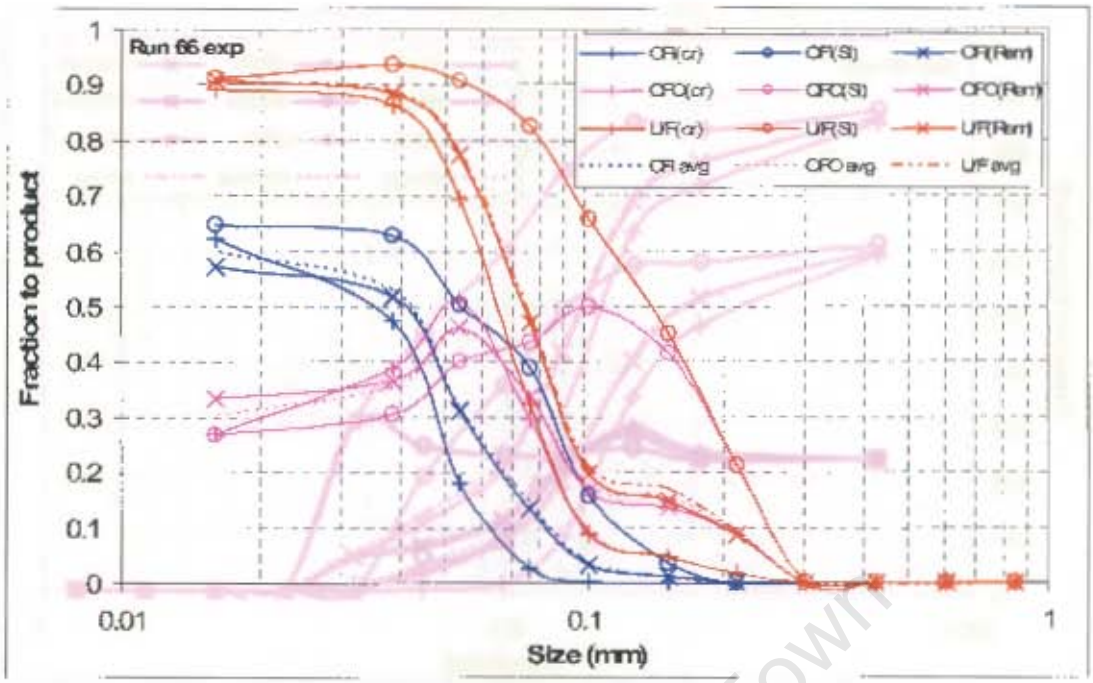


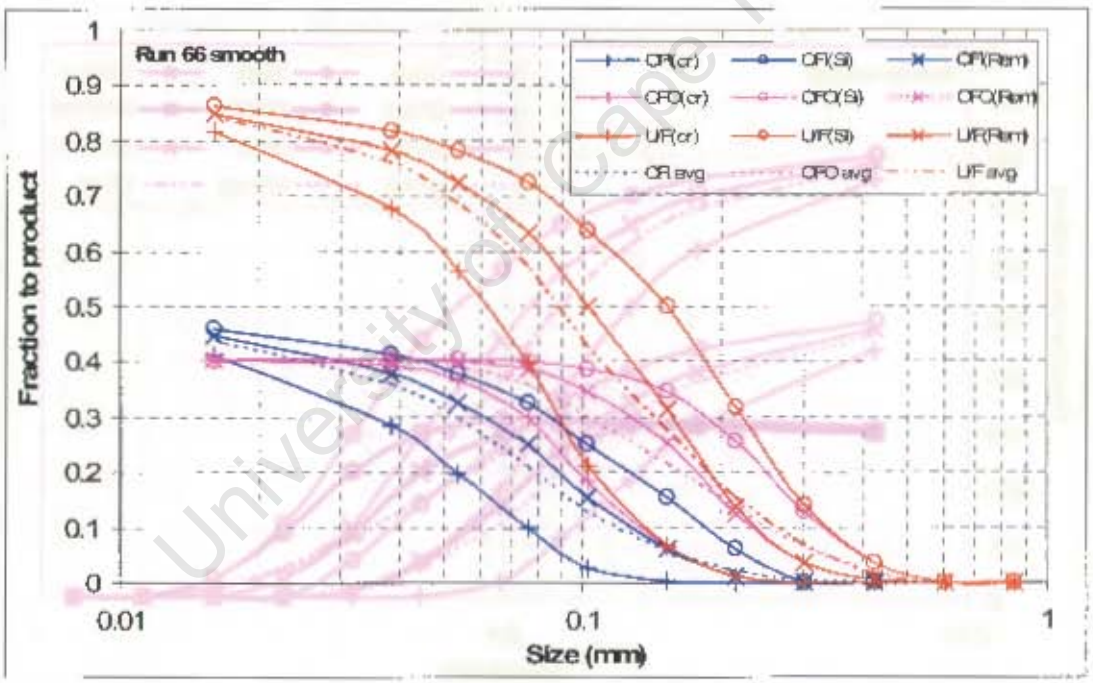
University of Cape Town



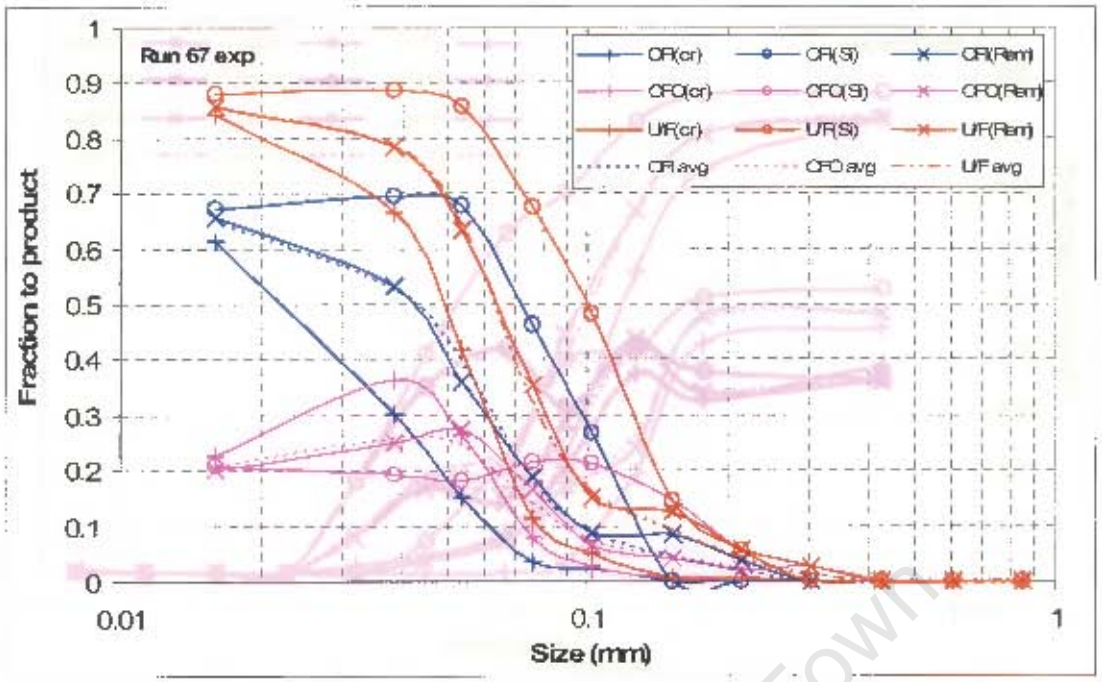


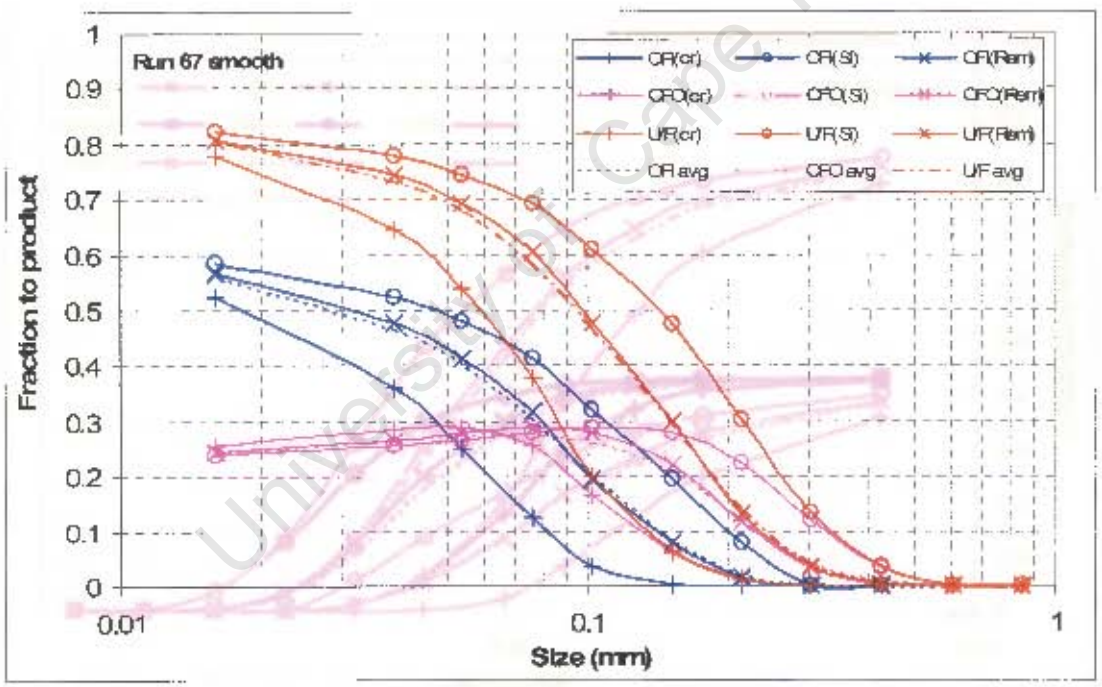
University of Cape Town



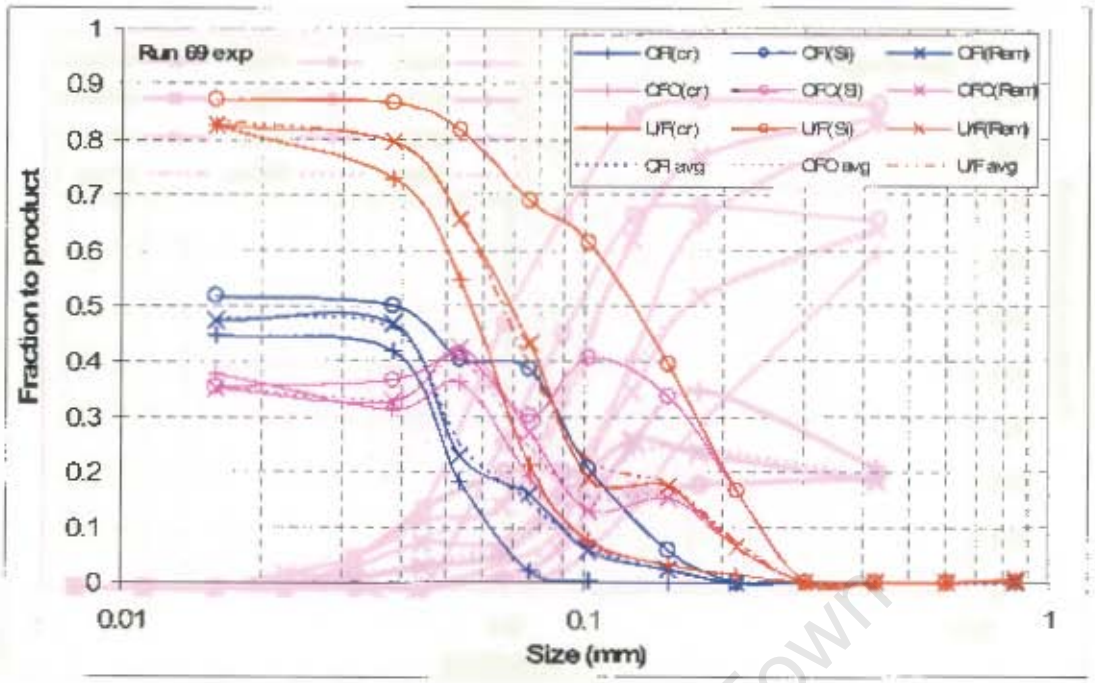


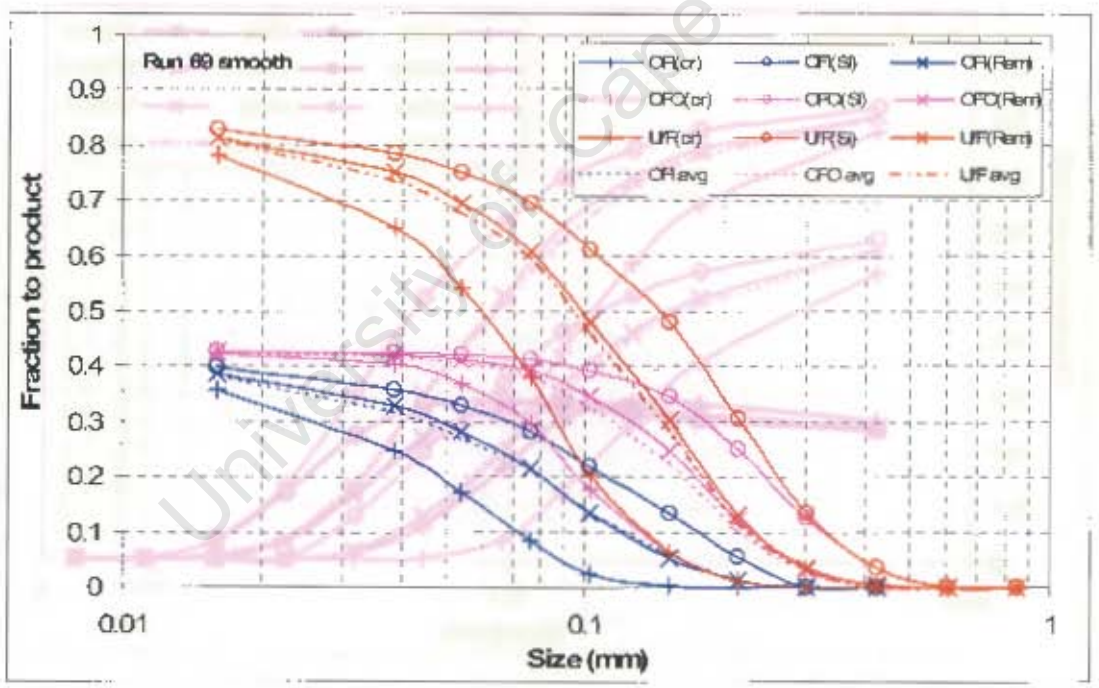
University of Cape Town



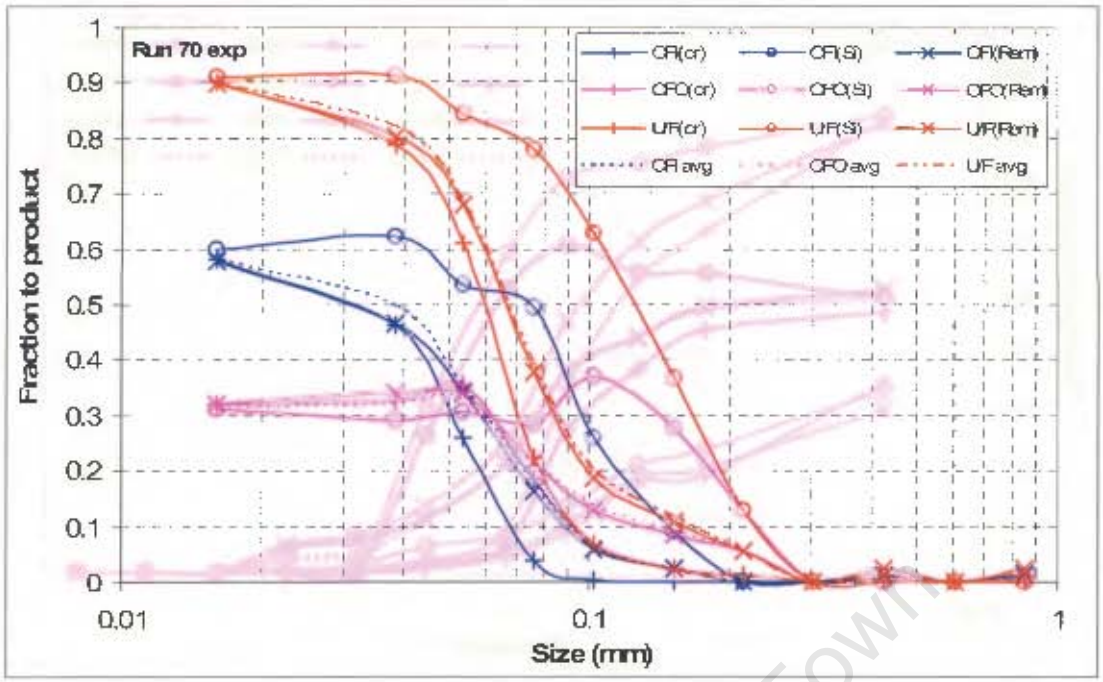


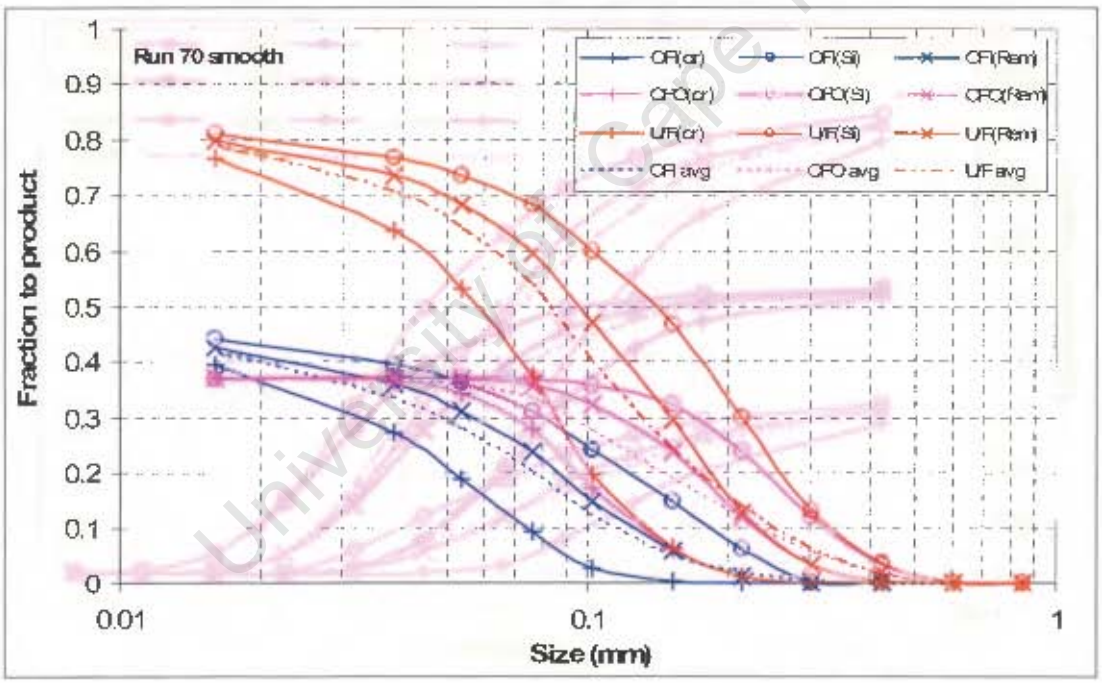
University of Cape Town



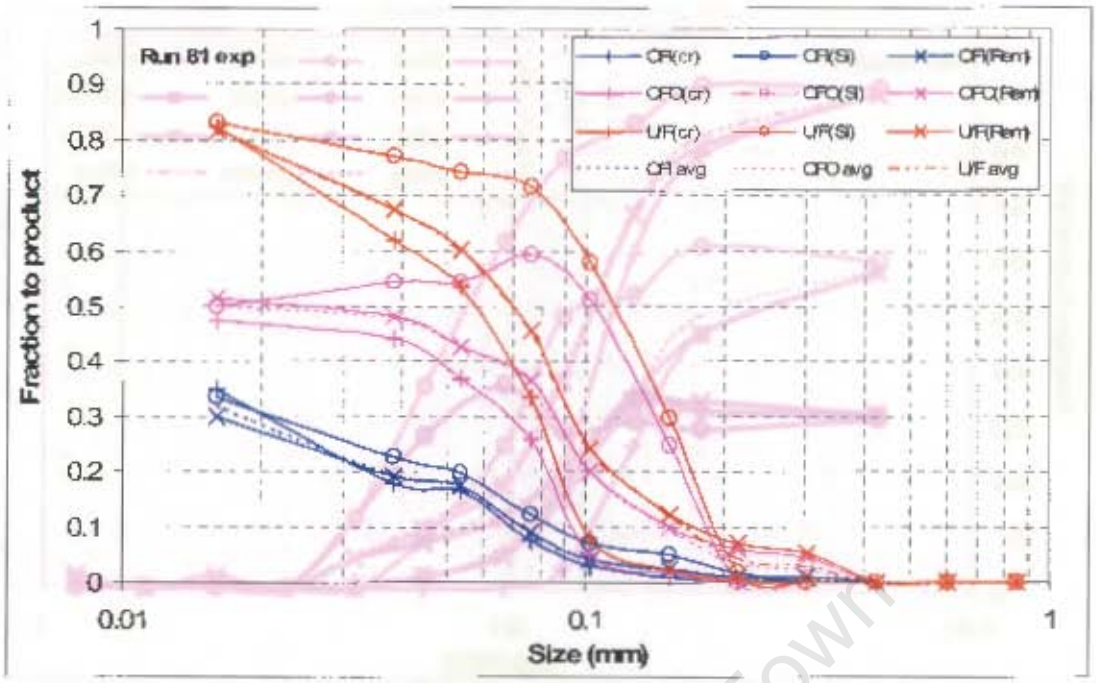


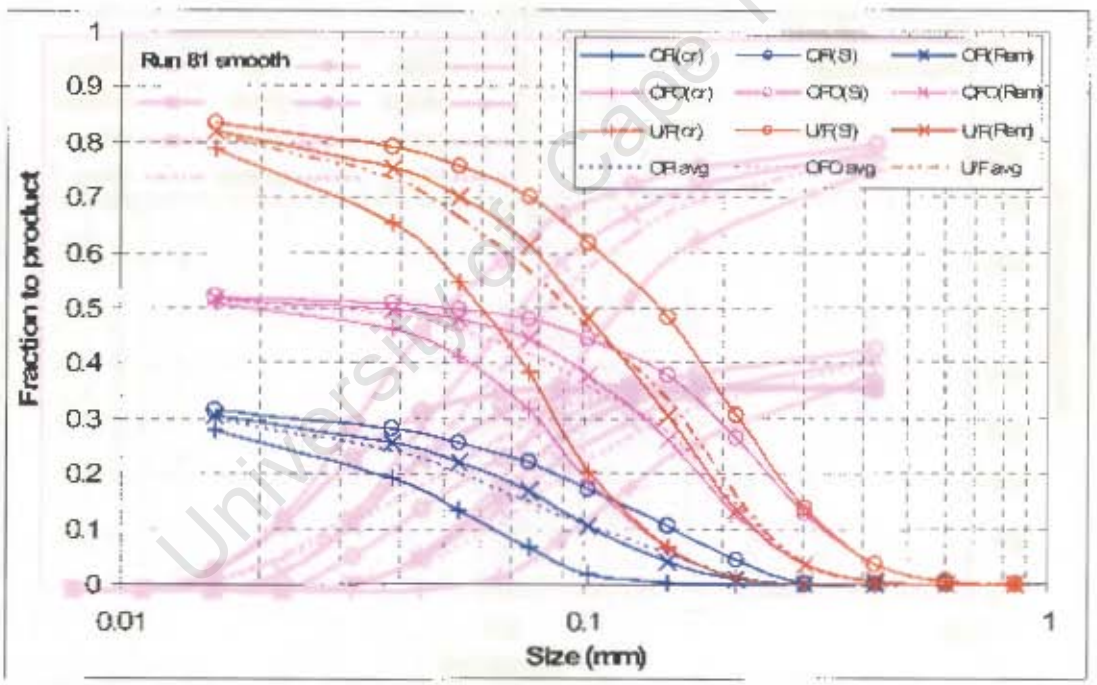
University of Cape Town



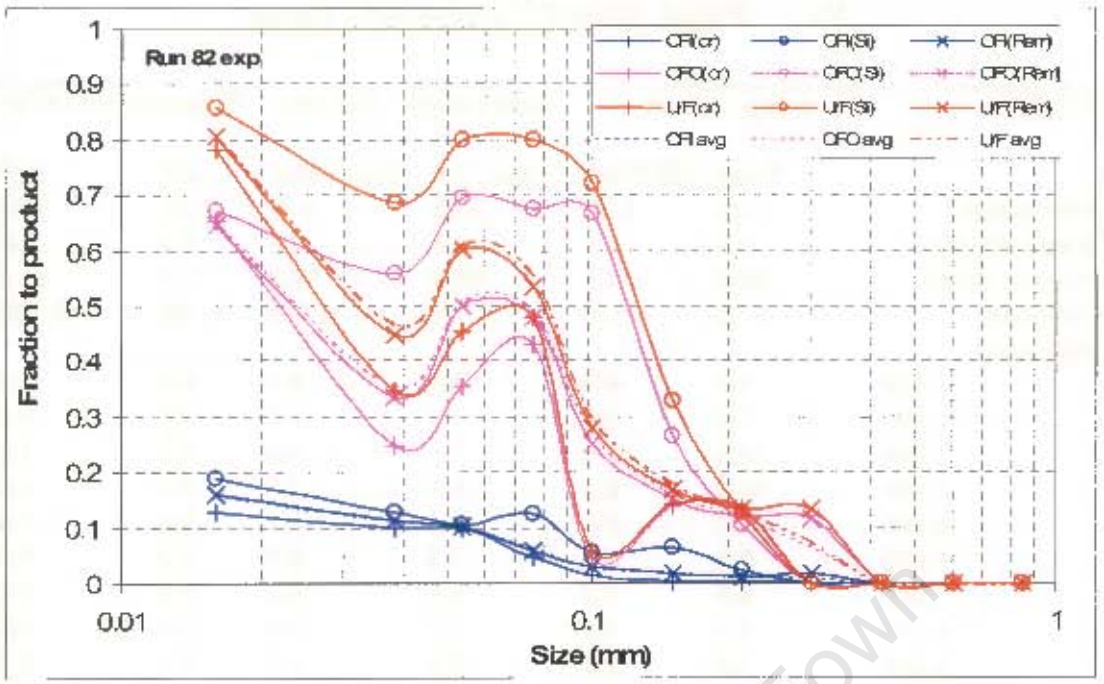


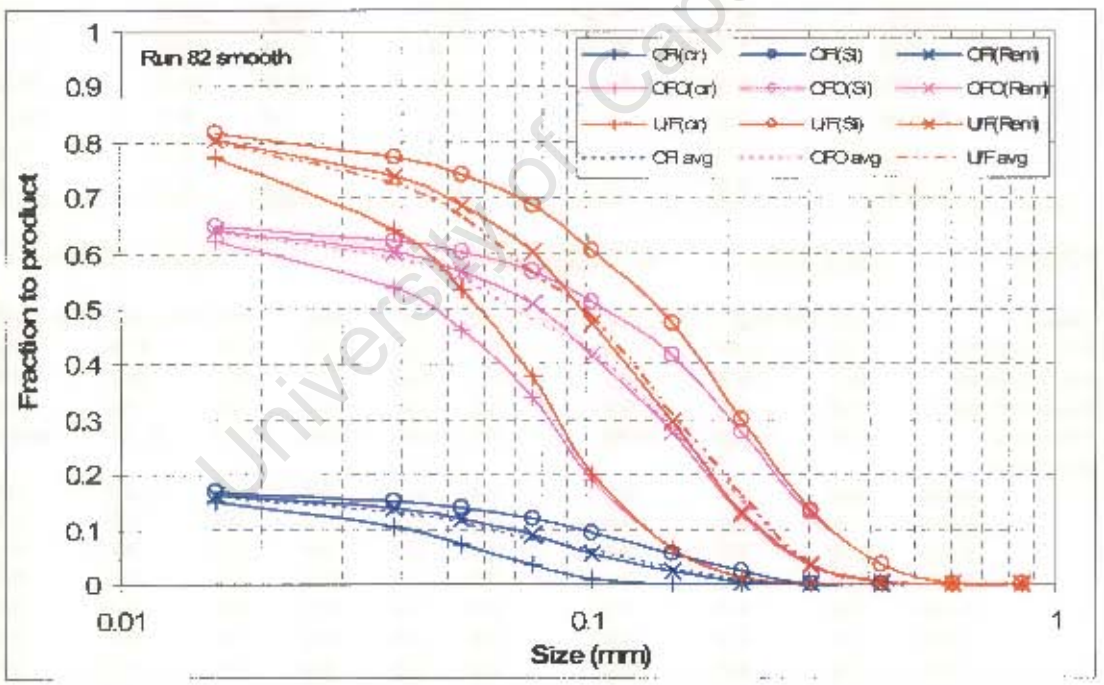
University of Cape Town





University of Cape Town





University of Cape Town

D. Pilot plant Testwork data

PTND 2	Dspig - 12 mm		Cone Length - 210 mm		Pressure - 122 kPa	
	Feed	Mill Prod.	Scn. O/S	Cyc. Feed	U/F	O/F
TPH Solids	1.02	3.69	0.20	3.49	2.47	1.02
Solids SG (t/m³)	3.8	3.8	3.8	3.8	3.8	3.8
Percent Solids	99.2	71.3	89.8	52.3	72.3	31.4
P80 (mm)	4.12	0.179	2.146	0.169	0.189	0.108
Size (mm)						
8.000	0.0	0.0	0.0	0.0	0.0	0.0
5.600	7.2	0.2	3.4	0.0	0.0	0.0
4.000	14.3	0.4	7.3	0.0	0.0	0.0
2.800	10.0	0.4	6.1	0.0	0.0	0.0
2.000	4.9	0.2	4.2	0.0	0.0	0.0
1.400	3.6	0.2	3.3	0.0	0.0	0.0
1.000	2.8	0.2	3.6	0.0	0.0	0.0
0.710	2.1	0.2	2.7	0.0	0.0	0.0
0.500	3.2	0.5	8.9	0.1	0.1	0.0
0.355	4.7	1.4	8.4	0.9	1.3	0.0
0.250	7.7	4.7	7.0	4.6	6.3	0.5
0.180	11.0	11.4	10.3	11.5	14.9	3.2
0.125	9.7	17.8	12.1	18.2	22.0	9.0
0.090	7.4	21.4	11.5	22.0	23.9	17.6
0.063	5.3	16.3	6.5	16.9	15.6	19.9
0.045	1.5	7.4	1.7	7.7	5.1	14.2
0.032	1.4	4.1	1.2	4.2	2.7	7.9
0.000	3.2	13.2	2.1	13.8	8.1	27.6

PTND 3	Dspig -12mm		Cone angle - 190 mm				Pressure - 144 kPa	
Stream	Feed	Mill Prod.	Scn. O/S	Cyc. Feed	U/F	OFO	OFI	PS - O/S	PS - U/S
TPH Solids (t/h)	1.05	4.81	0.18	4.63	3.43	0.87	0.33	0.15	0.18
Percent Solids	98.7	70.0	70.3	47.7	75.6	22.1	26.3	48.8	15.7
Solids SG (t/m³)	3.8	3.8	3.8	3.8	3.8	3.8	3.8	3.8	3.8
P80 (mm)	4.13	0.189	1.482	0.184	0.203	0.088	0.117	0.157	0.066
Size (mm)									
8.000	0.0	0.0	0.0	0.0	0.0	0.0	0.0	0.0	0.0
5.600	7.2	0.1	2.3	0.0	0.0	0.0	0.0	0.0	0.0
4.000	14.6	0.3	6.0	0.0	0.1	0.0	0.0	0.0	0.0
2.800	9.7	0.2	5.1	0.0	0.1	0.0	0.0	0.0	0.0
2.000	6.3	0.2	3.6	0.0	0.0	0.0	0.0	0.0	0.0
1.400	3.4	0.2	3.5	0.0	0.0	0.0	0.0	0.0	0.0
1.000	2.9	0.2	4.2	0.0	0.0	0.0	0.0	0.0	0.0
0.710	2.1	0.2	3.1	0.0	0.0	0.0	0.0	0.0	0.0
0.500	2.9	0.4	6.8	0.1	0.1	0.0	0.1	0.1	0.0
0.355	4.3	1.4	6.4	1.2	1.7	0.0	0.0	0.1	0.0
0.250	7.1	5.2	6.3	5.2	6.9	0.0	0.5	1.2	0.0
0.180	9.9	14.4	11.8	14.5	19.1	0.1	3.8	8.2	0.2
0.125	8.9	20.7	15.0	20.9	26.7	1.3	12.3	24.7	2.3
0.090	6.7	21.6	14.4	21.9	23.4	17.7	16.9	32.2	4.3
0.063	4.8	13.9	7.2	14.2	13.2	17.4	15.6	15.8	15.4
0.045	1.4	5.4	1.7	5.6	2.5	12.2	20.2	3.4	34.0
0.032	1.2	4.0	1.0	4.1	1.5	11.4	11.5	3.4	18.2
0.000	6.6	11.8	1.6	12.2	4.6	39.8	19.1	11.0	25.7

University of Cape Town

PTND 5	Dspig - 14 mm			Conical Length - 375 mm			Pressure - 136 kPa		
	Feed	Mill Prod.	Scn. O/S	Cyc. Feed	U/F	OFO	OFI	PS-O/S	PS - U/S
TPH Solids (t/h)	0.70	3.68	0.19	3.49	2.58	0.60	0.31	0.21	0.39
Solids SG (t/m³)	3.8	3.8	3.8	3.8	3.8	3.8	3.8	3.8	3.8
Percent Solids	98.7	72.5	70.9	54.1	71.4	34.7	27.9	46.9	27.6
P80 (mm)	4.30	0.168	0.478	0.164	0.182	0.104	0.083	0.145	0.078
Size (mm)									
8.000	0.0	0.0	0.0	0.0	0.0	0.0	0.0	0.0	0.0
5.600	9.2	0.1	1.3	0.0	0.0	0.0	0.0	0.0	0.0
4.000	14.5	0.2	3.1	0.0	0.0	0.0	0.0	0.0	0.0
2.800	10.2	0.1	2.6	0.0	0.0	0.0	0.0	0.0	0.0
2.000	5.1	0.1	1.8	0.0	0.0	0.0	0.0	0.0	0.0
1.400	3.6	0.1	1.8	0.0	0.0	0.0	0.0	0.0	0.0
1.000	2.7	0.1	1.9	0.0	0.0	0.0	0.0	0.0	0.0
0.710	2.1	0.2	2.6	0.0	0.0	0.0	0.0	0.0	0.0
0.500	3.0	0.7	4.2	0.5	0.7	0.0	0.0	0.0	0.0
0.355	4.4	1.6	5.1	1.5	2.0	0.0	0.0	0.0	0.0
0.250	7.3	3.9	5.1	3.9	5.1	0.4	0.1	1.0	0.0
0.180	10.2	9.9	10.6	9.9	12.6	2.9	1.2	8.0	0.1
0.125	8.8	17.4	15.1	17.5	21.1	8.2	5.0	20.0	1.8
0.090	7.1	24.0	19.9	24.3	27.8	16.2	10.7	26.2	10.7
0.063	4.9	17.6	12.4	17.9	17.9	19.5	14.3	18.6	20.0
0.045	1.5	9.5	5.4	9.7	7.8	15.4	15.0	10.2	18.2
0.032	1.1	3.6	1.4	3.7	1.8	8.4	9.9	4.7	10.4
0.000	4.3	10.9	5.8	11.2	3.1	29.1	43.7	11.2	38.8

PTND 6	Dspig - 12 mm	Cone Length - 475 mm		Pressure - 133 kPa
Stream	Cyc. Feed	U/F	OFO	OFI
TPH Solids (t/h)	3.48	2.41	0.53	0.54
Solids SG (t/m³)	3.8	3.8	3.8	3.8
Percent solids	49.1	66.9	36.1	26.7
P 80 (mm)	0.170	0.195	0.099	0.077
Size (mm)				
8.000	0.0	0.0	0.0	0.0
5.600	0.0	0.0	0.0	0.0
4.000	0.0	0.0	0.0	0.0
2.800	0.0	0.0	0.0	0.0
2.000	0.0	0.0	0.0	0.0
1.400	0.0	0.0	0.0	0.0
1.000	0.0	0.0	0.0	0.0
0.710	0.0	0.0	0.0	0.0
0.500	0.1	0.1	0.0	0.0
0.355	1.1	1.6	0.0	0.0
0.250	4.9	7.0	0.5	0.1
0.180	11.5	15.9	2.7	0.5
0.125	17.0	22.2	7.2	3.1
0.090	21.9	26.2	14.2	10.1
0.063	15.2	14.5	18.2	15.6
0.045	8.3	6.4	12.0	13.4
0.032	4.9	2.5	7.8	12.5
0.000	15.1	3.6	37.4	44.9

University of Cape Town

PTND 7	Dspig - 14 mm		Cone Length - 475 mm		Pressure - 96 kPa	
Stream	Feed	Mill Prod.	Scn. O/S	Cyc. Feed	U/F	O/F
TPH Solids (t/h)	0.71	3.82	0.26	3.56	2.85	0.71
Solids SG (t/m³)	3.8	3.8	3.8	3.8	3.8	3.8
Percent Solids	99.9	67.2	85.3	54.9	69.3	29.9
P80 (mm)	4.95	0.171	0.632	0.162	0.175	0.107
Size (mm)						
8.000	0.0	0.0	0.0	0.0	0.0	0.0
5.600	15.1	0.1	1.9	0.0	0.0	0.0
4.000	14.5	0.3	3.5	0.0	0.0	0.0
2.800	10.8	0.3	3.6	0.0	0.0	0.0
2.000	5.1	0.2	2.3	0.0	0.0	0.0
1.400	3.4	0.2	2.5	0.0	0.0	0.0
1.000	2.7	0.2	2.8	0.0	0.0	0.0
0.710	2.2	0.2	2.1	0.0	0.0	0.0
0.500	3.0	0.3	4.0	0.0	0.0	0.0
0.355	3.9	1.4	5.2	1.2	1.4	0.1
0.250	6.1	3.9	6.7	3.7	4.4	0.8
0.180	9.0	10.8	12.6	10.6	12.8	1.9
0.125	7.5	16.8	17.2	16.8	18.7	9.0
0.090	7.2	23.7	18.1	24.1	25.3	19.5
0.063	2.9	16.4	8.8	16.9	17.3	15.5
0.045	0.5	8.9	3.7	9.3	8.4	13.1
0.032	1.1	3.5	1.0	3.7	2.3	9.4
0.000	5.3	12.9	3.9	13.6	9.4	30.7

PTND 8	Dspig - 12 mm		Cone Length - 250 mm		Pressure - 125 kPa				
	Feed	Mill Prod.	O/S	Cyc. Feed	U/F	OFO	OFI	PS - O/S	PS - U/S
TPH Solids (t/h)	1.00	3.50	0.20	3.30	2.18	0.60	0.53	0.12	0.42
Solids SG (t/m³)	3.8	3.8	3.8	3.8	3.8	3.8	3.8	3.8	3.8
Percent Solids	99.8	74.4	92.5	55.3	74.3	32.0	45.7	54.3	28.0
P80 (mm)	4.21	0.175	3.13	0.166	0.188	0.093	0.127	0.155	0.072
Size (mm)									
8.000	0.0	0.0	0.0	0.0	0.0	0.0	0.0	0.0	0.0
5.600	8.6	0.5	7.9	0.0	0.0	0.0	0.0	0.0	0.0
4.000	14.0	0.5	7.9	0.0	0.0	0.0	0.0	0.0	0.0
2.800	10.8	0.4	6.3	0.0	0.0	0.0	0.0	0.0	0.0
2.000	4.8	0.2	3.7	0.0	0.0	0.0	0.0	0.0	0.0
1.400	3.9	0.2	3.4	0.0	0.0	0.0	0.0	0.0	0.0
1.000	2.7	0.2	3.5	0.0	0.0	0.0	0.0	0.0	0.0
0.710	2.3	0.3	5.0	0.0	0.0	0.0	0.0	0.0	0.0
0.500	3.1	0.5	8.4	0.0	0.0	0.0	0.0	0.0	0.0
0.355	4.5	1.2	5.4	0.9	1.4	0.0	0.2	0.1	0.0
0.250	7.5	3.6	4.3	3.6	5.2	0.6	1.2	1.3	0.0
0.180	10.8	11.1	8.1	11.2	16.0	1.2	5.6	10.4	0.1
0.125	8.9	19.5	12.0	20.0	27.4	3.8	13.7	22.2	1.8
0.090	7.7	21.1	12.5	21.6	24.3	16.1	20.4	28.8	8.2
0.063	4.6	14.4	6.1	14.9	13.7	17.1	15.4	15.3	17.4
0.045	2.1	6.4	2.5	6.7	3.9	12.0	8.0	6.6	16.0
0.032	0.7	2.6	0.8	2.7	0.9	8.5	3.4	2.8	7.7
0.000	3.1	17.4	2.4	18.3	7.2	40.7	32.1	12.4	48.8

University of Cape Town

PTND 9	Dspig - 12 mm		Cone Length - 475 mm				Pressure - 111 kPa		
	Feed	Mill Prod.	Scn. O/S	Cyc. Feed	U/F	OFO	OFI	PS - O/S	PS - U/S
TPH Solids (t/h)	0.90	3.39	0.21	3.18	2.02	0.69	0.47	0.26	0.43
Solids SG (t/m³)	3.8	3.8	3.8	3.8	3.8	3.8	3.8	3.8	3.8
Percent Solids	97.9	77.5	84.4	55.8	78.1	41.9	32.1	60.0	30.6
P80 (mm)	4.33	0.175	0.374	0.170	0.196	0.111	0.094	0.162	0.079
Size (mm)									
8.000	0.0	0.0	0.0	0.0	0.0	0.0	0.0	0.0	0.0
5.600	9.0	0.1	1.4	0.0	0.0	0.0	0.0	0.0	0.0
4.000	15.1	0.2	3.2	0.0	0.0	0.0	0.0	0.0	0.0
2.800	10.0	0.2	2.7	0.0	0.0	0.0	0.0	0.0	0.0
2.000	4.8	0.1	1.6	0.0	0.0	0.0	0.0	0.0	0.0
1.400	3.9	0.1	1.5	0.0	0.0	0.0	0.0	0.0	0.0
1.000	2.6	0.1	1.5	0.0	0.0	0.0	0.0	0.0	0.0
0.710	2.0	0.1	1.7	0.0	0.0	0.0	0.0	0.0	0.0
0.500	3.0	0.2	3.0	0.0	0.0	0.0	0.0	0.0	0.0
0.355	4.5	1.2	4.1	1.0	1.5	0.2	0.0	0.4	0.0
0.250	7.3	4.3	5.5	4.3	6.3	1.1	0.0	2.9	0.0
0.180	10.4	11.9	12.7	11.8	17.0	4.3	0.3	11.3	0.1
0.125	9.1	18.5	18.2	18.5	25.0	8.8	4.9	21.5	1.1
0.090	7.0	21.9	19.2	22.1	25.1	16.7	17.4	27.7	10.0
0.063	5.2	15.8	12.4	16.0	13.8	21.7	17.5	14.3	26.3
0.045	1.7	5.2	3.3	5.3	3.3	8.7	8.8	3.6	11.8
0.032	1.2	4.4	2.6	4.5	2.1	8.8	8.2	2.6	12.5
0.000	3.3	15.6	5.5	16.3	5.6	29.6	42.8	15.7	38.0

PTND 10	Dspig - 12 mm		Cone Length - 635 mm				Pressure - 134 kPa		
	Feed	Mill Prod.	Scn. O/S	Cyc. Feed	U/F	OFO	OFI	PS - O/S	PS - U/S
TPH Solids (t/h)	1.03	3.37	0.24	3.13	1.86	0.72	0.55	0.24	0.48
Solids SG (t/m³)	3.8	3.8	3.8	3.8	3.8	3.8	3.8	3.8	3.8
Percent Solids	99.8	76.2	82.0	53.0	73.0	43.6	32.2	51.0	30.5
P80 (mm)	4.19	0.179	0.474	0.173	0.203	0.116	0.089	0.179	0.085
Size (mm)									
8.000	0.0	0.0	0.0	0.0	0.0	0.0	0.0	0.0	0.0
5.600	8.0	0.1	1.6	0.0	0.0	0.0	0.0	0.0	0.0
4.000	14.4	0.3	3.2	0.0	0.0	0.0	0.0	0.0	0.0
2.800	9.8	0.2	2.8	0.0	0.0	0.0	0.0	0.0	0.0
2.000	4.7	0.1	1.6	0.0	0.0	0.0	0.0	0.0	0.0
1.400	3.8	0.1	1.6	0.0	0.0	0.0	0.0	0.0	0.0
1.000	2.7	0.1	1.8	0.0	0.0	0.0	0.0	0.0	0.0
0.710	2.2	0.2	2.2	0.0	0.0	0.0	0.0	0.0	0.0
0.500	2.8	0.3	4.3	0.0	0.0	0.0	0.0	0.0	0.0
0.355	4.4	1.3	5.5	1.0	1.7	0.1	0.0	0.4	0.0
0.250	8.2	4.7	5.2	4.6	7.0	1.9	0.0	5.6	0.0
0.180	9.9	12.2	9.7	12.4	19.1	4.6	0.0	13.7	0.0
0.125	9.0	18.7	16.7	18.9	27.8	9.4	1.0	27.9	0.1
0.090	6.7	20.5	18.4	20.7	21.9	19.5	18.3	25.7	16.4
0.063	6.5	13.8	13.2	13.8	11.5	17.8	16.4	11.1	21.2
0.045	2.0	6.7	4.7	6.9	3.3	11.3	12.9	4.2	14.9
0.032	0.8	2.8	1.5	2.9	0.9	5.6	5.9	1.5	7.7
0.000	4.0	17.8	6.0	18.6	6.4	29.8	45.3	10.0	39.6

University of Cape Town

PTND 11	Dspig - 12 mm		Cone Length - 375 mm					Pressure - 118 kPa	
	Feed	Mill Prod.	Scn. O/S	Cyc. Feed	U/F	OFO	OFI	PS - O/S	PS - U/S
TPH Solids (t/h)	1.01	3.50	0.23	3.27	1.95	0.94	0.38	0.31	0.63
Solids SG (t/m³)	3.8	3.8	3.8	3.8	3.8	3.8	3.8	3.8	3.8
Percent Solids	99.8	72.2	84.7	54.9	76.8	42.9	31.0	55.2	29.8
P80 (mm)	4.74	0.180	0.534	0.173	0.200	0.121	0.103	0.171	0.095
Size (mm)									
8.000	0.0	0.0	0.0	0.0	0.0	0.0	0.0	0.0	0.0
5.600	11.8	0.1	1.4	0.0	0.0	0.0	0.0	0.0	0.0
4.000	18.1	0.3	3.6	0.0	0.0	0.0	0.0	0.0	0.0
2.800	12.9	0.2	3.2	0.0	0.0	0.0	0.0	0.0	0.0
2.000	6.0	0.1	2.0	0.0	0.0	0.0	0.0	0.0	0.0
1.400	4.3	0.1	1.9	0.0	0.0	0.0	0.0	0.0	0.0
1.000	3.2	0.1	1.8	0.0	0.0	0.0	0.0	0.0	0.0
0.710	2.2	0.2	2.5	0.0	0.0	0.0	0.0	0.0	0.0
0.500	2.9	0.3	4.6	0.0	0.0	0.0	0.0	0.0	0.0
0.355	3.9	1.4	5.8	1.1	1.7	0.1	0.0	0.3	0.0
0.250	6.0	4.7	6.7	4.6	6.9	1.2	0.9	3.4	0.1
0.180	7.9	12.3	12.8	12.3	17.8	4.5	3.4	12.9	0.3
0.125	6.6	20.7	17.7	20.9	27.6	12.1	8.7	27.7	4.5
0.090	5.1	21.6	16.6	21.9	23.8	21.9	12.6	27.1	19.3
0.063	3.5	14.1	9.8	14.4	11.6	19.6	16.3	14.2	22.3
0.045	1.6	6.0	3.7	6.2	4.0	8.7	10.9	4.8	10.7
0.032	0.6	2.4	1.1	2.5	1.1	3.4	7.7	1.6	4.3
0.000	3.3	15.2	5.0	15.9	5.3	28.4	39.4	8.1	38.4

PTND 12	Dspig - 14 mm			Cone length - 635 mm				Pressure - 110 kPa	
Stream	Feed	Mill Prod.	Scn. O/S	Cyc. Feed	U/F	OFO	OFI	PS - O/S	PS - U/S
TPH Solids (t/h)	0.72	3.16	0.16	3.01	1.99	0.67	0.35	0.30	0.37
Solids SG (t/m³)	3.8	3.8	3.8	3.8	3.8	3.8	3.8	3.8	3.8
Percent Solids	99.8	73.3	83.8	54.4	75.3	39.4	29.6	52.5	27.4
P80 (mm)	4.31	0.163	0.406	0.159	0.179	0.109	0.073	0.148	0.065
Size (mm)									
8.000	0.0	0.0	0.0	0.0	0.0	0.0	0.0	0.0	0.0
5.600	9.2	0.1	0.9	0.0	0.0	0.0	0.0	0.0	0.0
4.000	14.4	0.1	2.2	0.0	0.0	0.0	0.0	0.0	0.0
2.800	10.2	0.1	2.2	0.0	0.0	0.0	0.0	0.0	0.0
2.000	4.9	0.1	1.5	0.0	0.0	0.0	0.0	0.0	0.0
1.400	3.7	0.1	1.5	0.0	0.0	0.0	0.0	0.0	0.0
1.000	2.9	0.1	1.8	0.0	0.0	0.0	0.0	0.0	0.0
0.710	2.2	0.1	2.2	0.0	0.0	0.0	0.0	0.0	0.0
0.500	2.9	0.2	4.4	0.0	0.0	0.0	0.0	0.0	0.0
0.355	4.6	0.9	5.6	0.7	1.0	0.1	0.0	0.1	0.0
0.250	8.1	3.3	6.1	3.2	4.5	0.8	0.2	1.7	0.1
0.180	10.1	10.3	11.0	10.3	14.0	4.1	1.3	9.0	0.0
0.125	8.2	18.8	18.1	18.8	24.9	8.5	3.9	18.9	0.0
0.090	7.9	24.6	21.5	24.7	30.2	17.4	7.8	31.1	6.3
0.063	4.6	13.7	10.9	13.8	14.3	13.1	12.4	10.8	15.1
0.045	2.1	7.0	4.3	7.2	5.2	13.2	6.8	15.2	11.5
0.032	0.5	3.0	1.4	3.1	1.5	4.8	9.1	2.7	6.4
0.000	3.5	17.4	4.4	18.1	4.3	38.1	58.5	10.4	60.5

University of Cape Town

PTND 13	Dspig - 12 mm			Cone Length - 210 mm			Pressure -118 kPa		
Stream	Feed	Mill Prod.	Scn. O/S	Cyc Feed	U/F	OFO	OFI	PS O/S	PS U/S
TPH Solids (t/h)	1.00	3.45	0.22	3.23	1.95	0.51	0.78	0.29	0.49
Solids SG (t/m³)	3.8	3.8	3.8	3.8	3.8	3.8	3.8	3.8	3.8
% Solids	99.6	73.5	86.9	53.0	73.1	31.2	43.0	49.5	28.5
P80(mm)	4.34	0.175	0.608	0.168	0.195	0.079	0.116	0.176	0.083
Size (mm)									
8.000	0.0	0.0	0.0	0.0	0.0	0.0	0.0	0.0	0.0
5.600	8.9	0.2	2.3	0.0	0.0	0.0	0.0	0.0	0.0
4.000	15.5	0.3	4.9	0.0	0.0	0.0	0.0	0.0	0.0
2.800	11.6	0.3	3.6	0.0	0.0	0.0	0.0	0.0	0.0
2.000	6.0	0.2	2.1	0.0	0.0	0.0	0.0	0.0	0.0
1.400	3.6	0.1	1.8	0.0	0.0	0.0	0.0	0.0	0.0
1.000	2.5	0.1	1.6	0.0	0.0	0.0	0.0	0.0	0.0
0.710	2.1	0.2	2.2	0.0	0.0	0.0	0.0	0.0	0.0
0.500	2.8	0.3	3.7	0.0	0.1	0.0	0.0	0.0	0.0
0.355	4.1	1.1	4.6	0.9	1.5	0.0	0.1	0.2	0.1
0.250	7.4	4.5	5.8	4.4	6.4	0.0	2.3	6.2	0.1
0.180	9.3	11.3	13.0	11.2	16.7	0.4	4.5	12.3	0.0
0.125	8.8	18.8	18.3	18.8	27.0	1.5	9.5	23.3	1.6
0.090	7.3	20.0	17.6	20.2	24.0	12.4	15.7	19.0	13.8
0.063	2.9	14.2	9.8	14.5	12.5	15.5	19.1	14.8	21.6
0.045	0.5	7.8	3.5	8.1	3.4	19.6	12.4	6.0	16.0
0.032	0.7	3.2	1.0	3.3	1.0	7.3	6.6	5.1	7.4
0.000	5.8	17.5	4.3	18.4	7.4	43.1	29.7	13.2	39.1

PTND 14	Dspig - 14 mm			Cone Length - 475 mm				Pressure -120 kPa		
Stream	Feed	Mill Prod.	Scn. O/S	Cyc Feed	U/F	OFO	OFI	PS O/S	PS U/S	Float feed
TPH Solids (t/h)	0.70	3.49	0.25	3.24	2.31	0.61	0.32	0.23	0.38	0.70
Solids SG (t/m³)	3.8	3.8	3.8	3.8	3.8	3.8	3.8	3.8	3.8	3.8
% Solids	99.5	70.2	85.4	57.9	70.9	41.9	36.6	47.7	28.9	32.0
P80(mm)	3.97	0.150	0.422	0.143	0.164	0.090	0.060	0.119	0.064	0.062
Size (mm)										
8.000	0.0	0.0	0.0	0.0	0.0	0.0	0.0	0.0	0.0	0.0
5.600	6.5	0.1	1.2	0.0	0.0	0.0	0.0	0.0	0.0	0.0
4.000	13.3	0.2	2.6	0.0	0.0	0.0	0.0	0.0	0.0	0.0
2.800	10.1	0.2	2.4	0.0	0.0	0.0	0.0	0.0	0.0	0.0
2.000	5.8	0.1	1.5	0.0	0.0	0.0	0.0	0.0	0.0	0.0
1.400	3.5	0.1	1.6	0.0	0.0	0.0	0.0	0.0	0.0	0.0
1.000	2.9	0.1	1.7	0.0	0.0	0.0	0.0	0.0	0.0	0.0
0.710	2.3	0.2	2.2	0.0	0.0	0.0	0.0	0.0	0.0	0.0
0.500	3.1	0.3	4.1	0.0	0.0	0.0	0.0	0.0	0.0	0.0
0.355	4.5	0.8	5.6	0.4	0.6	0.0	0.0	0.0	0.0	0.0
0.250	8.0	2.7	5.4	2.4	3.4	0.1	0.0	0.3	0.0	0.0
0.180	10.0	8.4	9.6	8.3	11.5	0.7	0.0	1.8	0.0	0.0
0.125	9.2	14.8	15.7	14.7	19.2	5.4	0.0	14.2	0.0	0.0
0.090	8.1	22.2	19.1	22.4	27.1	13.6	5.3	28.7	4.4	4.8
0.063	4.6	18.2	14.8	18.4	19.1	19.1	12.4	22.9	16.7	14.7
0.045	2.0	10.9	6.4	11.2	9.5	15.3	16.3	9.7	18.7	17.6
0.032	0.5	4.9	1.9	5.1	2.2	11.7	13.3	6.6	14.8	14.1
0.000	5.8	16.1	4.2	17.0	7.4	34.1	52.8	15.7	45.4	48.8

University of Cape Town

E. Efficiency curve parameters used in model development and Validation.

Table 1: Efficiency curve parameters used for model development.

Run No.	D50c U/F, mm	D50c OFl, mm	C-U/F	C-OFl	α - U/F	α - OFl
1	0.106	0.090	0.62	0.27	3.2	3.9
2	0.097	0.123	0.73	0.25	3.0	0.9
4	0.079	0.067	0.78	0.27	3.5	2.3
5	0.088	0.071	0.80	0.29	5.2	2.3
6	0.071	0.036	0.86	0.42	4.0	3.2
9	0.095	0.047	0.86	0.32	4.0	3.9
10	0.097	0.123	0.68	0.27	1.6	1.5
11	0.095	0.107	0.71	0.47	3.9	2.5
13	0.088	0.107	0.72	0.28	3.8	2.2
15	0.092	0.074	0.77	0.29	2.7	2.8
16	0.088	0.093	0.78	0.21	3.7	2.4
17	0.092	0.099	0.80	0.27	3.3	4.0
18	0.086	0.096	0.75	0.16	3.8	2.6
19	0.093	0.078	0.75	0.30	3.9	3.5
20	0.097	0.074	0.82	0.35	3.0	3.0
21	0.067	0.059	0.81	0.28	4.0	3.7
22	0.088	0.063	0.84	0.32	4.6	2.6
24	0.084	0.069	0.81	0.19	3.5	2.2
26	0.086	0.058	0.87	0.29	3.9	4.3
27	0.067	0.051	0.84	0.22	3.7	4.0
28	0.072	0.040	0.79	0.18	3.8	1.6
30	0.091	0.111	0.83	0.58	4.0	4.3
31	0.081	0.080	0.85	0.61	3.4	3.6
32	0.068	0.097	0.74	0.43	3.0	1.1
34	0.081	0.095	0.75	0.49	3.6	2.4
35	0.098	0.098	0.85	0.39	4.1	3.2
36	0.088	0.104	0.84	0.37	4.7	2.6
38	0.071	0.073	0.82	0.21	3.7	2.6
39	0.077	0.101	0.73	0.24	5.4	3.6
41	0.084	0.098	0.81	0.43	3.8	2.9
42	0.062	0.068	0.79	0.43	4.1	4.2
43	0.090	0.080	0.84	0.59	4.4	2.5
45	0.089	0.086	0.85	0.69	1.7	1.3

University of Pretoria

Table 2: Efficiency curve parameters used for model development Continued.

Run No.	D50c U/F, mm	D50c OFl, mm	C-U/F	C-OFl	α - U/F	α - OFl
46	0.065	0.066	0.86	0.64	3.6	3.2
47	0.068	0.066	0.83	0.62	3.4	3.7
48	0.069	0.065	0.84	0.63	2.9	4.0
49	0.077	0.052	0.84	0.41	3.1	3.8
50	0.083	0.062	0.84	0.34	3.3	4.0
52	0.093	0.152	0.88	0.36	5.0	3.5
53	0.107	0.155	0.88	0.33	3.0	1.9
54	0.079	0.093	0.82	0.23	2.5	3.3
55	0.072	0.103	0.90	0.30	3.9	4.1
56	0.085	0.104	0.91	0.27	3.9	4.0
57	0.084	0.095	0.88	0.27	3.7	3.0
58	0.083	0.100	0.90	0.34	4.0	1.5
60	0.072	0.104	0.90	0.22	2.3	2.2
61	0.091	0.077	0.89	0.55	5.0	2.3
63	0.072	0.060	0.87	0.51	3.9	4.0
64	0.087	0.075	0.88	0.61	4.0	4.0
65	0.079	0.067	0.83	0.53	3.1	3.5
67	0.069	0.062	0.85	0.62	3.8	3.2
68	0.071	0.065	0.84	0.55	3.7	3.9
69	0.075	0.057	0.85	0.43	3.9	4.0
70	0.073	0.062	0.84	0.47	3.1	3.2
72	0.090	0.077	0.87	0.46	5.4	4.0
73	0.072	0.093	0.89	0.44	2.2	2.7
74	0.076	0.072	0.85	0.54	5.0	2.4
75	0.073	0.067	0.86	0.37	5.2	4.3
76	0.097	0.115	0.82	0.22	3.7	1.6
77	0.104	0.076	0.84	0.34	2.2	3.2
78	0.081	0.068	0.82	0.53	3.8	4.0

University of Cape Town

University of Cape Town

University of Cape Town

University of Cape Town